University of Alberta

Renal proximal tubular handling of nucleosides by human nucleoside transporter proteins

by

Adam Nader Elwi

A thesis submitted to the Faculty of Graduate Studies and Research
in partial fulfillment of the requirements for the degree of

Doctor of Philosophy

Oncology

©Adam Nader Elwi
Fall 2009
Edmonton, Alberta

Permission is hereby granted to the University of Alberta Libraries to reproduce single copies of this thesis and to lend or sell such copies for private, scholarly or scientific research purposes only. Where the thesis is converted to, or otherwise made available in digital form, the University of Alberta will advise potential users of the thesis of these terms.

The author reserves all other publication and other rights in association with the copyright in the thesis and, except as herein before provided, neither the thesis nor any substantial portion thereof may be printed or otherwise reproduced in any material form whatsoever without the author's prior written permission.

Library and
Archives Canada

Published Heritage
Branch

395 Wellington Street
Ottawa ON K1A 0N4
Canada

Bibliothèque et
Archives Canada

Direction du
Patrimoine de l'édition

395, rue Wellington
Ottawa ON K1A 0N4
Canada

Your file Votre référence
ISBN: 978-0-494-51225-8
Our file Notre référence

NOTICE:
The author has granted a non-exclusive license allowing Library and Archives Canada to reproduce, publish, archive, preserve, conserve, communicate to the public by telecommunication or on the Internet, loan, distribute and sell theses worldwide, for commercial or non-commercial purposes, in microform, paper, electronic and/or any other formats.

The author retains copyright ownership and moral rights in this thesis. Neither the thesis nor substantial extracts from it may be printed or otherwise reproduced without the author's permission.

AVIS:
L'auteur a accordé une licence non exclusive permettant à la Bibliothèque et Archives Canada de reproduire, publier, archiver, sauvegarder, conserver, transmettre au public par télécommunication ou par l'Internet, prêter, distribuer et vendre des thèses partout dans le monde, à des fins commerciales ou autres, sur support microforme, papier, électronique et/ou autres formats.

L'auteur conserve la propriété du droit d'auteur et des droits moraux qui protège cette thèse. Ni la thèse ni des extraits substantiels de celle-ci ne doivent être imprimés ou autrement reproduits sans son autorisation.

In compliance with the Canadian Privacy Act some supporting forms may have been removed from this thesis.

While these forms may be included in the document page count, their removal does not represent any loss of content from the thesis.

Conformément à la loi canadienne sur la protection de la vie privée, quelques formulaires secondaires ont été enlevés de cette thèse.

Bien que ces formulaires aient inclus dans la pagination, il n'y aura aucun contenu manquant.

Canada

Examining Committee

Dr. Carol Cass, Department of Oncology

Dr. Michael Sawyer, Department of Oncology

Dr. Michael Weinfeld, Department of Oncology

Dr. James Young, Department of Physiology

Dr. Chris Cheeseman, Department of Physiology

Dr. Varsha Gandhi, Department of Experimental Therapeutics, The University of Texas M. D. Anderson Cancer Center

For my mother.

Abstract

Human cells possess multiple nucleoside transporters (NTs) that belong to either the human equilibrative or concentrative NT (hENT: hENT1/2/3/4; hCNT: CNT1/2/3) families. In the kidney, coupling of apical hCNT3 activities to basolateral hENT1/2 activities is hypothesized to mediate renal nucleoside proximal tubular absorption while apical ENT1 may have a role in secretion. The overall aim of this research was to increase understanding of the roles of hENTs and hCNTs in renal handling of physiological nucleosides and anti-cancer nucleoside analog drugs. This was achieved by investigating the distribution of hENTs and hCNTs in human kidney tissue and the function of hENTs and hCNTs in cellular uptake and transepithelial fluxes of nucleosides in cultured human renal proximal tubule cells (hRPTCs).

Immunolocalization of hCNT3 and hENT1 in human kidney tissue revealed that hENT and hCNT3 were present in apical membranes of proximal tubules. Production and characterization of adherent hRPTC cultures demonstrated endogenous hCNT3, hENT1, and hENT2 activities. These results provided evidence for the involvement of hCNT3, hENT1, and hENT2 in renal handling of nucleosides.

Comparison of adherent hRPTC cultures derived from kidneys from different individuals demonstrated that hCNT3 activities varied between cultures. Also, the extent of cellular uptake of fludarabine, an anti-cancer nucleoside drug, and degree of cytotoxicity was reflected in the different hCNT3 activities observed between cultures. These results suggested that hCNT3 plays an

important role in fludarabine renal handling and is a determinant of potential renal toxicities.

Production of polarized monolayer cultures of hRPTCs on transwell permeable inserts enabled the functional localization of hCNT3 and hENT1 to apical membranes and hENT2 to basolateral membranes. Transepithelial flux studies demonstrated that (i) apical-to-basolateral fluxes of adenosine were mediated by apical hCNT3 and basolateral hENT2, (ii) basolateral-to-apical fluxes of 2′-deoxyadenosine were mediated, in part, by apical hENT1 and basolateral hOATs, and (iii) apical-to-basolateral fluxes of fludarabine, cladribine, and clofarabine were mediated by apical hCNT3.

These studies showed that coupling of apical hCNT3 to basolateral hENT2 mediates proximal tubular nucleoside reabsorption, that coupling of basolateral human organic anion transporters (hOATs) to apical hENT1 mediates proximal tubular nucleoside secretion, and that hCNT3 is a key determinant of fludarabine proximal tubular reabsorption and cytoxicity.

Acknowledgements

This thesis was completed with the support of numerous people and they have my thanks. It is difficult to express my gratitude to my supervisor, Dr. Carol Cass, for taking me on and giving me the opportunity to work on several fruitful projects during the course of my studies. She is a great teacher who gave many useful suggestions, important advice, and constant encouragement throughout the course of this work. I am extremely grateful for her advice and tremendous patience during my research and scientific writing. I am equally indebted to my co-supervisor, Dr. Michael Sawyer, for providing scientific guidance and ideas during my studies, without which my research would not have been as relevant and timely.

Without the support of the wonderful staff and students in Dr. Carol Cass' laboratory, my research would not have been possible. I would particularly like to thank: Dr. Vijaya Damaraju for training and collaborating with me; Ms. Michelle Kuzma, Ms. Geraldine Baron, Ms. Delores Mowles, Ms. Pat Carpenter, Ms. Cheryl Santos, Ms. Lorelei Johnson, and Ms. Milada Selner for their technical expertise and support, Mr. Robert Paproski, Dr. Karen King, Dr. Kathryn Graham, Dr. Jing Zhang, Dr. Frank Visser, Dr. Allan Doucette, Dr. Thack Lang for their scientific criticisms and contributions, Ms. Yola and Ms. Lily Zombar for preparation of reagents, and Ms. Jennifer Au for her assistance as a summer student researcher.

My gratitude extends towards Dr. Michael Sawyer and our collaborators Dr. James Young, Dr. Stephen Baldwin, and Dr. John Mackey for their expert advice and provision of clinical samples. The provision of clinical samples, an integral part of my project, was made possible by Dr. Michael Sawyer's interactions with urologists at the University of Alberta Hospital including Dr. Gerald Todd and pathologists at the Anatomical Pathology Lab (University of Alberta Hospital) including Dr. Charlene Hunter.

I thank my supervisory committee (Dr. Carol Cass, Dr. Michael Sawyer, Dr. Michael Weinfeld, and Dr. James Young) for useful scientific discussions over the years. I am grateful for their time and effort in contributing to the development of my skills as a researcher.

I thank Dr. Xie-Jun Sun and the staff of the Cross Cancer Institute Cell Imaging Facility for technical assistance and direction with microscopy, the administrative staff of the Department of Oncology including Ms. Cheryl Erickson, Ms. Lori Jennings, and Ms. Cynthia Henderson for assistance with fellowship applications, the staff of the Abdul Khaliq Library including Ms. Linda Harris for assistance with scientific paper requests, and the faculty and students of the Department of Oncology and the Membrane Protein Research Group for their scientific discussions, interactions, and friendships. It was a pleasure interacting with them.

I thank my examining committee (Dr. Carol Cass, Dr. Michael Sawyer, Dr. James Young, Dr. Michael Weinfeld, Dr. Chris Cheeseman, Dr. Varsha Gandhi, and Dr. Andrew Shaw) for their thorough reading and discussion of my thesis.

My final thanks extend to my immediate family and friends for their tremendous love and support. My father, Alaa Elwi, and my mother, Azza

Darwish, provided me with every opportunity to pursue my heart's desire. My wife, Esther Kim, provided me with unconditional love, kindness, and understanding.

Table of Contents

Chapters **Page**

I. Introduction... 1

I.1 Review of human nucleoside and nucleobase transport biology.........2

I.1.1 Importance of physiological nucleosides and nucleobases........ 5

I.1.2 Pharmacology of synthetic nucleoside and nucleobase analog drugs 9

I.1.3 Human nucleoside transporter (hNT) protein family.................. 14

I.1.3.1 Human equilibrative nucleoside transporters (hENTs)...... 14

I.1.3.1.1 Characterization of hENTs.................................. 15

I.1.3.1.2 Regulation of hENTs...19

I.1.3.2 Human concentrative nucleoside transporters (hCNTs).... 20

I.1.3.2.1 Characterization of hCNTs.................................. 21

I.1.3.2.2 Regulation of hCNTs... 23

I.2 Human renal nucleoside and nucleobase transport biology................ 25

I.2.1 Overview of human renal transport biology........................... 25

I.2.2 Renal handling of nucleosides and nucleobases...................... 28

I.2.2.1 Renal handling of physiological nucleosides and nucleobases 28

I.2.2.1 Renal handling of synthetic nucleoside and nucleobase analog drugs.. 31

I.2.3 Distribution of hENTs and hCNTs in human kidney............. 32

1.2.4 Functions of hENTs and hCNTs in human kidney................ 35

I.3 Other transporter systems capable of transporting nucleotides, nucleosides, and nucleobases.. 38

I.4 Nephrotoxicity of nucleoside analog drugs............................... 42

I.5 Proposed model for renal handling of nucleosides..................... 46

I.6 Goals of the present work.. 48

I.7 Rationale of the experimental design... 51

I.8 Approach and model system: human renal proximal tubule cell (hRPTC) cultures.. 53

I.9 Bibliography.. 55

II. Materials and Methods......... 88

II.1 Materials.. 89

II.2 Human kidney tissue collection 91

II.3 Cell culture.. 93

II.3.1 Collagen coating of cell culture ware............................ 93

II.3.2 Growth and maintenance of human kidney proximal tubule cell line (HK-2).................. 94

II.3.3 Isolation, growth, and maintenance of adherent cultures of hRPTCs 94

II.3.4 Growth and maintenance of polarized monolayers of hRPTC cultures... 96

II.4 Staining and microscopy... 96

II.4.1 Brush border enzyme cytochemistry and light miscroscopy.... 97

II.4.2 Paraffin embedded tissue immunohistochemistry and light microscopy........ 98

II.4.3 Frozen tissue immunofluorescent staining and confocal microscopy........ 100

II.5 Transport assays........ 103

II.5.1 Protein Determinations........ 103

II.5.2 Uptake assays in adherent cultures of HK-2 cells and hRPTCs. 104

II.5.3 Uptake assays in polarized monolayers of hRPTC cultures...... 106

II.5.4 Transepithelial flux assays across polarized monolayer cultures of hRPTCs........ 107

II.5.5 Production of recombinant hCNT3 and measurement of nucleoside uptake in *Saccharomyces* (*S.*) *cerevisiae*........ 109

II.5.5.1 General molecular biology procedures........ 109

II.5.5.2 Plasmid construction........ 110

II.5.5.3 Measurement of nucleoside uptake in *S. cerevisiae* expressing recombinant hCNT3........ 111

II.6 Thin layer chromatography analysis........ 112

II.7 Determination of intracellular cyclic adenosine-3′,5′-monophosphate (cAMP)........ 113

II.8 Reverse transcriptase polymerase chain reaction (RT-PCR) analysis. 115

II.8.1 Total ribonucleic acid (RNA) preparations........ 115

II.8.2 RT-PCR........ 116

II.8.3 TaqMan™ real-time quantitation RT-PCR........ 117

II.9 Immunoblotting analysis ... 119

II.9.1 Membrane and protein preparations ... 119

II.9.1.1 Crude membrane preparations ... 119

II.9.1.2 Cell surface protein preparations ... 120

II.9.1.3 *S. cerevisiae* crude membrane preparations ... 121

II.9.2 Sodium dodecyl sulphate (SDS)-polyacrylamide gel electrophoresis and immunoblotting ... 122

II.10 Cytotoxicity assays ... 123

II.11 Data analysis ... 124

II.12 Bibliography ... 128

III. Distribution of human equilibrative and concentrative nucleoside transporters 1 and 3 (hENT1 and hCNT3) in human kidney proximal tubules ... 131

III.1 Introduction ... 132

III.2 Results ... 139

III.2.1 Distribution of hENTs and hCNTs in human kidney tissues ... 139

III.2.1.1 Expression messenger RNA transcripts for hENTs and hCNTs in human kidney cortex tissues ... 139

III.2.1.2 Identification of hENT1, hENT2, hCNT2, and hCNT3 in human kidney cortex tissues ... 140

III.2.1.3 Localization of hENT1 and hCNT3 in human kidney tissues ... 142

III.2.2 Characterization of nucleoside transport processes present in monolayer cultures of HK-2 cells.................................. 148

III.2.2.1 Expression of mRNA transcripts for hENTs and hCNTs in monolayer cultures of HK-2 cells.......................... 149

III.2.2.2 Identification of hENT1, hENT2, and hCNT3 in monolayer cultures of HK-2 cells....................................... 150

III.2.2.3 Characterization of hENT and hCNT activities in monolayer cultures of HK-2 cells....................................... 151

III.2.3 Characterization of nucleoside transport processes present in monolayer hRPTC cultures....................................... 154

III.2.3.1 Demonstration of the presence of proximal tubular brush border enzymes in monolayer hRPTC cultures......... 155

III.2.3.2 Demonstration of proximal tubular parathyroid hormone sensitivities and anti-diuretic hormone insensitivities in monolayer hRPTC cultures................................156

III.2.3.3 Demonstration of the presence of sodium-dependent, phloridzin-sensitive α-methyl-D-glucoside uptake in monolayer hRPTC cultures................................157

III.2.3.4 Characterization of nucleoside transport processes present in monolayer hRPTC1 cultures...............................158

III.3 Discussion... 161

III.4 Bibliography.. 184

IV. Human concentrative nucleoside transporter 3 is a determinant of 9-β-D-arabinosyl-2-fluoroadenine (fludarabine) transportability and cytotoxicity in cultures of human renal proximal tubule cells (hRPTCs) 191

IV.1 Introduction.. 192

IV.2 Results.. 199

IV.2.1 Expression of mRNA transcripts for hENTs and hCNTs in hRPTCs 199

IV.2.2 Identification of hENT and hCNT proteins in hRPTCs......... 199

IV.2.3 Relative hCNT3 mRNA expression and protein abundance in hRPTCs...201

IV.2.4 Characterization of hENT and hCNT activities in monolayer cultures of hRPTCs..202

IV.2.5 Fludarabine uptake into hRPTCs...................................206

IV.2.6 Fludarabine cytotoxicity to hRPTCs............................. 207

IV.3 Discussion...209

IV.4 Bibliography.. 222

V. Transepithelial fluxes of adenosine and 2′-deoxyadenosine across polarized monolayers of human renal proximal tubule cells (hRPTCs): the roles of human equilibrative and concentrative nucleoside transporters, hENT1, hENT2, and hCNT3.. 231

V.1 Introduction...232

V.2 Results..237

V.2.1 Formation of polarized monolayers................................ 237

V.2.2 Transepithelial fluxes of adenosine and 2′-deoxyadenosine......239

V.2.3 Cellular uptake of adenosine and 2′-deoxyadenosine from apical and basolateral surfaces..243

V.2.4 Expression of human organic anion transporter 2 (hOAT2) mRNA...247

V.2.5 hCNT3 protein abundance...248

V.2.6 Transportability of adenosine and 2′-deoxyadenosine by recombinant hCNT3..249

V.2.7 Fludarabine, cladribine, and clofarabine transepithelial fluxes and cellular uptake...250

V.3 Discussion...252

V.4 Bibliography...270

VI. Conclusion...277

VI.1 Model for renal proximal tubular handling of nucleosides by hENTs and hCNTs...279

VI.2 Other physiological roles of renal hNTs.............................288

VI.3 Clinical consequences of renal hNTs.................................290

VI.4 Bibliography.. 295

List of Tables

Table I-1. Summary of permeant selectivities and apparent affinities (K_m values) of hENTs for various permeants..58

Table I-2. Summary of inhibitor apparent affinities (K_i values) for hENTs for various inhibitors... 58

Table I-3. Summary of permeant selectivities and apparent affinities (K_m values) of hCNTs for various permeants 59

Table II-1. Summary of collected human kidney tissues and isolated hRPTC cultures... 126

Table II-2. TaqMan^{TM} oligonucleotide primers and probes 127

Table III-1. Comparison of relative hNT mRNA transcript levels in total RNA from four different human kidney cortex tissues and monolayer cultures of HK-2 cells.. 181

Table III-2. Summary of hENT1 immunohistochemistry and hCNT3 immunofluorescence staining studies in different human kidney tissues obtained from four different individuals 181

Table III-3. Demonstration of parathyroid hormone sensitivities of adherent hRPTC monolayer cultures 182

Table III-4. Demonstration of phloridzin-sensitive, sodium-dependent uptake of methyl-α-D-glucoside into adherent hRPTC monolayer cultures 183

Table IV-1. Summary of hCNT3 protein levels, hCNT3 activities, fludarabine uptake capacities (IC_{50} values for fludarabine inhibition of [^{3}H]-uridine uptake), and fludarabine cytotoxicities (EC_{50} values for fludarabine cytotoxicities) in hRPTCs..221

Table V-1. Summary of TEER measurements and immunofluorescent staining for tight junction protein ZO-1 and cell adhesion protein E-CAD in polarized hRPTC monolayer cultures..266

Table V-2. Analysis of adenosine and 2′-deoxyadenosine metabolites after apical-to-basolateral transepithelial fluxes of 1 μM [^{3}H]-adenosine and after basolateral-to-apical transepithelial fluxes of 1μM [^{3}H]-2′-deoxyadenosine across polarized hRPTC11 monolayers after 60 min........................... 267

Table V-3. Summary of 1 μM [^{3}H]-adenosine transepithelial fluxes and uptake in polarized hRPTC monolayers...267

Table V-4. Summary of 1 μM [^{3}H]-2′-deoxyadenosine transepithelial fluxes and uptake in polarized hRPTC monolayers.. 268

Table V-5. Recovery of adenosine in basolateral compartments and 2′-deoxyadenosine in apical compartments after apical-to-basolateral transepithelial fluxes of 1 μM [^{3}H]-adenosine and after basolateral-to-apical transepithelial fluxes of 1 μM [^{3}H]-2′-deoxyadenosine cross polarized hRPTC monolayers after 60 min... 269

Table V-6. Summary of apical-to-basolateral transepithelial fluxes and apical mediated uptake of 1 μM [^{3}H]-fludarabine, -cladribine, and –clofarabine in polarized hRPTC monolayers...269

List of Figures

Figure I-1. Structures of some major purine nucleotides, nucleosides, and nucleobases........ 55

Figure I-2. Structures of some major pyrimidine nucleotides, nucleosides, and nucleobases........ 56

Figure I-3. Structure of the nephron........ 57

Figure III-1. Demonstration of hENT1, hENT2, and hCNT3, but not hCNT2, in crude membrane preparations of four different human kidney cortex tissues........ 167

Figure III-2. Specificity of monoclonal antibodies against hENT1 and hCNT3 in human kidney tissues........ 168

Figure III-3. Localization of hENT1 and hCNT3 in proximal tubules........ 169

Figure III-4. Localization of hENT1 and hCNT3 in thick ascending limb of loops of Henle........ 170

Figure III-5. Localization of hENT1 and hCNT3 in collecting duct principal cells........ 171

Figure III-6. Localization of hENT1 and hCNT3 in collecting duct intercalated cells........ 172

Figure III-7. Demonstration of hENT1 and hCNT3 in crude membrane preparations of monolayer cultures of HK-2 cells........ 173

Figure III-8. Time courses of uptake of uridine by monolayer cultures of HK-cells........ 174

Figure III-9. Demonstration of the proximal tubular brush border enzymes, acid phosphatase, γ-glutamyl transferase, and alkaline phosphatase, in fifteen different monolayer hRPTC cultures 177

Figure III-10. Time courses of uptake of α-methyl-D-glucoside by monolayer hRPTC1 cultures..178

Figure III-11. Short time courses of uptake of uridine, thymidine, and inosine by monolayer cultures of hRPTCs... 179

Figure III-12. Long time courses of uptake of uridine, thymidine, and inosine by monolayer cultures of hRPTCs... 180

Figure IV-1. Demonstration of hENT1, hENT2, hCNT1, hCNT2, and hCNT3 mRNAs in hRPTCs... 216

Figure IV-2. Demonstration of hENT1, hENT2, and hCNT3, but not hCNT2, proteins in crude membrane preparations of hRPTCs.................................217

Figure IV-3. hRPTCs exhibit hENT1-, hENT2-, and hCNT3-mediated uptake activities...218

Figure IV-4. hRPTCs have different fludarabine uptake capacities and sensitivities to fludarabine cytotoxicity...219

Figure IV-5. Correlation of hCNT3 relative mRNA levels, total protein abundance levels, cell surface protein abundance levels, hCNT3 activity levels, fludarabine uptake levels, fludarabine apparent affinities, and sensitivities to fludarabine cytoxicity in hRPTCs... 220

Figure V-1. Demonstration that cultures of hRPTC11 on transwell inserts form polarized monolayers...259

Figure V-2. Demonstration of apical-to-basolateral fluxes of adenosine and basolateral-to-apical fluxes of 2′-deoxyadenosine across polarized hRPTC11 cultures..260

Figure V-3. Sodium dependence and inhibitor sensitivities of apical-to-basolateral fluxes of adenosine and basolateral-to-apical fluxes of 2′-deoxyadenosine across polarized hRPTC11 cultures..261

Figure V-4. Sodium dependence and inhibitor sensitivities of apical and basolateral uptake of adenosine and 2′-deoxyadenosine into polarized hRPTC11 cultures...262

Figure V-5. Expression of hOAT2 mRNA and abundance of hCNT3 protein on apical cell surfaces in polarized hRPTC cultures.............................. 263

Figure V-6. Transportability of adenosine and 2′-deoxyadenosine by recombinant hCNT3 in yeast..264

Figure V-7. Demonstration of preferential apical-to-basolateral fluxes and apical mediated uptake of fludarabine, cladribine, and clofarabine across polarized hRPTC11 cultures... 265

Figure VI-1. Model of renal proximal tubule handling of nucleosides by hNTs.. 294

List of abbreviations, symbols and nomenclature

%	per cent
×	times
ε	extinction coefficient
±	plus or minus
A	alanine
A_1	adenosine receptor subtype 1
A_{2A}	adenosine receptor subtype 2A
A_{2B}	adenosine receptor subtype 2B
A_3	adenosine receptor subtype 3
A_{595}	absorbance at 595 nanometre
A_{600}	absorbance at 600 nanometre
ABC	adenosine-5′-triphosphate-binding cassette
Acyclovir	2-amino-9-((2-hydroxyethoxy)methyl)-1H-purin-6(9H)-one
ade2	phosphoribosylaminoimidazole carboxylase recessive allele
Adefovir	1-[2-(phosphonomethoxy)-ethyl]adenine
ADH	antidiuretic hormone
ADP	adenosine-5′-diphosphate
AMP	adenosine-5′-monophosphate
Apricitabine	4-amino-1-[(2*R*,4*R*)-2-(hydroxymethyl)-1,3-oxathiolan-4-yl]pyrimidin-2(1*H*)-one

AQP2	aquaporin-2
ATP	adenosine-5′-triphosphate
ATPase	adenosine-5′-triphosphatase
BamHI	restriction enzyme *BamHI*
B cell	bursa-derived lymphocyte
BCRP	breast cancer resistance protein
BglII	restriction enzyme *BglII*
c	protein concentration
^{14}C	carbon-14
°C	degrees Celsius
C1	human kidney cortex tissue 1
C2	human kidney cortex tissue 2
C3	human kidney cortex tissue 3
C4	human kidney cortex tissue 4
C11	human kidney cortex tissue 11
C12	human kidney cortex tissue 12
C13	human kidney cortex tissue 13
C14	human kidney cortex tissue 14
C15	human kidney cortex tissue 15
$CaCl_2$	calcium chloride
cAMP	cyclic adenosine-3′-5′-monophosphate
Capecitabine	N4-pentyloxycarbamyl-5′-deoxy-5-fluorocytidine
cDNA	complementary deoxyribonucleic acid

C/EBP-α	human liver-enriched transcription factor
cGMP	cyclic guanosine-3′-5′-monophosphate
Ci	Curie
Cidofovir	1-[(*S*)-3-hydroxy-2-(phosphonomethoxy)propyl]cytosine
μCi/mL	microCurie per millilitre
cit	concentrative insensitive (to inhibitor) thymidine(-selective)
Cl^-	chloride ion
Cladribine	2-chloro-2′-deoxyadenosine
Clofarabine	2-chloro-9-(2′-deoxy-2′-fluoro-β-D-arabinofuranosyl)adenine
$\Omega\cdot cm^2$	ohmm times centimeter square
cm	centimetre
cm^2	centimetre square
CMM	complete minimal medium
CMM/GLU	complete minimal medium with 2 % weight (gram) per volume (100 millilitre) glucose
CNT	concentrative nucleoside transporter
CNT1	concentrative nucleoside transporter 1
CNT2	concentrative nucleoside transporter 2
CNT3	concentrative nucleoside transporter 3
CO_2	carbon dioxide

ΔC_t	cycle threshold corrected for RNA loading
$\Delta\Delta C_t$	cycle threshold corrected for RNA loading and normalized to arbitrary reference
$\Delta C_{t,\ reference}$	cycle threshold corrected for RNA loading of arbitrary reference
C_t	cycle threshold
Cytarabine	arabinofuranosylcytosine
DAKO EnVision+	Horseradish peroxidase conjugated dextran polymer
D	aspartate
dADP	2′-deoxyadenosine-5′-diphosphate
dAMP	2′-deoxyadenosine-5′-monophosphate
DAPI	4′,6-diamidino-2-phenylindole
dATP	2′-deoxy-5′-monophosphate
de novo	(from the beginning)
Deoxyribonucleotidase I	DNAse I
2′-Deoxytubercidin	4-amino-7-(2′-deoxy-beta-D-erythro-pentofuranosyl)-pyrrolo-(2,3-d)pyrimidine
Didanosine	2′,3′-dideoxyinosine
DNA	deoxyribonucleic acid
DMEM	Dulbecco's modified Eagle's medium
E	glutamate
EC_{50}	drug concentration resulting in 50 % reduction in cell viability

E-CAD	Epithelial Cadherin
ECL	Enhanced Chemiluminescence
E. coli	*Escherichia coli*
EDTA	ehylenediaminetetraacetic acid
e.g.	*exempli gratia* (for the sake of example)
EHNA	erythro-9-(2-hydroxy-3-nonyl)adenine
ei	equilibrative insensitive (to inhibitor)
es	equilibrative sensitive (to inhibitor)
ENT	equilibrative nucleoside transporter
ENT1	equilibrative nucleoside transporter 1
ENT2	equilibrative nucleoside transporter 2
ENT3	equilibrative nucleoside transporter 3
ENT4	equilibrative nucleoside transporter 4
FAM	6-carboxy-fluorescein
FBS	fetal bovine serum
Fialuridine	1-(2′-deoxy-2′-fluoro-1-β-D-arabinofuranosyl)-5-iodouracil
Fludarabine	9-β-D-arabinosyl-2-fluoroadenine
Δfui	high affinity uridine permease gene deletion
FUI1	high affinity uridine permease dominant allele
μg	microgram
g	gram
g	relative centrifugal force

G	glycine
GAPDH	glyceraldehyde-3-phosphate dehydrogenase
Gemcitabine	2′,2′-difluoro-2′-deoxycytidine
GFP	Green Fluorescent Protein
g/L	gram per litre
μg/L	microgram per litre
μg/mL	microgram per millilitre
H	histidine
^{3}H	hydrogen-3
H^{+}	proton
HCl	hydrochloric acid
hCNT	human concentrative nucleoside transporter
hCNT1	human concentrative nucleoside transporter 1
hCNT2	human concentrative nucleoside transporter 2
hCNT3	human concentrative nucleoside transporter 3
HeLa	human cervical cancer cell line
hENT	human equilibrative nucleoside transporter
hENT1	human equilibrative nucleoside transporter 1
hENT2	human equilibrative nucleoside transporter 2
hENT3	human equilibrative nucleoside transporter 3
hENT4	human equilibrative nucleoside transporter 4
hisd2000	histidinolphosphatase recessive allele
HK-2	human kidney proximal tubule cell line

H + L	Heavy + Light Chain
HNF3-γ	human liver-enriched transcription factor HNF3-γ
HNF4-α	human liver-enriched transcription factor HNF4-α
hNT	human nucleoside transporter
H_2O	water
hOAT	human organic anion transporter
hOAT1	human organic anion transporter 1
hOAT2	human organic anion transporter 2
hOAT3	human organic anion transporter 3
hOAT4	human organic anion transporter 4
hOCT	human organic cation transporter
hOCT1	human organic cation transporter 1
hPTH	human parathyroid hormone synthetic 1-34 fragment
hr	hour
hRPTC	human renal proximal tubule cell
hRPTC1	human renal proximal tubule cell culture 1
hRPTC2	human renal proximal tubule cell culture 2
hRPTC3	human renal proximal tubule cell culture 3
hRPTC4	human renal proximal tubule cell culture 4
hRPTC5	human renal proximal tubule cell culture 5
hRPTC6	human renal proximal tubule cell culture 6
hRPTC7	human renal proximal tubule cell culture 7

hRPTC8	human renal proximal tubule cell culture 8
hRPTC9	human renal proximal tubule cell culture 9
hRPTC10	human renal proximal tubule cell culture 10
hRPTC11	human renal proximal tubule cell culture 11
hRPTC12	human renal proximal tubule cell culture 12
hRPTC13	human renal proximal tubule cell culture 13
hRPTC14	human renal proximal tubule cell culture 14
hRPTC15	human renal proximal tubule cell culture 15
HTS	High Throughput System
^{125}I	iodine-125
I	isoleucine
IC_{50}	inhibitor concentration which reduces nucleoside uptake by 50 %
i.e.	*id est* (that is)
Ig	immunoglobulin
IgG	immunoglobulin isotype G
$IgG1_{K}$	immunoglobulin isotype $G1_{K}$
IgG2b	immunoglobulin isotype G2b
IgM	immunoglobulin isotype M
IL-6	interleukin-6
IFN-γ	interferon-γ
in situ	(in the place)
K	lysine

K1	human kidney tissue 1
K2	human kidney tissue 2
K3	human kidney tissue 3
K4	human kidney tissue 4
Kbp	kilobase pairs
KCl	potassium chloride
KH_2PO_4	potassium dihydrogen phosphate
K_i	inhibitor dissociation constant
K_m	permeant concentration resulting in half of maximal uptake rate
l	path length in centimetre
L	leucine
μL	microlitre
Lamivudine	L-2′,3′-dideoxy-3′-thiacytidine
LLC-PK$_1$	porcine kidney cell line
lys2	α-aminoadipate reductase recessive allele
μm	micrometre
μM	micromolar
M	molar
MATα	mating type locus α dominant allele
mCi	milliCurie
mCNT1	mouse concentrative nucleoside transporter 1
mCNT2	mouse concentrative nucleoside transporter 2

MDCK	Madin-Darby Canine Kidney cell line
MDR1	multidrug resistance protein 1
mENT1	mouse equilibrative nucleoside transporter 1
mENT2	mouse equilibrative nucleoside transporter 2
mENT3	mouse equilibrative nucleoside transporter 3
6-Mercaptopurine	3,7-dihydropurine-6-thione
$MgCl_2$	magnesium chloride
mg/L	milligram per litre
mg/mL	milligram per millilitre
$MgSO_4$	magnesium sulfate
min	minute
mL	millilitre
mm	millimetre
mM	millimolar
mmol	millimole
MRP	multidrug resistance-associated protein
MRP4	multidrug resistance-associated protein 4
MRP5	multidrug resistance-associated protein 5
MRP8	multidrug resistance-associated protein 8
mRNA	messenger ribonucleic acid
MTS	methoxyphenyl tetrazolium inner salt
Na^+	sodium ion
NaCl	sodium chloride

$Na_2EDTA \cdot 2H_2O$	disodium ethylenediaminetetraacetic acid salt
$NaHCO_3$	sodium hydrogen carbonate
Na_2HPO_4	disodium hydrogen phosphate
NBMPR	nitrobenzylmercaptopurine ribonucleoside
ng/L	nanogram per litre
nm	nanometre
nM	nanomolar
N	asparagine
NT	nucleoside transporter
N-terminus	amino terminal
OAT	organic anion transporter
OAT1	organic anion transporter 1
OAT2	organic anion transporter 2
OAT3	organic anion transporter 3
OAT4	organic anion transporter 4
OCT	organic cation transporter
OCT1	organic cation transporter 1
OCT2	organic cation transporter 2
% of control	percent of control
p	probability of obtaining a result at least as extreme as the one that was actually observed assuming that the null hypothesis is true (*i.e.*, there is no difference between the groups)

$P_{2\gamma2}$	purine receptor subtype 2γ2
pBluescript II KS(+)	cloning vector
PBS	phosphate buffered saline
pH	measure of aqueous hydrogen ion concentration
Pentostatin	2′-deoxycoformycin
pg/L	pictogram per litre
PMAT	plasma monoamine transporter
pmol	picomole
pmol/10^6 cell	picomole per 10^6 cell
pmol/mg	picomole per milligram protein
pmol/2 min/10^6 cell	picomole per 2 minute per 10^6 cell
pmol/10 min/10^6 cell	picomole per 10 minute per 10^6 cell
pmol/mg protein/10 min	picomole per milligram protein per 10 minute
pmol/mg protein/60 min	pocomole per milligram protein per 60 minute
PNRA	proximal nephrogenic renal antigen
P	proline
pCDNA3	mammalian expression vector
pCDNA3-hCNT3	mammalian expression vector containing gene for hCNT3
PCR	polymerase chain reaction
pGFP-C1	plasmid vector containing GFP gene for C-terminal fusion protein

pGFP-C1/hCNT3	plasmid vector containing gene for GFP-hCNT3 C-terminal fusion protein
Pseudouridine	5-(β-D-ribofuranosyl)uracil
pYPGE15	bacterial shuttle vector
pYPhCNT3	bacterial shuttle vector containing gene for hCNT3
Q	glutamine
R	arginine
r^2	correlation coefficient square
% radioactivity loaded	percent of radioactivity loaded
rCNT1	rat equilibrative nucleoside transporter 1
rCNT2	rat equilibrative nucleoside transporter 2
% reduction of control values	percent reduction of control
rENT1	rat equilibrative nucleoside transporter 1
rENT2	rat equilibrative nucleoside transporter 2
rENT4	rat equilibrative nucleoside transporter 4
R_f	retention factor
RIPA	radioimmunoprecipitation assay
RNA	ribonucleic acid
RPM	revolutions per minute
RT-PCR	reverse-transcription polymerase chain reaction
S	serine
S. cerevisiae	*Saccharomyces cerevisiae*
SDS	sodium dodecyl sulphate

Sec	second
SLC	Solute Carrier
SLC22A	Solute Carrier 22A
SLC28	Solute Carrier 28
SLC29	Solute Carrier 29
Sp1	human transcription factor Sp1
Stavudine	2′,3′-didehydro-3′-deoxythymidine
T	threonine
T cell	thymus lymphocyte
TEER	transepithelial electrical resistance
Tenofovir	1-[(*R*)-2-(phosphonomethoxy)propyl]adenine
TET	tetrochloro-6-carboxy-fluorescein
TGF-β1	tumor growth factor--β1
THP	Tamm-Horsfall protein
TNF-α	tumor necrosis factor-α
trp1	phosphoribosylanthranilate isomerase recessive allele
TRP1	phosphoribosylanthranilate isomerase dominant allele
Troxacitabine	L-1,3-dioxolane-cytidine
TTP	thymidine-5′-triphosphate
U/L	units per litre
ura3-52	orotidine-5′-phosphate decarboxylase mutant allele

UV	ultraviolet
V-ATPase	vacuolar type H^+-adenosine-5′-triphosphatase B1/2
V	valine
V_{max}	maximal uptake rate
v/v	volume (millilitre) per volume (millilitre)
v/v/v/v	volume (millilitre) pre volume (millilitre) per volume (millilitre) per volume (millilitre)
w/v	weight (gram) per volume (100 millilitre)
XhoI	restriction enzyme *XhoI*
Zalcitabine	2′,3′-dideoxycytidine
Zidovudine	3′-azido-2′,3′-dideoxythymidine
ZO1	Zonula Occludens 1

Chapter I

I. Introduction[1]

---

[1] An earlier version of this chapter has been published as a primary authored mini-review paper [Elwi AN, Damaraju VL, Baldwin SA, Young JD, Sawyer MB, Cass CE. Renal nucleoside transporters: physiological and clinical implications. Biochem Cell Biol. 2006; 84: 844-858]; contribution of Elwi AN was 90 %.

I.1 Review of human nucleoside and nucleobase transport biology[2]

Nucleosides and nucleobases are metabolites and precursors of nucleotides, which are vital to nucleic acid synthesis. As central metabolites in nucleic acid synthesis, various nucleoside and nucleobase analogs have been developed for use as drugs in a wide variety of treatments for cancer and viral infections [1]. Physiological nucleosides, such as adenosine play a myriad of roles in the regulation of multiple physiological processes, including cardiovascular and renal function, neurotransmission, and in their associated pathophysiologies [2]. Since physiological nucleosides and nucleoside drugs are relatively hydrophilic molecules, their cellular uptake and release is largely dependent on the activity of integral membrane transport proteins. The most prominent families involved in nucleoside transport are the Solute Carrier (SLC) 29 and SLC28 families of nucleoside transporters (NTs), whose members are known, respectively, as the equilibrative and concentrative NTs (ENTs: ENT1, ENT2, ENT3, ENT4; and CNTs: CNT1, CNT2, CNT3) [3,4]. Other transporter families, some members of which are involved in nucleoside transport, are the SLC22A family of organic cation and anion transporters (OCTs: OCT1; OATs: OAT1, OAT2, OAT3, OAT4) [5,6], and the adenosine triphosphate (ATP)-binding cassette (ABC) family of ATP-dependent efflux transporters including multidrug resistance protein (MDR1) [7], breast cancer resistance protein (BCRP) [8], and multidrug resistance-associated proteins (MRPs: MRP4, MRP5, MRP8) [9].

---

[2] Although much less is known about nucleobase transport in mammalian cells, because nucleobases are part of the same metabolic pathways as nucleosides, renal nucleobase transport ultimately affects the bioavailabilities of not just nucleobases but nucleosides as well. Therefore, it is included here with appropriate refrences when there is knowledge of nucleobase transport.

Nucleobase transport has been observed in several mammalian cellular systems. Proteins with nucleobase-transport activity identified thus far include ENT2 [10,11], ENT4[3] [12], OAT2[4] [13], OAT3[4] [14], MDR1 [15], MRP4, MRP5 [16], and MRP8 [17]. Sodium-independent and -dependent nucleobase transport processes mediated by, as yet, unidentified proteins have also been described [18-21]. Two novel mammalian genes with homologies to bacterial and fungal nucleobase transporters have been identified but they have not yet been functionally characterized [22].

NTs are essential for biosynthesis of nucleic acids by nucleoside salvage pathways [3,4] in cells that lack *de novo* nucleotide synthesis pathways (e.g., erythrocytes, B cell lymphocytes, bone marrow cells, and some brain cells) [23], in cells of tissues with high metabolic demands (e.g., muscle cells, activated B cell, and T cell lymphocytes) [24], and in cells undergoing periods of metabolic stress, limited food supply, and rapid embryonic growth [25]. For instance, human erythrocytes possess human ENT1 (hENT1) [26,27], porcine erythrocytes possess porcine ENT1[5] [28], and embryonic chicken erythrocytes possess chicken ENT1 [29], necessary for ATP production through guanosine and inosine salvage. For purine and pyrimidine nucleoside salvage, human B cell lymphocytes possess hENT1 and hCNT2 [30], rat T cell lymphocytes possess rat ENT1 (rENT1), rENT2, and rCNT2 [31], and murine bone marrow macrophages possess mouse

---

[3] Mouse equilibrative nucleoside transporter 4 (mENT4), but not human ENT4 (hENT4), transports adenine [12].

[4] While mouse organic anion transporter 2 and 3 (mOAT2, mOAT3) transport 5-fluorouracil, it is not known whether the same is true for hOAT2 and hOAT3 [13,14].

[5] Although, the primary focus of this work is human transporter proteins involved in nucleoside or nucleobase transport, when data is not available for the human proteins, data from various other animal sources is presented.

ENT1 (mENT1), mENT2, mCNT1, and mCNT2 [32]. Murine astrocytes possess mENT1, mENT2, and mCNT2 [33] for purine nucleotide salvage through adenosine and guanosine. Human skeletal muscle tissue possess hENT2 [34] and rat ventricular cardiomyocytes possess rENT4 [12], possibly for purine nucleotide salvage through hypoxanthine and adenosine [25], respectively. In addition, NTs are involved in regulation of extracellular pools of adenosine, a signalling molecule that modulates cellular function through specific interactions in various organ systems with cell surface receptors called adenosine receptors (A_1, A_{2A}, A_{2B}, and A_3) [2]. For instance, mice that lack the gene that encodes mENT1 have increased preferences for ethanol in drinking water but reduced responses to ethanol intoxication [35] and reduced anxiety-like behaviours [36]; presumably a result of altered extracellular levels of adenosine available for purinergic receptor signalling in specific brain regions. NTs are also involved in cellular uptake of nucleoside analog drugs, a requisite step for cytotoxic actions of most of these drugs. For instance, the abundance of hENT1 in pancreatic cancer tissues influences the therapeutic effectiveness of 2′,2′-difluoro-2′-deoxycytidine (gemcitabine) chemotherapy [37].

Clearly, NTs have well identified roles in nucleoside salvage, homeostasis, and drug efficacies and toxicities. Much remains to be learned about the organ-specific functions of NTs. For example, NTs in the kidney may influence the pharmacokinetics and normal tissue toxicities of nucleoside drugs. Systemic plasma and tissue levels of physiological nucleosides and their structurally related drugs, or their metabolites, may be determined by transport and metabolism in tissues, including, in large part, the kidney [38]. A better understanding of renal handling of nucleoside drugs will lead to strategies aimed at individualizing drug dosing to maximize therapeutic effects and minimize normal tissue toxicities. Therefore, it is of great interest to understand how NTs in the kidney influence renal handling, and hence the pharmacokinetics and normal tissue toxicities, of nucleoside drugs. The studies described in this thesis are aimed at providing further insights into the roles of hENTs and hCNTs in renal handling of physiological nucleosides and nucleoside analogs in humans. This chapter reviews renal human nucleoside and nucleobase transport biology beginning with overviews of the importance of physiological nucleosides, of the pharmacology of nucleoside analogs, and of hENT and hCNT protein families. A review of the current knowledge with respect to renal handling of physiological and pharmacological nucleosides, distribution and functions of renal hENTs and hCNTs, and nephrotoxicities of nucleoside analogs is followed by a proposal of a model of renal proximal tubular handling by hNTs. The hypothesis, objectives, and rationale of the experimental design of these studies are then presented.

I.1.1 Importance of physiological nucleosides and nucleobases

Physiological nucleosides, nucleobases, and their metabolic products have diverse and crucial roles in various biological processes including cellular division, metabolism, function, and structure. Nucleotides, which are essential for deoxyribonucleic acid (DNA) and ribonucleic acid (RNA) synthesis, can be obtained by *de novo* nucleotide synthetic pathways or by salvage of exogenous nucleosides and nucleobases. Cell types that are deficient in *de novo* nucleotide synthesis pathways rely on nucleoside and nucleobase salvage pathways to maintain intracellular nucleotide pools [23]. Even in some cell types, such as T lymphocytes, with intact *de novo* nucleotide synthesis pathways, salvage pathways have been shown to be more quantitatively relevant in maintaining intracellular nucleotide pools [39]. In addition, because *de novo* nucleotide synthesis pathways require relatively high levels of metabolic energy, the salvage pathways are often required to meet physiological needs during periods of metabolic stress, limited food supply, and rapid embryonic growth even in cells with *de novo* nucleotide synthesis capabilities [23-25].

In addition to their roles in metabolism, some nucleosides play major roles in cellular regulation as signalling molecules. Adenosine, through interactions with adenosine receptors, can induce cardiovascular vasodilation and reduce heart rate, modulate synaptic transmission, and act as both a cardioprotector and neuroprotector [2]. In the kidney, adenosine signalling through adenosine receptors, can lower renal glomerular filtration rate, stimulate sodium reabsorption in nephron proximal segments, inhibit sodium reabsorption in nephron medullary segments, and stimulate renin release inducing vasodilation [40]. Adenosine and guanosine are precursors, respectively, of 3′-5′-cyclic adenosine and guanosine monophosphate (cAMP and cGMP, respectively), second messengers in a variety of cell signalling processes [41,42]. Uridine, through interactions with pyrimidinoreceptors, can modulate synaptic transmission and hormone release [2]. As well, uridine and cytidine are vital to phospholipid synthesis through the formation of pyrimidine nucleotide-lipid conjugates [43]. Many nucleotides serve as allosteric regulators and coenzymes for various enzymatic reactions [43]. The less common modified nucleosides, such as 5-(β-D-ribofuranosyl)uracil (pseudouridine), are present in transfer RNA, ribosomal RNA, small nuclear RNA, and small nucleolar RNA molecules [44]. Some of the major physiological purine and pyrimidine nucleosides, nucleobases, and nucleotides are depicted in Figure I-1 and Figure I-2, respectively.

Cellular permeation of physiological nucleosides across plasma membranes is typically followed by phosphorylation to nucleotides by nucleoside kinases (e.g., 2′-deoxycytidine kinase, thymidine kinase, and adenosine kinase) while nucleobases are converted to nucleotides by phosphoribosyl transferases (e.g., hypoxanthine-guanine and adenine phosphoribosyl transferases) [43]. Nucleotides do not readily diffuse through plasma membranes because of the presence of negatively charged phosphate groups. As a result, phosphorylation and phosphoribosylation can serve, respectively, to trap nucleosides and nucleobases intracellularly [3,4] although some nucleotides are permeants of select members of the SLC22A and ABC transporter families [5-9]. Nucleosides and nucleobases derived from tissue turnover or excess dietary intake that are not salvaged are catabolised and excreted. Purine and pyrimidine, respectively, nucleosides and nucleobases are catabolised to uric acid and β-amino acids for excretion [43].

Circulating nucleosides come from several sources. The liver, which has a high capacity for *de novo* nucleotide synthesis, produces nucleosides that are released into the blood through NTs and can be subsequently salvaged by tissues with low or absent *de novo* nucleotide synthesis [3,4,23]. Turnover of blood cells is also a major source of circulating nucleosides as nucleic acids released into the blood are rapidly degraded into plasma nucleosides [23]. Circulating physiological nucleosides are also obtained by digestion of nucleic acids and nucleotides to nucleosides in the alimentary tract and their subsequent absorption in the small intestine [23]. Ecto-5′-nucleotidases on cell surfaces can also produce extracellular physiological nucleosides from their corresponding nucleotides [43].

With such diverse roles in biological processes, some nucleosides are valuable molecules while others are potentially toxic. Adenosine and 2′-deoxyadenosine are precursors to ATP and 2′-deoxyadenosine-5′-triphosphate (dATP), respectively, which play central roles in controlling intracellular nucleotide pools [45]. Ribonucleotide reductase is an intracellular enzyme that catalyzes formation of deoxyribonucleotides from corresponding ribonucleotides (the rate-limiting step in production of precursors for DNA synthesis) [45]. Ribonucleotide reductase is stimulated by ATP and inhibited by dATP in a tightly controlled manner [45]. High systemic concentrations of 2′-deoxyadenosine, can lead to cytotoxicity due to inhibition of ribonucleotide reductase and the resulting perturbation of intracellular nucleotide pools [46,47]. High systemic concentrations of 2′-deoxyadenosine can result from a genetic deficiency of adenosine deaminase, which catalyzes deamination of 2′-deoxyadenosine to 2′-deoxyinosine along its degradation pathway to uric acid, which is excreted as nitrogenous waste [48].

Like nucleosides, some nucleobases are valuable metabolites while others are potentially toxic. For instance, hypoxanthine is an important salvage source for purine nucleotides, particularly in bone marrow [49]. On the other hand, 2,8-dihydroxyadenine, formed intracellularly from adenine by xanthine oxidase, is insoluble at urine pH (pH 5-7) [50]. Adenine is normally returned to adenosine-5′-monophosphate pools by the salvage enzyme adenine phosphoribosyl transferase [43]. A rare genetic deficiency of adenine phosphoribosyl transferase results in high systemic concentrations of adenine and 2,8-dihydroxyadenine, which can lead to formation of kidney stones [50]. Given the high levels of energy expenditure for *de novo* nucleotide synthesis and the central importance of some nucleosides and nucleobases in homeostasis [23], it is not surprising that the kidney efficiently reabsorbs some physiological nucleosides and nucleobases (e.g., adenosine, hypoxanthine) and secretes others that can be potentially toxic at high concentrations (e.g., 2′-deoxyadenosine, adenine) [48,51,52].

I.1.2 Pharmacology of synthetic nucleoside and nucleobase analog drugs

Because physiological nucleosides have key roles as precursors to nucleotides, which are necessary for nucleic acid synthesis, many nucleoside and nucleobase analogs have been synthesized as potential therapeutics for treatment of cancer and viral diseases [1]. While most synthetic nucleoside analog drugs with intracellular modes of action to effect cytotoxicity gain entry to cells primarily through transporter proteins, a few, like L-1,3-dioxolane-cytidine (troxacitabine) and 2′,3′-didehydro-3′-deoxythymidine (stavudine), can permeate into cells via passive diffusion across lipid bilayers in sufficient quantities to effect cytotoxicity [53,54]. Nucleobase drugs also have intracellular modes of action to effect toxicity [1]. While nucleobases are less hydrophilic than their nucleoside counterparts, their cellular uptake through transporter proteins at physiological concentrations may be significant [3,10-21].

Despite the growing body of *in vitro* evidence for the importance of NTs in cytotoxic actions of synthetic nucleoside or nucleobase analog drugs, clinical evidence is only just becoming available [55]. Low levels of hENT1 immunohistochemical staining in pancreatic cancer tissues have recently been shown to predict poor outcome in patients undergoing gemcitabine treatment for pancreatic cancer, presumably a result of decreased cellular uptake of gemcitabine through hENT1 into cancer cells [37]. Although the abundance of proteins involved in nucleoside or nucleobase transport in the kidney may significantly influence pharmacokinetics and normal tissue toxicities of nucleoside or nucleobase drugs, no clinical evidence has yet been presented.

Among the more widely used anti-cancer nucleoside and nucleobase analogs are 6-thioguanine, 3,7-dihydropurine-6-thione (6-mercaptopurine), 1-β-D-arabinofuranosylcytosine (cytarabine), 9-β-D-arabinosyl-2-fluoroadenine (fludarabine), 2-chloro-2′-deoxyadenosine (cladribine), 2-chloro-9-(2′-deoxy-2′-fluoro-β-D-arabinofuranosyl)adenine (clofarabine) for treatment of haematological malignancies and 5-fluorouracil, gemcitabine, and N4-pentyloxycarbamyl-5′-deoxy-5-fluorocytidine (capecitabine) for treatment of solid tumors [55]. 6-Thioguanine, 6-mercaptopurine, cytarabine, fludarabine, cladribine, and clofarabine exhibit clinical activities against haematological malignancies, including acute lymphoblastic leukemias for 6-thioguanine and 6-mercaptopurine [56], acute myeloid leukemias for cytarabine [57], chronic lymphocytic leukemias for fludarabine [58], indolent lymphoid malignancies for cladribine [59], and acute lymphocytic leukemias for clofarabine [60]. Gemcitabine and capecitabine have a broad range of clinical activities against breast, ovarian, bladder, head and neck, and pancreatic cancers, while 5-fluorouracil (which, like capecitabine, is a prodrug of 5-fluoro-2′-deoxyuridine-5′-monophosphate) and its nucleoside derivatives 5-fluorouridine, 5-fluoro-2′-deoxyuridine, 5-fluoro-5′-deoxyuridine comprise an important class of anticancer drugs utilized in the treatment of disseminated cancers of the gastrointestinal tract, breast, and ovary [61-66]. Structures of some of the major anti-cancer purine and pyrimidine nucleoside and nucleobase drugs are depicted in Figure I-1 and Figure I-2, respectively.

Some of the more widely used anti-viral nucleoside analogs include 3′-azido-2′,3′-dideoxythymidine (zidovudine), 2′,3′-dideoxyinosine (didanosine), 2′,3′-dideoxycytidine (zalcitabine), L-2′,3′-dideoxy-3′-thiacytidine (lamivudine), and stavudine for treatment of human immunodeficiency viral infections [67], 9-β-D-arabinofuranosyladenine (vidarabine) and 9-(2-hydroxyethoxymethyl)guanine (acyclovir) for treatment of herpes simplex virus infections [68], 9-(1,3-dihydroxy-2-propoxymethyl)guanine (ganciclovir) for treatment of cytomegalovirus infections [69], and 1-(β-D-ribofuranosyl)-1*H*-1,2,4-triazole-3-carboxamide (ribavirin) for treatment of hepatitis C [70]. Structures of some of the major anti-viral purine and pyrimidine nucleoside analog drugs are depicted in Figure I-1 and Figure I-2, respectively.

As structural analogs of physiological nucleosides, nucleoside analog drugs are also moved into and out of cells by specialized transporter proteins [38,55]. Although, knowledge of nucleobase analog drug transport is limited, it appears to involve the same transporter proteins as physiological nucleobases [10-21]. Following cellular permeation, nucleoside and nucleobase analog drugs are converted to their mono-, di-, and tri-phosphorylated forms intracellularly, which exert their therapeutic actions through a variety of mechanisms to inhibit cancer cell proliferation or viral replication [38,55]. The nucleotide forms of 5-fluorouracil, which are also metabolites of capecitabine [71], are incorporated into RNA, resulting in inhibition of RNA processing [72], and into DNA, resulting in DNA strand breaks and inhibition of DNA synthesis [73]. Also, the metabolite of 5-fluorouracil and capecitabine, 5-fluoro-2′-deoxyuridine monophosphate, inhibits thymidylate synthase, and hence formation of thymidine-5′-triphosphate (TTP) necessary for DNA synthesis [74]. The incorporation of nucleotide triphosphate forms of cytarabine, gemcitabine, and fludarabine into DNA results in DNA chain termination and inhibition of DNA synthesis [75-80]. Similarly, the triphosphate nucleotide forms of cladribine and clofarabine are incorporated into DNA and result in DNA strand breaks and subsequent inhibition of DNA synthesis [81,82]. On the other hand, the incorporation of nucleotide triphosphate forms of 6-mercaptopurine and 6-thioguanine into DNA triggers apoptosis through the mismatch repair pathway [83,84]. The diphosphate nucleotide form of gemcitabine and the triphosphate nucleotide forms of fludarabine, cladribine, and clofarabine inhibit ribonucleotide reductase and perturb intracellular nucleotide pools in cancer cells, resulting in inhibition of DNA synthesis and hence cancer cell proliferation [77-80,85,86]. Additionally, some anti-cancer nucleoside analogs (*e.g.*, fludarabine) have RNA directed effects [87,88]. Anti-viral nucleoside analog drugs mediate their therapeutic actions primarily through incorporation of their nucleotide forms into viral DNA, resulting in DNA chain termination and inhibition of viral DNA synthesis, thus inhibiting viral replication [89].

While the pharmacokinetics of anti-cancer and -viral nucleoside and nucleobase analogs is typically well defined before widespread clinical usage [90], little is known about renal handling of these important drugs by kidney transporter proteins. Chemotherapy drug dosing and scheduling is typically based on empirical determinations in phase I trials, with stepwise escalation of doses to determine toxicities (termed *modified Fibonacci escalation*) [91]. Drug doses and schedules are established for the "average" patient based on pharmacokinetic observations from empiric phase I trials in groups of patients with shared characterisitics (e.g., age, sex, body surface area) [92,93], and occasionally takes into account whole organ functions (e.g., creatinine clearance for renal function, liver enzymes for hepatic function) [94-96]. For many nucleobase and nucleoside analogs, the kidney is the main route of elimination as these drugs undergo little if any oxidative metabolism in the liver [92,93]. Renal clearance of creatinine, which provides an estimate of glomerular filtration rates, provides no information about renal reabsorption or secretion of these important classes of antimetabolites that are not just passively filtered in the kidney [97]. Empirical dosing methodologies do not account for delayed elimination and unexpected toxicities [96]. Therefore, clinicians are unable to administer nucleoside or nucleobase analog drug doses with specific plasma concentration-time parameters that separate therapeutic effects from normal tissue toxicities in individual patients. If more was known about drug pharmacodynamics [96], clinical monitoring with dosage adjustments, based on target drug plasma concentrations, could overcome this barrier to tailored drug delivery [98]. A better understanding of the mechanisms behind renal handling of these antimetabolites would be expected to lead to strategies aimed at individualized chemotherapy [99-101].

I.1.3 Human nucleoside transporter (hNT) protein family

Early studies that were aimed at characterizing nucleoside transport processes used cultured cell lines, isolated cells or membrane preparations from tissues. With some exceptions (i.e., studies involving cells with a single transporter type such as human erythrocytes), the multiplicity of distinct functional transporter processes with overlapping, but distinct, permeant specificities and inhibitor sensitivities, confounded interpretation of many studies and made analyses of nucleoside influxes and effluxes complex. The cloning of NT complementary DNAs (cDNAs) and characterization of their encoded transporter proteins has clarified these multiple nucleoside transport processes. It is now well established that the majority of nucleoside transport is mediated by multiple transporters that fall into two families, the ENT or CNT families [3,4].

I.1.3.1 Human equilibrative nucleoside transporters (hENTs)

In the hENT family, four protein isoforms (hENT1/2/3/4) have been identified and characterized [3,10-12,27,34,102-111]. The properties of hENT1/2, which are plasma-membrane transporters, are well established. They translocate nucleosides bidirectionally down their concentration gradients, have broad permeant selectivities, and are widely distributed among tissues. They are functionally subdivided into two types based on their sensitivities to nitrobenzylmercaptopurine ribonucleoside (NBMPR) as equilibrative sensitive (*es*, hENT1) and equilibrative insensitive (*ei*, hENT2) [27,34,102]. hENT3 and hENT4 have only recently been characterized: hENT3 appears to be an intracellular pH-dependent NT with broad permeant selectivity [111], whereas hENT4 appears to be a cell surface pH-dependent adenosine transporter [12] originally identified and characterized as a brain serotonin transporter called plasma monoamine transporter (PMAT) [112,113].

I.1.3.1.1 Characterization of hENTs

The best understood members of the hENT family are hENT1/2, which are integral membrane proteins with 11 transmembrane helices [3,27,34,97]. Both hENT1/2 appear to be ubiquitously present in human tissues, including the kidney [27,34,97]. Both transport a wide range of purine and pyrimidine nucleosides, although hENT1 has higher apparent affinities (K_m) than hENT2, with the exception of inosine (Table I-1) [27,34,102,104]. Also, cytidine appears to be a poor permeant of hENT2 [108]. While hENT1 is potently inhibited by NBMPR, which has a K_i value of 5 nM [27], and by the coronary vasodilators dipyridamole and dilazep, which have K_i values of 20 nM and 50 nM, respectively [27,109], hENT2 is much less sensitive to these "classical" nucleoside transport inhibitors (Table I-2) [34,102,109]. While hENT2 can transport a broad range of purine and pyrimidine nucleobases (with the exception of cytosine), nucleobases are not permeants of hENT1 (Table I-I) [10,11,27,34,102,108]. The efficiencies of transport of nucleobases and nucleosides by hENT2 are expected to be similar despite its lower apparent affinities for nucleobases because its turnover numbers for nucleobase transport are higher than those for nucleoside transport [10].

With some exceptions, nucleoside analog drugs tend to be poorer permeants for hENT1 and hENT2 than their physiological counterparts [3]. Most purine and pyrimidine anti-cancer nucleoside drugs are permeants of hENT1 and hENT2 (Table I-1) [55]. Fludarabine, cladribine, and clofarabine are all permeants of hENT1 and hENT2 [110]. Just as cytosine and cytidine are poor permeants of hENT2 [10,104,108], gemcitabine is also a poor permeant of hENT2 compared to hENT1 [103]. Although it has long been assumed that hNTs in tumors are important for response to nucleoside drugs, clinical evidence has only recently become available [37]. It was found in pancreatic cancer patients who had received single-agent chemotherapy with gemcitabine that immunohistochemical deficiencies of hENT1 in tumor sections correlated with shorter overall survival times [37]. Some anticancer nucleobase analogs (e.g., 6-mercaptopurine, 6-thioguanine) are also permeants of hENT2 (Table I-1) whereas 5-fluorouracil appears to be transported by a different equilibrative transport process by, as yet, unidentified proteins [10,11,18,34,102]. As for anti-viral nucleoside analog drugs, hENT2 appears to be more important than hENT1 in their cellular transport [3].

For example, zidovudine is not a permeant of hENT1 but is a poor permeant of hENT2 (Table I-1) [106]. As well, zalcitabine and didanosine are better permeants of hENT2 than of hENT1 (Table I-1) [106].

The most recently characterized members of the hENT family are hENT3 and hENT4, which are both pH-dependent nucleoside transporters with predicted 11-transmembrane helix topologies [3,12,111]. The optimal pH for nucleoside transport is 5.5 for hENT3 and 6.5 for hENT4 [12,111]. Whether or not hENT3 and hENT4 are H^+/nucleoside co-transporters remains to be demonstrated experimentally.

hENT3 appears to be a pH-dependent NT with broad permeant selectivity for nucleosides and nucleobases, with the exception of hypoxanthine, and relative insensitivity to NBMPR, dilazep, and dipyridamole, much like hENT2 (Tables I-1, I-2) [111]. An endosomal/lysosomal targeting sequence with a dileucine motif is present in the N-terminus of hENT3 and is required for intracellular localization of hENT3 in HeLa cells [111]. hENT3 messenger RNA (mRNA) expression has been observed in multiple human tissues, including placenta, uterus, ovary, spleen, lymph node, and bone marrow with lower levels observed in brain and heart [111]. mENT3 mRNA and protein are present in crude membrane preprations of lung, liver, heart and, to a lesser extent, kidney [106]. Recently, the presence of hENT3 in lysosomes, mitochondria, and/or cell surface has been reported in human hepatocytes, placental tissues, and various cell lines [114]. The evidence that several mutations of the gene that encodes hENT3 cause the autosomal-recessive disorder H-syndrome, which is characterized by systemic and cutaneous pathologies, supports, in part, the potential role of hENT3 in mitochondria [115]. It has been suggested that the function of hENT3 may be to export nucleosides and nucleobases after nucleic acid degradation from lysosomes and import nucleosides and nucleobases into mitochondria for salvage [111].

hENT4 is a pH-dependent adenosine transporter, originally described as PMAT, a serotonin and 1-methyl-4-phenylpuridinium transporter in the brain [12,112,113]. hENT4 localizes to plasma membranes in transfected cells, accepts adenosine as the only known nucleoside permeant, and is slightly sensitive to NBMPR, dilazep, and dipyridamole (Tables I-1, I-2) [12]. Although mENT4 also transports adenine with low affinity, adenine is not a permeant of hENT4 [12]. hENT4 appears to be ubiquitous since its mRNA is found in most adult tissues, including the kidney [12,116]. In rat, rENT4 protein abundance is particularly high in the adult heart and brain and the protein has been found in plasma membranes of ventricular myocytes [12]. Physiological roles for hENT4/PMAT have been proposed in brain serotonin transport for neurotransmission modulation [112,113,117], in cardiac serotonin transport for regulation of cardiac development and function [12], and in cardiac adenosine transport for regulation of adenosine signaling during ischemic conditions [12]. Recently, uptake of the organic cation 1-methyl-4-phenylpuridinium in hENT4/PMAT-transfected cells was found to be reduced in the presence of a proton ionophore, suggesting that transport by hENT4/PMAT is coupled to inwardly directed proton gradients [116]. Furthermore, 1-methyl-4-phenylpuridinium uptake by hENT4/PMAT was inhibited by adenosine, cladribine, and 7-deaza-2′-deoxyadenosine (2′-

deoxytubercidin) [116]. It remains to be determined whether these nucleoside analogs are permeants of hENT4/PMAT.

I.1.3.1.2 Regulation of hENTs

Studies on regulation of the hENTs have focused largely on hENT1, which is present in the majority of human cells. The apparently ubiquitous presence of hENT1 in tissues and cells and the protein's broad permeant tolerance seem to categorize it as having a housekeeping function. Nevertheless, several studies have shown that expression of hENT1 mRNA, hENT1 protein abundance and hENT1 activity are under temporal regulation in a cell-specific manner [3]. In human cancer cell lines, abundance of transporter protein (as measured by quantification of NBMPR binding sites and only later identified as hENT1) is coordinated with the cell cycle with higher levels during G_2 [118,119]. Furthermore, this cell cycle dependent regulation of hENT1 abundance is dependent on intracellular deoxynucleotide pools with depletion of TTP levels resulting in upregulation of hENT1 abundance, consistent with a role in nucleoside salvage during periods of stress [118,119]. In contrast, expression of hENT1 mRNA is decreased during hypoxic conditions in cardiomyocytes, which is dependent on hypoxia inducible factor I (HIF-1) [120]. Analysis of the hENT1 promoter has revealed putative consensus sites for HIF-1, as well as for other transcription factors, including estrogen response element protein, myc-associated zinc finger protein, Sp1, AP-2, myogenin, interferon regulatory factor 2, cAMP response element binding protein, and proximal sequence element-binding transcription factor β sites [121]. Additionally, hENT1 activity is regulated by protein kinase C, purinoreceptor, and adenosine receptor activities in different cell culture systems [122-124]. hENT1 transport activity is up-regulated directly by protein kinase C δ/ε stimulation in human cancer cell lines by a mechanism that may involve post-translational modification at plasma membranes [122]. Alternatively, hENT1 activity is down-regulated by $P_{2\gamma 2}$ purinoceptor stimulation by ATP in cultured human umbilical vein endothelial cells by a mechanism that may involve reduction in hENT1 mRNA and protein levels [123]. mENT1 transport activity is acutely up-regulated in hypoxia challenged mouse cardiomyocytes through A_1 and A_3 adenosine receptors and protein kinase ε activation by a mechanism that may involve post-translational modification [124]. The protein kinase C and purinoceptor signaling pathways are present in renal epithelia and are known to regulate a variety of transporter processes in renal proximal tubules [125]; however, it is not known if and how hENT1 expression and activity are regulated in renal tubular cells.

I.1.3.2 Human concentrative nucleoside transporters (hCNTs)

hCNTs are integral membrane proteins that couple inwardly directed sodium gradients, and for hCNT3 also proton gradients, to uphill nucleoside translocation into cells. This is achieved by Na^+/nucleoside co-transport for hCNT1/2/3 and H^+/nucleoside co-transport for hCNT3. The hCNTs differ from hENTs in their permeant selectivities, apparent affinities, inhibitor sensitivities, and tissue distributions. In the CNT family, three human protein isoforms hCNT1/2/3 have been identified and characterized [4,103,110,126-136]. hCNT1/2/3 are uniformly insensitive to inhibition by NBMPR and exhibit different permeant selectivities

[126-129]. hCNT1 accepts pyrimidine nucleosides (concentrative insensitive thymidine selectivity, *cit*) [126]; hCNT2 accepts purine nucleosides (concentrative insensitive formycin B selectivity, *cif*) [127,128], and hCNT3 accepts both pyrimidine and purine nucleosides (concentrative insensitive broad selectivity, *cib*) [129]. All three transporters accept adenosine, 2′-deoxyadenosine, and uridine as permeants [126-129]. Three other concentrative nucleoside transport processes (concentrative sensitive, *cs*; concentrative sensitive guanosine selective, *csg*; *cit*-like system) have been functionally identified in freshly isolated leukemia cells [137], promyelocytic leukemia NB4 cells [138], and human kidney brush border membrane vesicles [139,140], respectively, although their molecular identities are, thus far, unknown. Of these, only the *cit*-like system, which also accepts the purine nucleoside guanosine as a permeant, has been observed in the kidney [139,140]. It has been suggested that the previously reported *cit*-like system, which also accepts guanosine as a permeant, is the result of natural occurring mutation in gene encoding hCNT1 that increases sensitivity of hCNT1-mediated nucleoside uptake to guanosine inhibition [141].

I.1.3.2.1 Characterization of hCNTs

mRNAs for all three hCNTs are expressed in various differentiated tissues including epithelial cells of the kidney [126-129]. hCNTs have higher apparent affinities for nucleosides than the hENTs (Table I-1) [103,110,126-129]. In contrast to hENTs, hCNTs are insensitive to the classical ENT inhibitors (Table I-2) [126-129]. While hCNT1/2 have Na^+-to-nucleoside coupling ratios of 1:1, hCNT3 has a Na^+-to-nucleoside coupling ratio of 2:1 [126-130]. The thermodynamic energy cost of transport by Na^+/permeant co-transporters is determined by the Na^+-to-permeant coupling ratio and limits the transmembrane permeant gradients that can be achieved [142]. Because the extracellular sodium concentration (~145 mM) is approximately 10-fold greater than the basal intracellular sodium concentration (~15 mM) in mammalian cells, a transporter with a 2:1 Na^+-to-nucleoside coupling ratio can achieve a transmembrane nucleoside concentration gradient approximately 10-fold greater than a transporter with a 1:1 Na^+-to nucleoside coupling ratio [142]. Physiologically, this means that hCNT3 can concentrate nucleosides significantly more than either hCNT1 or hCNT2 [4]. While hCNT1/2 are strictly Na^+/nucleoside co-transporters, hCNT3 exhibits pH-dependent nucleoside transport and is a H^+/nucleoside co-transporter [132,134-136]. hCNT3 can co-translocate nucleosides with sodium in a 2:1 Na^+-to-nucleoside coupling ratio, can co-translocate nucleosides with sodium and protons in a 2:1 Na^+,H^+-to-nucleoside coupling ratio, and can co-translocate nucleosides with protons in a 1:1 H^+-to-nucleoside coupling ratio [132,134-136]. As well, the permeant specificities appear to be different as H^+-coupled hCNT3 does not transport guanosine [132].

The permeant selectivities of hCNTs have been determined in recombinant expression systems. hCNT1 is pyrimidine nucleoside-selective but also transports the purine nucleoside adenosine and 2′-deoxyadenosine with high affinities but low capacities (Table I-1) [126,130]. hCNT2 is purine nucleoside-selective but also transports the pyrmidine nucleoside uridine (Table I-1) [127,128]. hCNT3 has broader selectivities and transports many purine and pyrmidine nucleosides (Table I-1) [129]. Permeant selectivities of hCNTs for anticancer and antiviral nucleoside drugs are similar to those of hCNTs for physiological nucleosides – i.e., hCNT1 transports pyrimidine nucleoside analogs, hCNT2 transports purine nucleoside analogs, and hCNT3 transports both pyrimidine and purine nucleoside analogs (Table I-1) [103,110,126-131,133]. Similar to hENTs, some nucleoside analogs are not transported as efficiently by hCNTs as their most structurally similar physiological nucleosides (Table I-1) [103,110,126-131,133]. While the therapeutic nucleoside analogs gemcitabine, 2′-deoxy-5-fluorouridine, and 5-fluorouridine are good permeants of hCNT1, 5′-deoxy-5-fluorouridine, zidovudine, cytarabine, and zalcitabine, are poorly transported by hCNT1 [103,126,131]. Similarly, the purine nucleoside analogs fludarabine, cladribine, and clofarabine are poor permeants of hCNT2 [110]. On the other hand, hCNT3 efficiently transports both pyrmidine and purine nucleoside analogs, including gemcitabine, fluoropyrmidine nucleoside analogs (5-fluorouridine, 2′-deoxy-5-fluorouridine, 5′-deoxy-5-fluorouridine), fludarabine, cladribine, and clofarabine [110,129,133]. While hCNT3 is also able to mediate sodium-nucleoside co-transport of anti-viral nucleoside analogs zidovudine and didanosine, it does not mediate their H^+/nucleoside co-transport [132].

I.1.3.2.2 Regulation of hCNTs

Knowledge of the regulation of hCNTs is a relatively unexplored area in nucleoside transport biology; however, two concepts have emerged from the few studies that have been performed. First, upregulation of CNT expression may be associated with differentiation or maturation of cells and downregulation may be associated with dedifferentiation of cells (as in tumors) [4]. For example, hCNT1 and hCNT2 staining is low in crypts but high in mature enterocytes in human duodenum tissue [143]. In the rat intestinal epithelial cell line IEC-6, dexamethasone induced differentiation results in upregulation of rCNT1 and rCNT2 expression [144]. In humans, lower levels of *cit* and *cif* transporter processes, now known to be mediated, respectively, by hCNT1 and hCNT2 [126-128], are present in fetal than in adult intestinal brush border membrane vesicles [145]. In rat liver, rCNT1 and rCNT2 proteins are present at higher levels in adult than in fetal hepatocytes [146]. Loss of expression of rCNT1 and rCNT2 has been observed in chemically induced and spontaneous hepatocarcinomas in rats [147] as has loss of hCNT1 and hCNT2 expression in hepatocyte cultures that have lost the hepatic phenotype [148]. Regulation of hCNT1 in human hepatocytes appears to be determined by the cytokines tumor necrosis factor-α (TNF-α) or interleukin-6 (IL-6) and the liver enriched transcription factors HNF4-α or C/EBP-α [148-150]. Similarly, the cytokine tumor growth factor--β1 (TGF-β1) and the liver enriched transcription factor HNF3-γ appear to regulate hCNT2 in human heptocytes [148-150]. In bone marrow mouse macrophages, mCNT2 is upregulated following activation by lipopolysaccharide or interferon-γ (IFN-γ) [151-153]. In gynaecologic tumours, loss of hCNT1 immunohistochemistry staining in cancer tissues as compared to normal tissues has been reported and is associated with poor prognosis [154]. Some patients with chronic lymphocytic leukemia undergoing fludarabine treatment had lower hCNT3 mRNA expression in their cancers than in normal cell populations, which is associated with lower complete response rates [155]. The second concept that has emerged is that CNTs may be regulated by their own permeants. For instance, rCNT1 expression in rat jejunum is increased during nucleotide starvation [156]. In rat hepatoma and liver parenchymal cells, adenosine modulates rCNT2 activity by signalling through A_1 adenosine receptors [157]. The signalling pathways that regulate hCNT expression or activity require further elucidation.

I.2 Human renal nucleoside and nucleobase transport biology

A perplexing question in nucleoside transporter biology has been why mammals possess multiple NT proteins with overlapping, and sometimes, almost identical permeant selectivities. In epithelial cells with polarized membrane domains, the distribution of hENTs and hCNTs with overlapping selectivities across epithelia is the basis for nucleoside vectorial transepithelial fluxes [3,4,38]. For example, the polarized distribution of transporter proteins in renal tubular epithelial cells is the mechanistic basis for the selective reabsorption and secretion of ions and solutes [158].

I.2.1 Overview of human renal transport biology

The kidney functions primarily in osmoregulation and excretion of metabolic waste products [158]. The functional units of the kidney are the nephrons, which are divided into renal corpuscles and nephron tubules (Figure I-3A) [158]. Bulk water, solutes, and ions of arterial blood are passively filtered into nephron tubules through glomeruli of renal corpuscles [158]. Nucleosides tend to have minimal binding to plasma proteins and hence are completely filtered into nephron tubules [159]. The filtrate passes through the nephron tubules whose renal epithelia alter luminal contents eventually producing urine to be excreted. Most of the filtrate is reabsorbed leaving excess water and metabolic waste products to be excreted as urine. Filtrate that is reabsorbed passes from the interstitial spaces of the serosal sides of nephron tubules by bulk flow into the surrounding leaky capillaries returning it to the blood [158].

Nephron tubules are segmented into morphologically and functionally distinct sections (Figure I-3A). The first section, termed the proximal convoluted tubule, is composed of epithelial cells whose luminal membranes have extensive microvilli projections, termed brush border membranes, which contain numerous membrane transporter proteins and enzymes (Figure I-3B) [158]. The proximal tubule, which has a high capacity for reabsorption of renal filtrate, is the main site of reabsorption of water, ions, and solutes. After passage through the proximal tubule, the remaining filtrate passes in turn into the loop of Henle, the distal convoluted tubule, the collecting tubule, and lastly the collecting duct. Each of these tubule segments affects the final contents of the nephron tubular lumen by various reabsorptive, secretory, and enzymatic processes, ultimately producing urine to be excreted.

Proximal tubules maintain an acidic pH of approximately 6.0 through Na^+/H^+-exchanger activities at apical membranes, with some contribution from apical H^+-adenosine-5′-triphosphatases (ATPases), resulting in eventual acid secretion [158]. Other apical membrane transport proteins include various Na^+/glucose and Na^+/amino acid co-transporters, K^+ channels, Cl^--formate exchangers, and aquaporins [158]. Basolateral membrane transport proteins include Na^+/K^+-ATPases and Na^+/dicarboxylate co-transporters [158]. The polarized distribution of Na^+/H^+-exchangers and H^+-ATPases to apical membranes and Na^+/K^+-ATPases and Na^+/dicarboxylate co-transporters to basolateral membranes establishes transepithelial gradients that can be harnessed by other transporter proteins to drive uphill uptake, and hence vectorial transepithelial fluxes of their permeants across renal tubular epithelial cells [158]. Apical Na^+/H^+-exchangers and H^+-ATPases establish proton gradients directed from tubular lumens into renal tubular epithelial cells while basolateral Na^+dicarboxylate co-transporters establish a dicarboxylate gradient directed from interstitial spaces into renal tubular epithelial cells [158]. Apical H^+/solute co-transporters and basolateral dicarboxylate/solute co-transporters drive solute reabsorption and secretion, respectively [158]. hENT4 and hCNT3 may utilize proton gradients to drive reabsorption of nucleosides [38,116,129,132,134-136] while some members of hOATs are dicarboxylate/nucleoside co-transporters that may utilize dicarboxylate gradients to drive secretion of other nucleosides [38]. Basolateral Na^+/K^+-ATPases maintain sodium gradients directed from tubular lumens and interstitial spaces into renal tubular epithelial cells that can be harnessed by apical sodium co-transporters to drive sodium and solute reabsorption [158]. hCNTs are Na^+/nucleoside co-transporters that utilize the sodium gradient to drive reabsorption of nucleosides in the kidney [38]. Na^+-dependent nucleobase transport processes in renal brush border membrane vesicles and renal epithelial cells have been reported, so the same may be true for nucleobases [19-22]. Additionally, basolateral Na^+/K^+-ATPases, by virtue of pumping three sodium ions out for every two potassium ions pumped in, maintain an electrogenic gradient directed from tubular lumens and interstitial spaces into renal tubular epithelial cells for cations (and outwards for anions) [158]. This electrogenic gradient can be harnessed by basolateral cation transporters or apical anion transporters to drive secretion of cationic and anionic solutes, respectively [158]. hOCT1 is one transporter that utilizes the electrogenic gradients to drive secretion of various cations in the kidney and may be involved in driving secretion of some nucleosides [38]. Also, the electrochemical gradient maintained by basolateral Na^+/K^+-ATPases establishes an osmotic gradient directed from tubular lumens into renal tubular epithelial cells, which drives water reabsorption with sodium reabsorption [158]. Lastly, several types of primary active transporters are present on apical membranes of renal tubular epithelial cells that utilize the hydrolysis of ATP to directly drive extrusion of various solutes into tubular lumens. Various members of the ABC superfamily of ATP-pumps present on apical membranes have been implicated in the direct secretion of some nucleosides [38].

I.2.2 Renal handling of nucleosides and nucleobases

The selective reabsorption or secretion of nucleosides or nucleobases is the result of their vectorial transport across nephron tubules by asymmetrically distributed transporter proteins in renal epithelial cells [38]. Nucleoside and nucleobase analog drugs, being structurally related molecules to their physiological counterparts, are also permeants of these transporter proteins and are selectively reabsorbed or secreted in the kidney [38].

I.2.2.1 Renal handling of physiological nucleosides and nucleobases

Some circulating physiological nucleosides and nucleobases (e.g., adenosine, hypoxanthine) are efficiently reabsorbed in the kidney [48,49,51]. Other nucleosides that have potential toxicities (e.g., 2′-deoxyadenosine, adenine) are secreted [48,50,52]. The strongest evidence for a role of hNTs in renal handling of nucleoside comes from pharmacokinetic studies in a patient with a genetic deficiency of adenosine deaminase and in humans and mice made pharmacologically deficient in adenosine deaminase by treatment with a potent inhibitor [48]. Specifically, adenosine was reabsorbed with no inhibition by either NBMPR or dipyridamole, both potent inhibitors of ENT-mediated transport processes [48]. On the other hand, 2′-deoxyadenosine, which is toxic at high concentrations [46,47], is secreted by a process that could be inhibited by both NBMPR and dipyridamole [48]. Studies in dogs injected with radiolabeled adenosine demonstrated significant renal reabsorption of adenosine, 70% of which was retained by renal tubular cells, and a three-fold increase in reabsorption of adenosine into the blood upon administration of dipyridamole [160]. Dipyridamole binds tightly to α1-acid glycoprotein in plasma [161], which reduces its bioavailability for inhibition of ENT1 and ENT2 transport activities. Since hENT1, canine ENT1 and mENT1 are more sensitive to dipyridamole than hENT2 and mENT2 (Table I-2) [27,34,109,162,163], it is likely that the observed *in vivo* effects of dipyridamole were due to inhibition of ENT1-mediated transport in kidney tubules. Since inhibition of transport at either apical or basolateral membranes would eliminate transepithelial fluxes, these results suggest that 2′-

deoxyadenosine secretion is dependent on ENT1 while adenosine reabsorption is not.

Much less is known about renal handling of other physiological nucleosides and nucleobases than adenosine and 2′-deoxyadenosine. Excretion of uridine has been observed in rhesus monkeys with elevated plasma uridine levels after treatment with exogenous uridine and 5-benzylacyclouridine, a uridine phosporylase inhibitor that blocks uridine catabolism by the liver, suggesting saturation of renal tubular reabsorption processes [164]. Likewise, xanthine renal tubular reabsoprtion is suggested from studies in humans in which administration of allopurinol or oxipurinol increased xanthine clearance rates [165]. Both reabsorption and secretion of pseudouridine has been observed in humans in different situations [166]. Elevated secretion of pseudouridine and other natural modified nucleosides, including 1-methyladenosine, 1-methylguanosine, and N^2,N^2-dimethylguanosine, is present in patients with chronic renal failure or with malignancies [166,167]. Relative to urinary excretion of pseudouridine, excretion of inosine, xanthine, and uridine is decreased, suggesting reabsorption of these nucleosides and nucleobases [166].

The majority of physiological nucleosides are thought to be reabsorbed from tubular lumens into interstitial spaces by kidney tubular epithelial cells through coupling of apically localized, sodium gradient-driven hCNTs or proton gradient-driven hCNT3 and hENT4 to basolaterally localized, equilibrating hENT1 and hENT2 [12,38,129,132,134-136]. It is currently unclear how the physiological nucleosides 2′-deoxyadenosine and pseudouridine are secreted from interstitial spaces to nephron lumens by kidney tubular epithelial cells. Basolaterally localized, electrogenic-driven hOATs or hOCTs may be coupled to apically localized, equilibrating hENT1 for 2′-deoxyadenosine secretion. While it is known that 2′-deoxytubercidin, an analog of 2′-deoxyadenosine, is a permeant of hOCT1 [168] and 2′-deoxyadenosine is a permeant of hOAT1 [169], it is not known whether pseudouridine is a permeant of hNTs, hOATs, or hOCTs.

I.2.2.2 Renal handling of synthetic nucleoside and nucleobase analog drugs

Even less is known about renal handling of therapeutic nucleoside and nucleobase analog drugs than their physiological counterparts. Although, the structural similarities of nucleoside and nucleobase analogs to physiological nucleosides suggest common mechanisms for renal handling, this is not necessarily the case. There are differences in transport capacities and permeant selectivites for hENTs and hCNTs (Tables I-1, I-3), as well as differences in the metabolism, between physiological and therapeutic nucleosides and nucleobases [55].

In mice, the fluoropyrmidine nucleobases and nucleosides have differential renal handling. 5-Fluorouracil undergoes net reabsorption as the unaltered nucleobase, which can be inhibited by dipyridamole [170,171]. On the other hand, 5′-deoxy-5-fluorouridine and 5-fluoro-2′-deoxyuridine undergo net secretion unaffected by dipyridamole, unlike uridine, which is reabsorbed [170,171]. This suggests that 5-fluoro-5′-deoxyuridine and 5-fluoro-2′-deoxyuridine secretions are not dependent on mENT1. The mechanism for 5-fluorouracil in the kidney is unknown but may involve sodium-dependent nucleobase co-transport processes [19-21]. On the other hand, the structural analogs 2′-deoxyadenosine and 4-amino-7-(2′-deoxy-beta-D-erythro-pentofuranosyl)-pyrrolo-(2,3-d)pyrimidine (2′-deoxytubercidin) undergo net secretion although the mechanisms appear to be different [48,172]. While 2′-deoxyadenosine secretion can be inhibited by NBMPR and is thus dependent on ENT1, 2′-deoxytubercidin secretion is not affected by NBMPR [48,172,173]. 2′-Deoxytubercidin has been explored as an anti-neoplastic agent but severe toxicities have limited its clinical utility [174].

The majority of anti-viral nucleoside analog drugs appear to undergo net tubular secretion [175-181]. Twenty percent of zidovudine is eliminated unchanged in the urine in humans and rats by net tubular secretion as is 70 % of lamivudine in humans and mice [175-177]. Additionally, the novel lamivudine analog 4-amino-1-[(2*R*,4*R*)-2-(hydroxymethyl)-1,3-oxathiolan-4-yl]pyrimidin-2(1*H*)-one (apricitabine) is secreted in mice [178]. The dideoxynucleoside analogs, didanosine, zalcitabine, and stavudine, are also secreted in humans [175]. Lastly, 90 % of 2-amino-9-((2-hydroxyethoxy)methyl)-1H-purin-6(9H)-one (acyclovir) is eliminated unchanged in the urine by active tubular secretion in humans [179]. Mounting evidence exists for the involvement of OATs, OCTs, MDR-1, and MRPs in renal secretion of anti-viral nucleoside analogs [180,181].

I.2.3 Distribution of hENTs and hCNTs in human kidney

Recent evidence has suggested roles for NTs in renal reabsorption of physiological nucleosides and nucleoside analogs [38]. The model proposes that hCNT1/2/3 in apical membranes and hENT1/2 in basolateral membranes of human kidney proximal tubule cells mediate vectorial fluxes of nucleosides from the lumen to the interstitial space across kidney epithelia [38]. Reabsorption would be driven through hCNT1/2/3 by sodium gradients established by basolateral Na^+/K^+-ATPases [38] and perhaps through hCNT3 and hENT4 by proton gradients established by apical Na^+/H^+-exchangers [12,116,129,132,134-136].

Expression of all seven hENT mRNA transcripts has been observed in human kidney through multiple tissue expression RNA arrays [3,4,27,34,102,111,112,116], although hENT3 mRNA expression in human kidney appears to be minimal [111]. hENT1 and hENT2 mRNA transcripts are found primarily in distal tubules and glomeruli while hCNT1 and hCNT2 mRNA transcripts are found primarily in proximal tubules by *in situ* hybridization in human kidney tissue [143]. The expression status of hCNT3 and hENT4 mRNA in human kidney proximal tubules is unknown.

Subcellular fractionation of animal and human kidney cortex membranes into brush border and basolateral membrane vesicles has allowed the study of NT activities in proximal tubule apical and basolateral membranes, respectively [182]. Cross-contamination of kidney brush border membrane and basolateral membrane vesicle preparations and contamination from organelle membranes tends to be low. However, the proportion of inside-out and rightside-out vesicles in a given vesicle preparation varies [182], sometimes confounding results. Nevertheless, early studies with kidney brush border and basolateral membrane vesicles indicated assymetrical distribution of CNTs and ENTs to apical and basolateral membranes, respectively [139,140,183-189]. Studies with human kidney brush border membrane vesicles identified a pyrimidine-nucleoside selective, sodium-dependent transport activity that also transports guanosine (*cit*-like transport process) before the cloning of hCNT1/2/3 [139,140]. Other studies have identified NT activities now known to be mediated by CNT1 and CNT2 in rat, rabbit and cow kidney brush border membrane vesicles, a NT activity now known to be mediated by ENT1 in rabbit kidney basolateral membrane vesicles, and a NT activity now known to be mediated by ENT1 in pig kidney brush border membrane vesicles [183-189]. Taken together, these studies support a model with ENT1 on basolateral surfaces and CNTs on apical surfaces of kidney proximal tubules, although they also suggested the presence of ENT1 on apical surfaces of kidney proximal tubules.

Relatively few studies have been performed to directly localize NT proteins in kidney tissues. Immunofluorescent studies of rCNT1 in rat kidney cortex demonstrated an apical localization in proximal tubules [190] that was later supported by immunohistochemistry studies of hCNT1 in human kidney tissue [143]. hCNT1 and hCNT2 staining was observed in apical membranes of human kidney proximal tubules and hENT1 staining in apical and basolateral membranes of proximal tubules adjacent to corticomedullary junctions [143]. Staining for hENT1 and hENT2 was observed primarily in basolateral membranes of human kidney distal tubules [135]. No localization studies have been reported in human kidney tissues for hCNT3, hENT3, or hENT4, although hENT4/PMAT protein has been detected in human kidney by immunoblotting of tissue lysates [116].

Fluorescent protein tagged transporters can be localized to apical or basolateral membranes in polarized renal epithelial cell lines grown on raised permeable cell culture supports – e.g., Madin-Darby canine kidney (MDCK) cells, a model for distal tubule epithelial cells, and LLC pig kidney (LLC-PK$_1$) cells, a model for proximal tubule epithelial cells [191]. Transepithelial fluxes of radiolabeled solutes can be studied across polarized monolayers of MDCK and LLC-PK$_1$ cells [192]. Several studies in these model systems have localized fluorescent protein-tagged hCNT1, rCNT1, rCNT2, hCNT3, hENT1, and hENT4 to apical membranes, hENT1 and hENT2 to basolateral membranes and hENT1 to mitochondria of transfected polarized kidney epithelial cell lines, MDCK and LLC-PK$_1$ [116,193-199]. The polarized distribution of ENTs and CNTs allowed preferential apical to basolateral transepithelial fluxes of nucleosides that were dependent on sodium gradients [199]. As well, trafficking of CNTs to apical membranes appears to be independent of glycosylation status [197].

I.2.4 Functions of hENTs and hCNTs in human kidney

In polarized renal epithelial cell lines co-transfected with hCNT1 and hENT1, apical-to-basolateral fluxes of adenosine but not 2′-deoxyadenosine occur at physiological concentrations [194], presumably because hCNT1 has a higher apparent affinity for adenosine than for 2′-deoxyadenosine, albeit with low capacity in comparison with pyrimidine nucleosides [126,130]. However, since hCNT2 and/or hCNT3 appear to be present together with hCNT1 in kidney proximal tubules [127-129,148,199,200], this may not be a physiologically relevant explanation for adenosine reabsorption and 2′-deoxyadenosine secretion given the low transport capacity of hCNT1 for adenosine and 2′-deoxyadenosine (Table I-3) [126,130]. hENT- and hCNT-mediated transport of nucleosides is unlikely to be saturated as circulating physiological and renal interstitial nucleoside concentrations (e.g., < 1 μM for adenosine) [201,202] are well below the apparent K_m values of hENT1/2/4 and hCNT1/2/3 for physiologic nucleosides (Tables I-1, I-3) [3,4]. It is unlikely that CNT1-mediated adenosine transport is physiologically relevant in renal handling of adenosine or 2′-deoxyadenosine because all three CNT mRNA transcripts are present in human kidneys [126-129] and rat proximal tubules [200], CNT2 protein is present in human kidney proximal tubules [143], and CNT3 activities are present in murine proximal tubules [199]. Rather, hCNT1 binding of adenosine may have a physiological role in limiting pyrimidine nucleoside conservation by hCNT1 or in abrogation of adenosine signaling by sequestering adenosine from purinergic receptors in the proximal tubular lumen.

In murine proximal convoluted tubule cells grown as polarized monolayers, endogenous CNT3 activity can mediate preferential sodium-dependent apical-to-basolateral transepithelial fluxes of cytidine [199]. Additionally, hCNT3 in transfected MDCK cells grown as polarized monolayers can mediate preferential sodium-dependent apical-to-basolateral transepithelial fluxes of radioisotope associated with cytidine, adenosine, gemcitabine, fludarabine, and 5′-deoxy-5-fluorouridine [199], although in some cases the fluxed species were different - i.e., cytidine was converted to uridine, adenosine was converted to nucleobases, and the nucleoside analogs were unchanged [199]. The transport of nucleobases, such as hypoxanthine derived from adenosine, across hCNT3-transfected MDCK polarized monolayers suggests a role for basolateral hENT2 in nucleobase renal handling as hENT2 is known to transport hypoxanthine [10]. It is not known if endogenous hCNT3 in proximal tubules is involved in transepithelial fluxes of purine and pyrimidine physiological and pharmacological nucleosides. Also, it is not known if hCNT3 is involved in transepithelial fluxes of purine anti-metabolites such as cladribine and clofarabine.

The apical localization of hENT4/PMAT in transfected MDCK cells grown as polarized monolayers and the presence of hENT4/PMAT protein in human kidney tissue [116] suggest its involvement in renal handling of adenosine utilizing the luminal proton gradients to drive adenosine reabsorption. This may have physiological relevance in the kidney proximal tubules which maintain an intratubular acidic pH [158]. Lastly, the apparent apical localization of hENT1 in proximal tubules suggested by studies in kidney brush border membrane vesicles [188,189] and transfected renal epithelial cell lines [194,195] has not been confirmed. Apical hENT1 may be involved in the secretory pathway of secreted nucleosides, such as 2′-deoxyadenosine, given that secretion of 2′-deoxyadenosine is dependent on ENT1.

It has been observed that overexpression of recombinant proteins in renal epithelial cell lines grown as polarized monoalyers sometimes saturates trafficking pathways and alters localization patterns [203,204]. One group avoided this by studying the role of endogenous CNT3 activities in transepithelial fluxes of various nucleosides in murine proximal convoluted tubule cells and observed sodium-dependent cytidine apical-to-basolateral fluxes [199]; however, species differences in transport capacities and affinities can confound applicability to humans. As well, the distal tubule-like MDCK and proximal tubule-like LLC-PK1 cell lines have characteristics of more than one tubular segment, with MDCK cells having pronounced brush border membranes and hydrolase activities, which are characteristic of proximal tubules [205,206], and LLC-PK$_1$ cells having responsiveness to anti-diuretic hormone, which is characteristic of distal tubules [207-209]. For these reasons, some researchers have turned to rabbit and human kidney tubule primary cultures to obtain more differentiated *in vitro* cell culture systems [210-211].

I.3 Other transporters capable of transporting nucleotides, nucleosides, and nucleobases

Most anti-cancer and anti-viral nucleoside drugs are poorer permeants of hNTs than their counterparts and their secretion is likely accomplished through kidney xenobiotic transporters [38]. Some nucleosides and nucleobases and their nucleotide metabolites are also permeants of xenobiotic transporters, including hOCT1, hOAT1/2/3/4, MDR1, MRP4/5/8, and BCRP [5-9]. These xenobiotic transporters, which are remarkable in their ability to transport structurally diverse compounds, were not initially thought to have overlapping permeant selectivities with NTs. However, recent studies (discussed below) have shown that many xenobiotic transporters, some of which are found in the kidney, can mediate resistance to various nucleoside and nucleobase drugs when overexpressed in cell lines and there are a few direct studies of transportability of nucleosides and/or their nucleotide metabolites by xenobiotic transporters [38].

The SLC22A family of transporters comprises the OCTs and the OATs [5,6]. OCTs mediate electrogenic-driven unidirectional facilitative diffusion of cationic compounds as well as unidirectional facilitative diffusion of anionic and uncharged compounds [5,6]. hOCT1/2 are both present in human kidney proximal tubules and rabbit OCT1/2 are putatively localized on basolateral membranes of rabbit proximal convoluted tubules and straight proximal tubules, respectively [212]. Evidence that OCTs may be involved in renal handling of nucleosides came from early studies of renal clearance of 2′-deoxytubericidin in mice [172,173]. While renal secretion of 2′-deoxyadenosine was not inhibited by cimetidine, an OCT inhibitor, renal secretion of 2′-deoxytubericidin, which is structurally almost identical to 2′-deoxyadenosine (Figure I-1), was inhibited by dosages of cimetidine that inhibit OCT1 but not OCT2 activity [48,168,172,173]. OCT1 is not necessary for renal secretion of 2′-deoxytubercidin as demonstrated in mice that lack the gene encoding OCT1 [213]. In mice, secretion of 5′-deoxy-5-fluorouridine was inhibited by cimetidine but not by probenecid while reabsorption of 5-fluorouracil was not inhibited by either cimetidine or probenecid [171]. In rats, secretion of zidovudine is partially inhibited by cimetidine [176]. Additionally, it has been shown that human OCT1 transports zidovudine, acyclovir, and ganciclovir [168,214]. Collectively, these data support a role for OCT1 in renal secretion of some nucleoside analogs by uptake of nucleosides across basolateral membranes into renal tubular epithelial cells.

Other candidates of the SLC22A family for renal handling of anti-viral nucleoside drugs are the OATs, which mediate transport of negatively charged compounds with broad structural diversity, including some nucleoside analogs [6]. OAT1 and OAT3 are dicarboxylate/permeant-exchangers whereby the dicarboxylate gradient supplies the driving force for uphill transport [6]. The mechanism of transport for OAT2 is currently unclear [6]. While hOAT1/2/3 are present on basolateral membranes of human kidney proximal tubules, hOAT4 is found on apical membranes [6]. Although transportability of zidovudine by all four human isoforms, hOAT1/2/3/4, and of ganciclovir by hOAT1 [214] has been demonstrated, their roles in renal handling of AZT and ganciclovir remains to be determined. hOAT2-mediated transport of 2′-deoxyguanosine and adenosine as well as cGMP and cAMP has been recently reported [169]. Additionally, hOAT2/3 appear to also transport the nucleobases 6-mercaptopurine and 6-thioguanine [13,14]. While the OAT inhibitor probenicid does not inhibit renal handling of several nucleosides, including adenosine, 2′-deoxyadenosine, 2′-deoxytubericidin, 5′-deoxy-5-fluorouridine [48,168,171-173], this may be a result of its low bioavailability -e.g., 80 % is bound to plasma proteins in dogs [215]. Nevertheless, probenecid does partially inhibit zidovudine secretion in rats, albeit to a lesser extent than cimetidine, indicating that zidovudine secretion may be mediated by OATs and OCTs. Therefore, there may be a role for hOAT1/2/3 in renal handling of some nucleosides, along with hOCT1, at the basolateral membrane of proximal tubules.

The large ABC family of proteins includes MDRs and MRPs, which are ATP-dependent efflux pumps that were originally identified as mediating resistance of cancer cells to drugs with an enormous diversity of bulky amphiphatic structures [7-9]. MDR1 protein (i.e., P-glycoprotein), which is present in apical membranes of kidney proximal tubules [7], has been implicated in resistance of transfected leukemia cell lines to 6-mercaptopurine and 6-thioguanine [15]. Decreased uptake of 6-mercaptopurine into MDR1-transfected cells was observed, suggesting that MDR1 plays a role in efflux of 6-mercaptopurine, or more likely its phosphorylated metabolites [15]. Although MDR1 appears not to have a significant role in renal secretion of dideoxynucleoside analogues, it may have a role in renal handling of phosphorylated metabolites of purine nucleosides and their drug analogs [15,180].

More recently, some MRPs have been found to mediate efflux of nucleoside and nucleobase anti-cancer drugs and nucleoside anti-viral drugs, thereby giving rise to drug resistance [for a review, see 8]. Specifically, MRP4 has been implicated in efflux of and resistance to various nucleoside drugs, nucleotide metabolites of nucleoside drugs, and nucleotide metabolites of nucleobase drugs in cancer cell lines [216]. MRP4 has an apical localization in human kidney proximal tubules [8]. Although MRP5 has also been linked to efflux and resistance of various nucleoside drugs, MRP5 does not appear to be present in human nephron tubules [217]. MRP4 in transfected cancer cell lines confers resistance to ganciclovir, 6-mercaptopurine and 6-thioguanine evidently because of increased efflux of the nucleoside monophosphate derivatives of 6-

mercaptopurine and 6-thioguanine and of ganciclovir and its nucleotide metabolites [16,218-220]. MRP4 has also been reported to transport other phosphorylated metabolites of nucleoside drugs, including the monophosphorylated forms of zidovudine and stavudine [16,221]. MRP5 also mediates ATP-dependent drug efflux of 6-thioguanine and 6-mercaptopurine and their monophosphorylated nucleotide forms [17,220]. MRP8, a recently identified member of the ABC family, has been implicated in efflux of 2′-deoxy-5-fluorouridine monophosphate and resistance to the fluoropyrimidines as well as to zalcitabine [222].

BCRP is another ATP-dependent efflux pump that is present in the kidney and is putatively localized on apical membranes of renal nephron tubules [9]. Recently, introduction of BCRP into cells by transfection of its cDNA was shown to confer resistance by mediating efflux of various purine nucleoside analogs, most notably cladribine [223]. The roles of these members of the ABC family of ATP-dependent efflux pumps in renal handling of nucleosides remain to be elucidated.

I.4 Nephrotoxicity of nucleoside and nucleobase analog drugs

During transepithelial fluxes of nucleoside drugs by renal NTs, whether it be reabsorption or secretion, renal epithelial cells may be exposed to significant drug levels. Nucleoside drugs in transit across renal epithelia could be phosphorylated and thereby trapped intracellularly by the same enzymes that phosphorylate physiological nucleosides, potentially giving rise to nephrotoxicity. Several anti-viral and anti-neoplastic nucleoside analog drugs have documented nephrotoxicities that can be dose-limiting. A major toxicity of 2′-deoxycoformycin (pentostatin) in humans is mild renal insufficiency, which is reversible [224]. Although 2′-deoxytubercidin is not used clinically, initial trials in cancer treatment in humans showed mild to severe renal toxicities [174,225]. Other common but manageable nephrotoxicities include proteinuria and hematuria (45 % and 35 % of patients, respectively) for gemcitabine [93]. Renal failure, a rare toxicity associated with gemcitabine and cytarabine, has been documented in case reports [93,226]. Nephrotoxicities associated with anti-viral nucleosides, which are also rare, have been observed with didanosine and ribavirin [227,228]. Two cases of Fanconi syndrome (nephrogenic diabetes insipidus and proximal tubular dysfunction) associated with didanosine treatment has been reported [227,229]; Fanconi syndrome is also associated with anti-viral nucleotide analog reverse transcriptase inhibitors 1-[(*R*)-2-(phosphonomethoxy)propyl]adenine (tenofovir), 1-[(*S*)-3-hydroxy-2-(phosphonomethoxy)propyl]cytosine (cidofovir), and 1-[2-(phosphonomethoxy)-ethyl]adenine (adefovir) [230,231]. Several cases of uric acid nephrolithiasis associated with ribavirin treatment have been reported and it may be common enough to warrant careful monitoring of susceptible patients [228]. Ribavirin treatment usually results in reversible hemolytic anemia in nearly all patients, hyperuricemia in 25 % of patients, and severe hemolysis in 5-10 % patients [232-234]. Although severe hyperuricemia may lead to uric acid nephrolithiasis in patients with risk factors such as dehydration, its incidence and severity in ribavirin treatment have not been reported [235].

Despite the rarity of renal failure induced by nucleoside drug therapy and the clinical manageability of other milder renal toxicities, nephrotoxicity associated with nucleoside analogs continues to present challenges to patient treatment. First, drug discovery and development is hampered at early clinical phases by unforeseen toxicities [236,237]. Second, patients with pre-existing renal dysfunction are more susceptible to nucleoside drug nephrotoxicity and are often precluded from treatment or given lower starting doses of drug [94,95]. Third, it is becoming apparent that traditional markers of nephrotoxicity (e.g., creatinine and blood urea nitrogen measurements) have several limitations [238]. They do not provide region-specific information and are not perturbed until significant kidney damage has occurred (~30 %) [238]. Furthermore, creatinine clearance is predictive of renal clearance of compounds that are filtered and excreted by the kidney but not of compounds such as nucleoside drugs that undergo regulated reabsorption and secretion. Better predictors of potential iatrogenic effects of nucleoside drugs, including nephrotoxicities, are needed. The ability to predict the toxicity profiles of new drugs in pre-clinical studies with genomic tools such as microarray analysis of predictive biomarkers is slowly becoming a reality [239,240]. For example, one study found that upregulation of some renal transporters were predictive biomarkers for a group of nephrotoxicants in an animal model [241].

There are several potential mechanisms of nephrotoxicity for nucleoside drugs. For the antiviral nucleoside drugs, direct cytotoxicity to renal tubular cells as a result of mitochondrial damage may be the major mitigating factor. For example, multi-organ toxicities of 1-(2′-deoxy-2′-fluoro-1-β-D-arabinofuranosyl)-5-iodouracil (fialuridine) predominantly affects multiple organs and tissues that have slow turnover of cells but a major dependence on mitochondrial functions (e.g., liver, kidney, brain, and pancreas) [242]. Under electron microscopy, liver specimens obtained after fialuridine treatment showed evidence of mitochondtrial toxicity [242]. Fialuridine incorporation into cellular and mitochondrial DNA in cell lines is associated with increased lactate production by cells, an indicator of mitochondrial toxicity [242]. As renal epithelial cells are non-dividing, cytotoxicity of nucleoside drugs may result from their toxicities to mitochondria of proximal tubule cells. Mitochondrial toxicity in normal tissues has been linked to several nucleoside analogs, including fialuridine in hepatitis B treatment [242], dideoxynucleoside analogs in anti-HIV treatments [243], and fludarabine in anti-cancer treatments [244]. Toxicity of fialuridine to polarized renal epithelial cells was found to be dependent on the presence of Yellow Fluorescent Protein (YFP)-tagged hENT1 in mitochondria [190]. Therefore, hENT1, and possibly also hENT3, in mitochondria of renal epithelia may play a role in nephrotoxicity of some nucleoside analogs. Evidence of the presence of actively transporting hENT1 and hENT4 in mitochondria supports this hypothesis [114,198].

A rare, but potentially fatal, complication of chemotherapy known as tumor lysis syndrome may occur in patients with hematological malignancies of high tumor burdens who are treated with nucleoside drugs such as fludarabine or cladribine [80,245-247]. Tumor lysis syndrome involves rapid killing of large numbers of tumor cells in the blood, leading to release of large amounts of nucleic acids and subsequent degradation of their purine nucleosides to uric acid, which in large amounts crystallizes in renal collecting tubules causing acute renal failure [248]. Tumor lysis syndrome occurs in approximately 5 % of patients treated with fludarabine or cladribine [249,250]. A mitigating factor in such patients may be direct cytotoxicity of these drugs to renal proximal tubules, which in turn leads to nephron flow defects that potentiate uric acid crystallization. It has not been established if fludarabine and cladribine are directly cytotoxic to renal proximal tubule cells. Reductions in glomerular filtration rates by volume depletion in patients with poor oral intake and severe vomiting and diarrhea, despite the kidney's ability to autoregulate, may result in uric acid crystallization in renal collecting tubules due to lower intratubular flow rates [248].

Proteinuria, which is found in some patients being treated with gemcitabine [93], is often associated with direct toxicity of certain drugs to podocytes (endothelial cells of glomeruli) [251]. Although, it is not known if NTs are present in podocytes, it is likely that hENT1, which is widely distributed among tissues, is present and mediates uptake of physiological nucleosides and nucleoside drugs from the plasma during the filtration process.

1.5 Proposed model for renal handling of nucleosides

The selective reabsorption or secretion of nucleosides is the result of their vectorial transport across nephron tubules by assymetrical distribution of their transporter proteins in the constituent kidney epithelial cells. Nucleoside analog drugs, being structurally related to their physiological counterparts, are also permeants of these transporter proteins and are selectively reabsorbed or secreted in the kidney. The mechanisms of nucleoside transport include facilitative diffusion by hENT1, hENT2, and hOAT2, pH-dependent nucleoside transport by hENT3 and hENT4, proton gradient-driven H^+/nucleoside co-transport by hCNT3, sodium gradient-driven Na^+/nucleoside co-transport by hCNT1, hCNT2, and hCNT3, electrogenic gradient-driven transport by hOCT1, electrogenic and dicarboxylate gradient-driven dicarboxylate/nucleoside-exchange by hOAT1 and hOAT3, proton gradient-driven OH^-/nucleoside-exchange by hOAT4, and ATP-dependent efflux (of nucleosides and their nucleotide metabolites) by MDR1, BCRP, MRP4, MRP5, and MRP8.

The model of kidney nucleoside reabsorption investigated in this thesis proposes that the proton gradient established by apical Na^+/H^+-exchangers and the sodium gradient established by basolateral Na^+/K^+-ATPases drives reabsorption of some nucleosides through coupling of apical hCNT1, hCNT2, hCNT3, and hENT4 to basolateral hENT1 and hENT2. In the model of kidney nucleoside secretion, the proton gradient established by apical Na^+/H^+-exchangers, the electrogenic gradient established by basolateral Na^+/K^+-ATPases and the dicarboxylate gradient established by basolateral Na^+/dicarboxylate co-transporters drives secretion of nucleosides through coupling of basolateral hOCT1, hOAT1, hOAT2, and/or hOAT3 to apical hENT1, hOAT4, MDR1, MRP4, and/or MRP8. hENT3 mRNA is present in minor amounts in kidney and hENT3 appears to be an intracellular transporter [111,114]. As well, MRP5 mRNA does not appear to be present in the kidney to a significant extent [8]. For nucleobases, reabsorption may be mediated by coupling putative apical sodium-dependent nucleobase transporters to basolateral hENT2 while secretion may be mediated by coupling of basolateral hENT2 to apical MDR1, MRP4, and MRP8.

The proposed model suggests that the ultimate direction and extent of a nucleoside's or a nucleobase's renal transepithelial transport is dependent on the relative localizations, cell surface levels, affinities, turnover numbers, and heterogeneous distribution along nephron tubular epithelial cells of the kidney transporter proteins involved. As well, the heterogeneity in ion gradients along nephron tubular segments and extent of a molecule's intracellular metabolism in nephron tubular epithelial cells will play a role in whether a particular nucleoside is reabsorbed or secreted by the kidney.

I.6 Goals of the present work

The work described herein aimed to enhance understanding of the roles of hNTs in renal proximal tubular handling of physiological nucleosides and nucleoside analog drugs. Since one of the known roles of the kidney is excretion of toxic metabolites and drugs, one might anticipate that nucleoside and nucleobase drugs would be secreted by the kidney. Nevertheless, the overlapping permeant selectivities of transporter proteins involved in nucleoside transport for physiological nucleosides and their cognate synthetic analog drugs predict that some nucleoside drugs will be reabsorbed. A comprehensive picture of the distribution of various transporter proteins involved in nucleoside transport in different nephron tubular segments would provide a framework for understanding transepithelial flux studies in renal epithelial cells representative of different nephron tubular segments. Much evidence has been collected over the years to implicate hNTs of renal proximal tubules in mediating reabsorption of some physiological nucleosides; however, little is known about the role of proximal tubule hNTs in mediating secretion of other physiological nucleosides (e.g., 2′-deoxyadenosine) and in renal handling of nucleoside analog drugs. The sites and mechanisms of nucleoside secretion in the kidney are not yet clear but growing evidence implicates xenobiotic transporters present in kidney proximal tubules in secretion of certain nucleosides. Thus, much of the bulk renal handling of physiological nucleosides and nucleoside analogs may occur in the kidney proximal tubules.

The overall goal of the research presented in this thesis was to examine the role of hENTs and hCNTs in renal handling of physiological nucleosides and nucleoside analog drugs. The 2:1 Na^+-to-nucleoside coupling ratio and H^+/nucleoside co-transport capabilities of hCNT3 [129,132,134-136] and the greater permeant tolerance of hENT2 for nucleobases [10] make a case for apical hCNT3 and basolateral hENT2 having primary roles in renal reabsorption of nucleosides. This is because hCNT3 has greater concentrating capacity than hCNT1/2 and is able to co-transport nucleosides under varying sodium and proton gradients in the nephron tubular lumen while hENT2 can equilibrate both nucleosides and nucleobases at the basolateral membrane [158]. On the other hand, the putative apical localization of hENT1 suggests it may have a role in renal secretion of nucleosides [143,183-189,194,195]. Therefore, it was hypothesized that in proximal tubules renal reasborption of nucleosides, such as adenosine, is mediated by coupling of apical hCNT3 to basolateral hENT1/2 while renal secretion of nucleosides, such as 2′-deoxyadenosine, is mediated, in part, by apical hENT1. Furthermore, it was hypothesized that some nucleoside analogs, such as fludarabine, in the process of being reabsorbed or secreted, are potentially cytotoxic to proximal tubules and that apical hCNT3 is a major determinant of the extent of fludarabine cytotoxicities.

The primary objectives of this thesis research were to:

1) establish the distribution of hCNT3 and hENT1 in human kidney proximal tubules (Chapter III):
    a. localize hCNT3 and hENT1 in human kidney tissue
    b. establish a human proximal tubular cell culture model system with endogenous hENT1/2 and hCNT3 transporter activities
2) determine the roles of hENT1/2 and hCNT3 in fludarabine accumulation and cytotoxicity in a human proximal tubular cell culture model system (Chapter IV):
    a. examine hENT1/2 and hCNT3 mRNA expression, protein abundances, and activities
    b. examine fludarabine accumulation and cytotoxicity
3) determine the roles of hENT1/2 and hCNT3 in transepithelial fluxes of purine nucleosides in polarized monlayers of a human proximal tubule cell culture model system (Chapter V):
    a. localize hENT1/2 and hCNT3 in polarized monolayers

b. examine the roles of hENT1/2 and hCNT3 in transepithelial fluxes of adenosine, 2′-deoxyadenosine, and their nucleoside analogs fludarabine, cladribine, and clofarabine

I.6 Rationale of the experimental design

First, a key to understanding the physiological roles of hNTs in renal handling of nucleosides would be to establish their distribution in human kidney tissue. Although the distributions of hENT1/2 and hCNT1/2 in human kidney tissue were reported after this study commenced [143], the distribution of hCNT3 remained uncertain. The localization of hENT1 and hCNT3 in human kidney tissue was possible because of the availability of antibodies directed against hCNT3 and hENT1 suitable for immunolocalization studies and of normal human kidney tissues, obtained from patients after partial or complete nephrectomy.

Second, another major key to understanding the physiological roles of hNTs in renal handling of nucleosides would be the establishment of nephron tubule segment-specific model systems with hNT phenotypes similar to those of proximal tubules *in vivo*. While the utility of generating recombinant nucleoside transporter proteins for detailed studies of distinct transport processes in the well established renal cell lines, MDCK and LLC-PK_1, cannot be overstated, it was decided that a more representative understanding of renal hNT biology would be garnered from studies of human renal cell culture models prepared from freshly isolated human kidney tissue. This is because: 1) production of recombinant hNTs in the MDCK and LLC-PK_1 cell lines could lead to altered localizations and cell surface levels not indicative of conditions present in renal tubules *in vivo*

[203,204]; 2) endogenous non-human NTs with different permeant selectivities and inhibitor sensitivities (*e.g.*, canine ENT1) [163] as well as the presence of other endogenous non-human transporters capable of transporting nucleoside (*e.g.*, porcine OCTs) [252] could complicate interpretation of nucleoside uptake or flux studies; and 3) MDCK and LLC-PK_1 cell lines have dedifferentiated characteristics with regards to their distal tubular and proximal tubular origins, respectively, and might not accurately reflect the physiology of their respective nephron tubules of origin [205-209]. Even though the usage of other renal proximal tubule cells of non-human origin (*e.g.*, mouse or rabbit) [210] with endogenous non-human NTs would avoid some of these confounding issues, the non-human NTs have different permeant selectivities than the human isoforms. The use of human renal cell cultures prepared from freshly isolated kidneys [211,253] increased the likelihood that the cultures would have the full complement of functional post-transcriptional and post-translational hNTs, making these research studies more physiologically applicable.

Third, based on the anatomy of the nephron, the bulk of renal handling of nucleosides is predicted to occur in proximal tubules as it does for many other solutes that are actively reabsorbed or secreted [158]. While it is important to understand the distribution and physiological roles of hNTs in all segments of the nephron to develop a complete picture of renal hNT biology, these studies focused on proximal tubules and a human renal cell culture system with proximal tubular origin and characterisitics, was developed.

Fourth, fludarabine was selected as the "model" drug to investigate potential cytotoxicity of nucleoside analogs to a human proximal tubular cell culture model system because of the severity of clinical fludarabine nephrotoxicity and its widespread clinical use [245,249,250]. The emerging clinical evidence that hNTs may be important in determining cytoxicity of nucleoside analogs *in vivo* [37] warranted examination of the roles of hENT1/2 and hCNT3 in cytotoxicity of a drug like fludarabine using a human proximal tubular cell culture model system.

Lastly, transepithelial fluxes of adenosine and 2′-deoxyadenosine analogs across transfected renal epithelial cell lines mediated by coupling of apical hCNT1 to basolateral hENT1 were previously investigated [194]. However, the proposed model for 2′-deoxyadenosine appears to be physiologically inadequate given the presence of hCNT2 and hCNT3, both of which have higher transport capacities for purine nucloeosides than hCNT1. During the course of the work described in this thesis, results of studies of transepithelial nucleoside fluxes driven by apical hCNT3 in transfected renal epithelial cell lines were reported [199]. However, it was felt that the strategy of the current work, which utilized non-transfected, polarized monolayers of a human proximal tubular cell culture model system, would provide a more realistic picture of transepithelial fluxes of adenosine, 2′-deoxyadenosine, and their nucleoside analogs fludarabine, cladribine, and clofarabine.

I.7 Approach and model system: human renal proximal tubule cell (hRPTC) cultures

The primary human proximal tubular cell culture model system employed in these studies were cultures of human renal proximal tubule cells (hRPTCs) produced from human kidney tissues of different individuals by well-established methods [253]. These hRPTC cultures isolated from human kidney tissue of different individuals provided a differentiated *in vitro* cell culture model system, with well-defined proximal tubular characteristics [253] that could be used to functionally assay multiple endogenous hNT activities by radiolabeled nucleoside uptake studies. Furthermore, the different hRPTC cultures provided a basis for comparison of the effects of different hNT activities on uptake and potential cytotoxicity of fludarabine to proximal tubule cells. Lastly, these hRPTC cultures could be readily induced to form polarized monolayers on transwell inserts by well-established methods [211], such that the roles of multiple endogenous hNTs in transepithelial fluxes of various physiological nucleosides and nucleoside analogs across proximal tubule cells could be studied.

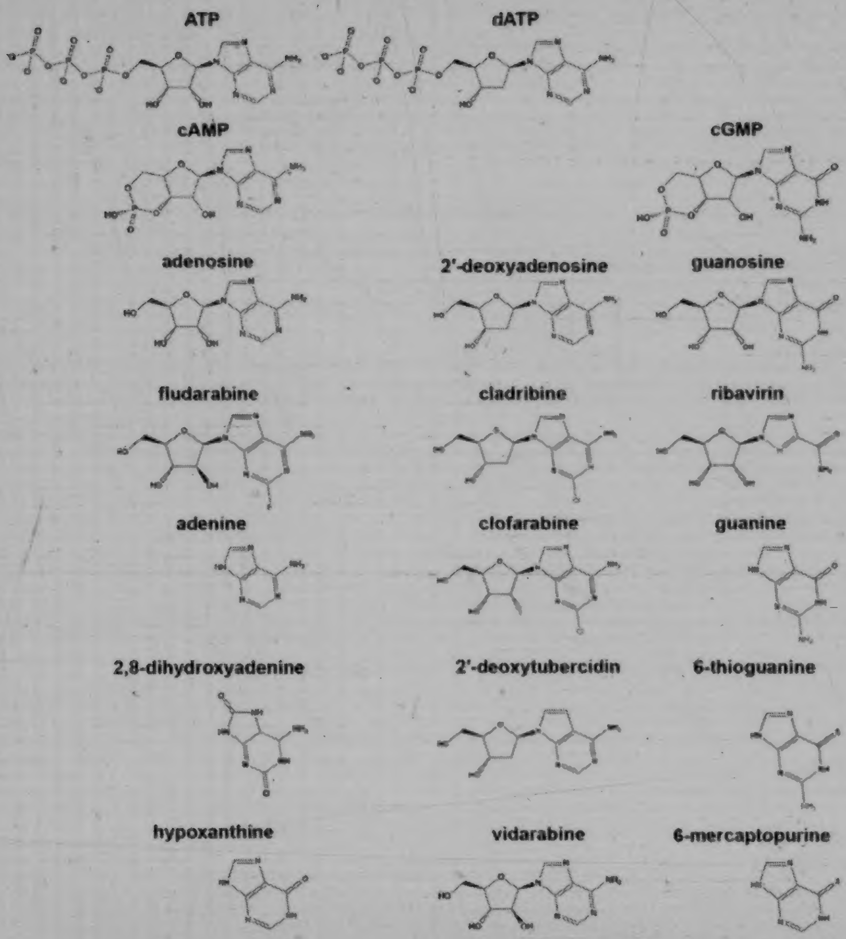
ATP
dATP
cAMP
cGMP
adenosine
2′-deoxyadenosine
guanosine
fludarabine
cladribine
ribavirin
adenine
clofarabine
guanine
2,8-dihydroxyadenine
2′-deoxytubercidin
6-thioguanine
hypoxanthine
vidarabine
6-mercaptopurine

Figure I-1. Structures of some major purine nucleotides, nucleosides, and nucleobases. ATP: adenosine-5′-triphosphate, cAMP: 3′-5′-cyclic adenosine monophosphate, cGMP: 3′-5′-cyclic guanosine monophosphate, cladribine: 2-chloro-2′-deoxyadenosine, clofarabine: 2-chloro-9-(2′-deoxy-2′-fluoro-β-D-arabinofuranosyl)adenine, dATP: 2′-deoxyadenosine-5′-triphosphate, 2′-deoxytubercidin: 4-amino-7-(2'-deoxy-beta-D-erythro-pentofuranosyl)-pyrrolo-(2,3-d)pyrimidine, fludarabine: 9-β-D-arabinosyl-2-fluoroadenine, 6-mercaptopurine: 3,7-dihydropurine-6-thione, ribavirin: 1-(β-D-ribofuranosyl)-1*H*-1,2,4-triazole-3-carboxamide, vidarabine: 9-β-D-arabinofuranosyladenine.

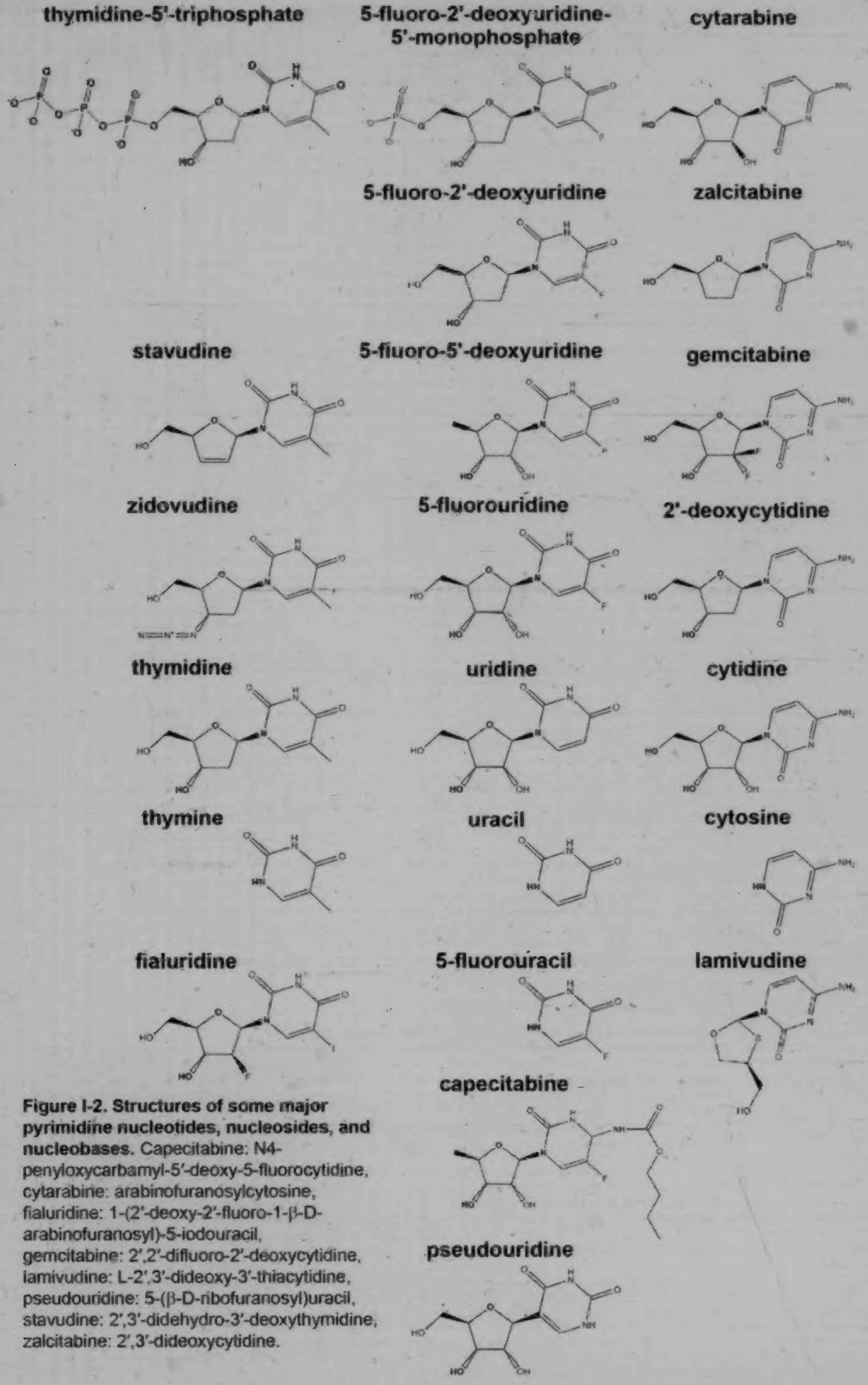

thymidine-5'-triphosphate

5-fluoro-2'-deoxyuridine-5'-monophosphate

cytarabine

5-fluoro-2'-deoxyuridine

zalcitabine

stavudine

5-fluoro-5'-deoxyuridine

gemcitabine

zidovudine

5-fluorouridine

2'-deoxycytidine

thymidine

uridine

cytidine

thymine

uracil

cytosine

fialuridine

5-fluorouracil

lamivudine

capecitabine

pseudouridine

Figure I-2. Structures of some major pyrimidine nucleotides, nucleosides, and nucleobases. Capecitabine: N4-penyloxycarbamyl-5′-deoxy-5-fluorocytidine, cytarabine: arabinofuranosylcytosine, fialuridine: 1-(2′-deoxy-2′-fluoro-1-β-D-arabinofuranosyl)-5-iodouracil, gemcitabine: 2′,2′-difluoro-2′-deoxycytidine, lamivudine: L-2′,3′-dideoxy-3′-thiacytidine, pseudouridine: 5-(β-D-ribofuranosyl)uracil, stavudine: 2′,3′-didehydro-3′-deoxythymidine, zalcitabine: 2′,3′-dideoxycytidine.

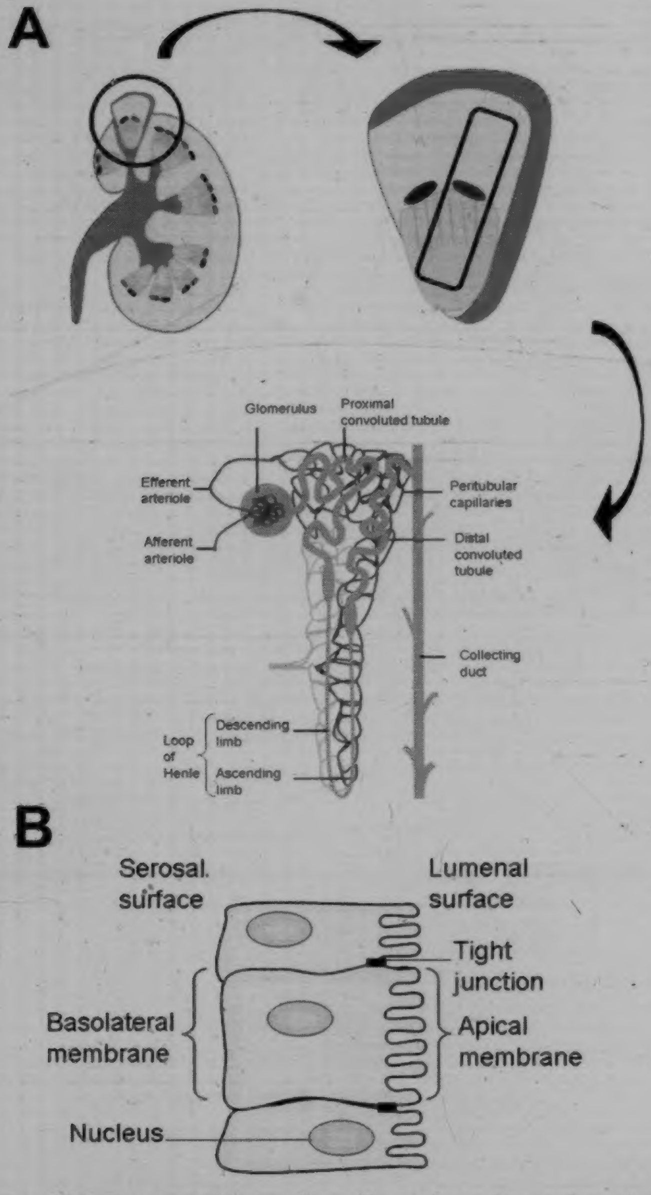
A
Glomerulus
Proximal convoluted tubule
Efferent arteriole
Afferent arteriole
Peritubular capillaries
Distal convoluted tubule
Collecting duct
Loop of Henle
Descending limb
Ascending limb
B
Serosal surface
Lumenal surface
Tight junction
Basolateral membrane
Apical membrane
Nucleus

Figure I-3. Structure of the nephron. The nephron, shown schematically in (A), is composed of the nephron tubules and associated capillaries. Blood enters and exits the nephron via afferent and efferent arterioles, respectively, and is filtered into the nephron tubules by the glomerulus. The major segments of nephron tubules include the proximal convoluted tubule, descending and ascending limbs of loop of Henle, distal convoluted tubule, and collecting duct, each of which alter the composition of renal filtrate by reabsorption and secretion processes. Peritubular capillaries and interstitial fluid surround the entire nephron structure such that there is a continuous transfer of fluid between lumen of renal tubules and blood of surrounding capillaries. The bulk of renal handling occurs in proximal convoluted tubule cells, shown schematically in (B), because of its extensive brush border membrane on the luminal (or tubule lumen-facing) surface. Proximal convoluted tubule cells are polarized epithelial cells with tight junctions separating apical membranes, the luminal surface, and basolateral membranes facing capillaries, the serosal surface.

Table I-1. Summary of permeant selectivities and apparent affinitities (K_m values) of hENTs for various permeants.

Nucleoside	hENT1		hENT2		hENT3		hENT4	
	Permeant[a]	K_m (μM)[b]	Permeant[a]	K_m (μM)[b]	Permeant[a]	K_m (μM)[b]	Permeant[a]	K_m (μM)[b]
adenosine	Yes	40	Yes	140	Yes	1900	Yes	780
2′-deoxyadenosine	Yes	-	Yes	-	-	-	-	-
fludarabine	Yes	107	Yes	-	Yes	-	-	-
cladribine	Yes	23	Yes	-	Yes	-	-	-
clofarabine	Yes	108	Yes	328	-	-	-	-
adenine	No	-	Yes	1100	Yes	-	No	-
hypoxanthine	No	-	Yes	700	No	-	No	-
guanosine	Yes	140	Yes	-	Yes	-	No	-
ribavirin	-	-	-	-	-	-	-	-
inosine	Yes	170	Yes	50	Yes	-	-	-
didanosine	Poor	7400	Yes	2300	Yes	-	-	-
6-mercaptopurine	-	-	Yes	-	-	-	-	-
6-thioguanine	-	-	Yes	-	-	-	-	-
uridine	Yes	260	Yes	250	Yes	2000	No	-
5-fluorouridine	Yes	-	Yes	-	Poor	-	-	-
2′-deoxy-5-fluorouridine	Yes	-	Yes	-	Yes	-	-	-
5′-deoxy-5-fluorouridine	Yes	-	Yes	-	-	-	-	-
uracil	No	-	Yes	2600			No	-
thymidine	Yes	300	Yes	710	-	-	No	-
zidovudine	No	-	Poor	-	Yes	-	-	-
thymine	No	-	Yes	1700	-	-	No	-
cytidine	Yes	580	Poor	5600	Yes	-	No	-
gemcitabine	Yes	160	Yes	740	Poor	-	-	-
cytarabine	Yes	-	Poor	-	-	-	-	-
zalcitabine	Poor	23000	Yes	>7500	Yes	-	-	-
References	3,27,103,104,106, 109.110		3,10,11,34,102-104.106.108-110		3,111		3,12	

a - Permeant selectivities denoted here are obtained from: 1) uptake studies in Xenopus oocytes and Saccharomyces cerevisae expressing recombinant hNTs and/or 2) uptake studies in mammalian cells expressing native or recombinant hNTs.

b - Reported apparent affinities (K_m values) of hNTs for nucleosides denoted here are obtained from uptake studies in mammalian cells expressing native or recombinant hNTs. Where studies have not been conducted in mammalian cells, reported apparent affinities (K_m values) of hNTs for nucleosides are obtained from uptake studies in Xenopus oocytes and/or Saccharomyces cerevisae expressing recombinant hNTs.

Table I-2. Summary of inhibitor apparent affinities (K_i values) of hENTs for various inhibitors

Transporter	Inhibitor K_i (μM)[a]			References
	NBMPR	Dilazep	Dipyridamole	
hENT1	0.005	0.02	0.05	3,27,109
hENT2	> 1	5	130	3,34,102,109
hENT3	>10	> 10	> 10	3,111
hENT4	> 1	> 1	> 1	3,12

a - Reported apparent inhibitor sensitivities (K_i values) denoted here were obtained from inhibition of uridine influx studies in Xenopus oocytes and/or Saccharomyces cerevisae expressing recombinant hENTs.

Table I-3. Summary of permeant selectivities and apparent affinities (K_m values) of hCNTs for various permeants.

Nucleoside	hCNT1		hCNT2		hCNT3	
	Permeant[a]	K_m (μM)[b]	Permeant[a]	K_m (μM)[b]	Permeant[a]	K_m (μM)[b]
adenosine	Poor	-	Yes	8	Yes	5 and 2[c]
2′-deoxyadenosine	Poor	-	Yes	-	Yes	-
fludarabine	No	-	Yes	-	Yes	-
cladribine	Poor	-	Yes	-	Yes	-
clofarabine	No	-	Yes	81	Yes	52
adenine	No	-	No	-	No	-
hypoxanthine	No	-	No	-	No	-
guanosine	No	-	Yes	-	Yes	5 and 9
ribavirin	No	-	Yes	18	Yes	14
inosine	No	-	Yes	13	Yes	4
didanosine	No	-	Yes	-	Yes	-
6-mercaptopurine	-	-	-	-	Yes	-
6-thioguanine	-	-	-	-	Yes	-
uridine	Yes	35	Yes	46 and 116	Yes	1 and 5
5-fluorouridine	Yes	18	-	-	Yes	-
2′-deoxy-5-fluorouridine	Yes	15	Yes	-	Yes	-
5′-deoxy-5-fluorouridine	Yes	209	Yes	-	Yes	-
uracil	No	-	No	-	No	-
thymidine	Yes	26	No	-	Yes	4 and 11
zidovudine	Yes	450	-	-	Yes	310
thymine	No	-	No	-	No	-
cytidine	Yes	3 and 120	Yes	-	Yes	3
gemcitabine	Yes	24	No	-	Yes	60
cytarabine	Poor	-	No	-	Yes	-
zalcitabine	Poor	-	No	-	Yes	-
References	4, 103, 110, 126, 130, 131, 134		4, 103, 110, 127, 128, 131, 134		4, 110, 129, 132-136	

a - Permeant selectivities denoted here are obtained from 1) uptake studies in Xenopus oocytes and Saccharomyces cerevisae expressing recombinant hNTs and/or 2) uptake studies in mammalian cells expressing native or recombinant hNTs.

b - Reported apparent affinities (K_m values) of hNTs for nucleosides denoted here are obtained from uptake studies in mammalian cells expressing native or recombinant hNTs. Where studies have not been conducted in mammalian cells, reported apparent affinities (K_m values) of hNTs for nucleosides are obtained from uptake studies in *Xenopus* oocytes and/or *Saccharomyces cerevisae* expressing recombinant hNTs.

c - Where two values are reported the first and second values represent K_m values obtained, respectively, in *Xenopus* oocytes and Saccharamyces cerevisae expressing recombinant hNTs.

I.8 Bibliography

1. Elion GB. The purine path to chemotherapy. Science. 1989; 244: 41-47.

2. Burnstock G. Purine and pyrimidine receptors. Cell Mol Life Sci. 2007; 64: 1471-1483.

3. Young JD, Yao SYM, Sun L, Cass CE, Baldwin SA. Human equilibrative nucleoside transporter (ENT) family of nucleoside and nucleobase transporter proteins. Xenobiotica. 2008; 38: 995-1021.

4. Pastor-Anglada M, Cano-soldado P, Errasti-murugarren E, Casado FJ. SLC28 genes and concentrative nucleoside transporter (CNT) proteins. Xenobiotica. 2008; 38: 972-994.

5. Ciarimboli G. Organic cation transporters. Xenobiotica 2008; 28: 936-971.

6. Srimaroeng C, Perry JL, Pritchard JB. Physiology, structure, and regulation of the cloned organic anion transporters. Xenobiotica 2008; 38: 889-935.

7. Zhou SF. Structure, function and regulation of P-glycoprotein and its clinical relevance in drug disposition. Xenobiotica 2008; 38: 802-832

8. Koshiba S, An R, Saito H, Wakabayashi K, Tamura A, Ishikawa T. Human ABC transporters ABCG2 (BCRP) and ABCG4. Xenobiotica 2008; 38: 863-888

9. Y, Hagiya Y, Adachi T, Hoshijima K, Kuo MT, Ishikawa T. MRP class of human ATP binding cassette (ABC) transporters: historical background and new research directions. Xenobiotica 2008; 28: 833-862

10. Yao SY, Ng AM, Vickers MF, Sundaram M, Cass CE, Baldwin SA, Young JD. Functional and molecular characterization of nucleobase transport by recombinant human and rat equilibrative nucleoside transporters 1 and 2. Chimeric constructs reveal a role for the ENT2 helix 5-6 region in nucleobase translocation. J Biol Chem. 2002; 277: 24938-24948.

11. Nagai K, Nagasawa K, Kihara Y, Okuda H, Fujimoto S. Anticancer nucleobase analogues 6-mercaptopurine and 6-thioguanine are novel

substrates for equilibrative nucleoside transporter 2. Int J Pharm. 2007; 333: 56-61.

12. Barnes K, Dobrzynski H, Foppolo S, Beal PR, Ismat F, Scullion ER, Sun L, Tellez J, Ritzel MW, Claycomb WC, Cass CE, Young JD, Billeter-Clark R, Boyett MR, Baldwin SA. Distribution and functional characterization of equilibrative nucleoside transporter-4, a novel cardiac adenosine transporter activated at acidic pH. Circ Res. 2006; 99: 510-519.

13. Kobayashi Y, Ohshiro N, Sakai R, Ohbayashi M, Kohyama N, Yamamoto T. Transport mechanism and substrate specificity of human organic anion transporter 2 (hOat2 [SLC22A7]). J Pharm Pharmacol. 2005; 57: 573-578.

14. Kobayashi Y, Ohshiro N, Tsuchiya A, Kohyama N, Ohbayashi M, Yamamoto T. Renal transport of organic compounds mediated by mouse organic anion transporter 3 (mOat3): further substrate specificity of mOat3. Drug Metab Dispos. 2004; 32: 479-483.

15. Zeng H, Lin ZP, Sartorelli AC. Resistance to purine and pyrimidine nucleoside and nucleobase analogs by the human MDR1 transfected murine leukemia cell line L1210/VMDRC.06. Biochem Pharmacol. 2004; 68: 911-21.

16. Reid G, Wielinga P, Zelcer N, de Haas M, van Deemter L, Wijnholds J, BaUatini J, Borst P. Characterization of the transport of nucleoside analog drugs by the human multidrug resistance proteins MRP4 and MRP5. Mol Pharmacol. 2003; 63: 1094-1103.

17. T, Bessho Y, Achiwa H, Ozasa H, Maeno K, Maeda H, Sato S, Ueda R. MRP8/ABCC11 directly confers resistance to 5-fluorouracil. Mol Cancer Ther. 2007; 6: 122-127.

18. Wohlhueter RM, McIvor RS, Plagemann PG. Facilitated transport of uracil and 5-fluorouracil, and permeation of orotic acid into cultured mammalian cells. J Cell Physiol. 1980; 104: 309-319.

19. Shayeghi M, Akerman R, Jarvis SM. Nucleobase transport in opossum kidney epithelial cells and Xenopus laevis oocytes: the characterisation, structure-activity relationship of uracil analogues and oocyte expression studies of sodium-dependent and -independent hypoxanthine uptake. Biochim Biophys Acta. 1999; 1416: 109-118.

20. Griffith DA, Jarvis SM. Characterization of a sodium-dependent concentrative nucleobase-transport system in guinea-pig kidney cortex brush-border membrane vesicles. Biochem J. 1994; 303: 901-905.

21. Griffith DA, Jarvis SM. High affinity sodium-dependent nucleobase transport in cultured renal epithelial cells (LLC-PK1). J Biol Chem. 1993; 268: 20085-20090.

22. Faaland CA, Race JE, Ricken G, Warner FJ, Williams WJ, Holtzman EJ. Molecular characterization of two novel transporters from human and mouse kidney and from LLC-PK1 cells reveals a novel conserved family that is homologous to bacterial and Aspergillus nucleobase transporters. Biochim Biophys Acta. 1998; 1442: 353-360.

23. Murray AW. The biological significance of purine salvage. Ann Rev Biochem. 1971; 40: 811-26.

24. Hellsten-Westing Y, Kaijser L, Ekblom B, Sjodin B. Exchange of purines in human liver and skeletal muscle with short-term exhaustive exercise. Am J Physiol Reg Int Comp Physiol. 1994; 266: R81-R86.

25. Carver JD, Walker A. The role of nucleotides in human nutrition. Nutr Biochem 1995; 6: 58-72.

26. Kwong FY, Davies A, Tse CM, Young JD, Henderson PJ, Baldwin SA. Purification of the human erythrocyte nucleoside transporter by immunoaffinity chromatography. Biochem J. 1988; 255: 243-249.

27. Griffiths M, Beaumont N, Yao SY, Sundaram M, Boumah CE, Davies A, Kwong FY, Coe I, Cass CE, Young JD, Baldwin SA. Cloning of a human nucleoside transporter implicated in the cellular uptake of adenosine and chemotherapeutic drugs. Nat Med. 1997; 3: 89-93.

28. Young JD, Jarvis SM, Clanachan AS, Henderson JF, Paterson AR. Nitrobenzylthioinosine: an in vivo inhibitor of pig erythrocyte energy metabolism. Am J Physiol. 1986; 251: C90-C94.

29. Mathew A, Grdisa M, Johnstone RM. Nucleosides and glutamine are primary energy substrates for embryonic and adult chicken red cells. Biochem Cell Biol. 1993; 71: 288-295.

30. Soler C, Felipe A, Casado FJ, Celada A, Pastor-Anglada M. Nitric oxide regulates nucleoside transport in activated B lymphocytes. J Leukoc Biol. 2000; 67: 345-349.

31. Sakowicz M, Szutowicz A, Pawelczyk T. Insulin and glucose induced changes in expression level of nucleoside transporters and adenosine transport in rat T lymphocytes. Biochem Pharmacol. 2004; 68: 1309-1320.

32. Soler C, García-Manteiga J, Valdés R, Xaus J, Comalada M, Casado FJ, Pastor-Anglada M, Celada A, Felipe A. Macrophages require different nucleoside transport systems for proliferation and activation. FASEB J. 2001; 15: 1979-1988.

33. Peng L, Huang R, Yu AC, Fung KY, Rathbone MP, Hertz L. Nucleoside transporter expression and function in cultured mouse astrocytes. Glia. 2005; 52: 25-35.

34. Griffiths M, Yao SY, Abidi F, Phillips SE, Cass CE, Young JD, Baldwin SA. Molecular cloning and characterization of a nitrobenzylthioinosine-insensitive (ei) equilibrative nucleoside transporter from human placenta. Biochem J. 1997; 328: 739-743.

35. Choi DS, Cascini MG, Mailliard W, Young H, Paredes P, McMahon T, Diamond I, Bonci A, Messing RO. The type 1 equilibrative nucleoside transporter regulates ethanol intoxication and preference. Nat Neurosci. 2004; 7: 855-861.

36. Chen J, Rinaldo L, Lim SJ, Young H, Messing RO, Choi DS. The type 1 equilibrative nucleoside transporter regulates anxiety-like behavior in mice. Genes Brain Behav. 2007; 6: 776-783.

37. Farrell JJ, Elsaleh H, Garcia M, Lai R, Ammar A, Regine WF, Abrams R, Benson AB, Macdonald J, Cass CE, Dicker AF, Mackey JR. Human equilibrative nucleoside ransporter 1 levels predict response to gemcitabine in patients with pancreatic cancer. Gastroenterol. 2008 [Epub ahead of print].

38. Pastor-Anglada M, Cano-Soldado P, Molina-Arcas M, Lostao MP, Larráyoz I, Martínez-Picado J, Casado FJ. Cell entry and export of nucleoside analogues. Virus Res. 2005; 107: 151-164.

39. Cohen A, Barankiewicz J, Lederman HM, Gelfand EW. Purine and pyrimidine metabolism in human T lymphocytes. Regulation of deoxyribonucleotide metabolism. J Biol Chem. 1983; 258: 12334-12340.

40. Vallon V, Muhlbauer B, Osswald H. Adenosine and kidney function. Physiol Rev. 2006; 86: 901-940.

41. Cooper DM. Regulation and organization of adenylyl cyclases and cAMP. Biochem J. 2003; 375: 517-529.

42. Lucas KA, Pitari GM, Kazerounian S, Ruiz-Stewart I, Park J, Schulz S, Chepenik KP, Waldman SA. Guanylyl cyclases and signaling by cyclic GMP. Pharmacol Rev. 2000; 52: 375-414.

43. Rudolph FB. The biochemistry and physiology of nucleotides. J Nutr. 1994; 124: 124S-130S.

44. Ishitani R, Yokoyama S, Nureki O. Structure, dynamics, and function of RNA modification enzymes. Curr Opin Struct Biol. 2008; 18: 330-339.

45. Nordlund P, Reichard P. Ribonucleotide reductases. Annu Rev Biochem. 2006; 75: 681-706.

46. Green H, Chan T-S. Pyrimidine starvation induced by adenosine in fibroblasts and lymphoid cells: role of adenosine deaminase. Science. 1973; 182: 836-837.

47. Klenow H. Further studies on the effect of deoxyadenosine on the accumulation of deoxyadenosine triphosphate and inhibition of deoxyribonucleic acid synthesis in Ehrlich ascites tumor cells in vitro. Biochim Biophys Acta. 1962; 61: 885-896.

48. Kuttesch JF Jr, Nelson JA. Renal handling of 2'-deoxyadenosine and adenosine in humans and mice. Cancer Chemother Pharmacol. 1982; 8: 221-229.

49. Tatersall MHN, Slowiaczek P, De Fazio A. Regional variation of human extracellular purine levels. J Lab Clin Med. 1983; 102: 411-420.

50. Wilkinson H, Samuell C, Stower M. 2,8-Dihydroxyadenine renal stones in a 41-year-old man Ann Clin Biochem. 2004; 41: 160-161.

51. Yamamoto T, Yokoyama H, Moriwaki Y, Takahashi S, Suda M, Hada T, Higashino K. The effect of completely purine-free diet of low sodium content on purine intermediates and end-product. Eur J Clin Nutr. 1990; 44: 659-664.

52. Ericson A, Groth T, Niklasson F, de Verdier CH. Plasma concentration and renal excretion of adenine and 2,8-dihydroxyadenine after administration of adenine in man. Scand J Clin Lab Invest. 1980; 40: 1-8.

53. Gourdeau H, Clarke ML, Ouellet F, Mowles D, Selner M, Richard A, Lee N, Mackey JR, Young JD, Jolivet RG, Lafrenier RG, Cass CE. Mechanisms of uptake and resistance to troxacitabine, a novel deoxycytidine nucleoside analogue, in human leukemic and solid tumor cell lines. Cancer Res. 2001; 61: 7217-7224.

54. August EM, Birks EM, Prusoff WH. 3'-Deoxythymidin-2'-ene permeation of human lymphocyte H9 cells by nonfacilitated diffusion. Mol Pharmacol. 1991; 39: 246-249.

55. Zhang J, Visser F, King KM, Baldwin SA, Young JD, Cass CE. The role of nucleoside transporters in cancer chemotherapy with nucleoside drugs Cancer Metastasis Rev. 2007; 26: 85-110.

56. Stanulla M, Schümann HJ, Vora A, Mitchell CD, Lennard L, Eden TOB, Kinsey SE, Lilleyman J, Richards SM. Toxicity and efficacy of 6-thioguanine versus 6- mercaptopurine in childhood lymphoblastic leukaemia : a randomised trial. Commentary. Lancet. 2006; 368: 1304-1306.

57. Bishop JF, Matthews JP, Young GA, Szer J, Gillett A, Joshua D, Bradstock K, Enno A, Wolf MM, Fox R, Cobcroft R, Herrmann R, Van Der Weyden M, Lowenthal RM, Page F, Garson OM, Juneja S. A randomized study of high-dose cytarabine in induction in acute myeloid leukemia. Blood. 1996; 87: 1710-1717.

58. Johnson S, Smith AG, Löffler H, Osby E, Juliusson G, Emmerich B, Wyld PJ, Hiddemann W. Multicentre prospective randomised trial of fludarabine versus cyclophosphamide, doxorubicin, and prednisone (CAP) for treatment

of advanced-stage chronic lymphocytic leukaemia. The French Cooperative Group on CLL. Lancet. 1996; 347: 1432-1438.

59. Robak T, Wierzbowska A, Robak E. Recent clinical trials of cladribine in hematological malignancies and autoimmune disorders. Rev Recent Clin Trials. 2006; 1: 15-34.

60. Jeha S, Gaynon PS, Razzouk BI, Franklin J, Kadota R, Shen V, Luchtman-Jones L, Rytting M, Bomgaars LR, Rheingold S, Ritchey K, Albano E, Arceci RJ, Goldman S, Griffin T, Altman A, Gordon B, Steinherz L, Weitman S, Steinherz P. Phase II study of clofarabine in pediatric patients with refractory or relapsed acute lymphoblastic leukemia. J Clin Oncol. 2006; 24: 1917-1923.

61. Abbruzzese JL New applications of gemcitabine and future directions in the management of pancreatic cancer. Cancer (Phila). 2002; 95: 941-945.

62. Burris HA 3rd, Moore MJ, Andersen J, Green MR, Rothenberg ML, Modiano MR, Cripps MC, Portenoy RK, Storniolo AM, Tarassoff P, Nelson R, Dorr FA, Stephens CD, Von Hoff DD. Improvements in survival and clinical benefit with gemcitabine as first-line therapy for patients with advanced pancreas cancer: a randomized trial. J Clin Oncol. 1997; 15: 2403-2413.

63. Lee KS, Ro J, Nam BH, Lee ES, Kwon Y, Kwon HS, Chung KW, Kang HS, Kim EA, Kim SW, Shin KH, Kim SK. A randomized phase-III trial of docetaxel/capecitabine versus doxorubicin/cyclophosphamide as primary chemotherapy for patients with stage II/III breast cancer. Breast Cancer Res Treat. 2008; 109: 481-489.

64. Cassidy J, Clarke S, Díaz-Rubio E, Scheithauer W, Figer A, Wong R, Koski S, Lichinitser M, Yang TS, Rivera F, Couture F, Sirzén F, Saltz L. Randomized phase III study of capecitabine plus oxaliplatin compared with fluorouracil/folinic acid plus oxaliplatin as first-line therapy for metastatic colorectal cancer. J Clin Oncol. 2008; 26: 2006-2012.

65. Bernhard J, Dietrich D, Scheithauer W, Gerber D, Bodoky G, Ruhstaller T, Glimelius B, Bajetta E, Schüller J, Saletti P, Bauer J, Figer A, Pestalozzi BC, Köhne CH, Mingrone W, Stemmer SM, Tàmas K, Kornek GV, Koeberle D, Herrmann R; Central European Cooperative Oncology Group. Clinical benefit and quality of life in patients with advanced pancreatic

cancer receiving gemcitabine plus capecitabine versus gemcitabine alone: a randomized multicenter phase III clinical trial--SAKK 44/00-CECOG/PAN.1.3.001. J Clin Oncol. 2008; 26: 3695-3701.

66. Scheithauer W, McKendrick J, Begbie S, Borner M, Burns WI, Burris HA, Cassidy J, Jodrell D, Koralewski P, Levine EL, Marschner N, Maroun J, Garcia-Alfonso P, Tujakowski J, Van Hazel G, Wong A, Zaluski J, Twelves C; X-ACT Study Group. Oral capecitabine as an alternative to i.v. 5-fluorouracil-based adjuvant therapy for colon cancer: safety results of a randomized, phase III trial. Ann Oncol. 2003; 14: 1735-1743.

67. Warnke D, Barreto J, Temesgen Z. Antiretroviral drugs. J Clin Pharmacol. 2007; 47: 1570-1579.

68. Suzuki M, Okuda T, Shiraki K. Synergistic antiviral activity of acyclovir and vidarabine against herpes simplex virus types 1 and 2 and varicella-zoster virus. Antiviral Res. 2006; 72: 157-161.

69. Mosca F, Pugni L. Cytomegalovirus infection: the state of the art. J Chemother. 2007; 19: 46-48.

70. Roffi L, Colloredo G, Pioltelli P, Bellati G, Pozzpi M, Parravicini P, Bellia V, Del Poggio P, Fornaciari G, Ceriani R, Ramella G, Corradi C, Rossini A, Bruno S; Gruppo Epatologico Lombardo. Pegylated interferon-alpha2b plus ribavirin: an efficacious and well-tolerated treatment regimen for patients with hepatitis C virus related histologically proven cirrhosis. Antivir Ther. 2008; 13: 663-673.

71. Miwa M, Ura M, Nishida M, Sawada N, Ishikawa T, Mori K, Shimma N, Umeda I, Ishitsuka H. Design of a novel oral fluoropyrimidine carbamate, capecitabine, which generates 5-fluorouracil selectively in tumours by enzymes concentrated in human liver and cancer tissue. Eur J Cancer. 1998; 34: 1274-1281.

72. Wilkinson DS, Tisty TD, Hanas RJ. The inhibition of ribosomal RNA synthesis and maturation in Novikoff hepatoma cells by 5-fluorouridine. Cancer Res. 1965; 35: 3014-3020.

73. Lonn U, Lonn S. DNA lesions in human neoplastic cells and cytotoxicity of 5-fluoropyrmidines. Cancer Res. 1986; 46: 3866-3870.

74. Santi DV, McHenry CS, Sommer A. Mechanisms of interactions of thymidylate synthetase with 5-fluorodeoxyuridylate. Biochem. 1974; 13: 471-480.

75. Major PP, Egan EM, Herrick DJ, Kufe DW. Effect of ARA-C incorporation on deoxyribonucleic acid synthesis in cells. Biochem Pharmacol. 1982; 31: 2937-2940.

76. Huang P, Chubb S, Hertel LW, Grindey GB, Plunkett W. Action of 2',2'-difluorodeoxycytidine on DNA synthesis. Cancer Res. 1991; 51: 6110-6117.

77. Huang P, Chubb S, Plunkett W. Termination of DNA synthesis by 9-beta-D-arabinofuranosyl-2-fluoroadenine. A mechanism for cytotoxicity. J Biol Chem. 1990; 265: 16617-16625.

78. Plunkett W, Huang P, Gandhi V. Metabolism and action of fludarabine phosphate. Semin Oncol. 1990; 17: 3-17.

79. Gandhi V, Huang P, Chapman A, Chen F, Plunkett W. Incorporation of fludarabine and 1-β-D-arabinosylcytosine 5′-triphosphates by DNA polymerase α: affinity, interaction, and consequences. Clin Cancer Res. 1997; 3: 1347-55.

80. Gandhi V, Plunkett W. Cellular and clinical pharmacology of fludarabine. Clin Pharmacokinet. 2002; 41: 93-103.

81. Seto S, Carrera CJ, Kubota M, Wasson DB, Carson DA. Mechanism of deoxyadenosine and 2-chlorodeoxyadenosine toxicity to nondividing human lymphocytes. J Clin Invest. 1985; 75: 377-383.

82. Parker WB, Shaddix SC, Chang CH, White EL, Rose LM, Brockman RW, Shortnacy AT, Montgomery JA, Secrist JA 3rd, Bennett LL Jr. Effects of 2-chloro-9-(2-deoxy-2-fluoro-beta-D-arabinofuranosyl)adenine on K562 cellular metabolism and the inhibition of human ribonucleotide reductase and DNA polymerases by its 5'-triphosphate. Cancer Res. 1991; 51: 2386-2394.

83. Swann PF, Waters TR, Moulton DC, Xu YZ, Zheng Q, Edwards M, Mace R. Role of postreplicative DNA mismatch repair in the cytotoxic action of thioguanine. Science. 1996; 273: 1109-1111.

84. Waters TR, Swann PF. Cytotoxic mechanism of 6-thioguanine: hMutSalpha, the human mismatch binding heterodimer, binds to DNA containing S6-methylthioguanine. Biochem. 1997; 36: 2501-2506.

85. Heinemann V, Xu YZ, Chubb S, Sen A, Hertel LW, Grindey GB, Plunkett W. Inhibition of ribonucleotide reduction in CCRF-CEM cells by 2',2'-difluorodeoxycytidine. Mol Pharmacol. 1990; 38: 567-572.

86. Parker WB, Bapat AR, Shen JX, Townsend AJ, Cheng YC. Interaction of 2-halogenated dATP analogs (F, Cl, and Br) with human DNA polymerases, DNA primase, and ribonucleotide reductase. Mol Pharmacol. 1988; 34: 485-491.

87. Huang P, Plunkett W. Action of 9-β-D-arabinofuranosyl-2-fluoroadenine on RNA metabolism. Mol Pharmacol. 1991; 39: 449-455.

88. Chen LS, Plunkett W, Gandhi V. Polyadenylation inhibition by the triphosphates of deoxyadenosine analogues. Leuk Res. 2008; 32: 1573-1581.

89. Stein DS, Moore KH. Phosphorylation of nucleoside analog antiretrovirals: a review for clinicians. Pharmacotherapy. 2001; 21: 11-34.

90. Donelli mG, D'Incalci M, Garattini S. Pharmacokinetic studies of anticancer drugs in tumor-bearing animals. Cancer Treat Rep. 1984; 68: 381.

91. Goldsmith MA, Slavik M, Carter SK. Quantitative prediction of drug toxicity in humans from toxicology in small and large animals. Cancer Res. 1975; 35: 1354.

92. Cassidy J, Twelves C, Cameron D, Steward W, O'Byrne K, Jodrell D, Banken L, Goggin T, Jones D, Roos B, Bush E, Weidekamm E, Reigner B. Bioequivalence of two tablet formulations of capecitabine and exploration of age, gender, body surface area, and creatinine clearance as factors influencing systemic exposure in cancer patients. Cancer Chemother Pharmacol. 1999; 44: 453-460.

93. Abbruzzese JL, Grunewald R, Weeks EA, Gravel D, Adams T, Nowak B, Mineishi S, Tarassoff P, Satterlee W, Raber MN, et al. A phase I clinical,

plasma, and cellular pharmacology study of gemcitabine. J Clin Oncol. 1991; 9: 491-498

94. Poole C, Gardiner J, Twelves C, Johnston P, Harper P, Cassidy J, Monkhouse J, Banken L, Weidekamm E, Reigner B. Effect of renal impairment on the pharmacokinetics and tolerability of capecitabine (Xeloda) in cancer patients. Cancer Chemother Pharmacol. 2002; 49: 225-234.

95. Venook AP, Egorin MJ, Rosner GL, Hollis D, Mani S, Hawkins M, Byrd J, Hohl R, Budman D, Meropol NJ, Ratain MJ. Phase I and pharmacokinetic trial of gemcitabine in patients with hepatic or renal dysfunction: Cancer and Leukemia Group B 9565. J Clin Oncol. 2000; 18: 2780-2787.

96. Powis G. Effect of human renal and hepatic disease on the pharmacokinetics of anticancer drugs. Cancer Treat Rev. 1982; 9: 85.

97. Coresh J, Stevens LA. Kidney function estimating equations: where do we stand? Curr Opin Nephrol Hypertens. 2006; 15: 276-284.

98. Thyss A, Milano G, Renée N, Vallicioni J, Schneider M, Demard F. Clinical pharmacokinetic study of 5-FU in continuous 5-day infusions for head and neck cancer. Cancer Chemother Pharmacol. 1986; 16: 64-66.

99. Liliemark JO, Plunkett W, Dixon DO. Relationship of 1-beta-D-arabinofuranosylcytosine in plasma to 1-beta-D-arabinofuranosylcytosine 5'-triphosphate levels in leukemic cells during treatment with high-dose 1-beta-D-arabinofuranosylcytosine. Cancer Res. 1985; 45: 5952-5957.

100. Plunkett W, Liliemark JO, Adams TM, Nowak B, Estey E, Kantarjian H, Keating MJ. Saturation of 1-beta-D-arabinofuranosylcytosine 5'-triphosphate accumulation in leukemia cells during high-dose 1-beta-D-arabinofuranosylcytosine therapy. Cancer Res. 1987; 47: 3005-3011.

101. Avramis VI, Biener R, Krailo M, Finklestein J, Ettinger L, Willoughby M, Siegel SE, Holcenberg JS Biochemical pharmacology of high dose 1-beta-D-arabinofuranosylcytosine in childhood acute leukemia. Cancer Res. 1987; 47: 6786-6792.

102. Crawford CR, Patel DH, Naeve C, Belt JA. Cloning of the human equilibrative, nitrobenzylmercaptopurine riboside (NBMPR)-insensitive nucleoside transporter ei by functional expression in a transport-deficient cell line. J Biol Chem. 1998; 273: 5288-5293.

103. Mackey JR, Yao SY, Smith KM, Karpinski E, Baldwin SA, Cass CE, Young JD. Gemcitabine transport in Xenobpus oocytes expressing recombinant plasma membrane mammalian nucleoside transporters. J Nat Cancer Inst. 1999; 91: 1876-1881.

104. Ward JL, Sherali A, Mo Z-P, Tse C-M. Kinetic and pharmacological properties of cloned human equilibrative nucleoside transporters, ENT1 and ENT2, stably expressed in nucleoside transporter-deficient PK15 cells. J Biol Chem. 2000; 275: 8375-8381.

105. Hyde RJ, Cass CE, Young JD, Baldwin SA. The ENT family of eukaryote nucleoside and nucleobase transporters: recent advances in the investigation of structure-function relationships and the identification of novel isoforms. Mol Membr Biol. 2001; 18: 53-63.

106. Yao SYM, Ng AML, Sundaram M, Cass CE, Baldwin SA, Young JD. Transport of antiviral 3'-deoxy-nucleoside drugs by recombinant human and rat equilibrative, nitrobenzylthioinosine (NBMPR)-insensitive (ENT2) nucleoside transporter proteins produced in Xenopus oocytes. Mol Membr Biol. 2001; 18: 161-167.

107. Acimovic Y, Coe IR. Molecular evolution of the equilibrative nucleoside transporter family: identification of novel family members in prokaryotes and eukaryotes. Mol Biol Evol. 2002; 19: 2199-2210.

108. Vickers MF, Kumar R, Visser F, Zhang J, Charania J, Raborn RT, Baldwin SA, Young JD, Cass CE. Comparison of the interaction of uridine, cytidine, and other pyrimidine nucleoside analogues with recombinant human equilibrative nucleoside transporter 2 (hENT2) produced in Saccharomyces cerevisiae. Biochem Cell Biol. 2002; 80: 639-644.

109. Visser F, Vickers MF, Ng AML, Baldwin SA, Young JD, Cass CE. Mutation of residue 33 of human equilibrative nucleoside transporters 1 and 2 alters sensitivity to inhibition of transport by dilazep and dipyridamole. J Biol Chem. 2002; 277: 395-401.

110. King KM, Damaraju VL, Vickers MF, Yao SY, Lang T, Tackaberry TE, Mowles DA, Ng AM, Young JD, Cass CE. A comparison of the transportability, and its role in cytotoxicity, of clofarabine, cladribine, and fludarabine by recombinant human nucleoside transporters produced in three model expression systems. Mol Pharmacol. 2006; 69: 346-353.

111. Baldwin SA, Yao SYM, Hyde RJ, Foppolo S, Barnes K, Ritzel MWL, Cass CE, Young JD. Functional Characterization of novel human mouse equilibrative nucleoside transporters (hENT3 and mENT3) located in intracellular membranes. J Biol Chem. 2007; 280: 15880-15887.

112. Engel K, Zhou M, Wang J. Identification and characterization of a novel monoamine transporter in human brain. J Biol Chem. 2004; 279: 50042-50049.

113. Engel K, Wang J. Interaction of organic cations with a newly identified plasma membrane monoamine transporter (PMAT). Mol Pharmacol. 2005; 68: 1397-1407.

114. Govindarajan R, Leung GP, Zhou M, Tse CM, Wang J, Unadkat JD. Facilitated Mitochondrial Import of Anti-viral and Anti-cancer Nucleoside Drugs by Human Equilibrative Nucleoside Transporter-3 (hENT3). Am J Physiol Gastrointest Liver Physiol. 2009; [Epub ahead of print].

115. Molho-Pessach V, Lerer I, Abeliovich D, Agha Z, Abu Libdeh A, Broshtilova V, Elpeleg O, Zlotogorski A. The H syndrome is caused by mutations in the nucleoside transporter hENT3. Am J Hum Genet. 2008; 83: 529-534.

116. Xia L, Engel K, Zhou M, Wang J. Membrane localization and pH-dependent transport of newly cloned organic cation transport (PMAT) in kidney cells. Am. J. Physiol. Renal Physiol. 2007; 292: F682-F690.

117. Zhou M, Engel K, Wang J. Evidence for significant contribution of a newly identified monoamine transporter (PMAT) to serotonin uptake in the human brain. Biochem Pharmacol. 2006; 73: 147-154.

118. Pressacco J, Wiley JS, Jamieson GP, Erlichman C, Hedley DW. Modulation of the equilibrative nucleoside transporter by inhibitors of DNA-synthesis. Brit J Cancer. 1995; 72: 939-942.

119. Pressacco J, Mitrovski B, Erlichman C, Hedley DW. Effects of thymidylate synthase inhibition on thymidine kinase activity and nucleoside transporter expression. Cancer Res. 1995; 55: 1505-1508.

120. Eltzschig HK, Abdulla P, Hoffman E, Hamilton KE, Daniels D, Schönfeld C, Löffler M, Reyes G, Duszenko M, Karhausen J, Robinson A, Westerman KA, Coe IR, Colgan SP. HIF-1-dependent repression of equilibrative nucleoside transporter (ENT) in hypoxia. J Exp Med. 2005; 202: 1493-1505.

121. Abdulla P, Coe IR. Characterization and functional analysis of the promoter for the human equilibrative nucleoside transporter gene, hENT1. Nucleosides Nucleotides Nucleic Acids. 2007; 26: 99-110.

122. Coe I, Zhang Y, McKenzie T, Naydenova Z. PKC regulation of the human equilibrative nucleoside transporter, hENT1. FEBS Lett. 2002; 517: 201-205.

123. Parodi J, Flores C, Aguayo C, Rudolph MI, Casanello P, Sobrevia L. Inhibition of nitrobenzylthioinosine-sensitive adenosine transport by elevated D-glucose involves activation of P2Y2 purinoceptors in human umbilical vein endothelial cells. Circ Res. 2002; 90: 570-577.

124. Chaudary N, Naydenova Z, Shuralyova I, Coe IR. The adenosine transporter, mENT1, is a target for adenosine receptor signaling and protein kinase C epsilon in hypoxic and pharmacological preconditioning in the mouse cardiomyocyte cell line, HL-1. J Pharmacol Exp Ther. 2004; 310: 1190-1198.

125. Dantzler WH. Regulation of renal proximal and distal tubule transport: sodium, chloride and organic anions. Comp Biochem Physiol. 2003; 136: 453-478.

126. Ritzel MW, Yao SY, Huang MY, Elliott JF, Cass CE, Young JD. Molecular cloning and functional expression of cDNAs encoding a human Na+ nucleoside cotransporter (hCNT1). Am J Physiol Cell Physiol. 1997; 272: C707-C714.

127. Wang J, Su SF, Dresser MJ, Schaner ME, Washington CB, Giacomini KM. Na+ dependent purine nucleoside transporter from human kidney: cloning and functional characterization. Am J Physiol Renal Physiol. 1997; 273: F1058-F1065.

128. Ritzel MW, Yao SY, Ng AM, Mackey JR, Cass CE, Young JD. Molecular cloning, functional expression and chromosomal localization of a cDNA encoding a human Na+/nucleoside cotransporter (hCNT2) selective for purine nucleosides and uridine. Mol Membr Biol. 1998; 15: 203-211.

129. Ritzel MW, Ng AM, Yao SY, Graham K, Loewen SK, Smith KM, Ritzel RG, Mowles DA, Carpenter P, Chen XZ, Karpinski E, Hyde RJ, Baldwin SA, Cass CE, Young JD. Molecular identification and characterization of novel human and mouse concentrative Na+ nucleoside cotransporter proteins (hCNT3 and mCNT3) broadly selective for purine and pyrimidine nucleosides (system cib). J Biol Chem. 2001; 276: 2914-2927.

130. Smith KM, Ng AM, Yao SY, Labedz KA, Knaus EE, Wiebe LI, Cass CE, Baldwin SA, Chen XZ, Karpinski E, Young JD. Electrophysiological characterization of a recombinant human Na+-coupled nucleoside transporter (hCNT1) produced in Xenopus oocytes. J Physiol. 2004; 558: 807-823.

131. Lang TT, Young JD, Cass CE. Interactions of nucleoside analogs, caffeine, and nicotine with human concentrative nucleoside transporters 1 and 2 stably produced in a transport-defective human cell line. Mol Pharmacol. 2004; 65: 925-933.

132. Smith KM, Slugoski MD, Loewen SK, Ng, AM, Yao SY, Chen XZ, Karpinski E, Cass CE, Baldwin SA, Young JD. The broadly selective human Na+/nucleoside cotransporter (hCNT3) exhibits novel cation-coupled nucleoside transport characteristics. J Biol Chem. 2005; 280: 25436-25449.

133. Hu H, Endres CJ, Chang C, Umapathy NS, Lee EW, Fei YJ, Itagaki S, Swaan PW, Ganapathy V, Unadkat JD. Electrophysiological characterization and modeling of the structure activity relationship of the human concentrative nucleoside transporter 3 (hCNT3). Mol Pharmacol. 2006; 65: 1542-1553.

134. Smith KM, Slugoski MD, Cass CE, Baldwin SA, Karpinski E, Young JD. Cation coupling properties of human concentrative nucleoside transporters hCNT1, hCNT2 and hCNT3. Mol Membr Biol. 2007; 24: 53-64.

135. Slugoski MD, Ng AM, Yao SY, Smith KM, Lin CC, Zhang J, Karpinski E, Cass CE, Baldwin SA, Young JD. A proton-mediated conformational shift

identifies a mobile pore-lining cysteine residue (Cys-561) in human concentrative nucleoside transporter 3. J Biol Chem. 2008; 283: 8496-8507.

136. Slugoski MD, Smith KM, Mulinta R, Ng AM, Yao SY, Morrison EL, Lee QO, Zhang J, Karpinski E, Cass CE, Baldwin SA, Young JD. A conformationally mobile cysteine residue (Cys-561) modulates Na+ and H+ activation of human CNT3. J Biol Chem. 2008; 283: 24922-34.

137. Paterson AR, Gati WP, Vijayalakshmi D, Cass CE, Mant MJ, Young JD, Belch AR. Inhibitor-sensitive, Na(+)-linked transport of nucleoside analogs in leukemia cells from patients (Meeting abstract). Proc Annu Meet Am Assoc Cancer Res. 1993; 24: A84.

138. Flanagan SA, Mecklinggill KA. Characterization of a novel Na+ dependent, guanosine specific, nitrobenzylthioionosine-sensitive transporter in acute promyelocytic leukemia cells. J Biol Chem. 1997; 272: 18026-18032.

139. Gutierrez MM, Brett CM, Ott RJ, Hui AC, Giacomini KM. Nucleoside transport in brush border membrane vesicles from human kidney. Biochimica et Biophysica Acta. 1992; 1105: 1-9.

140. Gutierrez MM, Gicomini KM. Substrate selectivity, potential sensitivity and stoichiometry of Na(+)-nucleoside transport in brush border membrane vesicles from human kidney. Biochimica et Biophysica Acta. 1993; 1149: 202-208.

141. Lai Y, Lee EW, Ton CC, Vijay S, Zhang H, Unadkat JD. Conserved residues F316 and G476 in the concentrative nucleoside transporter 1 (hCNT1) affect guanosine sensitivity and membrane expression, respectively. Am J Physiol Cell Physiol. 2005; 288: C39-C45.

142. Jacquez JA, Schafer JA. Na+ and K+ electrochemical potential gradients and the transport of alpha-aminoisobutyric acid in Ehrlich ascites tumor cells. Biochim Biophys Acta. 1969; 193: 368-383.

143. Govindarajan R, Bakken AH, Hudkins KL, Lai Y, Casado FJ, Pasto-Anglada M, Tse CM, Hayashi J, Unadkat JD. In situ hydribdization and immunolocalization of concentrative and equilibrative nucleoside transporters in the human intestine, liver, kidneys, and placenta. Amer J Physiol Reg Int Comp Physiol. 2007; 293: R1809-R1822.

144. Aymerich I, Pastor-Anglada M, Casado FJ. Long term endocrine regulation of nucleoside transporters in rat intestinal epithelial cells. J General Physiol. 2004; 124: 505-512.

145. Ngo LY, Patil SD, Unadkat JD. Ontogenic and longitudinal activity of Na(+)-nucleoside transporters in the human intestine. Amer J Physiol Gastro Liv Physiol. 2001; 280: 13-19.

146. Del Santo B, Tarafa G, Felipe A, Casado FJ, Pastor-Anglada M. Developmental regulation of the concentrative nucleoside transporters CNT1 and CNT2 in rat liver. J Hepatol. 2001; 34: 873-880.

147. Dragan Y, Valdes R, Gomez-Angelats M, Felipe A, Casado FJ, Pitot H, Pastor-Anglada M. Selective loss of nucleoside carrier expression in rat hepatocarcinomas. Heptol. 2000; 32: 239-246.

148. Fernandes-Veledo S, Jover R, Casado FJ, Gomez-Lechon MJ, Pastor-Anglada M. Transcription factors involved in the expression of SCL28 genes in human liver parenchymal cells. Biochem Biophys Res Commun. 2007; 353: 381-388.

149. Fernandez-Veledo S, Valdes R, Wallenius V, Casado FJ, Pastor-Anglada M. Up-regulation of the high-affinity pyrimidine-preferrin nucleoside transporter concentrative nucleoside transporter 1 by tumor necrosis factor-alpha and interleukin-6 in liver parenchymal cells. J Hepatol. 2004; 41: 538-544.

150. Valdes R, Fernandez-Veledo S, Aymerich I, Casado FJ, Pastor-Anglada M. TGF-beta transcreiptionally activates the gene encoding the high-affinity adenosine transporter CNT2 in rat liver parenchymal cells. Cell Mol Life Sci. 2006; 63: 2527-2537.

151. Soler C, Garcia-Manteiga J, Xaus J, Comalada M, Casado FJ, Pastor-Anglada M, Celada A, Felipe A. Macrophages require different nucleoside transport systems for proliferation and activation. FASEB J. 2001; 15: 1979-1988.

152. Soler C, Valdes R, Garcia-Manteiga J, Xaus J, Comalada M, Casado FJ, Modolell M, Nicholson B, MacLeod C, Felipe A, Celada A, Pastor-Anglada M. Lipopolysaccharide-induced apoptosis of macrophages determines the up-regulation of ceoncentrative nucleoside transporters Cnt1 and Cnt2

through tumor necrosis factor-alpha-dependent and independent mechanisms. J Biol Chem. 2001; 106: 195-204.

153. Valdes R, Ortega MA, Casado FJ, Felipe A, Giul A, Sanchez-Pozo A, Pastor- Soler C, Felipe A, Garcia-Manteiga J, Serra M, Guillen-Gomez E, CAsado FJ, MacLeod C, Modolell M, Pastor-Anglada M, Celada A. Interferon-gamma regulates nucleoside transport systems in macrophages through signal transduction ad activator of transduction factor 1 (STAT1)-dependent and –independent signalling pathways. Biochm J. 2003; 275: 777-783.

154. Farre X, Guillen-Gomez E, Sanchez L, Hardisson D, Plaza Y, Lloberas J, Casado FJ, Palacios J, Pastor-Anglada M. Expression of the nucleoside-derived drug transporters hCNT1, hENT1, and hENT2 in gynaecologic tumors. Int J Cancer. 2004; 112: 959-966.

155. Mackey JR, Galmarini CM, Graham KA, Joy AA, Delmer A, Dabbagh L, Glubrecht D, Jewell LD, Lai R, Lang T, Hanson J, Young JD, Merle-Béral H, Binet JL, Cass CE, Dumontet C. Quantitative analysis of nucleoside transporter and metabolism gene expression in chronic lymphocytic leukemia (CLL): Identification of fludarabine-sensitive and –insenstive populations. Blood. 2005; 105: 767-774.

156. Valdes R, Ortega MA, Casado FJ, Felipe A, Gil A, Sanchez-Pozo A, Pastor-Anglada M. Nutritional regulation of nucleoside transporter expression in rat small intestine. Gastroenterol. 2000; 119: 1623-1630.

157. Dufot S, Riera B, Fernandez-Veledo S, Casado V, Norman RI, Casado FJ, Lluis C, Franco R, Pastor-Anglada M. ATP-sensitive K(+) channels regulate the concentrative adenosine transporter CNT2 following activation by A(1) adenosine receptors. Mol Cell Biol. 2004; 24: 2710-2719.

158. Wheater PR, Burkitt HG, Daniels VG. Urinary system. In Wheaters Functional Histology: A Text and colour atlas. Edited by Wheater PR, Burkitt HG, Daniels VG. Churchill Livingstone: New York, 1987; pp. 236-257.

159. Dumez H, Guetens G, De Boeck G, Highley MS, de Bruijn EA, van Oosterom AT, Maes RA. In vitro partition of docetaxel and gemcitabine in human volunteer blood: the influence of concentration and gender. Anticancer Drugs. 2005; 16: 885-891.

160. Thompson CI, Sparks HV, Spielman WS. Renal handling and production of plasma and urinary adenosine. Am J Physiol Renal Physiol. 1985; 248: F545-F551.

161. Mahony C, Wolfram KM, Cocchetto DM, Bjornsson TD. Dipyridamole kinetics. Clin Pharmacol Ther. 1982; 31: 330-338.

162. Kiss A, Farah K, Kim J, Garriock RJ, Drysdale TA, Hammond JR. Molecular cloning and functional characterization of inhibitor-sensitive (mENT1) and inhibitor-resistant (mENT2) equilibrative nucleoside transporters from mouse brain. Biochem J. 2000; 352: 363-372.

163. Hammond JR, Stolk M, Archer RG, McConnell K. Pharmacological analysis and molecular cloning of the canine equilibrative nucleoside transporter 1. Eur J Pharmacol. 2004; 491: 9-19.

164. Sommadossi JP, Cretton EM, Kidd LB, McClure HM, Anderson DC, el Kouni MH. Effects of 5-benzylacyclouridine, an inhibitor of uridine phosphorylase, on the pharmacokinetics of uridine in rhesus monkeys: implications for chemotherapy. Cancer Chemother Pharmacol. 1995; 37: 14-22.

165. Turnheim K, Krivanek P, Oberbauer R. Pharmacokinetics and pharmacodynamics of allopurinol in elderly and young subjects. Br J Clin Pharmacol. 1999; 48: 501-509.

166. Dzúrik R, Lajdová I, Spustová V, Opatrný K Jr. Pseudouridine excretion in healthy subjects and its accumulation in renal failure. Nephron. 1992; 61: 64-67.

167. Seidel A, Brunner S, Seidel P, Fritz GI, Herbarth O. Modified nucleosides: an accurate tumour marker for clinical diagnosis of cancer, early detection and therapy control. Br J Cancer. 2006; 94: 1726-1733.

168. Chen R, Nelson JA. Role of organic cation transporters in the renal secretion of nucleosides. Biochem Pharmacol. 2000; 60: 215-219.

169. Cropp CD, Komori T, Shima JE, Urban TJ, Yee SW, More SS, Giacomini KM. Organic anion transporter 2 (SLC22A7) is a facilitative transporter of cGMP. Mol Pharmacol. 2008; 73: 1151-1158.

170. Nelson JA, Vidale E, Enigbokan M. Renal transepithelial transport of nucleosides. Drug Metab. 1998; 16: 789-792.

171. Enigbokan MA, Preston J, Hubbard C, Thompson JO. Characterization of and the influence of calcium channel blockers on the renal excretion of pyrimidine anticancer agents. Res Commun Chem Pathol Pharmacol. 1994; 83: 270-278.

172. Kuttesch JF Jr, Robins MJ, Nelson JA. Renal transport of 2'-deoxytubercidin in mice. Biochem Pharmacol. 1982; 31: 3387-3394.

173. Nelson JA, Kuttesch JR Jr, Herbert BH. Renal secretion of purine nucleosides and their analogs in mice. Biochem Pharmacol. 1983; 32: 2323-2327.

174. Bisel HF, Ansfield FJ, Mason JH, Wilson WL. Clinical studies with tubercidin administered by direct intravenous injection. Cancer Res. 1970; 30: 76-78.

175. Hoetelmans RMW. Clinical pharmacokinetics of antiretroviral drugs. AIDS Rev. 1999; 1: 167–178.

176. Aiba T, Sakurai Y, Tsukada S, Koizumi T. Effects of probenecid and cimetidine on the renal excretion of 3'-azido-3'-deoxythymidine in rats. J Pharmacol Exp Ther. 1995; 272: 94-99.

177. Moore KH, Yuen GJ, Raash RH, Eron JJ, Martin D, Mydlow PK, et al. Pharmacokinetics of lamivudine administered alone and with trimethoprimsulfamethoxazole. Clin Pharmacol Ther. 1996; 59: 550-558.

178. Nakatani-Freshwater T, Babayeva M, Dontabhaktuni A, Taft DR. Effects of trimethoprim on the clearance of apricitabine, a deoxycytidine analog reverse transcriptase inhibitor, and Lamivudine in the isolated perfused rat kidney. J Pharmacol Exp Ther. 2006; 319: 941-947.

179. Laskin OL, de Miranda P, King DH, Page DA, Longstreth JA, Rocco L, et al. Effects of probenecid on the pharmacokinetics and elimination of acyclovir in humans. Antimicrob Agents Chemother. 1982; 21: 804-807.

180. Leung S, Bendayan R. Role of P-glycoprotein in the renal transport of dideoxynucleoside analogues drugs. Can J Physiol Pharmacol. 1999; 77: 625-630.

181. Izzedine H, Launay-Vacher V, Deray G. Renal tubular transporters and antiviral drugs: an update. AIDS. 2005; 19: 455-462.

182. Boumendil-Podevin EF, Podevin RA. Isolation of basolateral and brush-border membranes from the rabbit kidney cortex. Vesicle integrity and membrane sidedness of the basolateral fraction. Biochim Biophys Acta. 1983; 735: 86-94.

183. Le Hir M, Dubach UC. Sodium gradient-energized concentrative transport of adenosine in renal brush border vesicles. Pfluegers Arch Eur J Physiol. 1984; 401: 58-63.

184. Le Hir M, Dubach UC. Uphill transport of pyrimidine nucleosides in renal brush border membrane vesicles. J Physiol. 1985; 404: 238-243.

185. Lee CW, Cheeseman CI, Jarvis SM. Transport characteristics of renal brush border Na(+) and K(+)-dependent uridine carriers. Amer J Physiol Renal Physiol. 1990; 258: F1203-F1210.

186. Williams TC, Jarvis SM. Multiple sodium-dependent nucleoside transport systems in bovine renal rush-border membrane vesicles. Biochem J. 1991; 274: 27-33.

187. Williams TC, Doherty AJ, Griffith DA, Jarvis SM. Characterization of sodium-dependent and sodium-independent nucleoside transport systems in rabbit brush-border and basolateral plasma-membrane vesicles from the renal outer cortex. Biochem J. 1989; 264: 223-231.

188. Sayos J, Blanco J, Ciruela F, Canela EI, Mallol J, Lluis C, Franco R. Regulation of nitrobenzylthioninosine-sensitive adenosine uptake by cultured kidney cells. Amer J Physiol Renal Physiol. 1994; 267: F758-F766.

189. Ciruela F, Blanco J, Canela EI, Lluis C, Franco R, Mallol J. Solubilization and molecular characterization of the nitrobenzylthioinosine binding sites from pig kidney brush-border membranes. Biochim Biophys Acta. 1994; 1191: 94-102.

190. Hamilton SR, Yao SYM, Ingram JC, Hadden DA, Ritzel MWL, Gallagheri MP, Henderson PJF, Cass CE, Young JD, Baldwin SA. Subcellular distribution and membrane topology of the mammalian concentrative Na^+-nucleoside cotransporter rCNT1. J Biol Chem. 2001; 276: 27981-27988.

191. Handler JS, Perkins FM, Johnson JP. Studies on renal cell function using cell culture technique. Am J Physiol Renal Physiol. 1980; 238: F1-F9.

192. Misfeldt DS, Hamamoto ST, Pitelka DR. Transepithelial transport in culture. Proc Natl Acad Sci USA. 1976; 73: 1212-1216.

193. Mangravite, LM, Lipschutz JH, Mostov KE, Giacomini KM. Localization of GFP-tagged concentrative nucleoside transporters in a renal polarized epithelial cell line. Am J Physiol Renal Physiol. 2001; 280: F879-F885.

194. Lai Y, Bakken AH, Unadkat JD. Simultaneous expression of hCNT1-CFP and hENT1-YFP in Madin-Darby canine kidney cells. Localization and vectorial transport studies. J Biol Chem. 2002; 277: 37711-37717.

195. Mangravite LM, Xiao G, Giacomini KM. Localization of human equilibrative nucleoside transporters, hENT1 and hENT2, in renal epithelial cells. Am J Physiol Renal Physiol. 2003; 284: F902-F910.

196. Mangravite LM, Badagnani I, Giacomini KM. Nucleoside transporters in the disposition and targeting of nucleoside analogs in the kidney. Eur J Pharmacol. 2003; 479: 269-281.

197. Mangravite LM, Giacomini KM. Sorting of rat SPNT in renal epithelium is independent of N-glycosylation. Pharm Res. 2003; 20: 319-323.

198. Lai Y, Tse CM, Unadkat JD. Mitochondrial expression of the human equilibrative nucleoside transporter 1 (hENT1) results in enhanced mitochondrial toxicity of antiviral drugs. J Biol Chem. 2004; 279: 4490-4497.

199. Errasti-Murugarren E, Pastor-Anglada M, Casado FJ. Role of CNT3 in the transepithelial flux of nucleosides and nucleoside-derived drugs. J Physiol. 2007; 582: 1249-60.

200. Rodriguez-Mulero S, Errasti-Murugarren E, Ballarin J, Felipe A, Doucet A, Casado FJ, Pastor-Anglada M. Expression of concentrative nucleoside transporters SLC28 (CNT1, CNT2, and CNT3) along the rat nephron: effect of diabetes. Kidney Int. 2005; 68: 665-672.

201. Saito H, Nishimura M, Shinano H, Makita H, Tsujino I, Shibuya E, Sato F, Miyamoto K, Kawakami Y. Plasma concentrations of adenosine during normoxia and moderate hypoxia in humans. Am J Respir Crit Care Med. 1999; 159: 1014-1018.

202. Zou AP, Nithipatikom K, Li PL, Cowley AW Jr. Role of renal medullary adenosine in the control of blood flow and sodium excretion. Am J Physiol Reg Int Comp Physiol. 1999; 45: R790-R798.

203. Masuda S, Sait H, Nonoguchi H, Tomita K, Inui K. mRNA distribution and membrane localization of the OAT-K1 organic anion transporter in rat renal tubules. FEBS Lett. 1977; 407: 127-131.

204. Brothers SP, Janovick JA, Conn PM. Unexpected effects of epitope and chimeric tags on gonadotropin-releasing hormone receptors: implications for understanding the molecular etiology of hypogonadotropic hypogonadism. J Clin Endocrinol Metab. 2003; 88: 6107-6112.

205. Louvard D. Apical membrane aminopeptidase appears at site of cell-cell contact in culture kidney epithelial cells. Proc Natl Acad Sci USA. 1980; 77: 4132-4136.

206. Richardson JWC, Scalera V, Simmons NL. Identification of two strains of MDCK cells which resemble separate nephron tubule segments. Biochim Biophys Acta. 1981; 673: 26-36.

207. Gstraunthaler G, Pfaller W, Kotanko P. Biochemical characterization of renal epithelial cell cultures (LLC-PK$_1$ and MDCK). Am J Physiol Renal Physiol. 1985; 248: F536-F544

208. Handler JS, Kreisberg JI. Biology of renal cells in culture. In The Kidney. Edited by BM Brenner and FC Jr Rector WB Saunders Co: Philadelphia, Pennsylvania, 1991; pp. 110-131.

209. Goldring SR, Dayer JM, Ausiello DA, Krane SM. A cell strain cultured from porcine kidney increases cyclic AMP content upon exposure to calcitonin or vasopressin. Biochem Biophys Res Commun. 1978; 83: 434-440.

210. Toutain H, Vauclin-Jacques N, Fillastre JP, Morin JP. Biochemical, functional, and morphological characterization of a primary culture of rabbit proximal tubule cells. Exp Cell Res. 1991; 194: 9-18.

211. Morshed KM, Ross DM, McMartin KE. Folate transport proteins mediate the bidirectional transport of 5-methyltetrahydrofolate in cultured human proximal tubule cells. J Nutr. 1997; 127: 1137-1147.

212. Karbach U, Kricke J, Meyer-Wentrup F, Gorboulev V, Volk C, Loffing-Cueni D, Kaissling B, Bachmann S, Koepsell H. Localization of organic cation transporters OCT1 and OCT2 in rat kidney. Am J Physiol Renal Physiol. 2000; 279: F679-687.

213. Chen R, Jonker JW, Nelson JA. Renal organic cation and nucleoside transport. Biochem Pharmacol. 2002; 64: 185-190.

214. Takeda M, Khamdang S, Narikawa S, Kimura H, Kobayashi Y, Yamamoto T, Cha SH, Sekine T, Endou H. Human organic anion transporters and human organic cation transporters mediate renal antiviral transport. J Pharmacol Exp Ther. 2002; 300: 918-924.

215. Kakizaki T, Yokoyama Y, Natsuhori M, Karasawa A, Kubo S, Yamada N, Ito N. Probenecid: its chromatographic determination, plasma protein binding, and in vivo pharmacokinetics in dogs. J Vet Med Sci. 2006; 68: 361-365

216. Ritter CA, Jedlitschky G, zu Schwabedissen HM, Grube M, Köck K, Kroemer HK. Cellular export of drugs and signaling molecules by the ATP-binding cassette transporters MRP4 (ABCC4) and MRP5 (ABCC5). Drug Met Rev. 2005; 1: 253-278.

217. Nies AT, Spring H, Thon WF, Keppler D, Jedlitschky G. Immunolocalization of multidrug resistance protein 5 in the human genitourinary system. J Urol. 2002; 167: 2271-2275

218. Adachi M, Sampath J, Lan LB, Sun D, Hargrove P, Flatley R, Tatum A, Edwards MZ, Wezeman M, Matherly L, Drake R, Schuetz J. Expression of MRP4 confers resistance to ganciclovir and compromises bystander cell killing. J Biol Chem. 2002; 277: 38998-39004.

219. Chen ZS, Lee K, Kruh GD. Transport of cyclic nucleotides and estradiol 17-beta-D-glucuronide by multidrug resistance protein 4. Resistance to 6-mercaptopurine and 6-thioguanine. J Biol Chem. 2001; 276: 33747-33754.

220. Wielinga PR, Reid G, Challa EE, van der Heijden I, van Deemter L, de Haas M, Mol C, Kuil AJ, Groeneveld E, Schuetz JD, Brouwer C, De Abreu RA, Wijnholds J, Beijnen JH, Borst P. Thiopurine metabolism and identification of the thiopurine metabolites transported by MRP4 and MRP5 overexpressed in human embryonic kidney cells. Mol Pharmacol. 2002; 62: 1321-1331.

221. Schuetz JD, Connelly MC, Sun D, Paibir SG, Flynn PM, Srinivas RV, Kumar A, Fridland A. MRP4: a previously unidentified factor in resistance to nucleoside-based antiviral drugs. Nat Med. 1999; 5: 1048-1051.

222. Guo Y, Kotova E, Chen ZS, Lee K, Hopper-Borge E, Belinsky MG, Kruh GD. MRP8, ATP-binding cassette C11 (ABCC11), is a cyclic nucleotide efflux pump and a resistance factor for fluoropyrimidines 2',3'-dideoxycytidine and 9'-(2'-phosphonylmethoxyethyl)adenine. J Biol Chem. 2003; 278: 29509-25914.

223. Takenaka K, Morgan JA, Scheffer GL, Adachi M, Stewart CF, Sun D, Leggas M, Ejendal KF, Hrycyna CA, Schuetz JD. Substrate overlap between Mrp4 and Abcg2/Bcrp affects purine analogue drug cytotoxicity and tissue distribution. Cancer Res. 2007; 67: 6965-6972.

224. Grever TB, Siaw MF, Jacob WF, Neidhart JA, Miser JS, Coleman MS, Hutton JJ, Balcerzak SP. The biochemical and clinical consequences of 2′-deoxycoformycin in refractory lymphoproliferative malignancy. Blood. 1981; 57: 406-417.

225. Grage TB, Rochlin DB, Weiss AJ, Wilson WL. Clinical studies with tubercidin administered after absorption into human erythrocytes. Cancer Res. 1970; 30: 79-81.

226. Slavin RE, Dias MA, Saral R. Cytosine arabinoside induced gastrointestinal toxic alterations in sequential chemotherapeutic protocols: a clinical-pathologic study of 33 patients. Cancer. 1978; 42: 1747-1759.

227. Crowther MA, Callaghan W, Hodsman AB, Mackie IC. Dideoxyinosine-associated nephrotoxicity. Aids. 1993; 7: 131-132.

228. Fontana RJ. Uric acid nephrolithiasis associated with interferon and ribavirin treatment of hepatitis C. Dig Dis Sci. 2001; 46: 920-924.

229. Izzedine H, Launay-Vacher V, Deray G. Fanconi syndrome associated with didanosine therapy. AIDS. 2005; 19: 844-845.

230. Rollot F, Nazal EM, Chauvelot-Moachon L, Kelaidi C, Daniel N, Saba M, Abad S, Blanche P. Tenofovir-related Fanconi syndrome with neprhogenic diabetes insipidus in a patient with acquired immunodeficiency syndrome: the role of lopinavir-ritonavir-didanosine. Clin Infect Dis. 2003; 37: 174-176.

231. Cundy KC. Clinical pharmacokinetics of the antiviral nucleotide analogues cidofovir and adefovir. Clin Pharmacokinet. 1999; 36: 127-143.

232. Davis GL, Esteban-Mur R, Rustgi V, Hoefs J, Gordon SC, Trepo C, Shiffman ML, Zeuzem S, Craxi A, Ling MH, Albrecht J. Interferon alfa-2b alone or in combination with ribavirin for the treatment of relapse of chronic hepatitis C. N Engl J Med. 1998; 339: 1493-1499.

233. Poynard T, Marcellin P, Lee SS, Niederau C, Minuk GS, Ideo G, Bain V, Heathcote J, Zeuzem S, Trepo C, Albrecht J. Randomised trial of interferon a2b plus ribavirin for 48 weeks or for 24 weeks versus interferon a2b plus placebo for 48 weeks for treatment of chronic infection with hepatitis C virus. Lancet. 1998; 352: 1426-1432.

234. McHutchison JG, Gordon SC, Schiff ER, Shiffman ML, Lee WM, Rustgi VK, Goodman ZD, Ling MH, Cort S, Albrecht JK. Interferon alfa-2b alone or in combination with ribavirin as initial treatment for chronic hepatitis C. N Engl J Med. 1998; 339:1485-1492.

235. Dibesceglie AM, Shindo M, Fong T, Fried MW, Swain MG, Bergasa NV, Axiotis CA, Waggoner JG, Park Y, Hoofnagle JH. A pilot study of ribavirin therapy for chronic hepatitis C. Hepatol. 1992; 16: 649-654.

236. Garrett MD, Workman P. Discovering novel chemotherapeutic drugs for the third millennium. Eur J Cancer. 1999; 35: 2010-2030.

237. Lesko LJ, Atkinson AJ Jr. Use of biomarkers and surrogate endpoints in drug development and regulatory decision making: criteria, validation, strategies. Annu. Rev. Pharmacol. Toxicol. 2001; 41: 347-366.

238. Duarte CG, Preuss HG. Assessment of renal function – glomerular and tubular. Clin Lab Med. 1993; 13: 33-52.

239. Kramer JA, Pettit SD, Amin RP, Bertram TA, Car B, Cunningham M, Curtiss SW, Davis JW, Kind C, Lawton M, Naciff JM, Oreffo V, Roman RJ, Sistare FD, Stevens J, Thompson K, Vickers AE, Wild S, Afshari CA. Overview on the application of transcription profiling using selected nephrotoxicants for toxicology assessment. Eviron. Health Perspect. 2004; 112: 460-464.

240. Huang Y, Anderle P, Bussey KJ, Barbacioru C, Shankavaram U, Dai Z, Reinhold WC, Papp A, Weinstein JN, Sadée W. Membrane transporters and channels: role of the transportome in cancer chemosensitivity and chemoresistance. Cancer Res. 2004; 64: 4294-4301.

241. Thukral S, Nordone PJ, Hu R, Sullivan L, Galambos E, Ftizpatrick VD, Healy L, Bass MB, Cosenza ME, Afshari CA. Prediction of nephrotoxicant action and identification of candidate toxicity-related biomarkers. Toxicol Pathol. 2005; 33: 343-355.

242. McKenzie R, Fried MW, Sallie R, Conjeevaram H, Di Bisceglie AM, Park Y, Savarese B, Kleiner D, Tsokos M, Luciano C, Pruett T, Stotka JL, Straus SE, Hoofnagle JH. Hepatic failure and lactic acidosis due to fialuridine (FIAU), an investigational nucleoside analogue for chronic hepatitis B. N Engl J Med. 1995; 333: 1099-1105.

243. Tsai CH, Doong SL, Johns DG, Driscoll JS, Cheng YC. Effect of anti-HIV 2'-beta-fluoro-2',3'-dideoxynucleoside analogs on the cellular content of mitochondrial DNA and on lactate production. Biochem Pharmacol. 1994; 48: 1477-1481.

244. Genini D, Adachi S, Chao Q, Rose DW, Carrera CJ, Cottam HB, Carson DA, Leoni LM. Deoxyadenosine analogs induce programmed cell death in chronic lymphocytic leukemia cells by damaging the DNA and by directly affecting the mitochondria. Blood. 2000; 96: 3537-3543.

245. List AF, Kummet TD, Adams JD, Chun HG. Tumor lysis syndrome complicating treatment of chronic lymphocytic leukemia with fludarabine phosphate. Am J Med. 1990; 89: 388-390.

246. Piro LD, Carrera CJ, Beutler E, Carson DA. 2-Chlorodeoxyadenosine: an effective new agent for the treatment of chronic lymphocytic leukemia. Blood. 1988; 72: 1069-1073.

247. McCroskey RD, Mosher DF, Spencer CD, Prendergast E, Longo WL. Acute tumor lysis syndrome and treatment response in patients treated for refractory chronic lymphocytic leukemia with short-course, high-dose cytosine arabinoside, cisplatin, and etoposide. Cancer. 1990; 66: 246-250.

248. Cairo MS, Bishop M. Tumor lysis syndrome: new therapeutic strategies and classification. Br J Haematol. 2004; 127: 3-11.

249. McEvoy GK. Fludarabine phosphate. In American Hospital Formulary Service - Drug Information. Edited by GK McEvoy. American Society of Health-System Pharmacists: Bethesda, Maryland. 2005; pp. 10:00.

250. McEvoy GK. Cladribine. In American Hospital Formulary Service - Drug Information. Edited by GK McEvoy. American Society of Health-System Pharmacists: Bethesda, Maryland. 2005; pp. 10:30.

251. Magil AB, Pichler RH, Johnson RJ. Osteopontin in chronic puromycin aminonucleoside nephrosis. J Am Soc Nephrol. 1997; 8: 1383-1390.

252. Chen R, Pan BF, Sakurai M, Nelson JA. A nucleoside-sensitive organic cation transporter in opossum kidney cells. Am J Physiol. 1999; 276: F323-F328.

253. Blackburn JG, Hazen-Martin DJ, Detrisac CJ, Sens DA. Electrophysiology and ultrastructure of cultured human proximal tubule cells. Kidney Int. 1988; 33: 508-516.

Chapter II

II. Materials and Methods

II.1 Materials

All chemicals used in this study were of analytical grade and obtained from Sigma-Aldrich (Oakville, ON, Canada), unless otherwise stated. Tissue-Tek® O.C.T compound was purchased from Sakura Finetek (Torrance, CA, USA). Allprotect Tissue Reagent was purchased from QIAGEN (Mississauga, ON, Canada). Dulbecco's modified Eagle's medium (DMEM), Ham's F12 medium, fetal bovine serum (FBS), trypsin-ethylenediaminetetraacetic acid (EDTA), glutamine, and penicillin-streptomycin-amphotericin B were purchased from Invitrogen (Burlington, ON, Canada). Collagen type I was purchased from Inamed Biomaterials (Fremont, CA). Selenium-insulin-transferrin, hydrocortisone, and epidermal growth factor were purchased from BD Biosciences (Mississauga, ON, Canada). Polyester membrane 12-well and polycarbonate membrane 6-well and High Throughput System (HTS) 24-well transwell permeable supports were purchased from Corning Life Sciences (Big Flats, NY, USA). Deoxyribonucleotidase I (DNAse I), oligonucleotide primers for reverse transcription polymerase chain reaction (RT-PCR) analysis, and 100-base pair deoxyribonucleic acid (DNA) ladders were purchased from Invitrogen (Burlington, ON, Canada). Oligonucleotide primers and fluorescently labeled oligonucleotide probes for quantitative TaqMan™ RT-PCR analysis were purchased from Applied Biosystems (Streetsville, ON, Canada). COMPLETE protease inhibitor tablets were purchased from Boehringer Mannheim (Lavel, PQ, Canada). DNA intercalating agent 4′,6-diamidino-2-phenylindole (DAPI) was purchased from Molecular Probes. Horseradish peroxidase conjugated dextran polymer (DAKO EnVision+) was obtained from DAKO Corporation (Carpentaria, CA, USA). Low range sodium dodecyl sulfate-(SDS)polyacrylamide gel electrophoresis standards were purchased from BIORAD (Hercules, CA, USA). Immobilon-P polyvinylidene fluoride membranes were purchased from Millipore (Bedford, MA, USA). Enhanced Chemiluminescence (ECL) was purchased from Amersham Pharmacia Biotech (Uppsala, Sweden). Fuji RX film was purchased from Fuji Medical Systems (Stanford, CT, USA). Aluminum-backed Silica Gel 60 thin layer chromatogram plates containing fluorescent indicator F254 were purchased from EMD Chemicals (Gibbstown, NJ, USA).

Anti-human equilibrative nucleoside transporter (hENT) 1 (hENT1) mouse (immunoglobulin, IgG, isotype G1$_{K}$; IgG1$_{K}$), anti-hENT2 mouse (IgG2b), anti-human concentrative nucleoside transporter (hCNT) 2 (hCNT2) mouse (IgG1$_{K}$), and anti-hCNT3 mouse (IgM) monoclonal antibodies were developed and characterized previously [1-4]. Monoclonal antibodies specific for the NT proteins were produced by immunization of mice with carrier proteins conjugated with synthetic peptides derived from hENT1, hENT2, hCNT2 or hCNT3 that corresponded to amino acids 254-271, 261-280, 30-51 or 45-69, respectively. Other antibodies used in this study were: anti-human proximal nephrogenic renal antigen (PNRA) mouse (IgG1$_{\kappa}$ isotype) monoclonal antibodies (Zymed Laboratories Inc., CA, USA), anti-human Tamm-Horsfall protein (THP) mouse (IgG2b) monoclonal antibodies (Cedarlane Laboratories, ON, Canada), anti-rat aquaporin-2 (AQP2) rabbit (IgG) polyclonal antibodies (Alpha Diagnostics, TX, USA), anti-human vacuolar type H^{+}-adenosine-5′-triphosphatase (ATPase) B1/2 (V-ATPase) rabbit (IgG) polyclonal antibodies (Santa Cruz Biotechnology, CA, USA), anti-human Zonula Occludens 1 (ZO1) mouse (IgG1$_{K}$) monoclonal antibodies (Zymed Laboratories Inc.), anti-human Epithelial Cadherin (E-CAD) mouse (IgG1$_{K}$) monoclonal antibodies (Zymed Laboratories Inc.), anti-β-actin rabbit (IgG) polyclonal antibodies (Sigma), mouse IgG1$_{K}$, IgG2b, and IgM isotype control monoclonal antibodies (Sigma), rabbit IgG isotype control polyclonal antibodies (Sigma), anti-mouse and -rabbit IgG (Heavy + Light chain; H + L) horseradish-peroxidase conjugated goat (IgG) polyclonal antibodies (Sigma), anti-mouse IgG (H + L) and IgM (H + L) AlexaFluor488 conjugated rabbit (IgG) polyclonal antibodies (Molecular Probes, Eugene, OR, USA), anti-mouse and -rabbit IgG (H + L) AlexaFluor546 conjugated goat (IgG) polyclonal antibodies (Molecular Probes).

Radioisotopes were purchased from Moravek Biochemicals (Brea, CA, USA): [methyl-^{14}C]-methyl-α-D-glucopyranoside (50 mCi/mmol), [5-^{3}H]-uridine (40 Ci/mmol), [methyl-^{3}H]-thymidine (20 Ci/mmol), [2,8-^{3}H]-inosine (50 Ci/mmol), and [8-^{3}H]-2-fluoroadenine-β-D-arabinofuranoside (15 Ci/mmol), [2,8-^{3}H]-adenosine (25 Ci/mmol), [2,8-^{3}H]-2′-deoxyadenosine (15 Ci/mmol) [8-H^{3}]-2-chloro-2′-deoxyadenosine (4 Ci/mmol), and [8-H^{3}]-2-chloro-2′-deoxy-2′-fluoroarabinosyl adenine (1 Ci/mmol). Ecolite scintillation fluid was purchased from MP Biomedicals (Irvine, CA, USA).

II.2 Human kidney tissue collection

Apparently normal parts of human kidney cortex were obtained from nephrectomized patients with renal cell carcinoma. Collected tissues contained no pathologic alterations as judged by a surgical pathologist (*i.e.*, derived from non-cancerous, non-diseased tissue). Ethics approval was obtained from the Research Ethics Board of the Alberta Cancer Board and the University of Alberta/Capital Health Research Ethics Board. Informed consent was obtained in accordance with ethics approval guidelines. No demographic data was collected as per the ethics approval guidelines.

The outer capsule and fat were removed from renal specimens; tissue was cut into small pieces, washed twice with ice-cold phosphate buffered saline (PBS: 137 mM NaCl, 2.7 mM KCl, 4.3 mM Na_2HPO_4, 1.47 mM KH_2PO_4, pH 7.4) to remove blood. Portions of each human kidney tissue (1 g each) obtained from four different individuals (designated K1 through K4) were formalin-fixed and paraffin-embedded for immunohistochemistry studies and embedded in Tissue-Tek® O.C.T compound and snap-frozen in a dry ice-methanol bath for immunofluorescent studies. After removal of medulla, 1-g portions of human kidney cortex tissue from nine different individuals (designated C1 through C4 and C11 through C15) were placed in Allprotect Tissue Reagent, snap frozen in liquid nitrogen and stored at -80 °C for use in preparing total ribonucleic acid (RNA) and crude membranes and 5-10-g portions of human kidney cortex tissue were placed in ice-cold DMEM with 15 % (v/v) FBS for isolation of cultures of human renal proximal tubule cells (hRPTCs; hRPTCs isolated from fifteen different individuals were designated hRPTC1 through hRPTC15).[1] Collected tissues and isolated cultures are summarized in Table II-1.

II.3 Cell culture

Cell culture manipulations were performed in laminar flow hoods using sterile cell culture techniques. All instruments and glassware were autoclaved and all media and buffers were filtered through 0.2-μm pore-size filters. All cultures used in these studies were periodically demonstrated to be free of *Mycoplasma* by direct culture in agar/cell-free medium (Provincial Health Laboratory, Edmonton, AB, Canada). Mycoplasma-free stock cultures were stored in 10 % (v/v) dimethyl sulfoxide with growth medium in liquid nitrogen. A Coulter Z2 electronic particle counter equipped with a size analyzer (Coulter Electronics, Burlington, ON, Canada) was routinely used to determine cell numbers

II.3.1 Collagen coating of cell culture ware

Cell culture ware (flasks, dishes, plates, coverslips, and transwell permeable supports) was collagen coated by completely covering cell culture surfaces in collagen type I (1 mg/mL) for 5 min, aspirating excess unbound collagen, and air drying in a laminar flow hood overnight at room temperature. Collagen-coated T-75 flasks used for expanding and sub-culturing cell cultures were then covered with 2.5 mL of FBS and incubated at 4 °C (1-7 days). Collagen-coated flasks, dishes, plates, coverslips, and transwell permeable supports used for experiments were not incubated with FBS but were stored at 4 °C (1-7 days). Collagen-coated cell culture ware was rinsed with PBS immediately before use.

---

[1] Human kidney tissues designated K1 through K4 corresponded to human kidney cortex tissues designated C1 through C4 that were obtained from the same four individuals. hRPTCs designated hRPTC1 through hRPTC4 were isolated from human kidney cortex tissues from four different individuals, who did not correspond to the four individuals from whom human kidney tissues K1 through K4 and human kidney cortex tissues C1 through C4 were isolated. Human kidney cortex tissues designated C11 through C15 corresponded to hRPTCs designated hRPTC11 through hRPTC15 isolated from the same five individuals.

II.3.2 Growth and maintenance of human kidney proximal tubule cell line (HK-2)

The human kidney proximal tubule cell line HK-2 was obtained from American Type Culture Collection (Manassa, VA, USA). HK-2 cells were maintained as adherent cultures on collagen type I-coated T-75 flasks in serum-free, hormonally defined medium containing DMEM-Ham's F-12 medium (50:50 by volume) supplemented with selenium (5 μg/L), insulin (5 mg/L), transferrin (5 mg/L), hydrocortisone (36 μg/L), epidermal growth factor (10 μg/L), triiodothyronine (4 ng/L), glutamine (2 mM), and penicillin-streptomycin-amphotericin B (0.1 U/L, 100 ng/L, and 250 pg/L, respectively) at 37 °C in a humidified atmosphere containing 5 % CO_2. The growth medium was replaced with fresh growth medium every three days. Sub-culturing was performed at regular intervals (4-6 days) by detachment with trypsin-EDTA (0.5 and 0.2 g/L, respectively) and seeding 1×10^6 cells per T-75 flask, unless otherwise stated. HK-2 cell cultures > 20 subculture generations were discarded and new cultures were started from *Mycoplasma*-free stock cultures stored frozen in 10 % (v/v) dimethyl sulfoxide with growth medium in liquid nitrogen.

II.3.3 Isolation, growth, and maintenance of adherent cultures of hRPTCs

Apparently normal regions of human kidney tissue obtained by complete or partial nephrectomy for renal cell carcinoma were used for isolation of cultures of hRPTCs from fifteen individuals (designated hRPTC1 through hRPTC15), using an enzyme-dissociation method as described previously [5]. Approximately 5-10 g portions of outer cortex tissue from each kidney specimen were finely minced with scissors and forceps in ice-cold PBS on a 35-mm glass dish. Minced pieces were collected with forceps and placed in a trypsinization flask containing 37°C enzyme digestion buffer: Hank's buffer (25 mM $NaHCO_3$, 25 mM 4-(2-hydroxyethyl)-1-piperazineethanesulfonic acid, pH 7.4), 0.5 mM ethylene glycol tetraacetic acid, 0.2 % (w/v) bovine serum albumin), 0.59 mg/mL $CaCl_2$, and 1 mg/mL collagenase type II. Trypsinization flasks were agitated at 37 °C for 15 min to carry out enzyme-dissociation of kidney cortical tissue. Digested mixtures were filtered through 70-μm mesh filter and filtrates containing human kidney cortical cells were collected on ice. The remaining human kidney cortical tissue was subjected to enzyme-dissociation two more times with collection of cortical cells by filtration as above. Pooled filtrates containing human kidney cortical cells were spun down at 300 × *g* at 4 °C, re-suspended in DMEM with 15 % (v/v) FBS, and seeded at 5×10^6 cells per collagen type I-coated T-75 flask. Typical initial yields were $5 - 7 \times 10^6$ cells per 1 g of human kidney cortex tissue.

Cultures containing kidney cortical cells were incubated at 37 °C in a humidified atmosphere containing 5 % CO_2 overnight, after which cultures were switched to serum-free, hormonally defined medium. Cultures of hRPTCs were maintained at 37 °C in a humidified atmosphere containing 5 % CO_2 with regular feeding (every 2-3 days). At confluency, hRPTCs were detached with trypsin-EDTA (0.5 and 0.2 g/L, respectively) and frozen in growth medium containing 10

% v/v dimethyl sulfoxide in liquid nitrogen for storage as generation 2 hRPTC cultures with 2 × 10^6 cells per cryovial.

Generation 2 hRPTC cultures were initiated and expanded to generation 7 hRPTC cultures by seeding with 1 × 10^6 cells per collagen type I-coated T-75 flask, growing in serum-free, hormonally defined medium, and sub-culturing by detachment with trypsin-EDTA (0.5 and 0.2 g/L, respectively). All experiments were performed on generation 7 hRPTC cultures, obtained from 6 total passages, unless otherwise stated.

II.3.4 Growth and maintenance of polarized monolayers of hRPTC cultures

hRPTC cultures (designated hRPTC11 through hRPTC15) from five different individuals were initiated at confluent densities on polyester membrane 12-well or polycarbonate membrane 6-well or HTS 24-well transwell permeable supports (0.5 × 10^6 cells per well, 1 × 10^6 cells per well, or 0.25 × 10^6 cells per well, respectively) and cultured for 10 days with feeding every 2 days. To monitor polarization of hRPTC cultures, transepithelial electrical resistance (TEER) across polarized monolayers of hRPTCs was measured periodically (2-4 days) using an Epithelial Tissue Voltohmmeter from World Precision Instruments (Berlin, Germany) according to the manufacturer's instructions. TEER values were measured in triplicate, corrected for background TEER values in transwell permeable supports with no hRPTCs, and normalized to culture surface areas of transwell inserts (per cm^2).

II.4 Staining and microscopy

Microscopy was performed in the Cross Cancer Institute Cell Imaging Facility (Edmonton, AB, Canada). All images were prepared using Adobe Photoshop from Adobe (San Jose, CA, USA).

II.4.1 Brush border enzyme cytochemistry and light microscopy

Cytochemistry for proximal tubule brush border enzymes (*i.e.*, alkaline phosphatise, γ-glutamyl transferase, and acid phosphatase) was assayed on each of the fifteen different hRPTCs (designated hRPTC1 through hRPTC15) using Alkaline Phosphatase, γ-Glutamyl Transferase, and Acid Phosphatase Cytochemistry Kits according to the manufacturer's instructions. hRPTC cultures were seeded onto collagen-coated #1 coverslips in 6-well plates at 1×10^4 cells per well and grown for 3 days as adherent cultures. Adherent cultures of hRPTCs on coverslips were washed with PBS, fixed at room temperature for 30 sec with Fixative Solution supplied in the kits (4.6 mM citric acid, 2.3 mM trisodium citrate, 3.1 mM NaCl, surfactant pH 3.6, 66 % v/v acetone, 3 % v/v formaldehyde), washed with deionized H_2O at 37 °C and incubated at 37 °C for 60 min with Staining Solution supplied in the kits (0.07 mg/mL fast garnet GBC base, 4 mM HCl with stabilizer, 1 mM sodium nitrite, acid, 0.1 M acetate pH 5.2) containing either (i) 0.13 mg/mL napthol AS-MX phosphate (for alkaline phosphatase cytochemistry), (ii) 0.13 mg/mL γ-glutamyl-4-methoxy-2-naphthylamide and 0.13 mg/mL glycylglycine (for γ-glutamyl transferase cytochemistry), or (iii) napthol AS-BI phosphoric acid (for acid phosphatase cytochemistry). The coverslips were then washed in deionized H_2O at 37 °C, counterstained for 2 min at room temperature with hematoxylin solution (6 g/L hematoxylin, 0.6 g/L aluminum sulphate, 52.8 g/L stabilizers), rinsed for 5 min in warm tap water, air dried for 30 min at room temperature, and mounted on slides with CytoMount from Sigma. Negative controls lacked the appropriate enzyme substrates – *i.e.*, napthol AS-MX phosphate (for alkaline phosphatase cytochemistry), γ-glutamyl-4-methoxy-2-naphthylamide (for γ-glutamyl transferase cytochemistry), or napthol AS-BI phosphoric (for acid phosphatise cytochemistry). Slides were imaged using a Zeiss Axioskop2 plus Microscope equipped with a F Fluar 10× or 20× lens and Zeiss Axiocam color camera (12 megapixels) with a 0.63x adaptor (Carl Zeiss MicroImaging Inc., Thornwood, NY, USA). Image processing was performed using Zeiss Axiovision Software 3.1 (Carl Zeiss MicroImaging, Inc.). Slides were scored as positive (or negative) for brush border enzymes if > 90 % (or < 90 %) of cells in three different fields of view contained intense granular staining [6].

II.4.2 Paraffin embedded tissue immunohistochemistry and light microscopy

Immunohistochemistry was performed on formalin-fixed, paraffin-embedded kidney tissue from each of four individuals (designated K1 through K4) as described elsewhere [7]. Sections (4-6 μm) of formalin-fixed, paraffin-embedded kidney tissue were dried in an oven at 59 °C for 2 hr, deparaffinised with three immersions in xylene baths (10 min each), washed serially in graded alcohol from 100 % (v/v) to 60 % (v/v), and rinsed in room temperature tap water. After rehydrating sections, slides were placed in 250 mL of high pH DAKO target antigen retrieval solution and microwaved in TT-mega Milestone (ESBE Scientific, Markahm, ON, Canada) under controlled temperature and high pressure for 10 min at 100 ºC. After cooling in water for 6 min, slides were rinsed with room temperature tap water and peroxidase blocked in 3 % H_2O_2 in methanol for 10 min then washed in room temperature running tap water for 10 min. After rinsing in PBS, slides were incubated overnight in a humidified chamber at 4 ºC with either anti-hENT1 monoclonal antibodies (~ 10 μg/mL) or incubated for 60 min at room temperature with mouse anti-human PNRA monoclonal antibodies (0.3 μg/mL), mouse anti-human THP monoclonal antibodies (0.5 μg/mL), rabbit anti-rat AQP2 polyclonal antibodies (4 μg/mL), or rabbit anti-human V-ATPase polyclonal antibodies (0.2 μg/mL). Negative controls consisted of slides incubated with isotype control antibodies: (i) 10 or 0.3 μg/mL mouse $IgG1_K$ isotype control monoclonal antibodies (for anti-hENT1 or -PNRA staining, respectively), (ii) 0.5 μg/mL mouse IgG2b isotype control monoclonal antibodies (for anti-THF staining), or (iii) 4 or 0.2 μg/mL rabbit IgG isotype control polyclonal antibodies (for anti-AQP2 and -V-ATPase staining, respectively). Slides were then washed three times in PBS (5 min each), incubated with DAKO En Vision+ goat anti-mouse dextran conjugate for 60 min at room temperature, and washed again three times in PBS (5 min each). Slides were then incubated with diaminobenzidine liquid chromagen for 5 min, rinsed with room temperature tap water, soaked in 1 % (v/v) $CuSO_4$ for 5 min, rinsed with room temperature tap water, counterstained with hematoxylin (6 g/L) for 2 min, and rinsed with warm running tap water for 5 min. After dehydrating specimens with serial washes in graded alcohol and xylene, slides with specimens were mounted with xylene mounting media and covered with #1 coverslips.

To validate the specificity of anti-hENT1 monoclonal antibodies, 500 μg/ml of the antigenic hENT1 peptide (residues 254-271; DLISKGEEPRAGKEESGVSVS[2]) or non-related antigenic hCNT3 peptide (residues 45-69; REHTNTKQDEEQVTVEQDSPRNREH[2]) were pre-incubated with anti-hENT1 monoclonal antibodies (10 μg/mL) for 30 min at room temperature before application to slides. To identify nephron segments positive for hENT1, consecutive sections were stained for defined tubule markers (PNRA, THP, AQP2, V-ATPase) as previously described [8]. Each tissue section that was stained for tubule markers was flanked by an adjacent tissue section that was stained for hENT1. Slides were imaged using a Zeiss Axioskop2 plus Microscope equipped with an F Fluar 40×/1.3 oil immersion lens and Zeiss Axiocam color camera (12 megapixels) with a 0.63× adaptor (Carl Zeiss MicroImaging, Inc.). Image processing was performed using Zeiss Axiovision Software 3.1. Images for adjacent tissue sections stained for specific tubule markers and hENT1 were collected so that the images obtained contained the same kidney tubules from consecutive sections. Immunhistochemistry staining experiments were performed in triplicate on kidney tissue obtained from four different individuals (designated K1 through K4).

II.4.3 Frozen tissue immunofluorescent staining and confocal microscopy

Immunofluorescent staining was performed on formalin-fixed, paraffin-embedded kidney tissues from each of four individuals (designated K1 through K4) as described elsewhere [9]. Cryostat sections (4–6 μm thick) of Tissue-Tek®

---

[2] Amino acid abbreviations are the following: alanine (A), asparagine (N), aspartate (D), glutamate (E), glutamine (Q), glycine (G), histidine (H), isoleucine (I), lysine (K), leucine (L), serine (S), proline (P), arginine (R), threonine (T), valine (V).

O.C.T compound-embedded kidney tissues were placed on glass microscope slides and dried at room temperature overnight, followed by fixing for 10 min in ice cold acetone, and air-drying for 30 min. Immunofluorescent staining of frozen kidney tissue sections on slides was performed in a humidified atmosphere using Whatman 3MM Chromaography paper soaked in PBS in a rectangular Petri dish. The slides were incubated for 30 minutes with 2 % goat serum in PBS to block non-specific antibody binding and then with anti-hCNT3 monoclonal antibodies (~ 10 μg/mL) for 30 min at room temperature, followed by washing three times with PBS (5 min per wash) using a Coplin jar. In a dark environment, the slides were then incubated with goat anti-mouse IgM AlexaFluor488 conjugated polyclonal antibodies (8 μg/mL) for 30 min at room temperature and washed three times with PBS (5 min per wash). All slides were mounted with # 1 coverslips using Mowiol mounting media (33.3 % w/v glycerol, 13.3 % w/v MOWIOL (Hoechst), 133.3 mM Tris pH 6.8) with 2.5 % w/v paraphenylenediamine and 1 μg/mL DAPI.

To validate the specificity of the anti-hCNT3 monoclonal antibodies, 500 μg/mL of the antigenic hCNT3 peptide or non-related hENT1 peptide were added to anti-hCNT3 monoclonal antibodies (~ 10 μg/mL) and incubated for 30 min at room temperature before application to slides. To identify nephron segments positive for hCNT3, double immunofluorescent labeling of frozen kidney tissue sections for hCNT3 and PNRA, THP, AQP2 or V-ATPase were performed, as previously described [8], by sequential incubations of: (i) mouse anti-human PNRA or THP monoclonal antibodies (0.3 or 0.5 μg/mL, respectively), (ii) goat anti-mouse AlexaFluor546 conjugated polyclonal antibodies (8 μg/mL), (iii) anti-hCNT3 monoclonal antibodies (10 μg/mL), and (iv) goat anti-mouse IgM AlexaFluor488 conjugated polyclonal antibodies (8 μg/mL), or (i) anti-hCNT3 monoclonal antibodies (10 μg/mL), (ii) goat anti-mouse IgM AlexaFluor488 conjugated polyclonal antibodies (8 μg/mL), (iii) rabbit anti-rat AQP2 or human V-ATPase polyclonal antibodies (4 or 0.2 μg/mL, respectively), and (iv) goat anti-rabbit AlexaFluor 546 conjugated polyclonal antibodies (8 μg/mL). Controls for double-labeling experiments included replacement of one or both of anti-PNRA, -THP, -AQP2 or -V-ATPase and anti-hCNT3 primary antibodies with equal concentrations of their respective isotype control mouse monoclonal or rabbit polyclonal antibodies (0.3 μg/mL mouse $IgG1_K$, 0.5 μg/mL mouse IgG2b, 4 μg/mL rabbit IgG, 0.2 μg/mL rabbit IgG, and 10 μg/mL mouse $IgG1_K$, respectively).

Immunofluorescent staining for human ZO-1 and E-CAD was performed on polarized monolayers of each of five hRPTCs isolated from different individuals (designated hRPTC11 through hRPTC15) that were grown on collagen-coated polyester membrane 12-well transwell permeable supports (seeded at 0.5×10^6 cells per well, 10 days in culture). Transwell permeable supports containing polarized monolayer cultures of hRPTCs were fixed in 4 % (w/v) paraformaldehyde for 10 min, permeabilized in 0.25 % (w/v) saponin, and then removed with a scalpel. The remainder of the staining procedure was performed at room temperature in a humidified atmosphere using 3MM paper soaked in PBS in a rectangular Petri dish. The cultures were incubated for 30 min with 4 % (w/v) goat serum in PBS after which they were incubated with mouse anti-human ZO-1 or E-CAD monoclonal antibodies (1 μg/mL) for 30 min and washed three times with PBS (5 min per wash). In a dark environment, slides were then incubated with goat anti-mouse AlexaFluor488 conjugated polyclonal antibodies (8 μg/mL) for 30 min, and washed three times with PBS (5 min per wash) after which # 1 coverslips were attached using MOWIOL mounting medium with 2.5 % w/v paraphenylenediamine and 1 μg/mL DAPI.

Labeled cells were viewed with a Zeiss laser scanning confocal microscope (LSM 510 version 3.2, Jena, Germany) mounted on an Axiovert 100M inverted microscope with a plan Neofluar 40×/1.3 oil immersion lens (Carl Zeiss MicroImaging, Inc.). Argon and helium-neon (HeNe) lasers were sequentially used to scan at wavelengths of 488 and 543 nm, respectively. An ultraviolet (UV) laser (364 nm) was used to excite DAPI-stained cells. Images were collected according to Nyquist sampling with a 560 nm long-pass filter for AlexaFluor546 signal, 505-550 nm band-pass filter for AlexaFluor488 signal and 385-470 nm band-pass filter for DAPI signal.

II.5 Transport assays

II.5.1 Protein Determinations

For uptake and transepithelial flux studies of polarized monolayer cultures of hRPTCs grown on collagen-coated HTS 24-well transwell permeable supports, protein content per well was determined by a colorimetric BIORAD protein assay of triplicate transwell permeable supports according to the manufacturer's instructions. Transwell permeable supports to which hRPTC cultures were attached were removed with a scalpel and solubilised for 10 min in ice-cold radioimmunoprecipitation assay (RIPA) buffer (50 mM Tris·HCl pH 8.0, 150 mM NaCl, 0.1 % (v/v) SDS, 0.5 % (w/v) sodium deoxycholate, 1 % (v/v) nonyl phenoxylpolyethoxylethanol) containing COMPLETE Protease Inhibitor tablets, 0.3 mM phenylmethylsulfonyl fluoride, and 0.5 mM dithiothreitol. After nuclei were spun down at 13 000 × *g* for 30 min at 4 ºC, 10-μL aliquots were removed and added to 0.8 mL of deionized H_2O and 0.19 mL of BIORAD reagent, containing Coomassie® Brilliant Blue G-250 dye. After incubating for 5 min at room temperature, the absorbance at 595 nm (A_{595}) was measured in plastic cuvettes using a UV-Visible Spectrophotometer (Thermo Fisher Scientific Inc., Waltham, MA, USA). Standard curves using known concentrations of bovine serum albumin were prepared to calculate sample protein concentrations using Beer's law ($A_{595} = \varepsilon \times c \times l$, where ε was the extinction coefficient determined from the slope of the standard curve, c was the sample protein concentrations, and l was the path length in cm).

II.5.2 Uptake assay in adherent cultures of HK-2 cells and hRPTCs

Uptake assays were performed as described previously [10] by assessing accumulation of radiolabeled compounds over time into adherent cultures of HK-2 cells and hRPTC cultures isolated from ten different individuals (designated hRPTC1 through hRPTC10). HK-2 cells or hRPTCs were seeded at confluent densities (0.4 × 10^6 cells per well) and maintained at confluence on collagen-coated 12-well plates for 5-7 days. For radiolabeled nucleoside uptake experiments, cells were washed twice at room temperature with buffer (3 mM

K_2HPO_4, 1.2 mM $CaCl_2$, 1 mM $MgCl_2$, 20 mM Tris/HCl, and 5 mM D-glucose pH 7.4) containing either sodium (144 mM NaCl), referred to as sodium-containing buffer, or N-methyl-D-glucamine (144 mM), referred to as sodium-free buffer. For radiolabeled-α-methyl-D-glucoside uptake experiments, cells were washed with buffers (5.4 mM KCl, 1.2 mM $CaCl_2$, 1 mM $MgSO_4$, 10 mM 4-(2-hydroxyethyl)-1-piperazineethanesulfonic-Tris pH 7.4) containing sodium (144 mM NaCl), referred to as sodium-containing buffer, or containing N-methyl-D-glucamine (144 mM), referred to as sodium-free buffer. Cells were then incubated with [^{14}C]-methyl-α-D-glucoside, [^{3}H]-uridine, -thymidine, -inosine, or -fludarabine (1 μCi/mL) in either sodium-containing buffer or sodium-free buffer with or without various additives (*i.e.*, potential permeants, inhibitors) for various time intervals up to 12 min. Cultures were "pre-incubated" with appropriate buffer containing dilazep, nitrobenzylmercaptopurine ribonucleoside (NBMPR), or phloridzin for 30 min when transport assays involved these inhibitors to allow steady-state inhibitor binding to transporter proteins [11]. To end uptake assays, cells were washed three times with ice-cold sodium-containing buffer, air dried, solubilised in 5 % (v/v) Triton X-100, and then transferred to vials with 10 mL Ecolite scintillation fluid for analysis of radioactivity by scintillation counting using a Beckman LS 6000 Scintillation Counter (Beckman Coulter Canada Inc., Mississauga, ON, Canada). Uptake values were normalized to total cell number per well as determined by trypsinization of triplicate wells (not exposed to radioactive compounds) with trypsin-EDTA (0.5 and 0.2 g/L, respectively) and cell counting. For comparison of transport activities by various hNT isoforms, uptake experiments were conducted with 1 μM [^{3}H]-uridine, because it is a permeant of six of the seven known hNTs. Transport activities for hENT2 and hCNT3 were calculated, respectively, by subtracting "background" uptake values of 1 μM [^{3}H]-uridine obtained in the presence of excess non-radiolabeled uridine (10 mM) from that obtained in (i) sodium-free buffer with 0.1 μM NBMPR or (ii) sodium-containing buffer with 200 μM dilazep. Transport activities for hENT1 were calculated by subtracting hENT2 activities from uptake values of 1 μM [^{3}H]-uridine obtained in sodium-free buffer. Three independent transport experiments, each with triplicate measurements, were performed on adherent cultures of hRPTCs isolated from ten different individuals (designated hRPTC1 through hRPTC10).

II.5.3 Uptake assays in polarized monolayers of hRPTC cultures

Uptake of radiolabeled nucleosides into polarized monolayer cultures of hRPTCs isolated from five different individuals (designated hRPTC11 through hRPTC15) that were grown on collagen-coated polycarbonate membrane HTS 24-well transwell permeable supports (seeded at 0.25 × 10^6 cells per well, 10 days in culture) was measured as described previously [12,13] with modifications. Apical and basolateral chambers of transwell permeable supports containing cells were (i) washed twice at room temperature with sodium-containing or sodium-free buffer, and then (ii) incubated for 60 min with 500 μM erythro-9-(2-hydroxy-3-nonyl)adenine (EHNA), where indicated, and 1 μM non-radiolabeled adenosine or 2′-deoxyadenosine in either sodium-containing or sodium-free buffer at pH 7.4 with or without various additives (*i.e.*, potential permeants, inhibitors). Cultures were "pre-incubated" for 60 min with appropriate buffers containing dilazep, NBMPR, cimetidine, or probenecid when transport assays involved these inhibitors. Uptake assays were initiated by adding either [^{3}H]-adenosine, -2′-deoxyadenosine, -fludarabine, -cladribine, or -clofarabine (10 μCi/mL) to apical or basolateral chambers. Uptake assays were stopped by washing cells on inserts three times with ice-cold sodium-containing buffer, after which they were air dried, solubilised in 5 % (v/v) Triton X-100, and then transferred to vials with 10 mL Ecolite scintillation fluid for analysis of radioactivity. Uptake values were normalized to total protein per well as determined by BIORAD protein assay of triplicate cultures (not exposed to radioactive nucleosides). Three independent uptake experiments, each with triplicate measurements, were performed on each of five different polarized monolayer cultures of hRPTCs cultures isolated from five different individuals (designated hRPTC11 through hRPTC15).

II.5.4 Transepithelial flux assays across polarized monolayer cultures of hRPTCs

Transepithelial fluxes of radiolabeled nucleosides across polarized monolayer cultures of hRPTCs isolated from five different individuals (designated hRPTC11 through hRPTC15) that were grown on collagen-coated polycarbonate membrane HTS 24-well transwell permeable supports (seeded at 0.25 × 10^6 cells per well, 10 days in culture) were measured as described previously [12,13] with modifications. Apical and basolateral chambers were (i) washed twice at room temperature with sodium-containing buffer or sodium-free buffer, and then (ii) incubated with 500 μM EHNA, where indicated, and non-radiolabeled adenosine (1 μM), 2′-deoxyadenosine (1 μM), fludarabine (10 μM), cladribine (10 μM), clofarabine (10 μM), or mannitol (1 μM or 10 μM) on both apical and basolateral sides in either sodium-containing or sodium-free buffer with or without various inhibitors for 60 min at room temperature to achieve steady state fluxes across the leaky monolayers as recommended elsewhere [14]. [^{3}H]-Adenosine, -2′-deoxyadenosine, -fludarabine, -cladribine, -clofarabine, or -mannitol (10 μCi/mL) was then added to apical or basolateral chambers and 10–μL samples were collected from the opposite side at timed intervals for 60 min with immediate replacement of removed samples with equal volumes of sodium-containing or sodium-free buffer to maintain osmotic pressure across monolayers [14]. Cultures were "pre-incubated" for 60 min with appropriate buffers containing dilazep, NBMPR, cimetidine, or probenecid before initiating transepithelial flux assays when assays involved these inhibitors. For analysis of radioactivity by scintillation counting, inserts were air dried, solubilised in 5 % (v/v) Triton X-100 and transferred to individual vials that contained 10 mL Ecolite scintillation fluid. Flux values were normalized to total protein content per well, which was determined by BIORAD protein assay of triplicate cultures (not exposed to radioactive nucleosides). Mannitol fluxes were used to estimate paracellular fluxes, which were subtracted from total nucleoside fluxes to obtain mediated nucleoside fluxes. Three independent flux experiments, each with triplicate measurements, were performed on each of five different polarized monolayer cultures of hRPTCs isolated from five different individuals (designated hRPTC11 through hRPTC15).

II.5.5 Production of recombinant hCNT3 and measurement of nucleoside uptake in *Saccharomyces* (*S.*) *cerevisiae*

II.5.5.1 General molecular biology procedures

S. cerevisiae strains were maintained in complete minimal medium (CMM) containing 0.67 % (w/v) yeast nitrogen base (Difco, Detroit, MI, USA), amino acids (as required to maintain auxotrophic selection) and 2 % (w/v) glucose (CMM/GLU). Agar plates contained CMM with various supplements and 2 % (w/v) agar (Difco). Plasmids were propagated in *Escherichia* (*E.*) *coli* strain DH5α (Invitrogen, Carlsbad, CA, USA) and maintained in Luria–Bertani broth (1 % w/v bacto-tryptone, 0.5 % w/v bacto-yeast extract, 1 % w/v NaCl, pH 7.0) with 100 μg/ml ampicillin at 37 °C with shaking at 200 revolutions per min (RPM). Transformation of *E. coli* strain DH5α (Invitrogen) was by heat-shock method according to the manufacturer's instructions. Mini, Midi, or Maxi Plasmid Purification Kits from QIAGEN were used for the preparation of plasmids according to the manufacturer's instructions. DNA samples were resolved by electrophoresis on 1 % w/v agarose gels in Tris/acetate/EDTA electrophoresis buffer (Tris-acetate, 3 mM $Na_2EDTA \cdot 2H_2O$, pH 8.5) alongside 1-kilobase DNA molecular weight markers (Invitrogen). Plasmid DNA for use as template in DNA sequencing was prepared using the QIAGEN Plasmid Purification Kit according to the manufacturer's instructions. DNA sequences were determined by *Taq* DyeDeoxy terminator cycle sequencing with an automated Model 310 DNA sequencer (Applied Biosystems, Foster City, CA) and analyzed with Edit/View/AutoAssembler software (Applied Biosystems).

II.5.5.2 Plasmid construction

E. coli shuttle vector pYPGE15 (containing the constitutive phosphoglycerate kinase promoter) [15] containing hCNT3 gene inserts were previously described [16]. The open reading frame of hCNT3 was PCR-amplified with *Pwo* polymerase (Boerhinger Mannheim/Roche Molecular Biochemicals, Laval, QC, Canada), according to the manufacturer's instructions, using hCNT3 complementary DNA (cDNA) in the original cloning vector pBluescript II KS(+) (Stratagene, La Jolla CA, USA) as the template and the following 5′-*BglII* and 3′-*XhoI* site containing primers (restriction sites underlined): 5′-*BglII*-hCNT3 (5′-CCAGATCTATGGAGCTGAGGAGTACAGCAGCCC-3′) and 3′-*XhoI*-hCNT3 (5′-GGCTCGAGTCAAAATGTATTAGAGATCCCATTGCAGT-3′). The *BglII*-hCNT3-*Xho*I fragment was subcloned into the polylinker in frame with the upstream Green Fluorescent Protein (GFP) open reading frame and the cytomegalovirus promoter of pGFP-C1 (Clontech, Mountain View, CA, USA) to produce the vector pGFP-C1/hCNT3, whose structure was confirmed by DNA sequencing. The open reading frame of hCNT3 was excised from pGFP-C1/hCNT3 using *BglII* and *XhoI* restriction enzymes and subcloned into mammalian expression vector pCDNA3 (Invitrogen) using compatible restriction sites *BamHI* and *XhoI*, producing pCDNA3-hCNT3 whose structure was confirmed by DNA sequencing. The hCNT3 open reading frames were amplified by PCR with *Pwo* polymerase, according to the manufacturer's instructions, using the vector pCDNA3-hCNT3 as the template and the following 5′-*BglII* and 3′-*XhoI* containing primers: 5′-*BglII*-hCNT3 and 3′-*XhoI*-hCNT3. The *BglII*-hCNT3-

*Xho*I fragment was subcloned into the yeast expression vector pYPGE15 [15], which is a high copy-number episomal vector that expresses the inserted DNA under the transcriptional control of a constitutive promoter (phosphoglycerate kinase promoter), producing pYPhCNT3 the structure of which was confirmed by DNA sequencing.

II.5.5.3 Measurement of nucleoside uptake in *S. cerevisiae* expressing recombinant hCNT3

Plasmids pYPhCNT3 were transformed into a *S. cerevisiae* strain, in which the endogenous high affinity uridine permease (*FUI1*) gene had been disrupted (*FUI1::TRP1* (*MATα, gal, ura3-52, trp1, lys2, ade2, hisd2000, Δfui::TRP1*)[3]) [16], using a standard lithium acetate method [17]. Uptake of varying concentrations of $[^3H]$-adenosine and -2′-deoxyadenosine into yeast was measured as described previously [16,18]. Yeast were grown in CMM/GLU to an absorbance at 600 nm (A_{600}) of 0.8 to 1.5, washed twice with fresh media, pH 7.4, and resuspended in CMM/GLU, pH 7.4, to an A_{600} of 4.0. Transport reactions were initiated by rapid mixing of 100 µl of yeast suspension with 100 µl of CMM/GLU, pH 7.4, containing various concentrations of $[^3H]$-adenosine or -2′-deoxyadenosine preloaded in a 96-well cell culture plate. The 96-well plate was placed on the semi-automated cell harvester (Micro96 HARVESTER; Skatron Instruments, Lier, Norway) and every 24 transport reactions were terminated simultaneously at graded time intervals by harvesting yeast on glass-fibre filters

---

[3] *S. Cerevisiae* genes/loci (uppercase refers to dominant allele, lower case refers to recessive allele, *Δ* refers to deletion-insertion): *TRP1* and *trp1*, phosphoribosylanthranilate isomerise; *MATα*, mating type locus α; *ura3-52*, orotidine-5′-phosphate decarboxylase (mutant); *lys2*, α-aminoadipate reductase; *ade2*, phosphoribosylaminoimidazole carboxylase, *hisd2000*, histidinolphosphatase).

(Skatron Instruments) with continued washing with demineralized water. The filters were air-dried for about 5 min, and the portions of the filter that corresponded to individual assays were excised and placed in scintillation vials with 10 mL Ecolite scintillation fluid. The amounts of radioactivity associated with the filters were determined by liquid scintillation counting.

II.6 Thin layer chromatography analysis

Transepithelial fluxes and uptake of [^{3}H]-adenosine and [^{3}H]-2′-deoxyadenosine in polarized monolayer cultures of hRPTCs isolated from five different individuals (designated hRPTC11 through hRPTC15) that were grown on collagen-coated HTS 24-well transwell permeable supports were assayed for 60 min as described above. Fifty-μL samples from apical or basolateral compartments were collected, acidified with ice cold perchloric acid to 7 % (v/v) and incubated for 1 hr. Transwell permeable supports to which cells were attached were cut out and incubated in ice-cold 7 % (v/v) perchloric acid for 1 hr. Acid-soluble extracts containing fluxed or intracellular nucleoside metabolites were removed and neutralized with equal volumes of ice cold 1 M KOH, followed by centrifugation at 10,000 × *g* for 10 min at 4 ºC. Supernatants were evaporated and resuspended in 10 μL of deionized H_2O. Aluminum-backed Silica Gel 60 thin layer chromatogram plates containing fluorescent indicator F254 were spotted with 1-μL portions of extracts together with 1-μL each of standard solutions that contained either 10 mM adenosine-5′-triphosphate (ATP), 2′-deoxyadenosine-5′-triphosphate (dATP), adenosine-5′-diphosphate (ADP), 2′-deoxyadenosine-5′-diphosphate (dADP), adenosine-5′-monophosphate (AMP), 2′-deoxyadenosine-5′-

monophosphate (dAMP), adenosine, 2′-deoxyadenosine, inosine, 2′-deoxyinosine, or hypoxanthine. Plates were developed using *n*-butanol/ethyl acetate/methanol/ammonium hydroxide (7:4:3:4 v/v/v/v) as described previously [19]. Metabolites were identified under UV light and retention factor (R_f) values were calculated and compared with those of the individual standards for identification. The UV-identified spots were cut out, and dissolved in 10 mL Ecolite scintillation fluid overnight at room temperature for analysis of radioactivity by scintillation counting. Results are expressed as % radioactivity loaded (determined by counting 1-µL portions of experimental extracts) for each identified metabolite. Three independent flux experiments, each with triplicate measurements, were performed individually on polarized monolayer cultures of hRPTCs isolated from five different individuals (designated hRPTC11 through hRPTC15).

II.7 Determination of intracellular cyclic adenosine-3′,5′-monophosphate (cAMP)

Hormonal responsiveness of individual adherent cultures of hRPTCs isolated from fifteen different individuals (designated hRPTC1 through hRPTC15) that were grown on collagen-coated 12-well plates (seeded at 0.4×10^6 cells/well, 5-7 days in culture) was assessed by determination of intracellular cAMP production after hormone stimulation using a Cyclic AMP Radioimmunoassay Kit (Biomedical Technologies Inc., Stoughton, MA, USA) according to the manufacturer's instructions. Triplicate wells containing hRPTCs were incubated with serum-free, hormonally defined medium containing 0.5 mM

1-methyl-3-isobutyl-xanthine and with or without either 1 μM human parathyroid hormone synthetic 1-34 fragment (hPTH), 1 μM antidiuretic hormone (ADH), or 5 μM forskolin (as a positive control) for 60 min at 37 °C in a humidified atmosphere containing 5 % (v/v) CO_2 as previously described [6]. Cells were washed with ice-cold PBS and incubated in 1 mL of ice-cold 5 % (v/v) trichloroacetic acid for 1 hr. Extracts containing intracellular cAMP were removed and centrifuged at 10,000 × *g* for 10 min at 4 °C. After removal of precipitates, supernatants were extracted with water-saturated diethyl ether three times in a screw crap centrifuge tube with centrifugation at 300 × *g* for 2 min at 4 °C to separate layers. Water-soluble extracts were collected into glass test tubes, adjusted to a final volume of 1 mL, and residual ether was removed by evaporation overnight at 4°C. Each assay tube contained (in order of addition): (i) either sample extracts (100 μL) or cAMP Standard Solutions with known cAMP concentrations supplied in the kit (100 μL), (ii) [^{125}I]S-Cyclic AMP-TME Tracer (~10,000 counts per minute total) supplied in the kit, (iii) either Non-Specific Binding Reagent (100 μL) containing rabbit γ-globulins (5 μg/mL) or Pre-conjugated Cyclic-AMP Antibody (100 μL) containing goat anti-cAMP antibodies (0.1 μg/mL) supplied in the kit, and (iv) Assay Buffer-Concentrate supplied in the kit to 500 μL total volume. The reaction mixtures were incubated for 20 hr at 4°C after which antibody complexes were precipitated by addition of $(NH_4)_2SO_4$ to a final concentration of 60 % (w/v). After centrifugation for 20 min at 4 °C, radioactivity was determined using a Beckman 5500 Gamma Counter (Beckman Coulter Canada Inc.). Normalized percent bound (% B/B_0) was calculated for each cAMP Standard Solutions with known cAMP concentrations by subtracting background counts obtained in the presence of Non-Specific Binding Reagent and by dividing values by background corrected counts obtained in the presence of the zero standard (containing no cAMP). cAMP standard curves were prepared by plotting % B/B_0 versus known cAMP concentrations (pmol per tube) of cAMP Standard Solutions on a semi-logarithmic plot. % B/B_0 was calculated for each experimental sample by subtracting background counts obtained in the presence of Non-Specific Binding Reagent and by dividing values by background corrected counts obtained in the presence of the zero standards (containing no cAMP). cAMP concentrations (pmol per tube) of experimental samples were determined by interpolation calculated % B/B_0 values from cAMP standard curves. These values represented cAMP concentrations (pmol per tube) of 100 µL aliquots of experimental samples which were taken from 1 mL total samples, which were then multiplied by dilution factor of 10 to obtain total intracellular cAMP in each experimental sample. Results are expressed as pmol of cAMP per 10^6 cells; cell numbers were determined by counting cells in triplicate wells (not extracted with trichloroacetic acid) by trypsinization with trypsin-EDTA (0.5 and 0.2 g/L, respectively). Three independent cAMP determinations, each with triplicate measurements, were performed individually on adherent cultures of hRPTCs isolated from fifteen different individuals (designated hRPTC1 through hRPTC15).

II.8 Reverse transcriptase polymerase chain reaction (RT-PCR) analysis

II.8.1 Total ribonucleic acid (RNA) preparations

Total RNA was isolated using GenElute Mammalian Total RNA Kit from Sigma according to the manufacturer's instructions from (i) 1 g of each of four different human kidney cortex tissues (designated C1 through C4) that were stored in Allprotect Tissue Reagent at -80 °C, (ii) 5×10^6 cells of adherent HK-2, and (iii) each of ten different hRPTC cultures (designated hRPTC1 through hRPTC10), grown for 5-7 days post-confluency on collagen-coated T-75 flasks and harvested by trypsinization with trypsin-EDTA (0.5 and 0.2 g/L, respectively),. Total RNA was treated with DNAse I to remove any contaminating genomic DNA before RT-PCR.

II.8.2 RT-PCR

RT-PCR was performed on total RNA preparations from each of four different human kidney cortex tissues (designated C1 through C4) and from each of ten different hRPTC cultures (designated hRPTC1 through hRPTC10) using Superscript™ One-Step RT-PCR with Platinum® *Taq* (Invitrogen). The oligonucleotide primers used for hENT1, hENT2, hCNT1, hCNT2, and hCNT3 amplification were the following: hENT1: 5′-gcttgaaggacccggggagc[4]-3′ and 5′-tggagaaggcaaaggcagcca[4]-3′; hENT2: 5′-tcccaggcccaagctcagga[4]-3′ and 5′-ggaaccgcaggcagaccagc[4]-3′; hCNT1: 5′-ctgtgtgggtcctcaccttcctg[4]-3′ and 5′-ggagagggccaaggcacaaggg[4]-3′; hCNT2: 5′-caaaggccagagcagctgatc[4]-3′; hCNT3: 5′-gaaacatgtttgactacccacag[4]-3′ and 5′-gtggagttgaaggcattctctaaaacgt[4]-3′; and hOAT2: 5′-gaggatgaacctgccacagt[4]-3′ and 5′-ctggcacagtggagcaagta[4]-3′ (Invitrogen) [20]. The RT-PCR reactions were set up in a total volume of 50 μL with the following (final concentrations shown): 1 × Superscript™ II Reverse Transcriptase and

---

[4] Nucleotide designations are: *a*, adenylate; *c*, cytidylate; *g*, guanylate; *t*, thymidine.

Platinum® *Taq* DNA Polymerase, 0.2 mM of each 2′-deoxynucleoside-5′-triphosphate (dNTP), 1.2 mM $MgSO_4$, 0.2 μM of each forward and reverse oligonucleotide, and autoclaved distilled water. Reaction mixtures were heated to 45 °C for 30 min and then to 94 °C for 2 min for cDNA synthesis. The PCR amplification conditions were as follows for 40 cycles: 94 °C for 1 min; either (i) 55 °C for 1 min for hENT1 or hENT2 amplification, (ii) 50 °C for 1 min for hCNT1 or hCNT2 amplification, (iii) 52 °C for 1 min for hCNT3 amplification, or (iv) 55 °C for 1 min for hOAT2 amplification; and 72 °C for 1 min. Afterwards, PCR reactions were heated to 72°C for 15 min and cooled to 4 °C. The samples were then run in a 1.2 % (w/v) agarose gel (0.8 mM Tris·acetate, 0.04 mM $Na_2EDTA \cdot 2H_2O$, pH 8.5; ethidium bromide). The expected sizes of the PCR products were 0.5 kilobase pairs (kbp) for hENT1, 0.43 kbp for hENT2, 0.8 kbp for hCNT1, 0.61 kbp for hCNT2, 0.48 kbp for hCNT3, and 0.59 kbp for hOAT2. Reverse transcriptase negative controls were used to control for contaminating genomic DNA. The identities of the amplified products were confirmed by DNA sequencing of excised bands. PCR amplification was performed on plasmid pYPGE15 (Invitrogen) [15] construct as negative controls or plasmid pYPGE15 containing hENT1, hENT2, hCNT1, hCNT2, or hCNT3 gene inserts as positive controls. Plasmid (pYpGE15) constructs containing hENT1, hENT2, hCNT1, hCNT2, or hCNT3 gene inserts were prepared as previously described [16,18].

II.8.3 TaqMan™ real-time quantitation RT-PCR

Quantitative real time TaqMan™ RT-PCR using gene-specific primers and fluorescent dye-labeled probes for hENT1, hENT2, hCNT1, hCNT2, and/or hCNT3 was performed as previously described [21] on total RNA samples from (i) adherent cultures of HK-2 cells, (ii) hRPTC1 isolated from one individual, (iii) human kidney cortex tissue from one individual (designated C1) and (iv) individual cultures of hRPTCs isolated from ten different individuals (designated hRPTC10 through hRPTC10). First, 1.0 μg of total RNA was reverse transcribed using the TaqMan™ Gold RT-PCR kit from Applied Biosystems (Foster City, CA, USA) in 50-μL reactions according to the manufacturer's instructions. Second, real time quantitative PCR was performed on 2 μL of reverse transcribed samples using a PRISM 7700 Sequence Detection System and TaqMan™ Universal PCR Master Mix kit from Applied Biosystems and hENT1, hENT2, hCNT1, hCNT2, or hCNT3-specific primers and fluorescently labeled probes (Table II-2). Oligonucleotide probes and primers for the housekeeping gene glyceraldehyde-3-phosphate dehydrogenase (GAPDH) were used to control for RNA pipetting and were purchased as a TaqMan™ RNA Control Reagent kit from Applied Biosystems. Reactions that lacked template were used as negative controls. Quantitative RT-PCR experiments were performed in triplicate on total RNA samples.

Relative expression values were calculated as described elsewhere [22]. First, cycle threshold (C_t) values for replicate PCR reactions were determined by setting a threshold level of fluorescence above background within the linear phase of the exponential PCR reaction. Validation assays (User Bulletin 2, Applied Biosystems) conducted with hNT and GAPDH cDNAs by Dr. K Graham (unpublished obsercations) demonstrated that they were amplified with equal efficiencies. To control for RNA loading, C_t values determined using GAPDH primers and probes were subtracted from C_t values determined using hNT-specific primers and probes on total RNA samples to obtain ΔC_t values. To normalize to the expression level of an arbitrary reference, ΔC_t values of an arbitrary reference were subtracted from all ΔC_t values to obtain $\Delta\Delta C_t$ values (*i.e.*, $\Delta\Delta C_t = \Delta C_t - \Delta C_{t,\ reference}$). Results are expressed as relative expression levels obtained from the equation $2^{-\Delta\Delta C_t}$.

II.9 Immunoblotting analysis

II.9.1 Membrane and protein preparations

Membrane and protein preparations were performed on ice at 0-4 ºC with ice-cold buffers that contain COMPLETE Protease Inhibitor tablets, 0.3 mM phenylmethylsulfonyl fluoride, and 0.5 mM dithiothreitol and with centrifugations at 4 ºC, unless otherwise stated. The protein content of protein preparations was determined using a BIORAD protein assay.

II.9.1.1 Crude membrane preparations

Crude membranes were prepared as previously described [23] from human kidney cortex tissue from (i) nine different individuals (designated C1 through C4 and C11 through C15), (ii) adherent cultures of HK-2 cells and (iii) adherent cultures of hRPTCs isolated from ten different individuals (designated hRPTC1 through hRPTC10). HK-2 cells and hRPTCs were seeded on five collagen-coated T-150 flasks at 10×10^6 cells per flask, grown as adherent cultures for 5-7 days post-confluency, washed with PBS, harvested (5×10^7 cells) with a cell scraper, and pelleted by centrifugation at 300 × *g* for 10 min. Human kidney cortex tissues, HK-2 cell pellets, and hRPTC pellets were incubated in swelling buffer (10 mM Tris-HCl, pH 7.5, 250 mM sucrose, 1 mM EDTA) for 30 min followed by homogenization using a Polytron® Homogenizer (Brinkmann Instruments, Westbury, NY, USA) at setting 6 for 2 min. Intact cells and nuclei were removed by low speed centrifugation (300 × *g*, 10 min) and crude membranes were centrifuged (15 000 × *g*, 30 min) and resuspended in swelling buffer. The resulting crude membranes were stored at -80 °C

II.9.1.2 Cell surface protein preparations

Cell surface protein preparations were produced using a Cell Surface Protein Isolation kit from Pierce (Rockford, IL, USA) according to the manufacturer's instructions and as previously described [24] from (i) 5×10^6 cells of adherent cultures of hRPTCs from each of ten different individuals (designated hRPTC1 through hRPTC10) and (ii) apical cell surfaces from 1×10^6 cells of polarized monolayer cultures of hRPTCs from each of five different individuals (designated hRPTC11 through hRPTC15). Duplicate sets of collagen-coated T-75 flasks or 6-well transwell permeable supports were seeded at 5×10^6 cells per flask or 1×10^6 cells per transwell permeable support, respectively, and grown for 5-7 days or 10 days post-confluency, respectively. Cell counting by trypsinization with trypsin-EDTA (0.5 and 0.2 g/L, respectively) was performed on one set of T-75 flasks and protein determination by BIORAD protein assay of RIPA buffer cell lysates was performed on one set of transwell permeable supports to ensure equal numbers of initial cells or total cellular protein, respectively. After washing cultures with PBS, cell surface proteins (in adherent cultures of hRPTCs on T-flasks and apical cell surface proteins of polarized monolayer cultures of hRPTCs on transwell permeable supports) with exposed lysine residues were biotinylated by addition of sulfosuccinimidyl-2-(biotinamido) ethyl-1,3-dithiopropionate (0.25 mg/mL) to flasks or apical chambers. After biotinylation for 30 min, reactions were quenched by addition of Quenching Solution supplied in the kit and biotinylated cells were harvested by scraping. After pelleting biotinylated cells by centrifugation at 300 × *g* for 10 min, cells were lysed in Lysis Buffer supplied in the kit using a Polytron® Homogenizer at setting 1.5 for five 1-sec bursts and incubated for 30 min with periodic vortexing every 5 min. After centrifuging cell lysates at 10,000 × *g* for 2 min, biotinylated proteins were isolated with Immobilized NeutrAvidin™ Gel slurry (50 % mixture) in spin columns. Biotinylated proteins were bound to NeutrAvidin™ Gel slurry (50 % mixture) for 60 min in spin columns at room temperature, washed with Wash Buffer supplied in the kit, and eluted with sample loading buffer (62.5 mM Tris•HCl, pH 6.8, 1 % w/v SDS, 10 % v/v glycerol, 5 % v/v β-mercaptoethanol, 50 mM dithiothreitol, 2 mg/mL bromophenol blue). The resulting cell surface protein preparations were stored at -80 °C.

II.9.1.3 *S. cerevisiae* crude membrane preparations

Yeast crude membrane preparations were prepared as previously described [16,18] from yeast transformed with plasmid (pYpGE15) containing (i) no insert as negative controls or (ii) hENT1, hENT2, hCNT2, and hCNT3 gene inserts as positive controls. Yeast transformed with plasmids were grown to an optical density at 600 nM of approximately 1.0 were (i) harvested by centrifugation at

500 × *g* for 5 min, (ii) resuspended in yeast breaking buffer (0.2 mM EDTA, 0.5 mM dithiothreitol, 10 mM Tris·HCl pH 7.5), (iii) lysed by vortexing in the presence of glass beads (425-600 μM) for 15 min, (iv) centrifuged at 500 × *g* for 5 min to remove unbroken cells and glass beads, and (v) centrifuged at 100,000 × *g* for 1 hr. The resulting control yeast crude membranes from yeast expressing (or not expressing) recombinant hENT1, hENT2, hCNT2, or hCNT3 were stored at -80 °C.

II.9.2 Sodium dodecyl sulphate (SDS)-polyacrylamide gel electrophoresis and immunoblotting

Various membrane or cell surface protein preparations and low range SDS-polyacrylamide gel electrophoresis standards (10 μL) were mixed in sample loading buffer (62.5 mM Tris•HCl, pH 6.8, 1 % w/v SDS, 10 % v/v glycerol, 5 % v/v β-mercaptoethanol, 2 mg/mL bromophenol blue). After denaturation at 95 °C for 5 min, samples were (i) run on SDS polyacrylamide gels (10 % w/v) at 100 V for 2 hr using a BIORAD Mini-PROTEAN 3 Electrophoresis System, (ii) transferred to Immobilon-P polyvinylidene fluoride membranes at 200 A for 2 hr using a Thermo Scientific Owl HEP-1 Semi Dry Electroblotting System, (iii) incubated in blocking solution (0.2 % v/v Tween-20, Tris-buffered saline, 5 % w/v skim milk powder) overnight at 4°C, (iv) incubated with either mouse anti-hENT1, -hENT2, -hCNT2, or -hCNT3 monoclonal antibodies (~ 1 μg/mL, 1:10 dilution of supernatant) in blocking solution for 2 hr at room temperature, (v) washed five times (5 min/wash) with washing solution (0.2 % v/v Tween-20, Tris buffered saline), (vi) incubated with goat anti-mouse IgG horseradish peroxidase conjugated polyclonal antibodies or in the dark with goat anti-mouse IgG AlexaFluor488 conjugated polyclonal antibodies (0.001 μg/mL) in blocking solution for 2 hr, and (vii) washed five times (5 min [erwash) with washing solution. For blots with goat anti-mouse horseradish peroxidase conjugated polyclonal antibodies, immunoreactive bands were visualized by ECL according to the manufacturer's instructions. Visualization was by exposure to Fuji RX film. For blots with goat anti-mouse AlexaFluor488 conjugated polyclonal antibodies, immunoreactive band intensities were quantified by fluorescence imaging using a Typhoon 9400 Variable Mode Imager from Amersham Biosciences (Sunnyvale, CA, USA). To control for protein loading, immunoblots containing crude membranes were incubated with stripping buffer (50 mM Tris pH 6.8, 2 % w/v SDS, 1 % v/v β-mercaptoethanol) at 50 °C for 30 min to remove primary and secondary antibodies and re-probed with rabbit anti-β-actin polyclonal antibodies (clone A2066; 4 μg/mL) followed by incubation with donkey anti-rabbit horseradish peroxidise or AlexaFluor488 conjugated polyclonal antibodies (0.001 μg/mL) using the same protocol as above. All immunoblots were produced in triplicate. Relative hCNT3 protein abundance in crude membrane preparations was calculated from triplicate experiments with background corrected hCNT3 band signal intensities (integrated intensity of all pixels in a particular band) normalized to β-actin band signal intensities. Relative hCNT3 protein quantities in cell surface and apical cell surface protein preparations were calculated from triplicate experiments with background corrected hCNT3 band signal intensities.

II.10 Cytotoxicity assays

Cytotoxicity assays were performed on adherent cultures of hRPTCs isolated from ten different individuals (designated hRPTC1 through hRPTC10) as previously described [25] using a CellTiter 96® AQ$_{ueous}$ Non-Radioactive Cell Proliferation Assay from Promega (Madison, WI, USA). The latter is a colorimetric assay that makes use of conversion of methoxyphenyl tetrazolium inner salt (MTS) compound to a coloured formazan product by mitochondrial dehydrogenase in metabolically active cells. Briefly, adherent cultures of hRPTCs were maintained on collagen-coated 96-well plates for 5-7 days at confluency after which they were incubated for 72 hr with or without various concentrations of fludarabine in growth media in triplicate wells. After fludarabine exposures, hRPTCs were incubated with MTS reagent for 1 hr, and absorbance at 490 nm was then measured using a 96-well plate reader from Molecular Devices (Sunnyvale, CA, USA). Three independent cytotoxicity experiments were performed in triplicate.

II.11 Data analysis

For experiments that measured inhibition of uridine uptake in hRPTC cultures, the concentrations that reduced mediated uridine uptake by 50 % (*i.e.*, IC_{50} values) were determined by non-linear regression analysis of the sigmoidal concentration-effect curves. For cytotoxicity experiments in hRPTC cultures, the concentrations resulting in 50 % reduction in cell viability (*i.e.*, EC_{50} values) were determined by non-linear regression analysis of sigmoidal dose-response curves. For experiments that measured concentration dependence of uptake rates of adenosine and 2′-deoxyadenosine into yeast producing recombinant hCNT3, the concentrations that yielded 50 % of maximum uptake rates (*i.e.*, K_m values) and maximum uptake rates (*i.e.*, V_{max} values) were determined by non-linear regression analysis of the parabolic rate versus concentration curves. Statistical comparisons of matched experimentally determined values were done by unpaired t tests and correlation analysis. Statistical analysis of variance within groups of experimentally determined values were done by one-way analysis of variance; where p values < 0.05, Tukey's post-test were performed to determine which values were significantly different from each other. All calculations and graphs were generated using GraphPad Prism® 4.0 (GraphPad Software Inc.; http://www.graphpad.com).

Table II-1. Summary of collected human kidney tissues and isolated hRPTC cultures

Individual	Paraffin-embedded kidney tissue	O.C.T.-embedded kidney tissue	Cortex tissue - Total RNA preparations	Cortex tissue - crude membrane	hRPTC cultures
1	K1	K1	C1	C1	-
2	K2	K2	C2	C2	-
3	K3	K3	C3	C3	-
4	K4	K4	C4	C4	-
5	-	-	-	-	hRPTC1
6	-	-	-	-	hRPTC2
7	-	-	-	-	hRPTC3
8	-	-	-	-	hRPTC4
9	-	-	-	-	hRPTC5
10	-	-	-	-	hRPTC6
11	-	-	-	-	hRPTC7
12	-	-	-	-	hRPTC8
13	-	-	-	-	hRPTC9
14	-	-	-	-	hRPTC10
15	-	-	-	C11	hRPTC11
16	-	-	-	C12	hRPTC12
17	-	-	-	C13	hRPTC13
18	-	-	-	C14	hRPTC14
19	-	-	-	C15	hRPTC15

Table II-2. TaqMan$^{\mathrm{TM}}$ oligonucleotide primers and probes

Gene	Sequence
hENT1	
Sense primer	5'-caccagcctcaggacagatacaa-3'
Antisense primer	5'-gtgaaatactgagtggccgtcat-3'
Probe[a]	5'-FAM-gtgaaatactgagtggccgtcat-3'
hENT2	
Sense primer	5'-atgagaacgggattcccagtag-3'
Antisense primer	5'-gctctgattccggctcctt-3'
Probe[b]	5'-TET-cagaaagtagctctgaccctggatcttgacct-3'
hCNT1	
Sense primer	5'-tctgtggatttgccaatttcag-3'
Antisense primer	5'-cggagcactatctgggagaagt-3'
Probe[b]	5'-TET-tgggaggcttgacctccatggtcc-3'
hCNT2	
Sense primer	5'-caaacaccacagcgcagtgt-3'
Antisense primer	5'-tgaccaagatcccaaagacaaa-3'
Probe[b]	5'-TET-cctaggcccgaaaacactgtcctcca-3'
hCNT3	
Sense primer	5'-gggtccctaggaatcgtgatc-3'
Antisense primer	5'-cgaggcgatatcacgctttc-3'
Probe[b]	5'-TET-cggactcacatcccatggctccttc-3'

a - FAM: 6-carboxy-fluorescein

b - TET: tetrochloro-6-carboxy-fluorescein

II.12 Bibliography

1. Mackey JR, Jennings LL, Clarke ML, Santos CL, Dabbagh L, Vsianska M, Koski SL, Coupland RW, Baldwin SA, Young JD, Cass CE. Immunohistochemical variation of human equilibrative nucleoside transporter 1 in primary breast cancers. Clin Cancer Res. 2002; 8: 110-6.

2. Vickers MF, Zhang J, Visser F, Tackaberry T, Robins MJ, Nielsen LP, Nowak I, Baldwin SA, Young JD, Cass CE. Uridine recognition motifs of human equilibrative nucleoside transporters 1 and 2 produced in Saccharomyces cerevisiae. Nucleosides Nucleotides Nucleic Acids. 2004; 23: 361-73.

3. Zhang J, Smith KM, Tackaberry T, Visser F, Robins MJ, Nielsen LP, Nowak I, Karpinski E, Baldwin SA, Young JD, Cass CE. Uridine binding and transportability determinants of human concentrative nucleoside transporters. Mol Pharmacol. 2005; 68: 830-9.

4. Zhang J, Visser F, Vickers MF, Lang T, Robins MJ, Nielsen LP, Nowak I, Baldwin SA, Young JD, Cass CE. Uridine binding motifs of human concentrative nucleoside transporters 1 and 3 produced in *Saccharomyces cerevisiae*. Mol Pharmacol. 2003; 64: 1512–20.

5. Todd JH, McMartin KE, Sens DA. Enzymatic isolation and serum-free culture of human renal cells. In Methods in Molecular Medicine: Human Cell Culture Protocols. Edited by Jones, GE. Humana Press Inc,: Totowa, NJ, 1995; Chapter 32.

6. Toutain H, Vauclin-Jacques N, Fillastre JP, Morin JP. Biochemical, functional, and morphological characterization of a primary culture of rabbit proximal tubule cells. Exp Cell Res. 1991; 194: 9-18.

7. Spratlin J, Sangha R, Glubrecht D, et al. The absence of human equilibrative nucleoside transporter 1 is associated with reduced survival in patients with gemcitabine-treated pancreas adenocarcinoma. Clin Cancer Res 2004; 10: 6956-61.

8. Kujala M, Tienari J, Lohi H, Elomaa O, Sariola H, Lehtonen E, and Kere J. SLC26A6 and SLC26A7 anion exchangers have a distinct distribution in human kidney. Nephron Exp Nephrol. 2005; 101: e50-58.

9. Mackey JR, Jennings LL, Clarke ML, Santos CL, Dabbagh L, Vsianska M, Koski SL, Coupland RW, Baldwin SA, Young JD, Cass CE. Immunohistochemical variation of human equilibrative nucleoside transporter 1 protein in primary breast cancers. Clin Cancer Res. 2002; 8: 110-6.

10. Graham KA, Leithoff J, Coe IR, et al. Differential transport of cytosine-containing nucleosides by recombinant human concentrative nucleoside transporter protein hCNT1. Nucleosides Nucleotides Nucleic Acids 2000; 19: 415-34.

11. Boumah CE, Hogue DL, Cass CE. Expression of high levels of nitrobenzylthioinosine-sensitive nucleoside transport in cultured human choriocarcinoma (BeWo) cells. Biochem J. 1992; 288: 987-96.

12. Morshed KM, McMartin KE. Reabsorptive and secretory 5-methyltetrahydrofolate transport pathways in cultured human proximal tubule cells. Am J Physiol Renal Physiol. 1997; 272: F380-8.

13. Morshed KM, Ross DM, McMartin KE. Folate transport proteins mediate the bidirectional transport of 5-methyltetrahydrofolate in cultured human proximal tubule cells. J Nutr. 1997; 127: 1137-47.

14. Morshed KM, McMartin KE. Transient alterations in cellular permeability in cultured human proximal tubule cells: implications for transport studies. In Vitro Cell Dev Biol Anim. 1995; 31: 107-14.

15. Brunelli JP, Paul ML. A series of yeast shuttle vectors for expression of cDNAs and other DNA sequences. Yeast. 9: 1299-1308, 1993.

16. Zhang J, Smith KM, Tackaberry T, Visser F, Robins MJ, Nielsen LP, Nowak I, Karpinski E, Baldwin SA, Young JD, and Cass CE. Uridine binding and transportability determinants of human concentrative nucleoside transporters. Mol Pharmacol. 2005; 68: 830-839.

17. Ito H, Fukuda Y, Murata K, and Kimura A. Transformation of intact yeast cells treated with alkali cations. J Bacteriol. 1983; 153: 163-168.

18. Vickers MF, Zhang J, Visser F, Tackaberry T, Robins MJ, Nielsen LP, Nowak I, Baldwin SA, Young JD, and Cass CE. Uridine recognition motifs of human

equilibrative nucleoside transporters 1 and 2 produced in Saccharomyces cerevisiae. Nucleosides Nucleotides Nucleic Acids. 2004; 23: 361-373.

19. Shimizu H, Daly JW, Creveling CR. A radioisotopic method for measuring the formation of adenosine 3′,5′-cyclic monophosphate in incubated slices of brain, J Neurochem. 1969; 16: 1609-1619.

20. García-Manteiga J, Molina-Arcas M, Casado FJ, Mazo A, Pastor-Anglada M Nucleoside transporter profiles in human pancreatic cancer cells: role of hCNT1 in 2′,2′-difluorodeoxycytidine- induced cytotoxicity. Clin Cancer Res. 2003; 9: 5000-8.

21. Ritzel MW, Ng AM, Yao SY, Graham K, Loewen SK, Smith KM, Ritzel RG, Mowles DA, Carpenter P, Chen XZ, Karpinski E, Hyde RJ, Baldwin SA, Cass CE, Young JD. Molecular identification and characterization of novel human and mouse concentrative Na+ nucleoside cotransporter proteins (hCNT3 and mCNT3) broadly selective for purine and pyrimidine nucleosides (system cib). J Biol Chem. 2001; 276: 2914– 2927.

22. Fink L, Seeger W, Ermert L, et al. Real-time quantitative RT-PCR after laser-assisted cell picking. Nat Med. 1998; 4: 1329-33.

23. Terada T, Saito H, Mukai M, Inui KI. Identification of the histidine residues involved in substrate recognition by a rat H^+/peptide cotransporter, PEPT1. FEBS Lett. 1996; 394: 196-200.

24. Handlogten ME, Hong SP, Westhoff CM, and Weiner ID. Apical ammonia transport by the mouse inner medullary collecting duct cell (mIMCD-3). Am J Physiol Renal Physiol. 2005; 289: F347-F358.

25. Malich G, Markovic B, Winder C. The sensitivity and specificity of the MTS tetrazolium assay for detecting the in vitro cytotoxicity of 20 chemicals using human cell lines. Toxicol. 1997; 124: 179-192.

Chapter III

III. Distribution of human equilibrative and concentrative nucleoside transporters 1 and 3 (hENT1 and hCNT3) in human kidney proximal tubules[1]

---

[1] An earlier version of this chapter has been published as a co-authored paper [Damaraju VL, Elwi AN, Hunter C, Carpenter P, Santos C, Barron GM, Sun X, Baldwin SA, Young JD, Mackey JR, Sawyer MB, Cass CE. Localization of broadly selective equilibrative and concentrative nucleoside transporters, hENT1 and hCNT3, in human kidney. Am J Physiol Renal Physiol. 2007; 293: F200-11.]; contribution of Elwi AN was 50%.

III.1 Introduction

Pharmacokinetic evidence suggests that some nucleosides are actively reabsorbed and secreted by the kidney through equilibrative and concentrative nucleoside transporters (ENTs and CNTs)[1-6]. Adenosine, a regulatory nucleoside that acts through binding to adenosine receptors [7], is found in plasma and its reabsorption in the human kidney has been demonstrated [1]. It has been suggested that toxic nucleosides (*e.g.*, 2′-deoxyadenosine) are selectively eliminated by renal secretion [1]. Renal reabsorption and secretion appear to involve different transport systems, since renal reabsorption of adenosine in mice was unaffected by classical nucleoside transport inhibitors (*e.g.*, NBMPR and dipyridamole), whereas renal secretion of 2′-deoxyadenosine and 5′-deoxy-5-fluorouridine was decreased by treatment with these inhibitors [2,3]. Human organic cation and anion transporters (hOCTs and hOATs may be involved in the renal secretion of nucleosides [4-6].

Human ENTs (hENTs) and hCNTs have been demonstrated in human kidney by functional studies [8], multiple tissue expression ribonucleic acid (RNA) arrays [9-18], *in situ* hybridization and immunohistochemistry studies [19], and immunoblotting studies [20]. Functional studies with human kidney brush border membrane vesicles revealed a single concentrative sodium-dependent nucleoside transport activity with pyrimidine-nucleoside selective (concentrative insensitive thymidine, *cit*) characteristics except that guanosine was also a permeant [8]. Expression of all seven hENT/CNT mRNA transcripts has been observed in the human kidney through multiple tissue expression RNA arrays [9-18], although hENT3 mRNA expression in human kidney appears to be minimal [12]. During the period that the current studies were being performed, others reported results of *in situ* hybridization studies in human kidney tissue that identified mRNA transcripts for hENT1 and hENT2 in distal tubules and glomeruli and for hCNT1 and hCNT2 in proximal tubules [19]. In the same report, the companion immunohistochemistry studies in human kidney tissues showed hCNT1 and hCNT2 staining in apical membranes of proximal tubules, hENT1 staining in apical and basolateral membranes of proximal tubules adjacent to corticomedullary junctions, and hENT1 and hENT2 staining in basolateral membranes of distal tubules [19]. hENT4/PMAT protein has been detected in human kidney by immunoblotting of tissue lysates [20]. It is uncertain whether or not hCNT3 is also present in human kidney and, if so, how it is distributed and localized in nephron tubules.

Asymmetric distribution of various transporters on cell surfaces is thought to determine the net absorption or secretion of nucleosides across epithelia [21]. For example, it has been proposed that absorption of nucleosides in the gastrointestinal tract is accomplished by sodium-dependent CNTs on apical surfaces and ENTs on basolateral surfaces, resulting in the net transport of dietary nucleosides from the intestinal lumen into blood [22]. A similar hypothesis has been proposed for renal reabsorption of nucleosides by proximal tubules based on the observed asymmetric localizations of recombinant hENT1- and hENT2-Green Fluorescent Protein (GFP) fusion proteins to basolateral membranes and rat CNT1- (rCNT1), rCNT2-, hCNT3- , and hENT1-GFP fusion proteins to apical membranes of transfected LLC pig kidney (LLC-PK$_1$) cells grown as polarized monolayers [23-25], a model for proximal tubule epithelial cells [26]. Previous studies in recombinant hENT1-Yellow Fluorescent Protein (YFP) and hCNT1-Cyan Fluorescent Protein (CFP) transfected LLC-PK$_1$ cells grown as polarized monolayers demonstrated preferential apical-to-basolateral transepithelial (*i.e.*, "reabsorptive") fluxes of adenosine and basolateral-to-apical transepithelial (*i.e.*, "secretive") fluxes of 2′-deoxyadenosine at physiological concentrations [27]. During the course of the current studies, recombinant hENT4/PMAT- and hCNT3-GFP fusion proteins were localized to apical membranes in transfected Madin Darby Canine Kidney (MDCK) cells grown as polarized monolayers [20,28], a model for distal tubule epithelial cells [29]. Additionally, functional studies that were performed in murine proximal convoluted tubule cells with endogenous CNT3 activities and grown as polarized monolayers demonstrated preferential sodium-dependent reabsorptive fluxes of cytidine and in recombinant hCNT3-GFP transfected MDCK cells, also grown as polarized monolayers, demonstrated sodium-dependent reabsorptive fluxes of adenosine, 9-β-D-arabinosyl-2-fluoroadenine (fludarabine), 2',2'-difluoro-2'-deoxycytidine (gemcitabine), 5′-deoxy-5-fluorouridine, 3'-azido-2',3'-dideoxythymidine (zidovudine), and 1-(β-D-ribofuranosyl)-1*H*-1,2,4-triazole-3-carboxamide (ribavirin) [28]. MDCK cells exhibit endogenous *es* activities mediated by canine ENT1 [29] and LLC-PK$_1$ cells exhibit endogenous ENT1 activities and small components of CNT2 activities [30]. Although these studies provided insights into the functions of proximal tubular hENTs and hCNTs, (i) overexpression of recombinant protein in renal epithelial cell lines is known to saturate trafficking pathways [31,32], (ii) difference in transport capacities and affinities exist between NTs of different species [33,34], and (iii) the distal tubule-like MDCK and proximal tubule-like LLC-PK1 cell lines have characteristics of more than one tubular segment [35-38].

Collectively, evidence from pharmacokinetic studies and transepithlial flux studies in non-human renal epithelial cell lines suggested that coupling of apical hCNTs to basolateral hENT1 and hENT2 in proximal tubules mediates reabsorption of nucleosides (*e.g.*, adenosine) and that apical hENT1 in proximal tubules may be involved in secretion of other nucleosides (*e.g.*, 2′-deoxyadenosine). It was hypothesized that hCNT3 and hENT1/2 would be present in apical and basolateral membranes, respectively, of human kidney proximal tubules because of: (i) the greater permeant tolerance, 2:1 Na^+-to-nucleoside coupling ratio, and H^+/nucleoside co-transport capabilities of hCNT3 [18,39] and (ii) the greater permeant tolerance of hENT2 for nucleobases [10-12]. Thus, hCNT3 has greater concentrating capacity than either hCNT1 or hCNT2 and is able to co-transport nucleosides under varying sodium and proton gradients in the nephron tubular lumen while hENT2 can equilibrate both nucleosides and nucleobases at the basolateral membrane. On the other hand, we postulated that hENT1 may also be present at the apical membrane of human kidney proximal tubules because renal secretion of 2′-deoxyadenosine is dependent on ENT1 in mice [1,3].

To increase understanding of renal nucleoside reabsorption and secretion processes, studies were undertaken to gain a more comprehensive picture of the distribution and localization of endogenous hENTs and hCNTs in human kidney. We assayed human kidney cortex tissues obtained from four different individuals for: (i) the presence, and relative levels, of messenger RNA (mRNA) transcripts for hENT1/2 and hCNT1/2/3 by quantitative TaqMan® reverse transcription polymerase chain reaction (RT-PCR) analysis, (ii) the presence of protein for hENT1/2 and hCNT2/3 in crude membranes by immunoblotting analysis, and (iii) the anatomic localizations of hENT1 and hCNT3 in human kidney tissues by immunohistochemistry and immunofluorescent staining analyses using established marker proteins for proximal tubules, thick ascending loops of Henle, and collecting ducts. Additionally, we established human cell culture systems of proximal tubular origin that exhibited endogenous hENT and hCNT activities and could be utilized for future studies of the functional roles of proximal tubular hENTs and hCNTs in renal handling of nucleosides. We examined the nucleoside transport processes present in monolayer cultures of the established human kidney proximal tubular cell line (HK-2) and of human renal proximal tubule cells (hRPTCs) developed as primary cultures from human kidney cortex tissues. Monolayer cultures of HK-2 cells were assayed for: (i) the presence, and relative levels, of mRNA transcripts for hENT1/2 and hCNT1/2/3 by quantitative TaqMan® RT-PCR analysis, (ii) the presence of hENT1/2 and hCNT3 in crude membranes by immunoblotting analysis, and (iii) the presence of activities for hENT1/2 and hCNT1/2/3 by radiolabeled nucleoside uptake studies. To establish the proximal tubular origin of cultures of hRPTCs isolated from human kidney cortex tissues of fifteen different individuals (designated hRPTC1 through hRPTC15), we determined: (i) brush border enzyme activities, (ii) parathyroid hormone sensitivities, and (iii) sodium-dependent, phloridzin sensitive methyl-α-methyl-D-glucoside uptake activities. Nucleoside transport processes present in monolayer cultures of hRPTC1, isolated from human kidney cortex tissue of one individual were characterized by radiolabeled nucleoside uptake studies.

These studies revealed that human kidney cortex tissues possess mRNAs encoding hENT1, hENT2, hCNT1, hCNT2 and hCNT3 by RT-PCR analysis, and protein for hENT1, hENT2, and hCNT3 by immunoblotting analysis. The anatomic locations of hENT1 in human kidney were determined by immunohistochemistry to be apical surfaces of proximal tubules and apical and basolateral surfaces of thick ascending loops of Henle and collecting ducts by immunohistochemistry. The anatomic locations of hCNT3 in human kidney were determined by immunofluorescent staining to be apical surfaces of proximal tubules and thick ascending loops of Henle. Characterization of nucleoside transporter processes present in monolayer cultures of HK-2 cells demonstrated the presence of mRNA transcripts encoding hENT1, hENT2 and hCNT3 by RT-PCR analysis, protein for hENT1 and hCNT3 by immunoblotting analysis, and hENT1 activities by radiolabeled uridine uptake studies. Fifteen different monolayer cultures of hRPTCs were shown to possess proximal tubular characteristics including the presence of brush border enzymes, the presence of sodium-dependent, phloridzin-sensitive α-methyl-D-glucose uptake, and sensitivities to parathyroid hormone. Characterization of nucleoside transporter processes present in monolayer cultures of hRPTC1 demonstrated the presence of hENT1, hENT2, and hCNT3 activities. These results suggest the involvement of hENT1, hENT2, and hCNT3 in renal handling of physiological nucleosides and nucleoside analog drugs.

III.2 Results

III.2.1 Distribution of hENTs and hCNTs in human kidney tissues

III.2.1.1 Expression of messenger RNA (mRNA) transcripts for hENTs and hCNTs in human kidney cortex tissues

Previous work demonstrated the presence of mRNA transcripts for all seven of the known hNTs, hENT1/2/3/4 and hCNT1/2/3, in human kidney tissues in multiple tissue RNA arrays [9-18]. Additionally, *in situ* hybridization studies in human kidney tissue demonstrated mRNA transcripts for hENT1 and hENT2 in distal tubules and glomeruli and mRNA transcripts for hCNT1/2 in proximal tubules [19]. In the current work, analysis of the expression of nucleoside transporter genes in four different human kidney cortex tissues obtained from four different individuals (designated C1 through C4, Table II-1) was undertaken using quantitative TaqMan® RT-PCR. This was also performed simultaneously on total RNA from monolayer cultures of HK-2 cells to determine whether this proximal tubular cell line expressed hNTs present in human kidney cortex tissues. The HK-2 cell line was established by immortalization of primary cultures of human proximal tubule cells isolated from adult human kidney cortex with human papillomavirus E6/E7 genes (40). It was chosen for investigation because of its: (i) human proximal tubular origin, (ii) maintenance of proximal tubular characteristics, and (iii) continuous and reproducible growth. The analysis was performed on total RNA using hENT1/2- and hCNT1/2/3-specific probes and primers as described in Materials and Methods (Section II.8). Relative mRNA transcript levels for each hNT were normalized to the sample possessing the lowest relative levels (arbitrary reference sample) as described in Materials and Methods (Section II.8) *i.e.*, HK-2 for hENT1 and hCNT3 and C4 for hENT2, hCNT1, and hCNT2).

Quantitative TaqMan® RT-PCR analysis identified the presence of mRNA transcripts for hENT1/2 and hCNT1/2/3 to varying levels in total RNA from four different human kidney cortex tissues and hENT1/2 and hCNT3, but not hCNT1/2, in total RNA from monolayer cultures of HK-2 cells (Table III-1). Relative levels of mRNA transcripts for hENT1, hCNT1 and hCNT3 varied over approximately 260-fold, 300-fold and 400-fold ranges, respectively, between the give total RNA preparations while those for hENT2 and hCNT2 varied over smaller ranges of approximately 12-fold and 10-fold, respectively (Table III-1). Although the relative levels of mRNA transcripts in HK-2 cells for hENT2 were comparable to those observed in four different human kidney cortex tissues, relative levels for hENT1 and hCNT3 were lower (p values < 0.01). hCNT1 and hCNT2 were undetectable in monolayer cultures of HK-2 cells, unlike in human kidney cortex tissues. Because proximal tubule epithelial cells are the predominant cell type in human kidney cortex tissues, constituting over 90% by mass [41,42], these results suggested that mRNA transcripts for hENT1/2 and hCNT1/2/3 are present in human kidney proximal tubules to varying levels while only mRNA transcripts for hENT1/2 and hCNT3 are present in monolayer cultures of HK-2 cells.

III.2.1.2 Identification of hENT1, hENT2, hCNT2 and hCNT3 in human kidney cortex tissues

During the course of the current studies, various hNT proteins were identified in human kidney tissue, including: (i) hCNT1 and hCNT2 in proximal tubules, hENT1 in proximal tubules adjacent to corticomedullary junctions, and hENT1 and hENT2 in distal tubules by immunohistochemistry [19] and (ii) hENT4 in tissue lysates by immunoblotting [20]. Since mRNA transcripts for hENT1/2 and hCNT1/2/3 were observed to varying levels in total RNA from human kidney cortex tissues C1 through C4, immunoblotting analyses were carried to determine which hNT proteins were present in crude membrane preparations. Immunoblotting was performed on crude membranes prepared from four human kidney cortex tissues using mouse monoclonal antibodies specific for hENT1, hENT2, hCNT2 or hCNT3 as described in Materials and Methods (Section II.9). Antibodies raised against a hCNT1-derived synthetic peptide failed to recognize hCNT1 in the positive controls (crude membranes from yeast producing recombinant hCNT1), therefore immunoblotting studies to detect hCNT1 in crude membranes from human kidney cortex tissues could not be performed.

The immunoblotting results are presented in Figure III-1. hENT1, hENT2 and hCNT3, but not hCNT2, were detected in crude membranes from all four human kidney cortex tissues. Immunoreactive bands exhibited the expected gel mobilities of hNT proteins – *i.e.*, 45-55 and 90 kDalton (kDa), respectively, for mammalian hENT1/2 and hCNT3 and 35-45 and 90 kDa, respectively, for recombinant hENT1/2 and hCNT3 produced in yeast (positive controls) (Figure III-1). The diffuse immunoreactive bands for hENT1 and hENT2 were likely due to different glycosylation states (Figure III-1) [43,44]. Multiple immunoreactive bands for hENT2 have been reported previously and were likely the result of proteolysis during preparation (Figure III-1) [45]. Despite the presence of mRNA transcripts for hCNT2 in total RNA of the four different human kidney cortex tissues that were analyzed, hCNT2 was not detected, indicating that it was either not present or below the limits of detection of the assay. Single immunoreactive bands for hCNT3 migrating at 90 kDa were observed. As the major cell type in human kidney cortex are proximal tubule epithelial cells [41,42], these results suggested that hENT1, hENT2 and hCNT3 were present in human kidney proximal tubules.

III.2.1.3 Localization of hENT1 and hCNT3 in human kidney tissues

During the course of the current studies, hCNT1 and hCNT2 were reported to be present in apical membranes of proximal tubules, hENT1 to be present in apical and basolateral membranes of proximal tubules adjacent to corticomedullary junctions, and hENT1 and hENT2 to be present in basolateral membranes of distal tubules [19]. In the current study, since hENT1, hENT2 and hCNT3 were detected in crude membranes of four different human kidney cortex tissues by immunoblotting, localization studies were undertaken to assess their anatomic distributions in human kidney tissues obtained from four different individuals (designated K1 through K4, Table II-1). Since hCNT2 protein was not detected in immunoblotting analyses of crude human kidney cortex membranes, localization of hCNT2 in human kidney tissues was not undertaken.

Two established methods were assessed for use in immunolocalization studies with hENT1, hENT2 and hCNT3 [47]. First, immunohistochemistry of paraffin-embedded tissues was employed because it preserves morphology of tissue ultrastructure well but does require antigen retrieval as formalin fixation can mask antigenic epitopes [46]. Second, immunofluorescent staining of frozen tissues was employed because it allows labeling of cells for multiple antigens (*i.e.* double immunofluorescent staining) but does not preserve morphology because of denaturing acetone fixation [46]. The methods employed were based on previous studies of immunohistochemistry methods of staining paraffin-embedded tissues [47] or staining frozen tissues [48] with anti-hENT1 mouse monoclonal antibodies as described in Materials and Methods (Section II.4). Immunofluorescence staining of frozen tissues with anti-hENT1 or -hENT2 mouse monoclonal antibodies yielded negative results, possibly due to low protein abundance, whereas staining with anti-hCNT3 antibodies was clearly positive. Immunohistochemistry staining of paraffin-embedded tissues with anti-hENT2 and -hCNT3 monoclonal antibodies yielded high non-specific background staining even with dilutions of antibodies, possibly due to antigenic epitope masking with formalin fixation. Paraffin embedded human kidney tissue sections fixed with formalin and frozen tissue sections fixed with acetone post-sectioning exhibited good immunoreactivity for hENT1 and hCNT3, respectively (Figure III-2a,d). Since neither of these methods worked for hENT2, it was not possible to localize hENT2 in kidney tissues.

The specificity of hENT1 and hCNT3 staining was demonstrated in Figure III-3 by immunostaining of human kidney tissue with anti-hENT1 or -hCNT3 antibodies in the presence or absence of immunogenic peptides. In human kidney tissue, immunohistochemistry with anti-hENT1 antibodies in the absence of immunogenic peptides showed apical hENT1 staining (Figure III-2a) and immunofluorescent staining with anti-hCNT3 antibodies showed apical hCNT3 staining (Figure III-2d). Apical staining was defined as luminal surface staining inside tubules demarcated by nuclei counterstains with hematoxylin or 4'-6-diamidino-2-phenylindole (DAPI). Pre-adsorption of anti-hENT1 antibodies with excess immunogenic peptide corresponding to amino acids 254-271 of hENT1 abolished positive apical staining (Figure III-2c), whereas pre-adsorption with the hCNT3-specific immunogenic peptide corresponding to amino acids 45-69 of hCNT3 had no effect (Figure III-2b), demonstrating specificity of the interaction of the primary antibodies with immunoreactive material (*i.e.*, hENT1) on apical surfaces. Similarly, pre-adsorption of anti-hCNT3 antibodies with excess immunogenic peptide of hCNT3 abolished positive apical staining (Figure III-2f), whereas pre-adsorption with hENT1-specific immunogenic peptide had no effect (Figure III-2e). The kidney tubules shown in Figure III-2a-c were identified as proximal tubules due to their morphology – *i.e.*, cuboidal epithelium with fewer nuclei, extensive interdigitations between cells, and occluded lumens [49].

Immunohistochemistry studies performed at the same time as the current work, which localized hENT1, hENT2, hCNT1 and hCNT2 along nephron tubules, employed morphological identification of specific nephron tubule segments [19]. To gain a more comprehensive understanding of the distributions and localizations of hENT1 and hCNT3 in specific nephron tubule segments, immunostaining studies for hENT1 and hENT2 employed antigen identification of specific nephron tubule segments [50]. Immunohistochemistry staining of consecutive human kidney tissue sections (for hENT1 localization studies) and double immunofluorescent (for hCNT3 localization studies) were performed as described in Materials and Methods (Section II.4) along with antibodies specific for the various nephron segment-specific marker proteins [50]. The marker proteins were: (i) proximal nephrogenic renal antigen (PNRA) for proximal tubule identification, (ii) Tamm-Horsfall protein (THP) for thick ascending loop of Henle identification, (iii) aquaporin 2 (AQP2) for collecting duct principal cell identification and (iv) V-type H^+-adenosine-5′-triphosphatase type B1/2 (V-ATPase) for collecting duct intercalated cell identification [50]. The studies described in Figures III-3, III-4, III-5 and III-6 utilized human kidney tissues obtained from the same individual (designated K1, Table II-1).

Localization of hENT1 in proximal tubules was assessed by light microscopy with immunohistochemistry of consecutive sections with antibodies against PNRA and hENT1 (Figure III-3a-c,i). Proximal tubule marker PNRA staining is found on apical surfaces of immunohistochemistry sections (Figure III3-b) and of immunofluorescent sections (Figure III-3e-g). Cortical proximal tubules, indicated by PNRA positivity of adjacent sections (Figure III-3b), exhibited intense hENT1 staining on apical, but not basolateral, surfaces (Figure III-3a,c). PNRA-negative tubules have a distinctly different hENT1 staining pattern with apical and basolateral membrane staining on apical surfaces of proximal tubules (Figure III-3a-c). Localization of hCNT3 in proximal tubules was demonstrated by confocal microscopy with double immunofluorescence staining with antibodies against PNRA and hCNT3 and counterstaining with 4'-6-diamidino-2-phenylindole (DAPI), which stains nuclei, (Figure III-3d-h). PNRA and hCNT3 co-localize on apical surfaces of proximal tubules (Figure III-3d-g), although some intracellular staining of hCNT3 was also present (Figure III-3g). Intracellular localization of hCNT3 has been observed previously in mitochondria of cell cultures of the human cervical cancer cell line, HeLa (King KM & Cass CE, unpublished observations). Intracellular localizations of hENT1 to mitochondria in transfected MDCK cells grown as polarized monolayers [51] and of hENT3 to endosomes/lysosomes in transfected HeLa cells [13] has also been documented. Isotype control staining for PNRA/hENT1 (Figure III-3i) and PNRA/hCNT3 (Figure III-3h) were negative.

Localization of hENT1 and hCNT3 in thick ascending loops of Henle was assessed by immunohistochemistry of consecutive sections with antibodies against THP and hENT1 (Figure III-4a-c,i) and by double immunofluorescence staining of sections with antibodies against THP and hCNT3 (Figure III-4d-h). Thick ascending loop of Henle marker THP staining is found in lumens and on apical surfaces in immunohistochemistry sections (Figure III-4b) and in apical membranes in immunofluorescent staining sections (Figure III-4e-g). Thick ascending loops of Henle, indicated by THP positivity of adjacent sections (Figure III-4b), exhibited moderate hENT1 staining on apical and basolateral surfaces (Figure III-4a,c). THP-negative tubules also show distinct apical and basolateral membrane staining patterns, which may represent collecting ducts (see results of Figure III-5,6 below) or some other unidentified nephron tubule segment. Double immunofluorescence staining with antibodies against THP and hCNT3 and counter staining with DAPI showed co-localization of THP and hCNT3 on apical surfaces when images were merged (Figure III-4d-g). Some intracellular hCNT3 staining was observed in THP-positive tubules (Figure III-4g) possibly related to its presence in endosomes/lysosomes or mitochondria. Not all THP-positive tubules had hCNT3 staining (Figure III-4d-f), which may represent distal tubules that also secrete THP to some extent [50]. . Isotype control staining for THP/hENT1 (Figure III-4i) and THP/hCNT3 (Figure III-3h) were negative.

Localization of hENT1 and hCNT3 in collecting ducts was demonstrated by immunohistochemistry of consecutive sections with antibodies against hENT1 and AQP2 (Figure III-5a-c,i) or V-ATPase (Figure III-6a-c,i) and double immunofluorescent staining of sections with antibodies against hCNT3 and AQP2 (Figure III-5d-h) or V-ATPase (Figure III-5d-h). Collecting duct principal cell marker AQP2 staining is found on apical surfaces in immunohistochemistry (Figure III-5b) and immunofluorescent staining (Figure III-5e-g) sections. Collecting intercalated cell marker V-ATPase is found in cytoplasmic domains in immunohistochemistry (Figure III-6b) and immunofluorescent staining (Figure III-6e-g) sections. Immunohistochemistry with antibodies against hENT1 and two markers of collecting ducts (AQP2, V-ATPase) in adjacent tissue sections showed moderate apical and basolateral surface localization of hENT1 in collecting duct cells identified by both principal cell marker AQP2 (Figure III-5a-c) and intercalated cell marker V-ATPase staining (Figure III-6a-c) in adjacent sections. In contrast, double immunofluorescence staining with antibodies against hCNT3 and either AQP2 or V-ATPase showed little, if any, co-localization of hCNT3 with AQP2 (Figure III-5d-g) or V-ATPase (Figure III-6d-g), indicating absence of hCNT3 in collecting ducts. Isotype control staining for AQP2/hENT1 (Figure III-5i), V-ATPase/hENT1 (Figure III-6i), AQP2/hCNT3 (Figure III-5h) and V-ATPase/hCNT3 (Figure III-6h) THP/hCNT3 (Figure III-3h) were negative.

Localization of hENT1 and hCNT3 in human kidney tissues obtained from three other individuals (designated K2 through K4, Table II-1) yielded similar findings to those obtained above for K1 and the results for all four are summarized in Table III-2. Taken together, these results indicated that: (i) hENT1 and hCNT3 were both present in apical membranes of cortical proximal tubule cells, (ii) hENT1 was present in basolateral and apical membranes of thick ascending loops of Henle, distal convoluted tubules, and collecting ducts, and (iii) hCNT3 was present in apical membranes of thick ascending loops of Henle, but not in collecting ducts.

III.2.2 Characterization of nucleoside transport processes present in monolayer cultures of HK-2 cells

Previous studies identified an endogenous "hCNT1-like" pyrimidine-nucleoside selective concentrative transporter activity in human kidney brush border membrane vesicles [21]. Since we observed (i) mRNA transcripts for hENT1/2 and hCNT1/2/3 in total RNA of human kidney cortex tissues (Table III-1), (ii) hENT1, hENT2 and hCNT3 in crude membranes of human kidney cortex tissues (Figure III-1), and (iii) hENT1 and hCNT3 on apical membranes of human kidney tissues (Figures III-3, Table III-2) of four different individuals (K1 through K4, Table II-1), we sought to identify a cell culture system with proximal tubular characteristics and the nucleoside transport processes observed in human kidney proximal tubules (*i.e.*, hENT1, hENT2 and hCNT3). To this end, the nucleoside transporter processes present in human kidney proximal tubular cell line HK-2 were characterized. The HK-2 cell line was established by immortalization of primary cultures of proximal tubule cells isolated from adult human kidney cortex with human papillomavirus E6/E7 genes (40). It was chosen for investigation because of its: (i) human proximal tubular origin, (ii) maintenance of proximal tubular characteristics including presence of brush border enzymes, presence of sodium-dependent, phloridzin-sensitive sugar transport, and responsiveness to parathyroid hormone, and (iii) continuous and reproducible growth with doubling time of ~72 hours [40].

III.2.2.1 1 Expression of mRNA transcripts for hENTs and hCNTs in monolayer cultures of HK-2 cells

To determine if monolayer cultures of HK-2 cells possessed the same hNT mRNA transcripts as were observed in human kidney cortex tissues (Table III-1), quantitative TaqMan® RT-PCR was performed on HK-2 total RNA using hENT1/2- and hCNT1/2/3-specific probes and primers as described in Materials and Methods (Section II.8). Quantitative TaqMan® RT-PCR analysis identified the presence of mRNA transcripts for hENT1, hENT2 and hCNT3 in total RNA from monolayer cultures of HK-2 cells. The relative levels of mRNA transcripts in HK-2 cells for hENT1 and hCNT3 were lower (p values < 0.01) and for hENT2 were comparable to those observed in four different human kidney cortex tissues. Unlike human kidney cortex tissues, mRNA transcripts for hCNT1 and hCNT2 were undetectable in monolayer cultures of HK-2 cells. These results suggested that mRNA transcripts for hENT1, hENT2 and hCNT3 were present in monolayer cultures of HK-2 cells, although hENT1 and hCNT3 mRNA transcripts were relatively lower than in human kidney cortex tissues.

III.2.2.2 Identification of hENT1, hENT2, and hCNT3 in monolayer cultures of HK-2 cells

To determine which hNT proteins were present in monolayer cultures of HK-2 cells, immunoblotting analysis was performed on HK-2 crude membrane preparations using anti-hENT1, anti-hENT2 and anti-hCNT3 monoclonal antibodies as described in Materials and Methods (Section II.9). The results are presented in Figure III-7. Since no mRNA transcripts for hCNT2 or hCNT2 were detectable in HK-2 cells, immunoblotting analyses for these proteins were not performed. hENT1 and hCNT3 were detected in HK-2 membranes but, unlike crude membranes of human kidney cortex tissues (Figure III-7), hENT2 was not detected. Immunoreactive bands exhibited the expected gel mobilities of hNT proteins – *i.e.*, 45-55 and 90 kDa, respectively, for mammalian hENT1/2 and hCNT3 and 35-45 and 90 kDa, respectively, for recombinant hENT1/2 and hCNT3 produced in yeast (positive controls) (Figure III-7). The diffuse immunoreactive bands for hENT1 and hENT2 were likely due to different glycosylation states (Figure III-1) [43,44]. Multiple immunoreactive bands for hENT2 have been reported previously and were likely the result of proteolysis during preparation (Figure III-7) [45].These results suggested that the key proximal tubular transporters hENT1 and hCNT3, but not hENT2, were present in monolayer cultures of HK-2 cells.

III.2.2.3 Characterization of hENT and hCNT activities in monolayer cultures of HK-2 cells

To determine if monolayer cultures of HK-2 cells exhibited the hNT activities expected to be present in proximal tubule cells (*i.e.*, hENT1 and hCNT3, and possibly hENT2) based on the results of immunoblotting (Section II.2.1.2) and localization studies (Section II.2.1.3), hNT activities were measured by monitoring uptake of radiolabeled nucleosides into monolayer cultures of HK-2 cells as described in Materials and Methods (Section II.5).

Cellular uptake of radiolabeled nucleosides into whole cells of monolayer cultures monitored over time in sodium-containing or sodium-free buffers in the presence or absence of potential inhibitors was used to functionally dissect the hNT processes present in HK-2 cells here, and in hRPTCs elsewhere (see below). To assess hNT-mediated uptake, radiolabeled nucleoside (uridine, thymidine, inosine, or adenosine) uptake was monitored in various buffers containing the presence (non-mediated uptake) or absence (total uptake) of excess non-radiolabeled nucleoside (10 mM uridine or 1 mM thymidine, inosine, or adenosine). hNT-mediated uptake was calculated by subtracting non-mediated uptake from total uptake. To assess the total hNT-mediated uptake, in which hENT1/2 and hCNT1/2/3 are all active, radiolabeled nucleoside uptake was monitored in sodium-containing buffer to allow function of both sodium-independent hENT1/2 and sodium-dependent hCNT1/2/3.

To assess hCNT-mediated uptake, in which hCNT1/2/3 are active but not hENT1/2, radiolabeled nucleoside uptake was monitored in sodium-containing buffer with 200 μM dilazep to allow function of sodium-dependent hCNT1/2/3, but not dilazep-sensitive hENT1/2 (Table I-2). To assess the presence hCNT1-mediated uptake, in which hCNT1 was active but not hENT1/2 or hCNT2/3, radiolabeled uridine or thymidine uptake was monitored in sodium-containing buffer with 200 μM dilazep and 1 mM non-radiolabeled inosine to allow function of sodium-dependent pyrimidine-selective hCNT1, but not purine-transporting hCNT2/3 (Table I-3) or dilazep-sensitive hENT1/2 (Table I-2). To assess the presence of hCNT2-mediated uptake, in which hCNT2 was active but not hENT1/2 or hCNT1/3, radiolabeled uridine or inosine uptake was monitored in sodium-containing buffer with 200 μM dilazep and 1 mM non-radiolabeled thymidine to allow function of purine-selective hCNT2, but not pyrimidine-transporting hCNT1/3 (Table I-3) or dilazep-sensitive hENT1/2 (Table I-2). Monitoring of radiolabeled thymidine or inosine uptake was monitored in sodium-containing buffer with 200 μM dilazep, to allow function of sodium-dependent hCNT1/2/3 but not dilazep-sensitive hENT1/2 (Table I-2), and the presence or absence of excess 1 mM non-radiolabeled inosine or thymidine, respectively, where inhibition of uptake by each of thymidine or inosine to non-mediated levels in the presence of excess 10 mM non-radiolabeled uridine demonstrated the presence of hCNT3. Monitoring of uptake of radiolabeled uridine in sodium-containing buffer with 200 μM dilazep, to allow function of sodium-dependent hCNT1/2/3 but not dilazep-sensitive hENT1/2 (Table I-2), in the presence or absence of excess 1 mM non-radiolabeled thymidine or inosine was also used to demonstrate the presence of hCNT3-mediated uptake, where inhibition of uptake by each of thymidine or inosine to non-mediated levels in the presence of excess 10 mM non-radiolabeled uridine demonstrated the presence of hCNT3.

To assess total hENT-mediated uptake, in which hENT1/2 but not hCNT1/2/3 are active, uptake of radiolabeled uridine was monitored in sodium-free buffer to allow function of sodium-independent hENT1/2, but not sodium-dependent hCNT1/2/3. To assess the presence of hENT2-mediated uptake, in which hENT2 was active but not hENT1 or hCNT1/2/3, uptake of radiolabeled uridine was monitored in sodium-free buffer with 0.1 μM NBMPR to allow function of sodium-independent hENT2, but not NBMPR-sensitive hENT1 (Table I-2) or sodium-dependent hCNT1/2/3. Monitoring of radiolabeled uridine uptake in sodium-free buffer, to allow function of sodium-independent hENT1/2 but not sodium-dependent hCNT1/2/3, in the presence or absence of 0.1 μM NBMPR was used to demonstrate the presence of hENT1-mediated uptake, where inhibition by the presence of 0.1 μM NBMPR (Table I-2) demonstrated the presence of hENT1.

Uptake of 1 μM [^{3}H]-uridine into monolayer cultures of HK-2 cells was linear for up to ten min (Figure III-8b), suggesting that uptake time courses provided a good approximation of initial rates of uptake. Linearity was also demonstrated in preliminary experiments in which uptake was measured for one min at five-sec intervals (Figure III-8a). Uptake of 1 μM [^{3}H]-uridine in sodium-containing buffer was inhibited almost completely in the presence of excess (10 mM) non-radiolabeled uridine (Figure III-8b), indicating that uridine uptake was primarily mediated. Uptake of uridine in: (i) sodium-free buffer was similar to that in sodium-containing buffer (Figure III-8b) and in (ii) sodium-containing buffer with 200 μM dilazep was reduced to levels observed in the presence of 10 mM non-radiolabeled uridine (Figure III-8b). These results indicate the presence both of hENT-, but not hCNT-, mediated uptake processes in monolayer cultures of HK-2 cells. Uptake of uridine in sodium-free buffer was completely inhibited by NBMPR at 0.1 μM, a concentration that inhibits hENT1 but not hENT2 (Figure III-8c), indicating the presence of hENT1-, but not hENT2-, mediated uptake processes. These results suggested that monolayer cultures of HK-2 cells exhibited only hENT1 activity, with little, if any, evidence of hENT2 or hCNT3 activity. Because of the lack of endogenous hCNT3 activities, no further studies were undertaken with monolayer cultures of HK-2 cells.

III.2.3 Characterization of nucleoside transport processes present in monolayer hRPTC cultures

Although all seven hNTs are present in human kidney, the current studies demonstrate that hENT1 and hCNT3, and possibly hENT2, are present in human kidney proximal tubules. Since monolayer cultures of HK-2 cells lacked the full complement of hNTs demonstrated to be present in human kidney proximal tubules in the current studies (– *i.e.*, hENT1 and hCNT3, and possibly hENT2), we sought to determine whether another cell culture system with proximal tubular characteristics, hRPTCs, possessed these hNTs. To this end, fifteen different hRPTCs were established from human kidney cortex tissue of fifteen different individuals (hRPTC1 through hRPTC15, Table II-1) as described in Materials and Methods (Section II.2), their proximal tubular characteristics were defined, and the nucleoside transport processes in one of the cultures (hRPTC1) were characterized.

III.2.3.1 Demonstration of the presence of proximal tubular brush border enzymes in monolayer hRPTC cultures

Previous studies established that monolayer cultures of hRPTCs (or of rabbit RPTCs) exhibit brush border enzyme activities for acid phosphatase, γ-glutamyl transferase, and alkaline phosphatase, enzymes considered to be markers of *in vivo* proximal tubule cells [41,42]. To determine if these brush border enzymes were present in the hRPTCs established from different human kidney cortex tissues, brush border enzyme cytochemistry staining was performed on hRPTCs grown as monolayer cultures on slides as described in Materials and Methods (Section II.4). Slides were scored as positive (or negative) for brush border enzymes if > 90 % (or < 90 %) of cells in three different fields of view contained moderate to intense granular staining as described in Materials and Methods (Section II.4). All fifteen different hRPTCs showed epithelial cell morphology (Figure III-9A-C), typical of renal tubular cell cultures [41,42], and were positive for brush border enzymes acid phosphatase, γ-glutamyl transferase, and alkaline phosphatase (Figure III-9A-C). Brush border cytochemistry staining for these enzymes in hRPTCs showed moderate to intense granular staining in majority of cells (> 90%) in three different fields of view (representative images are shown for each of fifteen different hRPTCs in Figure III-9). These results suggested that hRPTCs retained brush border enzymes present in human kidney proximal tubules.

III.2.3.2 Demonstration of proximal tubular parathyroid hormone sensitivities and anti-diuretic hormone insensitivities in monolayer hRPTC cultures

Human kidney proximal tubules are known to be sensitive to parathyroid hormone but insensitive to anti-diuretic hormone while collecting tubules are insensitive to parathyroid hormone but sensitive to anti-diuretic hormone [52]. Parathyroid hormone and anti-diuretic hormone act through stimulation of cell surface receptors, resulting in activation of adenylate cyclase which converts adenosine-5′-triphosphate (ATP) into cyclic adenosine-5′-monophosphate (cAMP) leading to an inhibition of Na^+-phosphate co-transport processes located in proximal tubule brush border membranes and increase in water permeability in collecting ducts, respectively [52]. Previous studies established that monolayer hRPTC (or rabbit RPTC) cultures retained parathyroid hormone sensitivities and anti-diuretic hormone insensitivities characteristic of *in vivo* proximal tubules [41,42]. To determine if this was the case for the hRPTC cultures isolated from fifteen different individuals (hRPTC1 through hRPTC15, Table II-1) in this study, the cultures were treated with either parathyroid hormone, anti-diuretic hormone, or forskolin (positive control) and total intracellular cAMP levels were determined as described in Materials and Methods (Section II.7). Forskolin was used as a positive control because it is a potent stimulant of adenylate cyclise [40,41]. The results are presented in Table III-3. All fifteen hRPTCs displayed significantly higher levels of total intracellular cAMP when treated with parathyroid hormone or forskolin as compared to untreated cultures (negative controls) (p values ranging from < 0.05 to < 0.001). In contrast, no significant differences in intracellular cAMP levels were observed when hRPTCs were treated with anti-diuretic hormone as compared to untreated cultures (negative controls). These results suggested that hRPTCs retained parathyroid hormone sensitivities and anti-diuretic hormone insensitivities characteristic of human kidney proximal tubules [41,42].

III.2.3.3 Demonstration of the presence of sodium-dependent, phloridzin-sensitive α-methyl-D-glucoside uptake in monolayer hRPTC cultures

To determine if monolayer cultures of hRPTCs exhibited glucose transporter activities known to be present in proximal tubule cells *in vivo*, uptake of α-methyl-D-glucoside into monolayer hRPTC cultures was investigated by monitoring uptake of radiolabeled α-methyl-D-glucoside into monolayer hRPTC cultures isolated from fifteen different individuals (hRPTC1 through hRPTC15) as described in Materials and Methods (Section II.5). Uptake of radiolabeled α-methyl-D-glucoside was linear for up to five min (Figure III-10B), suggesting that uptake time courses provided a good approximation of initial rates of uptake. Linearity was also demonstrated in preliminary experiments in which uptake was measured for one min at five-sec intervals (Figure III-10A). Uptake of 100 μM $[^3H]$-α-methyl-D-glucoside into monolayer hRPTC1 cultures in sodium-containing buffer was reduced in the presence of 1 mM phloridzin, an inhibitor of the sodium-glucose linked transporter (SGLT1), and in sodium-free buffer (p values < 0.0001), indicating that α-methyl-D-glucoside uptake was primarily sodium-dependent and phloridzin-sensitive. These results were confirmed for all fifteen different hRPTC cultures and the results are summarized in Table III-4.

III.2.3.4 Characterization of nucleoside transport processes present in monolayer hRPTC1 cultures

Taken together, the results thus far suggested that hRPTCs retained *in vivo* proximal tubular characteristics including: (i) the presence of brush border enzymes, (ii) parathyroid hormone sensitivity and anti-diuretic hormone insensitivity, and (iii) the presence of sodium-dependent, phloridzin-sensitive α-methyl-D-glucoside uptake processes. The next step was to determine which nucleoside transport processes were present in monolayer hRPTC1 cultures to assess whether or not they retained key proximal tubular hNTs known to be present in human kidney proximal tubules – *i.e.*, hENT1 and hCNT3, and possibly hENT2. Uptake of radiolabeled nucleosides into hRPTCs was monitored over time in sodium-containing or sodium-free buffers in the presence or absence of potential inhibitors to functionally dissect the hNT processes that were responsible, as described for HK-2 cultures above (see Section III.2.2.3). Because uridine is a permeant of hENT1/2 (Table I-1) and hCNT1/2/3 (Table I-3), thymidine is a permeant of hCNT1/3 (Table I-3), and inosine is a permeant of hCNT2/3 (Table I-3), uptake studies were performed with radiolabeled uridine, thymidine, or inosine in the presence or absence of excess unlabeled uridine (10 mM), thymidine (1 mM), and inosine (1 mM). Because hENT1/2 are sodium-independent and hCNT1/2/3 are sodium-dependent, uptake studies were performed in sodium-containing or sodium-free buffers. Because hENT1/2 are dilazep-sensitive and hENT1 is NBMPR-sensitive (Table I-2), uptake studies were performed in sodium-containing or sodium-free buffer in the presence or absence of 200 μM dilazep and 0.1 μM NBMPR. Uptake time courses for 10 μM [^{3}H]-uridine, -thymidine, and -inosine were linear for up to ten min (Figure III-12), indicating that the time courses provided a good approximation of initial rates of uptake – i.e., of transport activities. Confirmation that these time courses represented initial rates of uptake for uridine (Figure III-11A), thymidine (Figure III-11B), and inosine (Figure III-11C) was demonstrated in preliminary experiments in which uptake was measured for one min at five-sec intervals.

Uptake of 10 μM [^{3}H]-uridine in sodium-containing buffer was inhibited almost completely in the presence of excess (10 mM) non-radiolabeled uridine (Figure III-12A), indicating that uridine uptake was primarily mediated in hRPTC1 cultures. Dilazep, when present in sodium-containing buffer at a concentration (200 μM) that inhibits both hENT1 and hENT2 activities, increased uridine uptake ($p < 0.01$) Figure III-12A), a result that can be explained by the inhibition of uridine efflux through bidirectional hENTs while still allowing uptake via unidirectional hCNTs. Uptake of [^{3}H]-uridine in sodium-free buffer was lower than in sodium-containing buffer ($p < 0.01$) and could be further reduced by 200 μM dilazep to levels observed in the presence of 10 mM non-radiolabeled uridine (Figure III-12D), indicating the presence both of hCNT- and hENT-mediated uptake processes in monolayer hRPTC1 cultures. Uptake of [^{3}H]-uridine in sodium-free buffer was only partially inhibited by NBMPR at 0.1 μM, a concentration that inhibits hENT1 but not hENT2 [6,48], indicating the presence of both hENT1- and hENT2-mediated uptake processes in monolayer hRPTC1 cultures (Figure III-12D). Uptake of 1 μM [^{3}H]-thymidine, which is transported by hCNT1 and hCNT3 but not by hCNT2, in sodium-containing buffer with 200 μM dilazep was completely inhibited by either 1 mM non-radiolabeled thymidine or inosine, both of which are transported by hCNT3 but not of hCNT1; this result (Figure III-12B) demonstrated the presence of hCNT3-mediated uptake processes in monolayer hRPTC1 cultures. Similarly, uptake of 1 μM [^{3}H]-inosine in sodium-containing buffer with 200 μM dilazep was completely inhibited by either 1 mM non-radiolabeled thymidine or inosine (Figure III-12C), also demonstrating the presence of hCNT3-mediated, but not of hCNT1- or hCNT2-mediated, uptake processes in monolayer hRPTC1 cultures. Collectively, these results suggested that monolayer hRPTC1 cultures exhibited nucleoside transport processes, hENT1, hENT2, and hCNT3s.

III.3 Discussion

A previous model for renal reabsorption of nucleosides by renal tubules from lumen into the blood mediated by coupling of apical sodium-dependent hCNT1/2/3 to basolateral equilibrating hENT1/2 has been proposed based on asymmetric localization of recombinant hNT-GFP fusion proteins in transfected LLC-PK_1 cells, a pig kidney epithelial cell line with proximal tubular characteristics [25]. However, this proposed model has been inadequate in explaining selective nucleoside secretion by renal tubules (*e.g.*, 2′-deoxyadenosine) [1-4]. Moreover, direct evidence of the presence of hENTs and hCNTs in human kidney proximal tubules has been largely limited to a few studies including: (i) hENT1/2/3/4 and hCNT1/2/3 mRNA transcripts observed in human kidney tissue RNA [9-18], (ii) hCNT1-like activities observed in human kidney brush border membrane vesicles [8], and (iii) hENT4/PMAT protein observed in human kidney tissue lysates [20]. hCNT1/2/3 seem to be restricted to apical membranes in polarized transfected LLC-PK_1 cells, whereas the locations of hENT1/2 are controversial and have been reported in apical and basolateral membranes [23-25,27,28]. The current study characterized the distribution and anatomic locations of several hNTs in human kidney tissue of four different individuals (K1 through K4, Table II-1) by immunohistochemistry and immunofluorescent staining analyses (Table III-2). It was shown that human kidney cortical proximal tubules possess apical hENT1 and hCNT3, thick ascending loops of Henle possess apical hENT1 and hCNT3 and basolateral hENT, and collecting ducts possess apical and basolateral hENT1 but not hCNT3.

Additionally, we established a suitable cell culture system, hRPTCs, in which monolayers cultures obtained from one individual, hRPTC1, were shown to possess hNTs demonstrated to be present human kidney proximal tubules in the current studies (*i.e.*, hENT1, hCNT3, and possibly hENT2) and could be used in future studies to characterize the functional roles of renal proximal tubule hNTs.

Results from *in situ* hybridization and immunohistochemistry studies in human kidney identified: (i) mRNA transcripts for hCNT1/2 in proximal tubules, (ii) hCNT1/2 protein in apical membranes of proximal tubules, (iii) mRNA transcripts for hENT1/2 in distal tubules, and (iv) hENT1/2 protein in apical and basolateral membranes of distal tubules, and (v) hENT1 protein in apical and basolateral membranes of proximal tubules adjacent to corticomedullary junctions [19]. The apical location of hENT1 in proximal tubules agreed with results of the current study; however, basolateral hENT1 was not observed in proximal tubules. While the former study employed morphological identification of different nephron tubule segments [19], the current study employed more precise identification by immunohistocemistry of consecutive tissue sections (for hENT1 localization studies) or double immunofluorescent staining (for hCNT3 localization studies) with nephron tubule segment-specific markers: (i) PNRA for proximal tubules, (ii) THP for thick ascending loops of Henle, (iii) AQP2 for principal collecting duct cells, and (iv) V-ATPase for intercalated collecting duct cells (Figures III-3 - III-6). Differences in observed staining patterns between these studies may be a result of differences in detection limits between antibodies.

The location of hCNT3 on apical membranes of human kidney proximal tubules observed in the current study suggested that hCNT3 is a key transporter in renal nucleoside reabsorption (Figure III-4). It should be noted that hCNT3 has a greater concentrating capacity and permeant tolerance than either hCNT1 or hCNT2 [14-18] and is also a H^+-nucleoside co-transporter [39], capable of driving both purine and pyrimidine nucleoside reabsorption under the varied sodium and proton gradients.

On the other hand, hENT1 may be a key transporter involved in renal nucleoside secretion owing to its observed location on apical membranes of human kidney proximal tubules (Figure III-4). This would be consistent with the results of previous work, which showed that 2′-deoxyadenosine secretion in mice is dependent on ENT1 [15,16]. While the driving forces behind nucleoside secretion at the basolateral membrane are still unknown, mounting evidence suggests the involvement of hOCTs and hOATs in renal nucleoside secretion [17-19]. Furthermore, the lack of hENT1 on basolateral membranes of human kidney proximal tubules, demonstrated in the present study (Figure III-4), implicates hENT2 as a basolateral transporter mediating equilibration of nucleoside across basolateral membranes. As some nucleosides are expected, and have been observed [28], to undergo metabolism to nucleobases during proximal tubular reabsorption (*e.g.*, adenosine to hypoxanthine in the absence of adenosine deamination), complete reabsorption would require a basolateral transporter capable of mediating nucleobases transport. The hypothesis that hENT2 is a basolateral transporter in proximal tubules is supported by hENT2 having a greater permeant tolerance for both nucleosides and nucleobases than hENT1, which is only able to transport nucleosides [9-12].

Although a complete picture of distribution and function of hENTs and hCNTs in each nephron tubule segment is necessary for understanding the roles of hNTs in renal handling of nucleosides, the anatomy of the kidney suggests that, like many other solutes, the majority of reabsorption occurs in the proximal tubules. Despite the possibility that nucleoside secretion may occur in different nephron tubule segments, the observed location of hENT1 in proximal tubules in the current study suggested that secretion may also occur in proximal tubules. Therefore, subsequent characterization of nucleoside transport processes present into two cell culture model systems of proximal tubular origin, HK-2 cells and hRPTCs, was undertaken with the goal of identifying a suitable model system for future characterization of functional roles of proximal tubule hNTs. Collectively, TaqMan® RT-PCR analyses of Total RNA (Table III-1) and immunoblotting analyses of crude membranes from four human kidney cortex tissues (Figure III-1), and immunohistochemistry and immunofluorescent staining studies of kidney tissues (Figure III-3, Table III-2) from four different individuals (K1 through K4, Table II-1) suggested that hENT1 and hCNT3, and possibly hENT2, were the key hNTs present in human kidney. As monolayer cultures of HK-2 cells possessed only hENT1 activity (Figure III-8) and lacked hENT2 protein by immunoblotting analysis (Figure III-7) and hCNT3 activities by radiolabeled nucleoside uptake studies (Figure III-8), they were deemed an unsuitable model system to characterize the functional roles of endogenous proximal tubule hNTs. While the possibility of transfecting HK-2 cells with recombinant hNTs was explored, this was not pursued because the main goal of this research was to study endogenous hNTs in human kidney proximal tubules. In contrast, monolayer cultures of hRPTC1 from one individual possessed hENT1, hENT2, and hCNT3 activities by radiolabeled nucleoside uptake studies (Figure III-11,12). hRPTCs that were obtained from fifteen different individuals (hRPTC1 through hRPTC15, Table II-1) were demonstrated to exhibit several well-defined proximal tubular characteristics including: (i) the presence of brush border enzymes acid phosphatase, γ-glutamyl transferase, and alkaline phosphatase (Figure III-9), (ii) parathyroid hormone sensitivities and anti-diuretic hormone insensitivities (Table III-3), and (iii) sodium-dependent, phloridzin-sensitive α-methyl-D-glucoside uptake (Figure III-10, Table III-4). Although hRPTCs are heterogeneous cell populations, since the majority of cells have a proximal tubular origin and maintain such characteristics [41,42], methods including microdissection [53], immunodissection [54], and percoll gradient fractionation [55] to obtain more homogenous cell populations were not explored. This was because: (i) of the low yield of such isolation procedures, (ii) the requirement for large populations of high-density multiple replicate sub-cultures for radiolabeled nucleoside uptake studies, and (iii) the methods demand fastidious immunologic and cell type characterization to be successful. The presence of multiple endogenous hNTs, demonstrated to be present in human kidney proximal tubules *in situ* in the current studies, (*i.e.*, hENT1, hENT2, and hCNT3) in hRPTC1 cultures warranted further investigation.

In summary, results using RT-PCR, immunoblotting, immunohistocemistry, immunofluorescence staining, and nucleoside uptake studies demonstrated hENT1 and hCNT3, and possibly hENT2, to be the major nucleoside transporter proteins in human kidney proximal tubules. hENT1 was found on apical surfaces of proximal tubules and apical and basolateral surfaces of thick ascending loops of Henle and collecting ducts, whereas hCNT3 was found on apical surfaces of proximal tubules and thick ascending loops of Henle. These results were consistent with a primary role for hCNT3 in reabsorption of nucleosides from apical surfaces of proximal tubules; they suggest that hENT1, which was observed on apical, but not basolateral, surfaces, may be involved in nucleoside secretion, raising the possibility that hENT2 (or some other transporter type) moves nucleosides across basolateral surfaces of proximal tubules during reabsorption. Nucleoside transporters are likely involved in regulating renal levels of extracellular adenosine, which has a multiplicity of physiological and pathophysiological functions, including lowering of glomerular filtration rates, stimulating Na^+ reabsorption in proximal segments, and inhibiting Na^+ reabsorption in medullary segments [56]. The current study opens several potential avenues of research that will determine roles of nucleoside transporters in renal handling of physiological nucleosides and nucleoside drugs as well as in adenosine modulated renal physiology and pathophysiology.

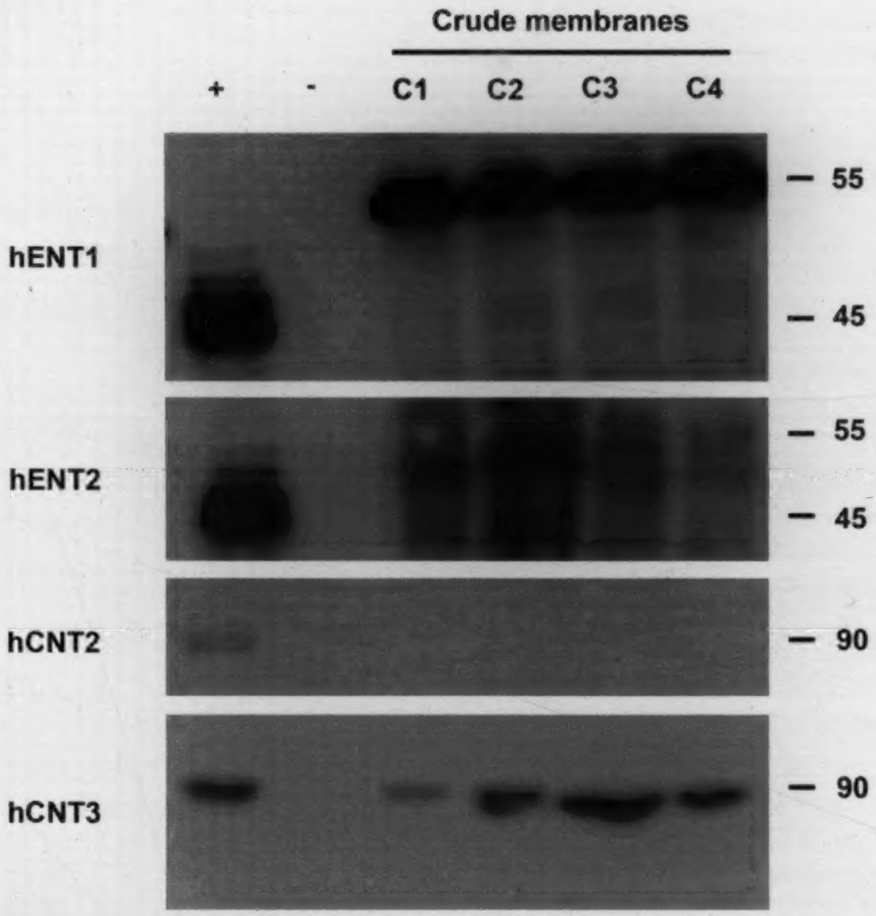

Figure III-1. Demonstration of hENT1, hENT2, and hCNT3, but not hCNT2, in crude membrane preparations of four different human kidney cortex tissues. hENT1, hENT2, hCNT2, and hCNT3 were assessed by immunoblotting using anti-hNT specific monoclonal antibodies in crude membranes (20 μg protein per sample) isolated from four different human kidney cortex tissues (designated C1 through C4) as described in Materials and Methods (Section II.9). Positive controls (+) consisted of crude membrane preparations from yeast transfected with plasmids that contained the indicated hNT cDNA insert and negative controls (-) consisted of crude membrane preparations from yeast transfected with plasmids without inserts. Bands were visualized using horseradish peroxidase-conjugated anti-mouse IgG antibodies and enhanced chemiluminescence. Gel mobilities in kDa are denoted by the dashes and numbers beside each immunoblot.

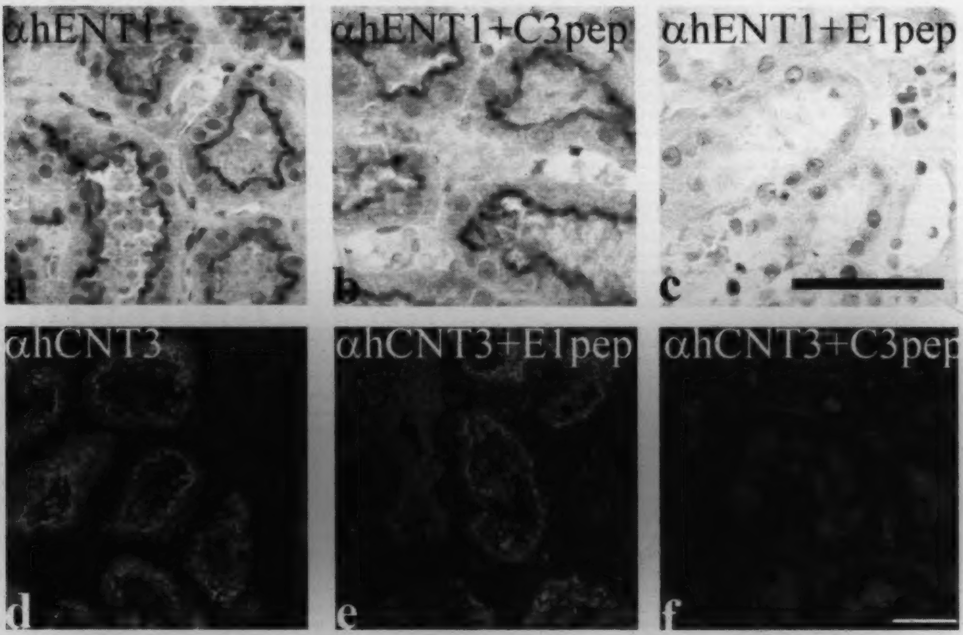

Figure III-2. Specificity of monoclonal antibodies against hENT1 and hCNT3 in human kidney tissues. The specificity of anti-hENT1 antibodies (αhENT1) was confirmed by immunohistochemistry as described in Materials and Methods (Section II.4) of human kidney tissue obtained from one individual (designated K1, Table II.1) under the following conditions: (a) hENT1 staining in the absence of hENT1 peptides (E1 pep) or hCNT3 peptides (C3 pep), (b) hENT1 staining in the presence of C3 pep, and (c) hENT1 staining in the presence of E1 pep. The specificity of anti-hCNT3 antibodies (αhCNT3) was confirmed by immunofluorescence staining of human kidney cortex tissue obtained from one individual (K1) under the following conditions: (d) hCNT3 staining in the absence of E1 pep or C3 pep, (e) hCNT3 staining in the presence of E1 pep, and (F) hCNT3 staining in the presence of C3 pep. Hematoxylin (a-c) and DAPI (d-f) counterstains for nuclei are shown in blue. Scale bars shown are 50 μm.

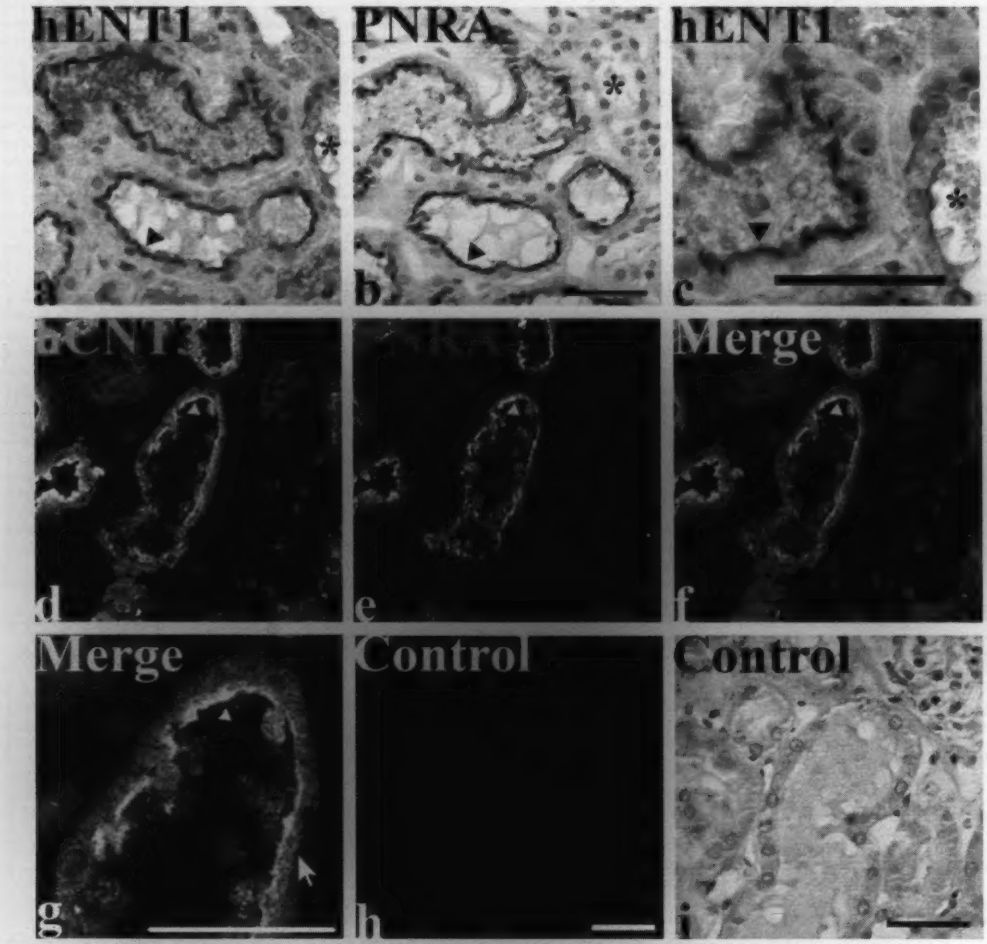

Figure III-3. Localization of hENT1 and hCNT3 in proximal tubules. Immuno-histochemistry with anti-hENT1 antibodies and immunofluorescence with anti-hCNT3 antibodies was performed on human kidney tissue obtained from one individual (K1, Table II-1) as described in Section II.4. (a-c,i) hENT1 and PNRA immunohistochemistry of consecutive tissue sections. hENT1 localization to apical membranes of proximal tubules (a,c) is indicated by the arrow heads. * denotes a PNRA-negative tubule (a-c). Proximal tubule marker PNRA localization to apical membranes (b) is indicated by the arrow head. Isotype control staining for hENT1 and PNRA are negative (i). hCNT3 and PNRA double immunofluorescence staining of human kidney tissue sections (d-h). hCNT3 in (d) and proximal tubule marker PNRA in (e) co-localization to apical membranes of proximal tubules in merge (f,g; hCNT3 in green, PNRA in red; merge in yellow), indicated by the arrow heads in (d-g). The arrow (←) indicates intracellular staining of hCNT3 in proximal tubule cells (g). Isotype control staining for hCNT3 and PNRA are negative (h). Hematoxylin (a-c,i) and DAPI (d-h) counterstains for nuclei are shown in blue. Scale bars shown are 50 μm.

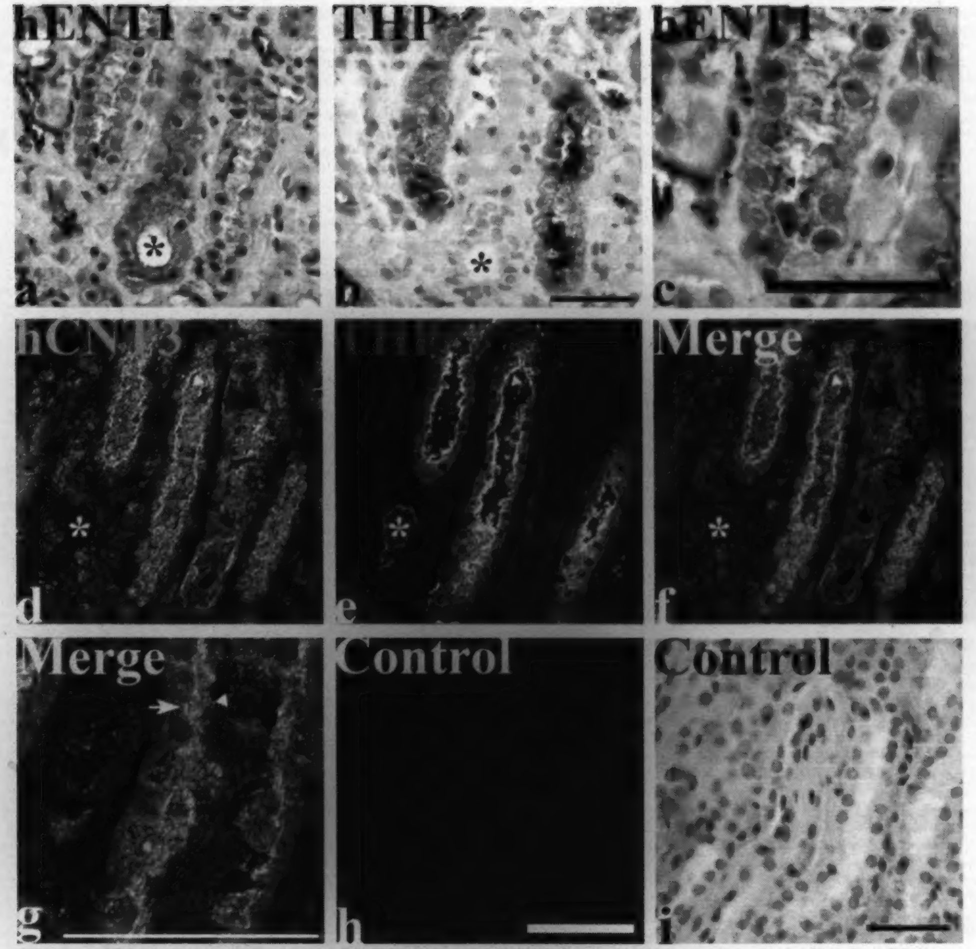

Figure III-4. Localization of hENT1 and hCNT3 in thick ascending limb of loops of Henle. Immunohistochemistry with anti-hENT1 antibodies and immunofluorescence with anti-hCNT3 antibodies was performed on human kidney tissue obtained from one individual (K1, Table II-1) as described in Section II.4. (a-c,i) hENT1 and THP immunohistochemistry of consecutive sections. hENT1 localizes to apical and basolateral membranes of thick ascending loops of Henle (a,c), indicated by the arrow heads in (c). * denotes a THP-negative tubule (a,b). Loop of Henle marker THP localizes to apical membranes and lumens (b). Isotype control staining for hENT1 and THP are negative (i). (d-h) hCNT3 and THP double immunofluorescence staining. hCNT3 in (d) and loop of Henle marker THP in (e) co-localize to apical membranes of thick ascending loops of Henle in merge (f,g; hCNT3 in green, THP in red, merge in yellow), indicated by the arrow heads in (d-g). *THP-positive tubule (e-f). The arrow (←) indicates intracellular staining of hCNT3 in thick ascending loops of Henle (g). Isotype control staining for hCNT3 and THP are negative (h). Hematoxylin (a-c,i) and DAPI (d-h) counterstains for nuclei are shown in blue. Scale bars shown are 50 μm.

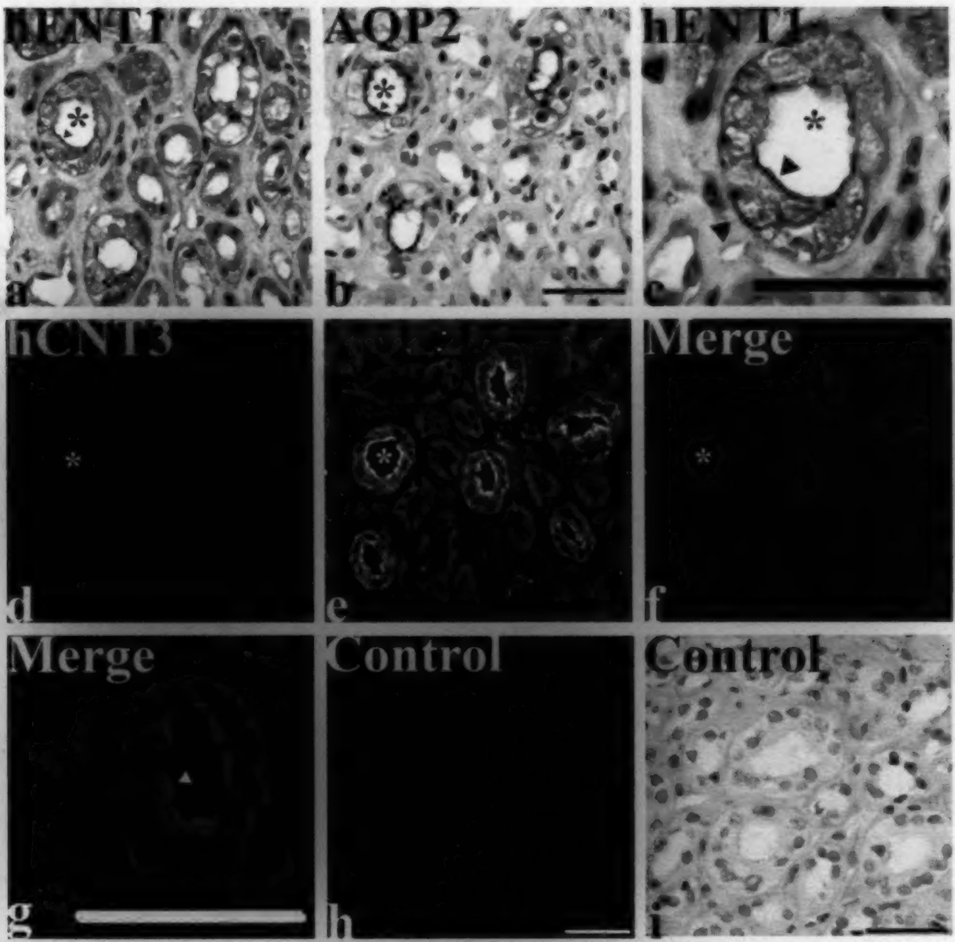

Figure III-5. Localization of hENT1 and hCNT3 in collecting duct principal cells. Immunohistochemistry with anti-hENT1 and immunofluorescence with anti-hCNT3 antibodies was performed on human kidney tissue obtained from one individual (K1, Table II-1) as described in Section II.4. (a-c,i) hENT1 and AQP2 immunohistochemistry of consecutive sections. hENT1 localizes to apical and basolateral membranes of collecting ducts principal cells (a,c), indicated by the arrow heads. * denotes a AQP2-positive tubule (a-c). Principal cell marker AQP2 localizes to apical membranes of collecting ducts (b, indicated by the arrow head. Isotype control staining for hENT1 and AQP2 are negative (i). (d-h) Double immunofluorescence staining with hCNT3 in (d) and collecting duct principal cell marker AQP2 in (e) shows absence of hCNT3 staining in collecting ducts in merge (f,g; hCNT3 in green, AQP2 in yellow, merge in yellow). Principal cell marker AQP2 in red localizes to apical membranes of collecting ducts (e-g), indicated by the arrow head in (g). * denotes AQP2-positive tubule. Isotype control staining for hCNT3 and THP are negative (h). Hematoxylin (a-c,i) and DAPI (d-h) counterstains for nuclei are shown in blue. Scale bars shown are 50 μm.

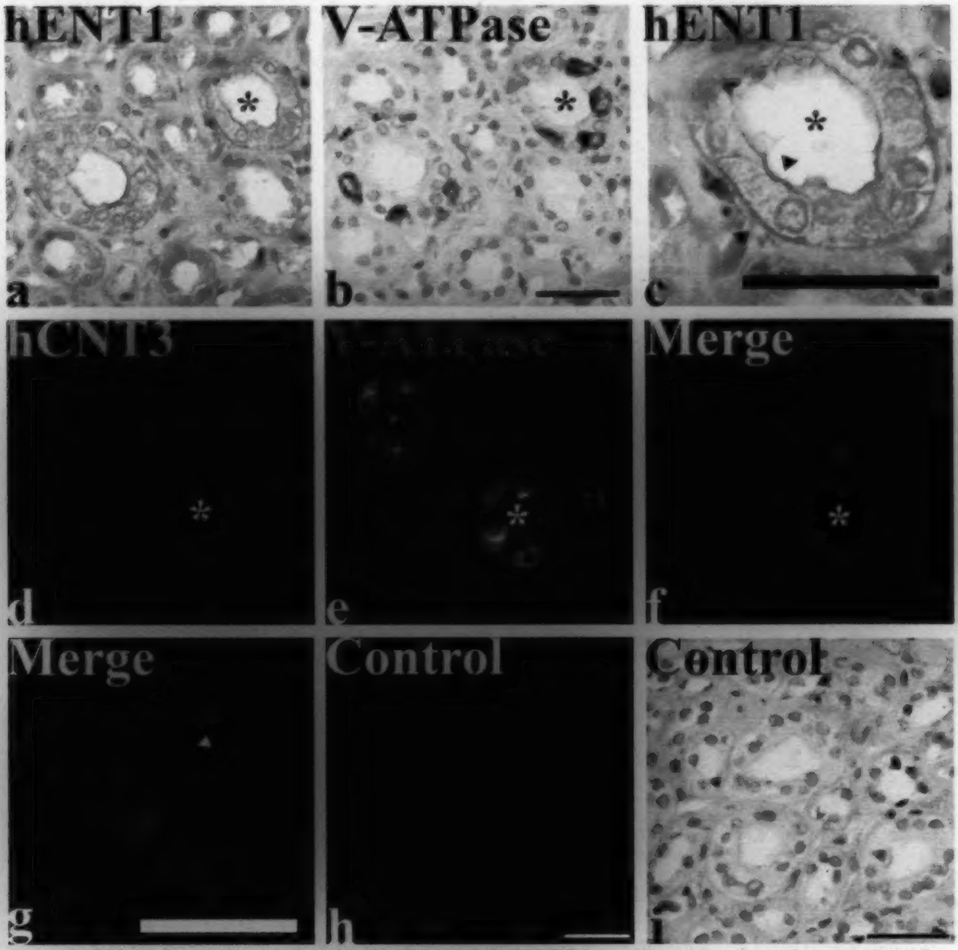

Figure III-6. Localization of hENT1 and hCNT3 in collecting duct intercalated cells. Immunohistochemistry with anti-hENT1 and immunofluorescence with anti-hCNT3 anti-bodies was performed on human kidney tissue obtained from one individual (K1, Table II-1) as described in Section II.4. (a-c,i) hENT1 and V-ATPase immunohistochemistry of consecutive sections. hENT1 localizes to apical and basolateral membranes of collecting ducts intercalated cells (a,c), indicated by the arrow heads in (c). * denotes a V-ATPase-positive tubule (a-c). Intercalated cell marker V-ATPase localizes intracellularly in collecting ducts (b). Isotype control staining for hENT1 and V-ATPase are negative (i). (d-h) Double immunofluorescence staining with hCNT3 in (d) and intercalated cell marker V-ATPase in (e) shows absence of hCNT3 staining in collecting ducts in merge (f,g; hCNT3 in green, V-ATPase in red, merge in yellow). * denotes a V-ATPase-positive tubule (d-f). Intercalated cell marker V-ATPase in red localizes intracellularly of collecting ducts (e-g), indicated by the arrow head in (g). Isotype control staining for hCNT3 and V-ATPase are negative (h). Hematoxylin (a-c,i) and DAPI (d-h) counterstains for nuclei are shown in blue. Scale bars shown are 50 μm.

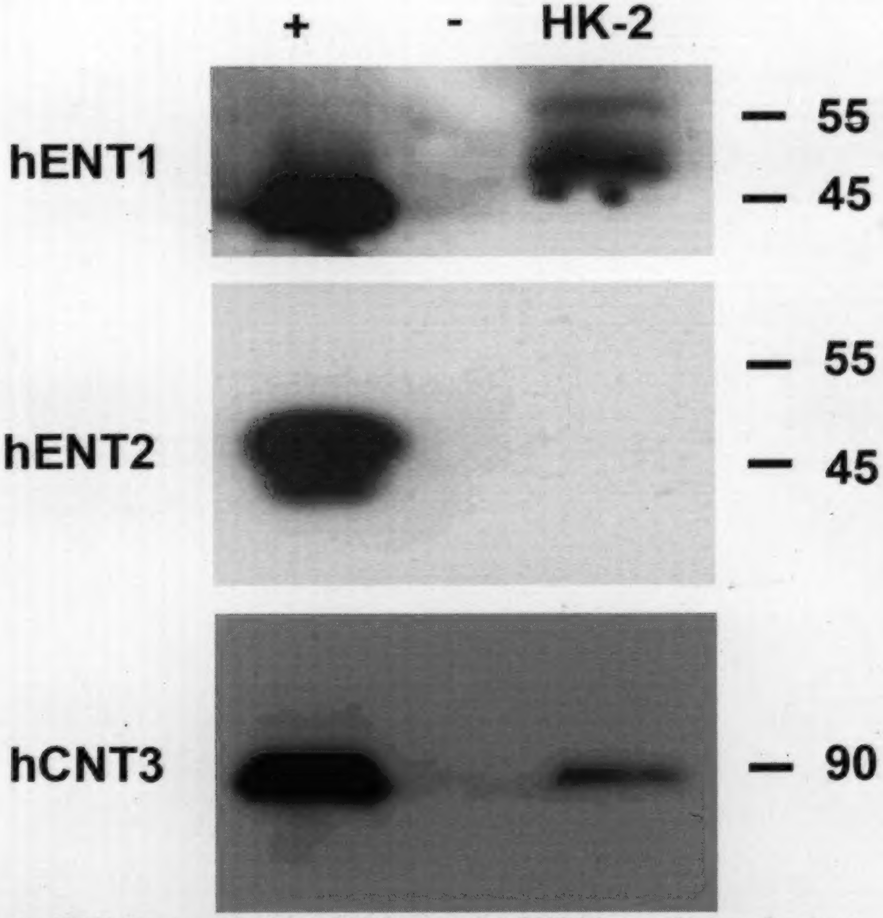

Figure III-7. Demonstration of hENT1 and hCNT3 in crude membrane preparations of monolayer cultures of HK-2 cells. hENT1, hENT2, and hCNT3 were assessed by immunoblotting using anti-hNT specific monoclonal antibodies in crude membranes (20 μg protein per sample) isolated from monolayer cultures of HK-2 cells as described in Materials and Methods (Section II.9). Positive controls (+) consisted of crude membrane preparations from yeast transfected with plasmids that contained the indicated hNT cDNA insert and negative controls (-) consisted of crude membrane preparations from yeast transfected with plasmids without inserts. Bands were visualized using horseradish peroxidase-conjugated anti-mouse IgG antibodies and enhanced chemiluminescence. Gel mobilities in kDa are denoted by the dashes and numbers beside each immunoblot.

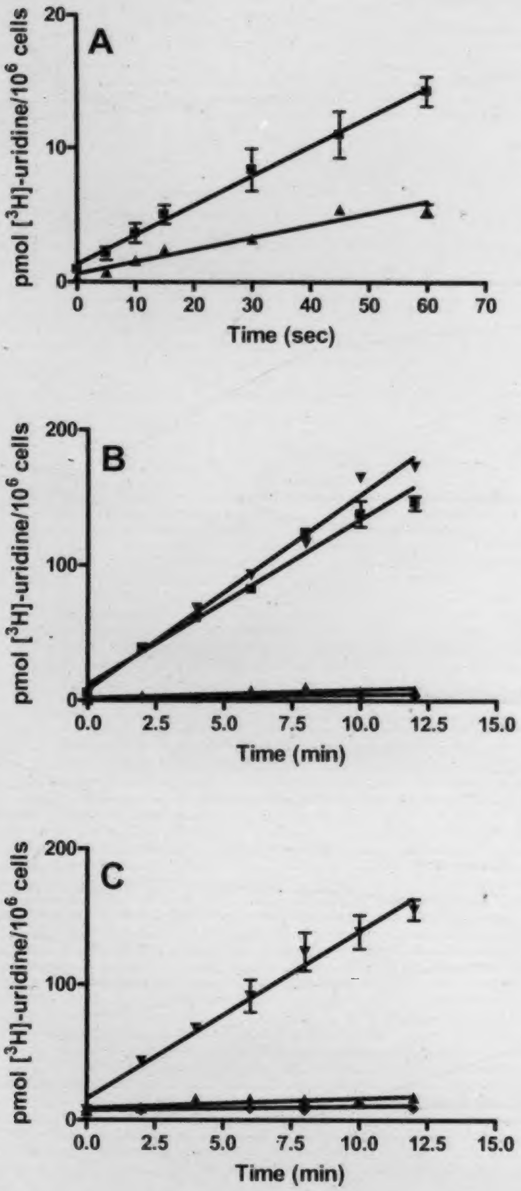

Figure III-8. Time courses of uptake of uridine by monolayer cultures of HK-2 cells. Uptake of 10 μM [^{3}H]-uridine in (A) sodium-containing buffer alone (■), or with 10 mM uridine (▲), of 10 μM [^{3}H]-uridine in (B) in sodium-containing buffer alone (▼), or with 10 mM uridine (♦), or 200 μM dilazep (▲) or sodium-free buffer alone (■), and of 1 μM [^{3}H]-uridine in (C) sodium-free buffer alone (▼) or with 0.1 μM NBMPR (▲) or 10 mM uridine (♦) was monitored over time into monolayer cultures of HK-2 cells as described in Materials and Methods (Section II.5). Values plotted are means (± standard deviations) from three independent experiments. Points for which error bars are absent had errors equal or smaller than the border size of the points.

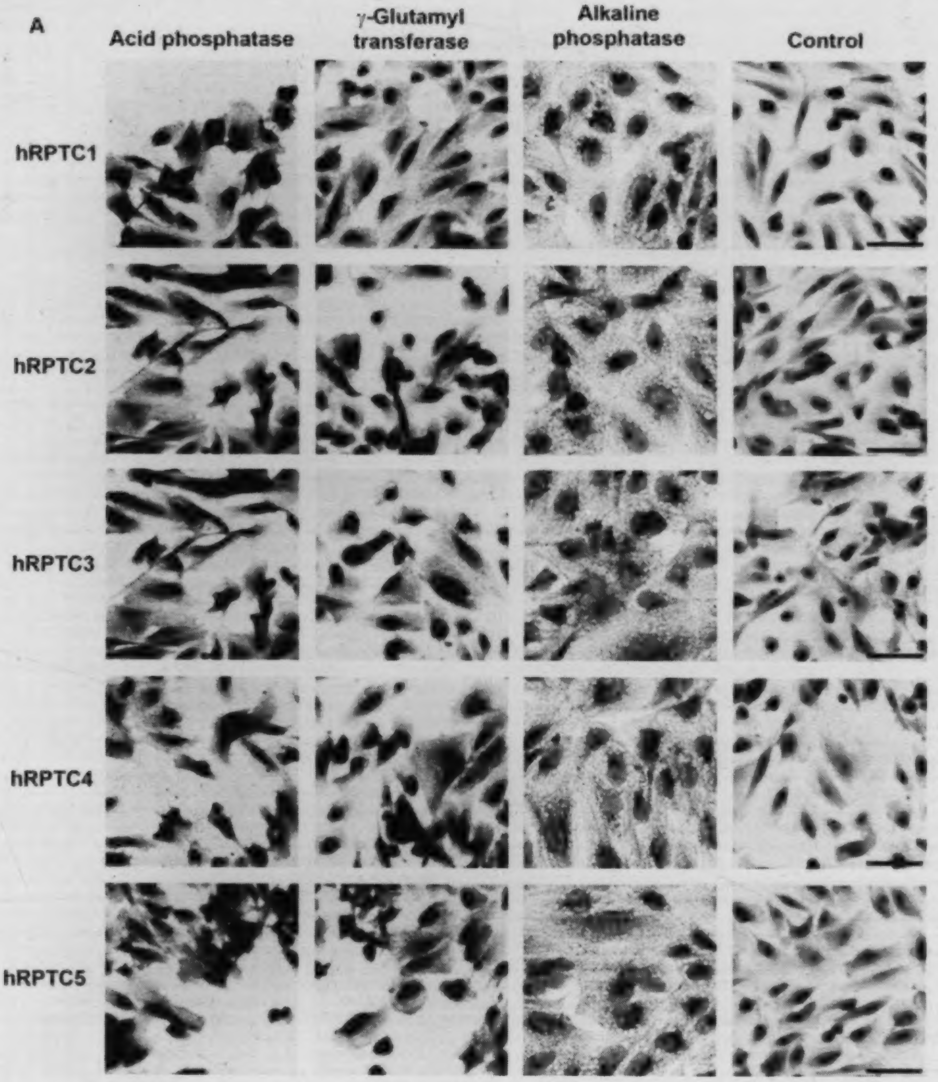
A
Acid phosphatase
γ-Glutamyl transferase
Alkaline phosphatase
Control
hRPTC1
hRPTC2
hRPTC3
hRPTC4
hRPTC5

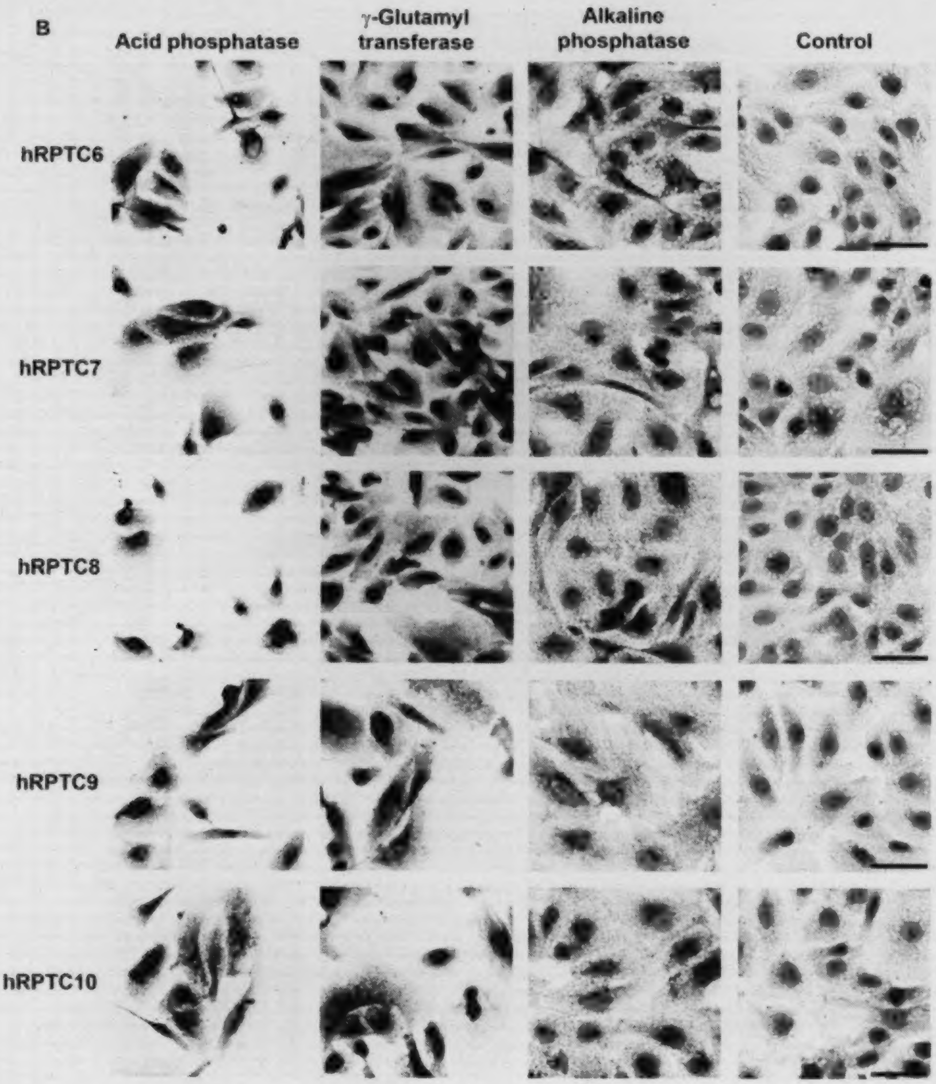
B
Acid phosphatase
γ-Glutamyl transferase
Alkaline phosphatase
Control
hRPTC6
hRPTC7
hRPTC8
hRPTC9
hRPTC10

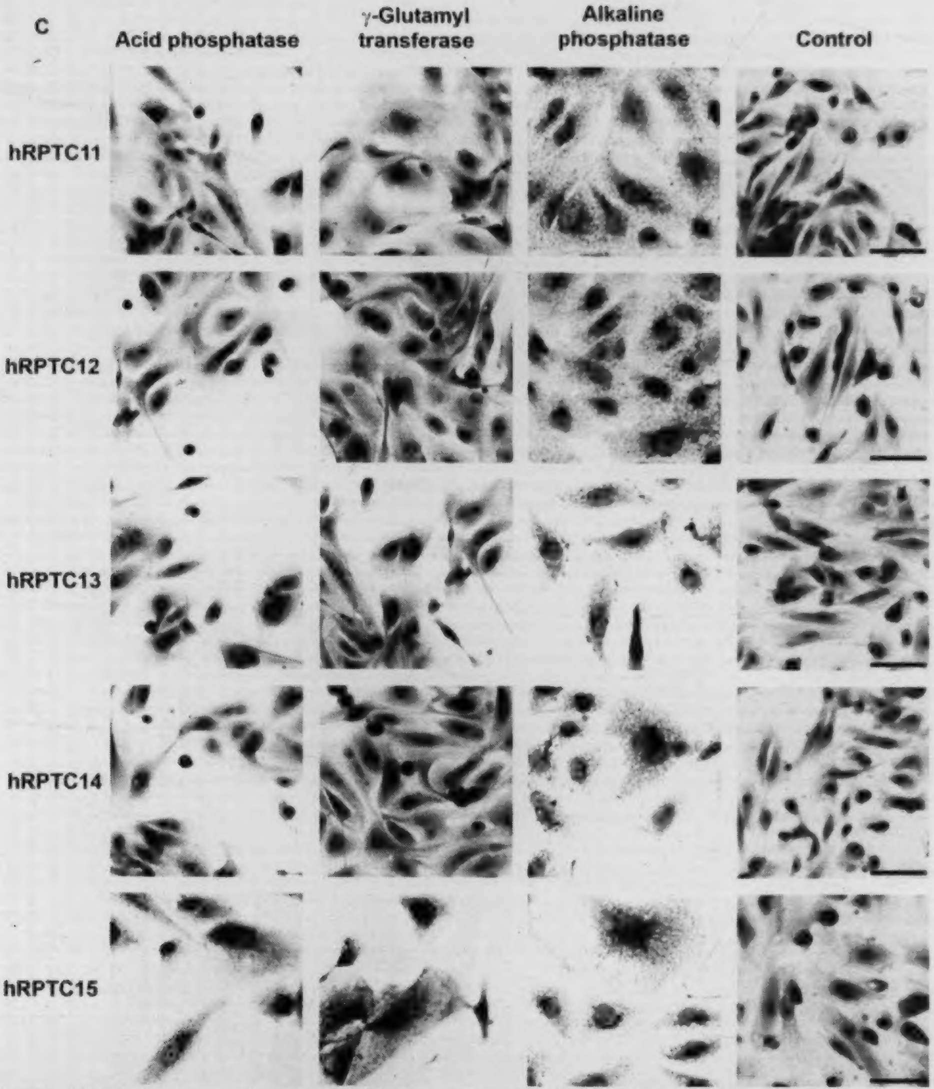
C
Acid phosphatase
γ-Glutamyl transferase
Alkaline phosphatase
Control
hRPTC11
hRPTC12
hRPTC13
hRPTC14
hRPTC15

Figure III-9. Demonstration of the proximal tubular brush border enzymes, acid phosphatase, γ-glutamyl transferase, and alkaline phosphatase, in fifteen different monolayer hRPTC cultures. Brush border cytochemistry staining for acid phosphatase, γ-glutamyl transferase, and alkaline phosphatase was performed on monolayer cultures of (A) hRPTC1 through hRPTC5, (B) hRPTC6 through hRPTC10, and (C) hRPTC11 through hRPTC15 as described in Materials and Methods (Section II.4). Hematoxylin counterstain for nuclei is shown in blue. Scale bars are 50 μm.

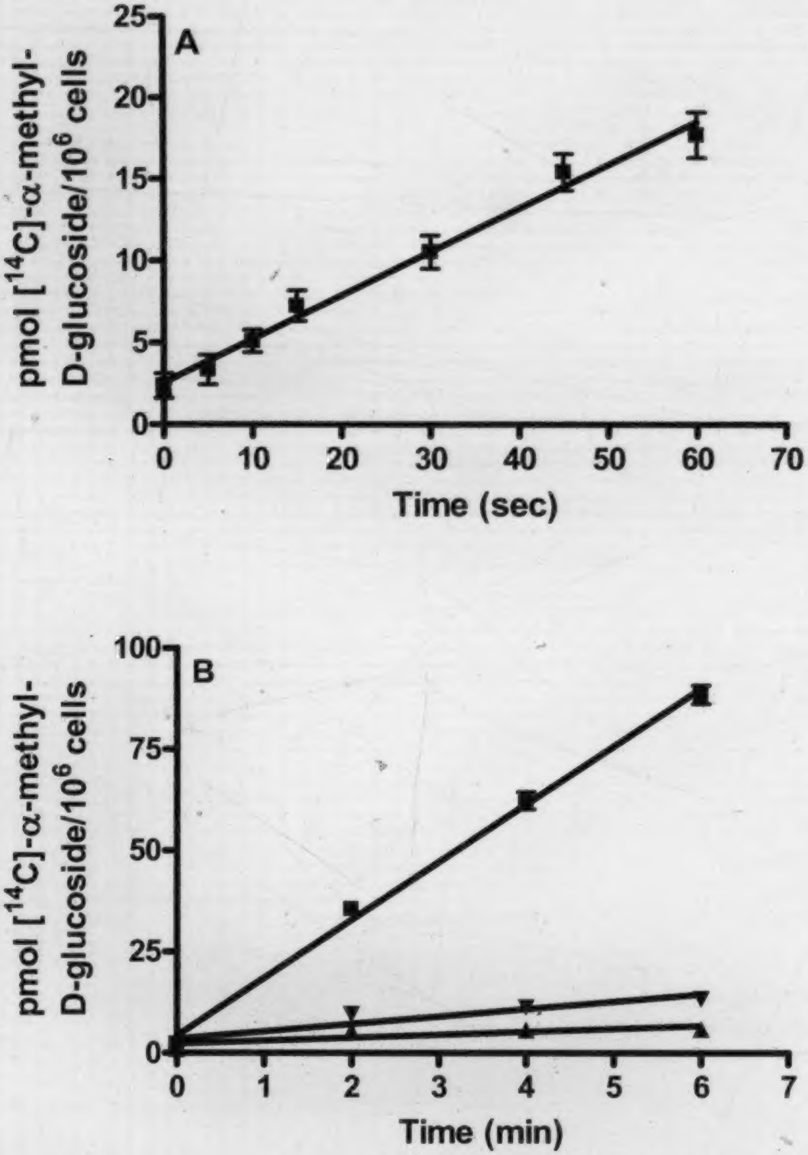

Figure III-10. Time courses of uptake of α-methyl-D-glucoside by monolayer hRPTC1 cultures. Uptake of 100 μM [^{3}H]-α-methyl-D-glucoside into monolayer hRPTC1 cultures was monitored over time in (A) sodium-containing buffer alone (■) or (B) in sodium-containing buffer alone (■) with 1 mM phloridzin (▲) or in sodium-free buffer alone (▼) as described in Materials and Methods (Section II.5). Values plotted are means (± standard deviations) from three independent experiments. Points for which error bars are apparently absent had errors equal or smaller than the border size of the points.

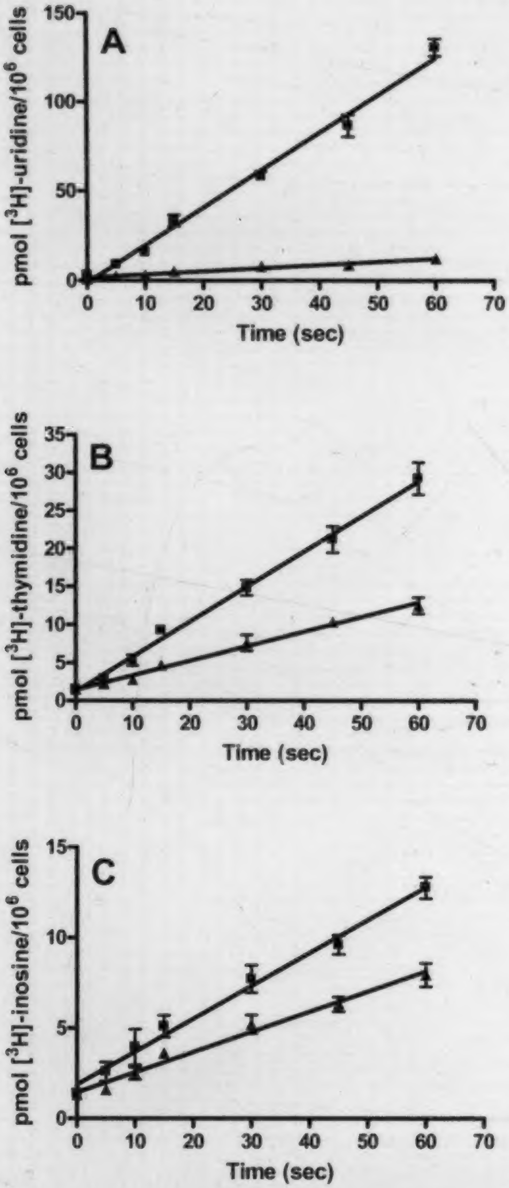

Figure III-11. Short time courses of uptake of uridine, thymidine, and inosine by monolayer cultures of hRPTCs. Uptake of 10 µM (A) [^{3}H]-uridine, (B) [^{3}H]-thymidine, and (C) [^{3}H]-inosine in sodium-containing buffer alone (■) or with 10 mm uridine (▲) in (A), 1 mM thymidine (▲) in (B), or 1 mM inosine (▲) in (C) was monitored over time into one (hRPTC1) of fifteen different hRPTC cultures as described in Materials and Methods (Section II.5). Values plotted are means (± standard deviations) from three independent experiments. Points for which error bars are apparently absent had errors equal or smaller than the border size of the points.

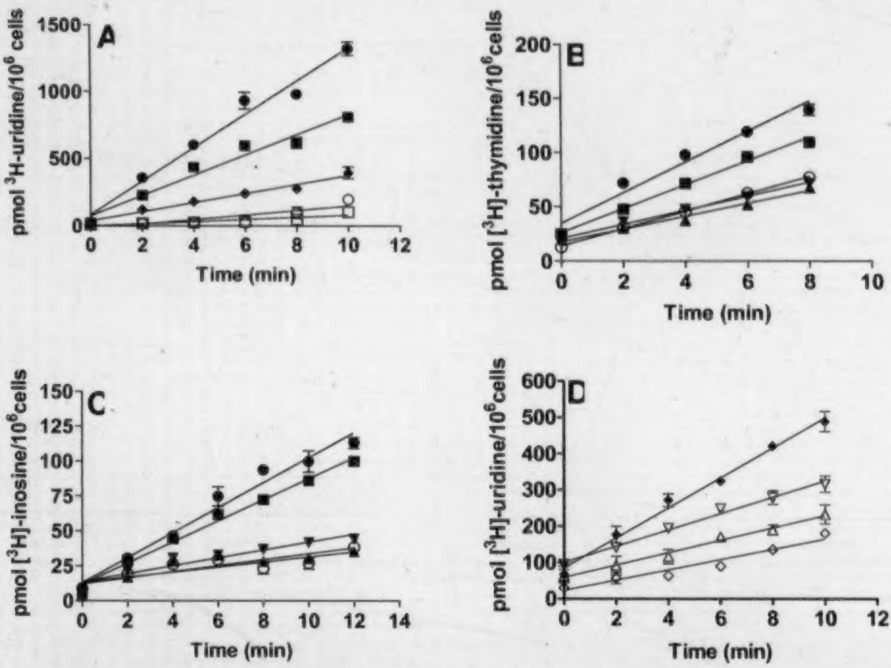

Figure III-12. Long time courses of uptake of uridine, thymidine, and inosine by monolayer cultures of hRPTCs. Uptake of 10 μM (A) [^{3}H]-uridine, (B) [^{3}H]-thymidine, and (C) [^{3}H]-inosine in sodium-containing buffer and (D) 10 μM [^{3}H]-uridine in sodium-free buffer with or without various inhibitors was monitored over time into one (hRPTC1) of fifteen different hRPTC cultures. The symbols denote the following buffers and inhibitors: sodium-containing buffer alone (■) or with 10 mM uridine (□) or 200 μM dilazep alone (●) or with 10 mM uridine (○), 1 mM thymidine (▼), or 1 mM inosine (▲); sodium-free buffer (♦) with 0.1 μM NBMPR (▽), 200 μM dilazep (Δ), or 10 mM uridine (◊). Values plotted are means (± standard deviations) from three independent experiments. Points for which error bars are apparently absent had errors equal or smaller than the border size of the points.

Table III-1. Comparison of relative hNT mRNA transcript levels in total RNA from four different human kidney cortex tissues and monolayer cultures of HK-2 cells.^{a}

Probe	Fold Expression				
	Human kidney cortex tissue				HK-2
	C1	C2	C3	C4	
hENT1	260.2 ± 4.5	446 ± 2.4	18.9 ± 0.2	5.9 ± 0.3	1.0 ± 0.7^{b}
hENT2	8.6 ± 0.5	12.8 ± 0.3	2.5 ± 0.2	1.0 ± 0.3^{b}	12.4 ± 0.7
hCNT1	299.8 ± 4.9	534 ± 3.8	11.85 ± 0.2	1.0 ± 0.4^{b}	undetectable
hCNT2	2.1 ± 0.6	10.1 ± 0.3	4.5 ± 0.3	1.0 ± 0.4^{b}	undetectable
hCNT3	435.9 ± 7.4	154.7 ± 8.2	179 ± 3.1	10.5 ± 0.6	1.0 ± 0.8^{b}

a - TaqMan RT-PCR was performed as described in Materials and Methods (Section II.8).
b - Relative levels were normalized to these arbitrary reference samples as described in Materials and Methods (Section II.8.3).

Table III-2. Summary of hENT1 immunohistochemistry and hCNT3 immunofluorescence staining studies in different human kidney tissues obtained from four different individuals.^{a}

Human kidney tissue	hENT1 immunohistochemistry			
	Proximal tubule marker PNRA	Thick ascending loop of Henle marker THP	Collecting duct principal cell marker AQP2	Collecting duct intercalated cell marker V-ATPase
K1	intense apical membrane	moderate apical and basolateral membrane	moderate apical and basolateral membrane	moderate apical and basolateral membrane
K2	intense apical membrane	moderate apical and basolateral membrane	moderate apical and basolateral membrane	moderate apical and basolateral membrane
K3	intense apical membrane	moderate apical and basolateral membrane	moderate apical and basolateral membrane	moderate apical and basolateral membrane
K4	intense apical membrane	moderate apical and basolateral membrane	moderate apical and basolateral membrane	moderate apical and basolateral membrane

Human kidney tissue	hCNT3 immunofluorescence staining			
	Proximal tubule marker PNRA	Thick ascending loop of Henle marker THP	Collecting duct principal cell marker AQP2	Collecting duct intercalated cell marker V-ATPase
K1	apical membrane	apical membrane	negative	negative
K2	apical membrane	apical membrane	negative	negative
K3	apical membrane	apical membrane	negative	negative
K4	apical membrane	apical membrane	negative	negative

a - Immuno-histochemistry with anti-hENT1 antibodies and immunofluorescence with anti-hCNT3 antibodies was performed on human kidney tissue obtained from four different individuals (K1 through K4, Table II-1) as described in Materials and Methods (Section II.4).

Table III-3. Demonstration of parathyroid hormone sensitivities of adherent hRPTC monolayer cultures.[a]

Culture	Total intracellular cAMP pmol cAMP/10^6 cells			
	Control - untreated	Parathyroid hormone	Anti-diuretic hormone	Forskolin
hRPTC1	424 ± 37	719 ± 67 **	401 ± 32	1092 ± 108 ***
hRPTC2	760 ± 46	1284 ± 118 **	788 ± 77	1307 ± 124 **
hRPTC3	994 ± 146	1387 ± 86 *	930 ± 93	1731 ± 41 **
hRPTC4	630 ± 117	855 ± 36 *	645 ± 102	1125 ± 55 **
hRPTC5	485 ± 66	685 ± 47 *	426 ± 79	712 ± 52 **
hRPTC6	542 ± 19	654 ± 29 **	504 ± 28	754 ± 42 **
hRPTC7	638 ± 59	1212 ± 156 **	674 ± 49	1329 ± 151 **
hRPTC8	650 ± 68	1068 ± 135 **	634 ± 44	1207 ± 143 **
hRPTC9	451 ± 83	842 ± 66 **	402 ± 49	859 ± 71 **
hRPTC10	591 ± 47	803 ± 26 **	624 ± 65	931 ± 76 **
hRPTC11	366 ± 58	612 ± 21 **	443 ± 40	735 ± 28 ***
hRPTC12	429 ± 47	687 ± 51 **	463 ± 85	798 ± 87 **
hRPTC13	661 ± 33	755 ± 42 *	628 ± 38	841 ± 69 *
hRPTC14	629 ± 41	788 ± 26 **	680 ± 64	850 ± 94 *
hRPTC15	579 ± 26	712 ± 49 *	595 ± 93	787 ± 51 **

a - Hormone treatments and determination of total intracellular cAMP was performed as described in Materials and Methods (Section II.7). Values represent means ± standard deviations of three independent experiments.

* denotes values significantly different than control by paired t-test ($p < 0.05$)

** denotes values significantly different than control by paired t-test ($p < 0.01$)

*** denotes values significantly different than control by paired t-test ($p < 0.001$)

Table III-4. Demontration of phloridzin-sensitive, sodium-dependent uptake of methyl-α-D-glucoside into adherent hRPTC monolayer cultures.[a]

Culture	methyl-α-D-glucopyranoside uptake pmol /2 min/10^6 cells		
	Sodium-containing buffer		Sodium-free buffer
	Control	1 mM phloridzin	
hRPTC1	36.7 ± 1.3	5.2 ± 0.5 *	2.4 ± 0.8 *
hRPTC2	51.5 ± 4.9	5.3 ± 0.8 *	2.5 ± 0.6 *
hRPTC3	61.3 ± 1.8	5.0 ± 1.7 *	1.9 ± 0.2 *
hRPTC4	20.0 ± 3.6	5.8 ± 1.6 *	1.3 ± 0.3 *
hRPTC5	25.8 ± 4.6	5.8 ± 1.1 *	2.6 ± 0.8 *
hRPTC6	24.7 ± 1.9	5.2 ± 1.6 *	1.9 ± 0.4 *
hRPTC7	48.4 ± 2.5	5.6 ± 0.4 *	2.4 ± 0.3 *
hRPTC8	28.0 ± 2.5	6.0 ± 2.1 *	1.3 ± 0.1 *
hRPTC9	40.1 ± 8.0	4.8 ± 1.2 *	1.3 ± 0.3 *
hRPTC10	52.8 ± 8.1	4.3 ± 1.5 *	1.5 ± 0.5 *
hRPTC11	23.1 ± 4.7	6.4 ± 0.5 *	1.9 ± 0.3 *
hRPTC12	29.0 ± 3.0	6.8 ± 1.1 *	2.0 ± 0.5 *
hRPTC13	31.8 ± 2.6	6.1 ± 1.8 *	2.2 ± 1.3 *
hRPTC14	15.8 ± 4.0	5.9 ± 1.7 *	1.4 ± 0.4 *
hRPTC15	19.4 ± 1.3	4.7 ± 2.2 *	2.1 ± 1.0 *

a - Uptake assays were performed as described in Materials and Methods (Section II.5). Values represent means ± standard deviations of three independent experiments.

* denotes values significantly different than control by paired t-test ($p < 0.0001$)

III.4 Bibliography

1. Kuttesch JF Jr, Nelson JA. Renal handling of 2'-deoxyadenosine and adenosine in humans and mice. Cancer Chemother Pharmacol. 1982; 8: 221-229.

2. Nelson JA, Kuttesch JR Jr, Herbert BH. Renal secretion of purine nucleosides and their analogs in mice. Biochem Pharmacol. 1983; 32: 2323-232.

3. Nelson, J.A., Vidale, E., and Enigbokan, M. 1998. Renal transepithelial transport of nucleosides. Drug Metab. 16: 789-792.

4. Kuttesch JF Jr, Robins MJ, Nelson JA. Renal transport of 2'-deoxytubercidin in mice. Biochem Pharmacol. 1982; 31: 3387-3394.

5. Aiba T, Sakurai Y, Tsukada S, Koizumi T. Effects of probenecid and cimetidine on the renal excretion of 3'-azido-3'-deoxythymidine in rats. J Pharmacol Exp Ther. 1995; 272: 94–99.

6. Chen R, Nelson JA. Role of organic cation transporters in the renal secretion of nucleosides. Biochem Pharmacol. 2000; 60: 215-219.

7. Burnstock G. Purine and pyrimidine receptors. Cell Mol Life Sci. 2007; 64: 1471-1483.

8. Gutierrez MM, Brett CM, Ott RJ, Hui AC, Giacomini KM. Nucleoside transport in brush border membrane vesicles from human kidney. Biochimica et Biophysica Acta. 1992; 1105: 1-9.

9. Griffiths M, Beaumont N, Yao SY, Sundaram M, Boumah CE, Davies A, Kwong FY, Coe I, Cass CE, Young JD, Baldwin SA. Cloning of a human nucleoside transporter implicated in the cellular uptake of adenosine and chemotherapeutic drugs. Nat Med. 1997; 3: 89-93.

10. Griffiths M, Yao SY, Abidi F, Phillips SE, Cass CE, Young JD, Baldwin SA. Molecular cloning and characterization of a nitrobenzylthioinosine-insensitive (ei) equilibrative nucleoside transporter from human placenta. Biochem J. 1997; 328: 739-743.

11. Crawford CR, Patel DH, Naeve C, Belt JA. Cloning of the human equilibrative, nitrobenzylmercaptopurine riboside (NBMPR)-insensitive nucleoside transporter ei by functional expression in a transport-deficient cell line. J Biol Chem. 1998; 273: 5288–5293.

12. Yao SY, Ng AM, Vickers MF, Sundaram M, Cass CE, Baldwin SA, Young JD. Functional and molecular characterization of nucleobase transport by recombinant human and rat equilibrative nucleoside transporters 1 and 2. Chimeric constructs reveal a role for the ENT2 helix 5-6 region in nucleobase translocation. J Biol Chem. 2002; 277: 24938-24948.

13. Baldwin SA, Yao SYM, Hyde RJ, Foppolo S, Barnes K, Ritzel MWL, Cass CE, Young JD. Functional Characterization of novel human mouse equilibrative nucleoside transporters (hENT3 and mENT3) located in intracellular membranes. J Biol Chem. 2007; 280: 15880-15887.

14. Barnes K, Dobrzynski H, Foppolo S, Beal PR, Ismat F, Scullion ER, Sun L, Tellez J, Ritzel MW, Claycomb WC, Cass CE, Young JD, Billeter-Clark R, Boyett MR, Baldwin SA. Distribution and functional characterization of equilibrative nucleoside transporter-4, a novel cardiac adenosine transporter activated at acidic pH. Circ Res. 2006; 99: 510-519.

15. Ritzel MW, Yao SY, Huang MY, Elliott JF, Cass CE, Young JD. Molecular cloning and functional expression of cDNAs encoding a human Na+ nucleoside cotransporter (hCNT1). Am J Physiol Cell Physiol. 1997; 272: C707– C714.

16. Wang J, Su SF, Dresser MJ, Schaner ME, Washington CB, Giacomini KM. Na+ dependent purine nucleoside transporter from human kidney: cloning and functional characterization. Am J Physiol Renal Physiol. 1997; 273: F1058– F1065.

17. Ritzel MW, Yao SY, Ng AM, Mackey JR, Cass CE, Young JD. Molecular cloning, functional expression and chromosomal localization of a cDNA encoding a human Na+/nucleoside cotransporter (hCNT2) selective for purine nucleosides and uridine. Mol Membr Biol. 1998; 15: 203– 211.

18. Ritzel MW, Ng AM, Yao SY, Graham K, Loewen SK, Smith KM, Ritzel RG, Mowles DA, Carpenter P, Chen XZ, Karpinski E, Hyde RJ, Baldwin SA, Cass CE, Young JD. Molecular identification and characterization of novel human and mouse concentrative Na+ nucleoside cotransporter

proteins (hCNT3 and mCNT3) broadly selective for purine and pyrimidine nucleosides (system cib). J Biol Chem. 2001; 276: 2914– 2927.

19. Govindarajan R, Bakken AH, Hudkins KL, Lai Y, Casado FJ, Pasto-Anglada M, Tse CM, Hayashi J, Unadkat JD. In situ hydribdization and immunolocalization of concentrative and equilibrative nucleoside transporters in the human intestine, liver, kidneys, and placenta. Amer J Physiol Reg Int Comp Physiol. 2007; 293: R1809-R1822.

20. Xia L, Engel K, Zhou M, Wang J. Membrane localization and pH-dependent transport of newly cloned organic cation transport (PMAT) in kidney cells. Am. J. Physiol. Renal Physiol. 2007; 292: F682-F690.

21. Pastor-Anglada M, Cano-Soldado P, Molina-Arcas M, Lostao MP, Larráyoz I, Martínez-Picado J, Casado FJ. Cell entry and export of nucleoside analogues. Virus Res. 2005; 107: 151-164.

22. Chandrasena G, Giltay R, Patil SD, Bakken A, Unadkat JD. Functional Expression of Human Intestinal Na+ Dependent and Na+ Independent Nucleoside Transporters in Xenopus Laevis Oocytes. Biochem Pharmacol. 1997; 53: 1909-1918.

23. Mangravite, LM, Lipschutz JH, Mostov KE, Giacomini KM. Localization of GFP-tagged concentrative nucleoside transporters in a renal polarized epithelial cell line. Am J Physiol Renal Physiol. 2001; 280: F879-F885.

24. Mangravite LM, Xiao G, Giacomini KM. Localization of human equilibrative nucleoside transporters, hENT1 and hENT2, in renal epithelial cells. Am J Physiol Renal Physiol. 2003; 284: F902-F910.

25. Mangravite LM, Badagnani I, Giacomini KM. Nucleoside transporters in the disposition and targeting of nucleoside analogs in the kidney. Eur J Pharmacol. 2003; 479: 269-281.

26. Handler JS, Perkins FM, Johnson JP. Studies on renal cell function using cell culture technique. Am J Physiol Renal Physiol. 1980; 238: F1-F9.

27. Lai Y, Bakken AH, Unadkat JD. Simultaneous expression of hCNT1-CFP and hENT1-YFP in Madin-Darby canine kidney cells. Localization and vectorial transport studies. J Biol Chem. 2002; 277: 37711-37717.

28. Errasti-Murugarren E, Pastor-Anglada M, Casado FJ. Role of CNT3 in the transepithelial flux of nucleosides and nucleoside-derived drugs. J Physiol. 2007; 582: 1249-60.

29. Hammond JR, Stolk M, Archer RG, McConnell K. Pharmacological analysis and molecular cloning of the canine equilibrative nucleoside transporter 1. Eur J Pharmacol. 2004; 491: 9-19.

30. Griffith DA, Doherty AJ, and Jarvis SM. Nucleoside transport in cultured LLC-PK1 epithelia. Biochim et Biophys Acta. 1992; 1106: 303-310.

31. Brothers SP, Janovick JA, Conn PM. Unexpected effects of epitope and chimeric tags on gonadotropin-releasing hormone receptors: implications for understanding the molecular etiology of hypogonadotropic hypogonadism. J Clin Endocrinol Metab. 2003; 88: 6107-6112.

32. Louvard D. Apical membrane aminopeptidase appears at site of cell-cell contact in culture kidney epithelial cells. Proc Natl Acad Sci USA. 1980; 77: 4132-4136.

33. Young JD, Yao SYM, Sun L, Cass CE, Baldwin SA. Human equilibrative nucleoside transporter (ENT) family of nucleoside and nucleobase transporter proteins. Xenobiotica. 2008; 38: 995-1021.

34. Pastor-Anglada M, Cano-soldado P, Errasti-murugarren E, Casado FJ. SLC28 genes and concentrative nucleoside transporter (CNT) proteins. Xenobiotica. 2008; 38: 972-994.

35. Richardson JWC, Scalera V, Simmons NL. Identification of two strains of MDCK cells which resemble separate nephron tubule segments. Biochim Biophys Acta. 1981; 673: 26-36.

36. Gstraunthaler G, Pfaller W, Kotanko P. Biochemical characterization of renal epithelial cell cultures (LLC-PK_1 and MDCK). Am J Physiol Renal Physiol. 1985; 248: F536-F544.

37. Handler JS, Kreisberg JI. Biology of renal cells in culture. In The Kidney. Edited by BM Brenner and FC Jr Rector, WB Saunders Co: Philadelphia, Pennsylvania, 1991; pp. 110-131.

38. Goldring, SR, Dayer JM, Ausiello DA, Krane SM. A cell strain cultured from porcine kidney increases cyclic AMP content upon exposure to calcitonin or vasopressin. Biochem Biophys Res Commun. 1978; 83: 434-440.

39. Slugoski MD, Smith KM, Mulinta R, Ng AM, Yao SY, Morrison EL, Lee QO, Zhang J, Karpinski E, Cass CE, Baldwin SA, Young JD. A conformationally mobile cysteine residue (Cys-561) modulates Na+ and H+ activation of human CNT3. J Biol Chem. 2008; 283: 24922-34.

40. Ryan MJ, Johnson G, Kirk J, Fuerstenberg SM, Zager RA, Torok-Storb B. HK-2: an immortalized proximal tubule epithelial cell line from normal adult human kidney. Kidney Int. 1994; 45: 48-57.

41. Todd JH, McMartin KE, Sens DA. Enzymatic isolation and serum-free culture of human renal cells. In Methods in Molecular Medicine: Human Cell Culture Protocols. Edited by Jones, GE. Humana Press Inc,: Totowa, NJ, 1995; Chapter 32.

42. Toutain H, Vauclin-Jacques N, Fillastre JP, Morin JP. Biochemical, functional, and morphological characterization of a primary culture of rabbit proximal tubule cells. Exp Cell Res. 1991; 194: 9-18.

43. Ward JL, Sherali A, Mo ZP, and Tse CM. Kinetic and pharmacological properties of cloned human equilibrative nucleoside transporters, ENT1 and ENT2, stably expressed in nucleoside transporter-deficient PK15 cells. Ent2 exhibits a low affinity for guanosine and cytidine but a high affinity for inosine. J Biol Chem. 2000; 275: 8375-81.

44. Vickers MF, Mani RS, Sundaram M, et al. Functional production and reconstitution of the human equilibrative nucleoside transporter (hENT1) in *Saccharomyces cerevisiae*. Interaction of inhibitors of nucleoside transport with recombinant hENT1 and a glycosylation-defective derivative (hENT1/N48Q). Biochem J. 1999; 339: 21-32.

45. Jennings LL, Hao C, Cabrita MA, et al. Distinct regional distribution of human equilibrative nucleoside transporter proteins 1 and 2 (hENT1 and hENT2) in the central nervous system. Neuropharm. 2001;40:722-31.

46. Harlow E, Lane D. In *Using Antibodies: a laboratory manual*. Cold Spring Harbor, NY: Cold Spring Harbor Laboratory Press, 1999.

47. Spratlin J, Sangha R, Glubrecht D, et al. The absence of human equilibrative nucleoside transporter 1 is associated with reduced survival in patients with gemcitabine-treated pancreas adenocarcinoma. Clin Cancer Res 2004; 10: 6956-61.

48. Mackey JR, Jennings LL, Clarke ML, Santos CL, Dabbagh L, Vsianska M, Koski SL, Coupland RW, Baldwin SA, Young JD, Cass CE. Immunohistochemical variation of human equilibrative nucleoside transporter 1 protein in primary breast cancers. Clin Cancer Res. 2002; 8: 110-6.

49. Wheater PR, Burkitt HG, Daniels VG. Urinary system. In Wheaters Functional Histology: A Text and colour atlas. Edited by Wheater PR, Burkitt HG, Daniels VG. Churchill Livingstone: New York, 1987, pp. 236-257.

50. Kujala M, Tienari J, Lohi H, Elomaa O, Sariola H, Lehtonen E, and Kere J. SLC26A6 and SLC26A7 anion exchangers have a distinct distribution in human kidney. Nephron Exp Nephrol. 2005; 101: e50-58.

51. Lai Y, Tse CM, Unadkat JD. Mitochondrial expression of the human equilibrative nucleoside transporter 1 (hENT1) results in enhanced mitochondrial toxicity of antiviral drugs. J Biol Chem. 2004; 279: 4490–4497.

52. François M. Sites of hormone action in the mammalian nephron. Am J Physiol Renal Fluid Electrolyte Physiol. 1981; 240: F159-164.

53. Wilson PD, Dillingham MA, Breckon R, Anderson RJ. Defined human renal tubular epithelia in culture: growth, characterization, and hormonal response. Am J Physiol. 1985; 248: F436-443,

54. Smith WL, Garcia-Perez A. Immunodissection: use of monoclonal antibodies to isolate specific types of renal cells. Am J Physiol. 1985; 248: F1-7.

55. Chen TC, Curthoys NO, Lagenaur CF, Puschett JB. Characterization of primary cell cultures derived from rat renal proximal tubules. In Vitro Cell Dev Biol. 1989; 25: 714-722.

56. Vallon V, Muhlbauer B, and Osswald H. Adenosine and kidney function. Physiol Rev. 2006; 86: 901-940.

Chapter IV

IV. Human concentrative nucleoside transporter 3 (hCNT3) is a determinant of 9-β-D-arabinosyl-2-fluoroadenine (fludarabine) transportability and cytotoxicity in cultures of human renal proximal tubule cells (hRPTCs)[1]

---

[1] An earlier version of this chapter has been published as a co-authored paper [Elwi AN, Damaraju VL, Kuzma ML, Baldwin SA, Young JD, Sawyer MB, Cass CE. Human concentrative nucleoside transporter 3 is a determinant of fludarabine transportability and cytotoxicity in human renal proximal tubule cell cultures. Cancer Chemother Pharmacol. 2009; 63: 289-301.]; contribution of Elwi AN was 90 %.

IV.1 Introduction

Nucleoside analog chemotherapy plays a central role in the treatment of hematological malignancies, especially since the advent of purine nucleoside analogs that are resistant to adenosine deaminase, which catalyzes their conversion to inactive forms [1]. 9-β-D-Arabinosyl-2-fluoroadenine (fludarabine) was one of the first purine nucleoside analogs to be used to treat adult and pediatric hematologic malignancies [2]. More specifically, fludarabine has become a standard treatment of indolent lymphoproliferative disorders such as chronic lymphocytic leukemia and low grade non-Hodgkin's lymphoma [3,4]. Fludarabine is administered as a more soluble pro-drug fludarabine-5′-monophosphate (Fludara®) either orally [5] or intravenously by rapid bolus injections [6], short term infusions [7], or continuous infusions [8]. Fludara® is quickly dephosphorylated in the small intestine or plasma to fludarabine by 5′-nucleotidases [9]. Following cellular uptake, fludarabine is sequentially phosphorylated intracellularly to its monophosphate, diphosphate, and triphosphate forms by intracellular kinases, most notably to its monophosphate form by deoxycytidine kinase [10,11]. In proliferating cells, fludarabine's main mechanisms of cytotoxic actions are through inhibition by fludarabine-5′-triphosphate of deoxyribonucleic acid (DNA) synthesis [11] by: (i) competition with 2′-deoxyadenosine-5′-triphosphate (dATP) as a substrate for DNA polymerase α, β, γ, and ε, thus being incorporated into elongating DNA strands and acting as a DNA chain terminator [12-17], and (ii) inhibition of ribonucleotide reductase, thus reducing cellular 2′-deoxynucleotide pools and potentiating its actions as a DNA chain terminator [13-15]. Reduction of intracellular (2′-deoxy)nucleotide-5′-triphosphate (dNTP/NTP) pools below physiological concentrations relieves direct inhibition of apoptosome formation by (d)NTPs, and hence apoptosis, through decreases in (d)NTP binding of cytochrome c [18]. In addition to inhibition of DNA synthesis, fludarabine-5′-triphosphate exhibits ribonucleic acid (RNA) directed effects, including inhibition of RNA transcription [19] and polyadenylation [20]. Cytotoxicity of fludarabine to quiescent non-dividing cells has been observed and may be related to RNA directed effects [19,20] or inhibition of DNA repair processes [21]. Because of the multiple mechanisms of action of fludarabine, rationally designed combination therapies have been exploited in the clinic, including biochemical modulation of 1-β-D-arabinofuranosylcytosine (cytarabine) for treatment of acute myelogeneous leukemia [22,23].

Fludarabine is mainly eliminated from the body by renal excretion [24]. Fludarabine-5′-triphosphate accumulation in, and elimination from, leukemia cells are relatively constant parameters in an individual but exhibit significant inter-patient variability [24]. Plasma pharmacokinetics of the free drug, fludarabine, exhibit long terminal half lives of 30 hr and persistent low plasma concentrations of free drug (<0.1 μM) 24-72 hr after administration [24]. Inter-patient variability in drug elimination can result in unpredictable normal tissue toxicities and response rates from empirical chemotherapy dosing methodologies. Although the common dose-limiting toxicities of fludarabine are neutropenia, thrombocytopenia, and lymphopenia [2], other toxicities include somnolence, fatigue, nausea, vomiting, pulmonary toxicity, autoimmune complications, and occasionally acute renal failure associated with tumor lysis syndrome [2,25-27].

Permeation of nucleoside analogs across plasma membranes, the first step in nucleoside analog cytotoxicity, is accomplished primarily by activity of the human equilibrative and concentrative nucleoside transporters (hENTs and hCNTs) [28-42]. Fludarabine transport by hENT1, hENT2, hCNT2, and hCNT3 has been demonstrated in a variety of recombinant expression systems [43] with fludarabine transportability correlating positively with sensitivity to cytotoxicity in a human leukemic cell line, CEM [43]. While the apparent affinity of recombinant hENT1 for fludarabine is higher than its apparent affinity for uridine (K_m values of 107 μM versus 250 μM), the apparent affinity of recombinant hCNT3 for fludarabine is lower than its apparent affinity for uridine (K_m values of 353 μM versus 20 μM) [43]. Because uridine is a permeant of six of the seven human NTs (hNTs), its transportability is often used as a benchmark for comparison of transportabilities of other nucleosides and nucleoside drugs [28,29].

Several studies suggest that nucleosides are actively reabsorbed and secreted in kidneys through the concerted actions of hENTs, hCNTs, and possibly human organic cation and anion transporters (hOCTS and hOATs) [44-49]. Adenosine is reabsorbed through ENT1-and OCT-independent processes [44,47] while 2′-deoxyadenosine, which is toxic at high concentrations [50,51], is secreted by ENT1-dependent, but OCT-independent, processes [44,47]. 7-Deaza-2'-deoxyadenosine (2′-deoxytubercidin) is secreted by ENT1-dependent, but OAT-independent, processes that may utilize OCT1 [45,46,49], although OCT1 is not necessary for its secretion [52]. The fluoropyrimidine nucleosides, 5'-deoxy-5-fluorouridine and 5-fluoro-2'-deoxyuridine, undergo net secretion unaffected by the ENT inhibitor dipyridamole but inhibited by the OCT inhibitor cimetidine [47]. The anti-viral nucleoside analog 3'-azido-2',3'-dideoxythymidine undergoes net tubular secretion by OAT- and OCT-dependent processes [48]. A pyrimidine-nucleoside selective, sodium-dependent NT activity, similar to the activity now known to be mediated by hCNT1, was identified in studies with human kidney brush border membrane vesicles [53]. Several studies have localized hCNT1, rat CNT2 (rCNT2), and hCNT3 to apical membranes and hENT1 and hENT2 to basolateral membranes of transfected animal kidney epithelial cell lines grown as polarized monolayers [54-57]. Asymmetric distribution of CNTs and ENTs to apical and basolateral membranes of kidney epithelial cells, respectively, results in vectorial fluxes of nucleosides from the lumen to the interstitial space across kidney epithelia, driven by sodium gradients established by basolateral Na^+K^+ATPases [57].

In the experiments described in Chapter III of this thesis, hENT1 and hCNT3 in human kidney tissues were localized to apical brush border membranes of proximal tubules, the main site of solute reabsorption in nephrons. Furthermore, primary cultures of human renal proximal tubule cells (hRPTCs) from a single individual were shown to exhibit endogenous hENT1, hENT2, hCNT3 activities, and all three proteins were also demonstrated to be present in human kidney proximal tubules *in situ* from four different individuals (Chapter

III). At the time the current studies were in progress, one group reported hENT4 in human kidney tissue lysates and also localized recombinant hENT4 to apical membranes of transfected animal kidney epithelial cell lines [58]. Another group demonstrated the presence of hCNT1 and hCNT3 in apical membranes of proximal tubules, hENT1 in apical and basolateral membranes of proximal tubules adjacent to corticomedullary junctions, and hENT1 and hENT2 in apical and basolateral membranes of distal tubules [59]. Also, subsequent to the current study, hCNT3 was reported to mediate adenosine and fludarabine apical-to-basolateral fluxes in transfected animal kidney epithelial cell lines grown as polarized monolayers [60].

Taken together, the evidence presented in Chapter III suggested that apical hCNT3 is a main contributor to nucleoside reabsorption and apical hENT1 may play a role in selective nucleoside secretion in human kidney proximal tubules. In addition, hENT2 may be the basolateral transporter that is coupled to apical hCNT3 for nucleoside reabsorption. The contributions of endogenous hENTs and hCNTs in proximal tubular handling of physiological nucleosides and nucleoside analogs, such as fludarabine, are still poorly understood. Therefore, the roles of endogenous hENT1, hENT2, and hCNT3 in fludarabine accumulation into, and cytotoxicity to, hRPTC cultures isolated from human kidney cortex tissues of ten different individuals (hRPTC1 through hRPTC10, Table II-1) were investigated in the studies described in this chapter.

It was hypothesized that hENT1, hENT2, and hCNT3 activities would be present in hRPTCs to varying levels, that fludarabine accumulation would be determined by hCNT3 activity levels, and that fludarabine would be cytotoxic to hRPTCs. These predictions were based on previous observations of: (i) varied levels of other transporter types in hRPTCs, including hOCT1/2 and hOAT1/2/3/4 as determined by immunoblotting and uptake studies [61], (ii) varied abundance of hENT1 and hCNT3 in other tissues, including epithelial tissues, as determined by immunohistochemistry [62-68], and (iii) cytotoxicity of fludarabine to non-dividing quiescent cells [21], similar in growth properties to differentiated renal epithelial cells. To address the underlying mechanisms of proximal tubular handling of fludarabine by hNTs, hENT- and hCNT-mediated processes were characterized in monolayer cultures of ten different hRPTC cultures by reverse transcription polymerase chain reaction (RT-PCR), immunoblotting, and radiolabeled nucleoside uptake assays. hRPTCs possessed mRNA transcripts encoding hENT1/2 and hCNT1/2/3 as well as hENT1/2 and hCNT3 proteins and activities. The relationships of hCNT3 mRNA, protein, and activity levels with cellular uptake of fludarabine in hRPTCs were assessed. The different hRPTC cultures exhibited varying levels of hCNT3 mRNA, protein, and activities, and hCNT3 protein abundance and activity levels correlated positively with the extent of fludarabine accumulation. Although fludarabine nephrotoxicity is rare, it can be life threatening. Since there are no reported studies of fludarabine cytotoxicity to renal proximal tubule cells, *in vitro* cytotoxicity of fludarabine to hRPTCs was assessed to determine if fludarabine is directly toxic to renal tubule cells. The different hRPTC cultures exhibited varying sensitivities to fludarabine cytotoxicity that showed a modest positive correlation with the extent of fludarabine accumulation mediated by hCNT3. These results suggested that hCNT3 is a primary determinant of fludarabine uptake and cytotoxicity in hRPTCs. Variations in hCNT3 abundance in renal proximal tubules, and hence nucleoside reabsorption, may explain interpatient variability in fludarabine's pharmacokinetics and toxicities.

IV.2 Results

IV.2.1 Expression of mRNA transcripts for hENTs and hCNTs in hRPTCs

The presence of hENT1, hENT2, hCNT1, hCNT2, and hCNT3 transcripts in total RNA isolated from human kidney cortex tissues, comprised primarily of proximal tubules, was demonstrated in the experiments described in Chapter III. To establish that hRPTCs were a suitable model for studying kidney NTs, their NT mRNA expression levels were determined as described in Materials and Methods (Section II.8). Transcripts for all five NTs observed in kidney tissues *(i.e.*, hENT1, hENT2, hCNT1, hCNT2, and hCNT3) were also observed in total RNA isolated from four different hRPTC cultures (hRPTC1 through hRPTC4, Table II-1) as determined by RT-PCR with gene specific primers (Figure IV-1). The identities of the amplified bands were confirmed by their predicted PCR product sizes (0.50 kb for hENT1, 0.43 kb for hENT2, 0.80 kb for hCNT1, 0.61 kb for hCNT2, and 0.48 kb for hCNT3) and by sequence analysis of representative bands that were excised from the gels. Genomic DNA contamination was not detected in RT-PCR reactions without reverse transcriptase. The presence of transcripts for hCNT1 and hCNT2 in hRPTCs was expected since cDNAs of both were isolated from kidney cDNA libraries [37-39] and transcripts for both were detected in total RNA of human kidney cortex tissues (Chapter III).

IV.2.2 Identification of hENT and hCNT proteins in hRPTCs

The presence of hENT1, hENT2, and hCNT3 in crude membrane preparations from human kidney cortex tissues from four individuals was demonstrated in the experiments of Chapter III by immunoblotting. hCNT2 protein was not observed, either because it was not present or was below the limits of detection of the assay, and immunoblotting studies to detect hCNT1 were not undertaken since the antibodies raised against a hCNT1-derived synthetic peptide failed to recognize hCNT1 in the positive controls (electropherograms of membrane preparations of yeast producing recombinant hCNT1).

Since the expression studies shown in Figure IV-1 demonstrated transcripts for hENT1, hENT2, hCNT1, hCNT2, and hCNT3 in hRPTCs, immunoblotting experiments (Figure IV-2) were undertaken to determine which NT proteins were present in crude membranes of ten different adherent cultures of hRPTCs (hRPTC1 through hRPTC10, Table II-1). hENT1, hENT2, and hCNT3, but not hCNT2, were detected by immunoblotting in crude membranes from all ten cultures with anti-hNT specific monoclonal antibodies. Visualized bands exhibited the expected gel mobilities of NT proteins – i.e., 45-55 and 90 kDalton (kDa), respectively, for mammalian hENT1/hENT2 and hCNT3 and 35-45 and 90 kDA, respectively, for recombinant hENT1/hENT2 and hCNT3 produced in yeast. hENT1 and hENT2 are known to be heterogeneously glycosylated in mammalian cells [69,70] and the presence of diffuse bands with both anti-hENT1 and hENT2 antibodies was most likely a result of different glycosylation states. The presence of multiple bands in hENT2 immunoblots has been reported previously [69,70] and may have been a result of proteolysis during preparation. Despite the presence of mRNA transcripts for hCNT2 in the hRPTC cultures that were analyzed, no hCNT2 immunostaining was detected in any of the crude membrane preparations, indicating that hCNT2 was either not present or was below the limits of resolution of the assay. Single bands for hCNT3 migrating at 90 kDa were detected in immunoblots of hRPTC crude membranes, indicating the presence of hCNT3.

The results of the experiments of Figures IV-1,2 established that the NT mRNA and proteins that were detected in hRPTCs corresponded well with those that were detected in human kidney cortex tissues in similarly conducted experiments of Chapter III. Therefore, adherent cultures of hRPTCs were used as a model system to further study the functional roles of kidney hENTs and hCNTs in renal handling of nucleosides and nucleoside analogs.

IV.2.3 Relative hCNT3 mRNA expression and protein abundance in hRPTCs

The presence of hENT1 and hCNT3 proteins in apical brush border membranes of proximal tubules in human kidney tissues shown in the experiments of Chapter III suggested involvement of hCNT3 in nucleoside reabsorption from the proximal tubule lumen and of hENT1, which was not detected in basolateral membranes, in nucleoside secretion into the proximal tubule lumen. Additionally, the presence of functional hENT1, hENT2, and hCNT3 was demonstrated in hRPTCs from a single individual by measuring uridine, thymidine, and inosine transport under a variety of diagnostic conditions (Chapter III, Section III.2.3.4), suggesting that hCNT3 is the main contributor to nucleoside reabsorption in proximal tubules. The development of separate cultures of hRPTCs from kidneys of ten different individuals (hRPTC1 through hRPTC10, Table II-1) enabled assessment of variability in hCNT3 mRNA expression levels, protein abundance, and transport activities in cultures from a group of genetically different individuals, as well as relationships between these parameters among heterogeneous hRPTC cultures.

Transcript levels for hCNT3, determined by TaqMan™ quantitative RT-PCR as described in Materials and Methods (Section II.8), varied over a 16-fold range (p values < 0.01) between the different hRPTCs (Table IV-1). The relative abundance of hCNT3 protein was determined in crude membrane preparations (total hCNT3 protein abundance) and cell surface protein preparations by immunoblotting analysis as described in Materials and Methods (Section II.9). Total and cell surface hCNT3 protein abundance varied over 13- and 35-fold ranges, respectively (p values < 0.01) between the ten different hRPTC cultures (Table IV-1), and there was a modest positive correlation between hCNT3 total and cell surface protein abundance for the different hRPTC cultures (Figure IV-5B; r^2 0.5674, $p < 0.05$). However, there was no correlation between relative hCNT3 mRNA levels and either hCNT3 total or cell surface protein abundance for the different hRPTC cultures (Figure IV-5A; r^2 0.0529 and 0.1003, respectively).

IV.2.4 Characterization of hENT and hCNT activities in monolayer cultures of hRPTCs

The results of the transport experiments of Chapter III demonstrated hENT1, hENT2, and hCNT3 activities in cultures from a single individual (hRPTC1). Since cell surface protein abundance of hCNT3 varied significantly between hRPTC cultures from ten different individuals, experiments were undertaken to determine if relative hNT activities also varied. Uptake of radiolabeled nucleosides into hRPTCs was monitored over time in sodium-containing buffers or sodium-free buffers in the presence or absence of potential inhibitors to functionally dissect the hNT processes present as described previously for monolayer cultures of HK-2 cells (Section III.2.2.3) and hRPTC1 (Section III.2.3.4). Because uridine is a permeant of hENT1/2 (Table I-1) and hCNT1/2/3 (Table I-3), thymidine is a permeant of hCNT1/3 (Table I-3), and inosine is a permeant of hCNT2/3 (Table I-3), uptake studies were performed with radiolabeled uridine in the presence or absence of excess unlabeled uridine (10 mM), thymidine (1 mM), and inosine (1 mM). Because hENT1/2 are sodium independent and hCNT1/2/3 are sodium dependent, uptake studies were performed in sodium-containing or sodium-free buffers. Because hENT1/2 are dilazep-sensitive and hENT1 is NBMPR-sensitive (Table I-2), uptake studies were performed in sodium-containing or sodium-free buffer in the presence or absence of 200 μM dilazep and 0.1 μM NBMPR. Linearity of uridine uptake was previously demonstrated in preliminary experiments conducted with hRPTC1 cultures in which uptake was measured for 1 min at five-sec intervals (Chapter III, Figure III-11A).

Results for uptake of 1 μM [^{3}H]-uridine into monolayer cultures of hRPTC1 under various experimental conditions are shown in the bar graphs of Figure IV-3A, which is derived from the uptake results shown in Figure III-11. Uptake of [^{3}H]-uridine in sodium-containing buffer was inhibited almost completely in the presence of excess (10 mM) non-radiolabeled uridine, indicating that uridine uptake was primarily mediated (Figure IV-3A). Dilazep, when present in sodium-containing buffer at a concentration (200 μM) that inhibits both hENT1 and hENT2 activities, increased uridine uptake ($p < 0.01$) Figure IV-3A), a result that can be explained by the inhibition of uridine efflux through bidirectional hENTs while still allowing uptake via unidirectional hCNTs. Uptake of [^{3}H]-uridine in sodium-free buffer was lower than in sodium-containing buffer ($p < 0.01$) and could be further reduced by 200 μM dilazep to levels observed in the presence of 10 mM non-radiolabeled uridine (Figure IV-3A), indicating the presence both of hCNT- and hENT-mediated uptake processes. Uptake of [^{3}H]-uridine in sodium-free buffer was only partially inhibited by NBMPR at 0.1 μM (Figure IV-3A), a concentration that inhibits hENT1 but not hENT2 (Table I-2), indicating the presence of both hENT1- and hENT2-mediated uptake processes. It is likely that the transport experiments shown in Figure IV-3 assessed primarily apical NT activities since hRPTCs grown as confluent adherent cultures had differentiated into polarized monolayers (Chapter V, Section V.2.1).

To compare hENT1-, hENT2-, and hCNT3-mediated uptake activities in the ten different hRPTC cultures, uptake of 1 μM [^{3}H]-uridine was monitored over 10 min under conditions that allowed estimation of hNT activities as described for hRPTC1 (see Figure IV-3A; Materials and Methods; Section II.5). The procedure was as follows: (i) hCNT3-mediated activities were obtained by subtracting non-mediated uptake values (in the presence of excess non-radiolabeled uridine, 10 mM) from those in sodium-containing buffer with 200 μM dilazep; (ii) hENT2-mediated activities were obtained by subtracting non-mediated uptake values from those in sodium-free buffer with 0.1 μM NBMPR; and (iii) hENT1-mediated uridine uptake activities were obtained by subtracting hENT2-mediated and non-mediated uptake values from total uptake values in sodium-free buffer. hENT1 activities (Figure IV-3B) varied over 16-fold (p values < 0.01), hENT2 activities (Figure IV-3C) varied over 4-fold (p values < 0.01), and hCNT3 activities (Figure IV-3D) varied over 30-fold (p values < 0.01). Results for hCNT3 activities in different hRPTCs are summarized in Table IV-1.

While positive correlations were found between hCNT3 activities and relative cell surface or total hCNT3 protein abundance in each of the ten different hRPTC cultures (Figure IV-5C; Table IV-1) as expected (r^2 0.9439, $p < 0.0001$ and r^2 0.6191, $p < 0.01$), no correlation was found between hCNT3 activities and relative hCNT3 mRNA transcript levels (r^2 0.0326). hENT1 and hENT2 activities tended to be relatively low compared to hCNT3 activities (Figures IV-3B-D, p values < 0.01), suggesting that hCNT3 was the major contributor to nucleoside uptake.

Despite the lack of significant correlation between relative hCNT3 mRNA levels and either total or cell surface protein abundance or hCNT3 activities in the different hRPTC cultures, some with relatively high hCNT3 mRNA levels also exhibited relatively high hCNT3 total and cell surface protein abundances and activities, (*e.g.*, hRPTC3, 8, and 5, Table IV-1, Figure IV-5A) and others with relatively low hCNT3 mRNA levels also exhibited relatively low hCNT3 total and cell surface protein abundances and hCNT3 activities (*e.g.*, hRPTC4 and 10, Table IV-1, Figure IV-5A). Additionally, although there was a significant positive correlation between relative hCNT3 total and cell surface protein abundances and hCNT3 activities, some cultures with relatively high hCNT3 total protein abundances had relatively low hCNT3 cell surface protein abundance and hCNT3 activities (*e.g.*, hRPTC6, Table IV-1, Figure IV-5B,C). These results suggested that there are multiple levels of regulation for hCNT3 in different hRPTC cultures — *e.g.*, mRNA transcription, protein translation, and export to the plasma membrane.

IV.2.5 Fludarabine uptake into hRPTCs

Since fludarabine is a permeant of hCNT3 [43], the observed variations in the abundance of hCNT3 protein and activities in hRPTC cultures from different individuals grown under identical conditions suggested that its uptake would vary correspondingly. Fludarabine, which is widely used clinically, exhibits considerable inter-patient variability in renal elimination and normal tissue toxicities [24]. Therefore, uptake of [^{3}H]-fludarabine in sodium-containing buffer over 10 min was monitored in the ten different cultures (hRPTC1 through hRPTC10, Table II-1) at 1 μM (Section II.5), since this concentration is observed during the terminal elimination phase of fludarabine in patients [24].

Total cellular uptake of 1 μM [^{3}H]-fludarabine was almost completely inhibited in the presence of 10 mM non-radiolabeled uridine (Figure IV-4A), indicating that fludarabine uptake was primarily mediated. The component of total fludarabine uptake that was mediated was calculated by subtracting non-mediated uptake observed in the presence of 10 mM non-radiolabeled uridine from total cellular uptake for each of the ten different hRPTCs and the results are summarized in Table IV-1. The average values of mediated uptake of fludarabine among the different hRPTC cultures were significantly different (p values < 0.01) (Figure IV-4A, Table IV-1) and correlated positively with estimated hCNT3 activities, also shown in Table IV-1 and Figure IV-5D (r^2 0.9534, $p < 0.0001$), suggesting that hCNT3 was a primary determinant of fludarabine handling by hRPTCs.

To further study relationships between hCNT3 activities and fludarabine uptake, concentration-dependent fludarabine inhibition of uptake of [^{3}H]-uridine, which is a permeant of hENT1, hENT2 and hCNT3, was assayed in the ten different hRPTC cultures under conditions for which these hNTs were all functional (Figure IV-4B shows results for hRPTC2 cultures). Fludarabine inhibited uptake of 1 μM [^{3}H]-uridine in a dose-dependent fashion and the concentrations resulting in 50% inhibition of mediated uridine uptake (IC_{50} values), which were determined by non-linear regression, ranged from 12 μM to 142 μM (Table IV-1 summarizes results for the ten cultures). Because the three hNTs exhibited different activities in the various hRPTC cultures (probably reflecting different relative NT quantities), the IC_{50} values provided a rough measure of the composite "apparent affinities" of the hNTs for fludarabine, with the lowest IC_{50} values representing the highest composite apparent affinities. The composite apparent affinity of a particular culture would be expected to be most influenced by that of the hNT present in greatest abundance (i.e., with the greatest activity) in plasma membranes. A positive correlation was found between mediated fludarabine uptake values and IC_{50} values for fludarabine inhibition of uridine uptake (Table IV-1, Figure IV-5E) (r^2 0.9831, $p < 0.0001$).

IV.2.6 Fludarabine cytotoxicity to hRPTCs

The relationship between fludarabine uptake and cytotoxicity was also assessed. Fludarabine cytotoxicity, which was investigated by the MTS assay in hRPTC cultures exposed to graded concentrations of fludarabine over 72-hr periods as described in Materials and Methods (Section II.10), showed dose-dependent cell killing (Figure IV-4C shows results for hRPTC2 cultures and Table IV-1 summarizes results for the ten different hRPTC cultures). The fludarabine concentrations that killed 50% of cells relative to untreated control cultures (EC_{50} values) ranged from 40 to > 200 μM. Cultures used in these experiments were non-dividing and had been confluent for five to seven days as described in Materials and Methods (Sections II.3 and II.10).

A modest negative correlation between mediated fludarabine uptake values and sensitivities to fludarabine cytotoxicity (EC_{50} values) was found (Figure IV-4D, Table IV-1) (r^2 0.7356, $p < 0.01$). Closer analysis of the data revealed that the different hRPTC cultures fell into two clusters: (i) those with lower sensitivities to fludarabine cytotoxicity (EC_{50} values, 80 to > 200 μM) and lower mediated fludarabine uptake values (1.3 to 1.9 pmol/10min/10^6cells) (Figure IV-D,); and (ii) those with higher sensitivities to fludarabine cytotoxicity (EC_{50} values, 40 to 52 μM) but also higher mediated fludarabine uptake values (3.0 to 5.4 pmol/10min/10^6cells) (Figure IV-D).

IV.3 Discussion.

Empirical dosing methodologies currently in use for chemotherapeutic nucleoside analogs do not take into account interpatient variabilities in tumor response, drug metabolism, or drug elimination. Individually tailored dosing regimens that consider these factors would greatly benefit patient treatment. This study focused on understanding variabilities in renal elimination of the nucleoside analog fludarabine by examining NTs in normal human renal epithelial cells grown *in vitro*. Cultures of human renal proximal tubule primary cells, termed hRPTCs, were isolated from ten individuals (hRPTC1 through hRPTC10, Table II-1) and their *in vitro* NTs were characterized at mRNA, protein, and activity levels, respectively, by RT-PCR of total RNA, immunoblotting of crude membrane and cell surface protein preparations, and whole cell radiolabeled nucleoside uptake experiments. Although all ten hRPTC cultures exhibited hENT1, hENT2, and hCNT3 mRNA, protein, and cell surface activities, the magnitude of these parameters differed significantly between cultures derived from different individuals. hCNT3 total and cell surface protein and transport activities correlated positively with mediated uptake of fludarabine, indicating that hCNT3 was an important determinant of fludarabine uptake in hRPTCs. The authors of a recent report of studies in renal epithelial cell lines transfected with cDNA encoding hCNT3 made a similar case for hCNT3 as a determinant of transepithelial fluxes of nucleoside analogs [60].

The presence of hENT1, hENT2, and hCNT3 mRNA, protein, and transport activities in hRPTCs fits well with current models of renal nucleoside handling

[57]. Because proximal tubules are the main sites of reabsorption of solutes in nephrons, both hENTs and hCNTs in hRPTCs are likely to be involved in transepithelial vectorial fluxes in a reabsorptive direction. The high levels of hENT1 and hCNT3 activities and low levels of hENT2 activities observed in hRPTCs suggested that hENT1 and hCNT3 are the primary luminal hNT activities in proximal tubule cells. This is consistent with the results of the localization studies of hENT1 and hCNT3 in fixed human kidney tissues described in Chapter III – i.e., that hENT1 and hCNT3 are localized to brush border membranes of proximal tubules.

While earlier studies in human brush border membrane vesicles identified an activity now known to be hCNT1-like [53], no hCNT1 activities were identified in any of the hRPTC cultures in experiments reported in this chapter. The results suggested that hCNT3 is the predominant hCNT in human renal proximal tubules. The ability of hCNT3 to utilize the sodium gradient to a greater extent than hCNT1 or hCNT2 (2:1 versus 1:1 sodium-to-nucleoside coupling ratio) [37-40] to drive uphill transport of nucleosides and to also utilize the proton gradient [41] fits with the finding of hCNT3 being the major renal hCNT driving reabsorption of nucleosides from the acidic proximal tubular lumen.

There was no correlation between relative hCNT3 mRNA levels and either hCNT3 total or cell surface protein abundance in the different hRPTC cultures. In proliferating versus differentiated HL-60 cells, a 17-fold range of hCNT3 mRNA expression was demonstrated and was accompanied by corresponding absence and presence of hCNT3 activities [40]. In contrast, a positive correlation between hCNT3 total and cell surface protein abundance and hCNT3 activities was observed in the current work, suggesting that hCNT3 cell surface levels and activities are determined by total hCNT3 protein levels in hRPTCs. hRPTC cultures will be a useful model system to further explore regulation of hCNT3 mRNA expression, protein abundance, and activities.

A central question that is raised by the results described in this chapter is why hNT cell surface abundance varied between different hRPTC cultures. Single nucleotide polymorphisms (SNPs) in hNTs have been investigated previously as a source of inter-individual differences in NT activities. Two SNPs identified for hCNT1 and hCNT3 have direct effects on their activities in recombinant expression systems [71]; however, their low prevalence discounts them as plausible explanations for the observed differences in hNT activities in the different hRPTC cultures assayed. Rather, differences in regulatory protein abundances or activities that effect transcriptional, translational, and/or post-translational regulation of hNTs may be responsible for the observed variations of transport. Although it is possible that the observed differences may have been a result of different growth states of the various cultures, this is unlikely as care was taken to ensure that all experiments were performed on non-proliferating cells (*i.e.*, cells had been confluent for five to seven days, Section II.3). Previous studies have identified significant variations in abundance of other transporters between different hRPTC cultures, namely the organic cation transporters [61].

Since fludarabine, and other nucleoside analogs, undergo primarily renal elimination, hNT levels in human kidney epithelial cells may determine total systemic exposures to these drugs and hence efficacy and normal tissue toxicities. Interpatient heterogeneity in renal hCNT3 abundance, and therefore activity, may have profound effects on the extent of fludarabine luminal uptake and hence fludarabine reabsorption. Patients with relatively higher renal hCNT3 activities may experience higher fludarabine systemic exposures and therefore, different tumor responses and normal tissue toxicities.

Renal epithelial cells, being effectors of transporter-mediated reabsorption and secretion in kidneys, are likely exposed continuously to cytotoxic xenobiotics. As such, hRPTCs are expected to be relatively more resistant to cytotoxic drugs such as fludarabine than other epithelial tissues, although fludarabine cytotoxicity to the various hRPTCs ranged from 40 to 100 μM. While peak plasma concentrations of fludarabine observed in patients undergoing fludarabine treatment are lower (3 μM) than the observed EC_{50} values for fludarabine cytotoxicity to hRPTC cultures, persistent low plasma concentration of free drug (<0.1 μM; 24-72 hr) have been observed [24]. Because kidneys filter blood plasma volume several times over in 24 hr, the continuous exposure of kidney epithelial cells to even low plasma concentration of fludarabine may lead to significant accumulation of fludarabine 5'-triphosphate levels in kidney proximal tubule cells. Additionally, the range of peak plasma concentrations of fludarabine in renally challenged patients may be much higher than in normal patients.

Sensitivity to fludarabine cytotoxicity against hRPTC cultures, as assessed by EC_{50} values of concentration-effect curves, was positively correlated, albeit weakly, to mediated uptake of fludarabine, hCNT3 activities and cell surface protein abundance. The different hRPTC cultures comprised two groups with differing fludarabine transportabilities and sensitivities to cytotoxicity. The first group exhibited lower uptake and sensitivity to fludarabine cytotoxicity, while the second group exhibited higher, although varied, uptake and higher sensitivity to cytotoxicity. The first group appeared to be relatively more resistant to fludarabine because of lower hCNT3 activities, resulting in lower fludarabine uptake, than the second group. Within the second group, the various hRPTC cultures exhibited similar sensitivities to fludarabine despite different hCNT3 activities, which could be explained by cytotoxicity being a multi-step process, with permeation through NTs being the first step and intracellular activation by kinases being subsequent steps. Notably, fludarabine has been shown to be cytotoxic to non-proliferating plasma cells by virtue of DNA repair inhibition [21], which is consistent with the observed cytotoxicity of fludarabine to non-proliferating hRPTCs. Precedent for interpatient variations in hENT1 abundance comes from hENT1 immunohistochemical studies in primary breast cancers, non-Hodgkin's lymphoma, and primary pancreatic cancers and in hCNT3 abundance in chronic lymphocytic leukemia, in which hENT1 and hCNT3 staining intensities varied significantly and independently of pathological and clinical features [62-68].

While the work described in this chapter assessed the contribution of NT-mediated uptake to fludarabine cytotoxicity in hRPTCs, it is well established that cellular uptake is only the first step in pathways leading to nucleoside analog cytotoxicity. Conversion of fludarabine to its monophosphate, diphosphate, and triphosphate forms by intracellular kinases, most notably its monophosphate form by deoxycytidine kinase is the second step in the uptake pathway leading to fludarabine cytotoxicity to normal and cancerous cells [72]. It is likely that the intracellular levels of fludarabine 5'-triphosphate, the cytotoxic form of fludarabine which inhibits ribonucleotide reductase and DNA synthesis [24], that are achieved in cultures of hRPTCs, are also be primary determinants of fludarabine cytotoxicity to hRPTCs.

A positive correlation was observed between fludarabine-mediated uptake and IC_{50} values for concentration-dependent fludarabine inhibition of radiolabeled uridine uptake. The latter provided a rough measure of the composite apparent affinities of the NTs of the various hRPTC cultures for fludarabine, with lower values representing higher affinities. The apparent affinity of hENT1 for fludarabine is higher than its apparent affinity for uridine (K_m values, 107 versus 250 μM, respectively), whereas the apparent affinity of hCNT3 for fludarabine is lower than its apparent affinity for uridine (K_m values, 353 versus 20 μM, respectively) [30,40,43]. Although hENT2 is known to transport fludarabine [43], the K_m value for fludarabine interaction with hENT2 has not been reported. The composite apparent affinities for fludarabine of individual hRPTC cultures, which exhibited different levels of hENT1, hENT2, and hCNT3 activities, were due to the relative levels of these activities and their individual affinities for fludarabine. As hCNT3 was the dominant contributor to fludarabine uptake in hRPTCs and the affinity of hCNT3 for fludarabine is less than that of hENT1, the composite apparent affinity for fludarabine was expected to decrease (*i.e.*, increased IC_{50}

values) as hCNT3 activity increased. Additionally, there is no *a priori* relationship between affinity and total cellular accumulation in physiological milieus, because total cellular accumulation will depend upon a combination of affinity, turnover number, and total cell surface abundance of transporter.

In summary, hENT1, hENT2, and hCNT3 were present in hRPTC cultures, a differentiated model system of proximal tubules, and hCNT3 was shown to be an important determinant of fludarabine uptake and toxicity. The experiments described in this chapter established monolayer cultures of hRPTCs as an excellent model system for studying roles of multiple transporters in proximal tubular handling of nucleosides and nucleoside analogs. An understanding of determinants of individual patient differences in renal elimination of nucleoside analogs could lead to methods for individualizing chemotherapy regimens and improving patient treatment.

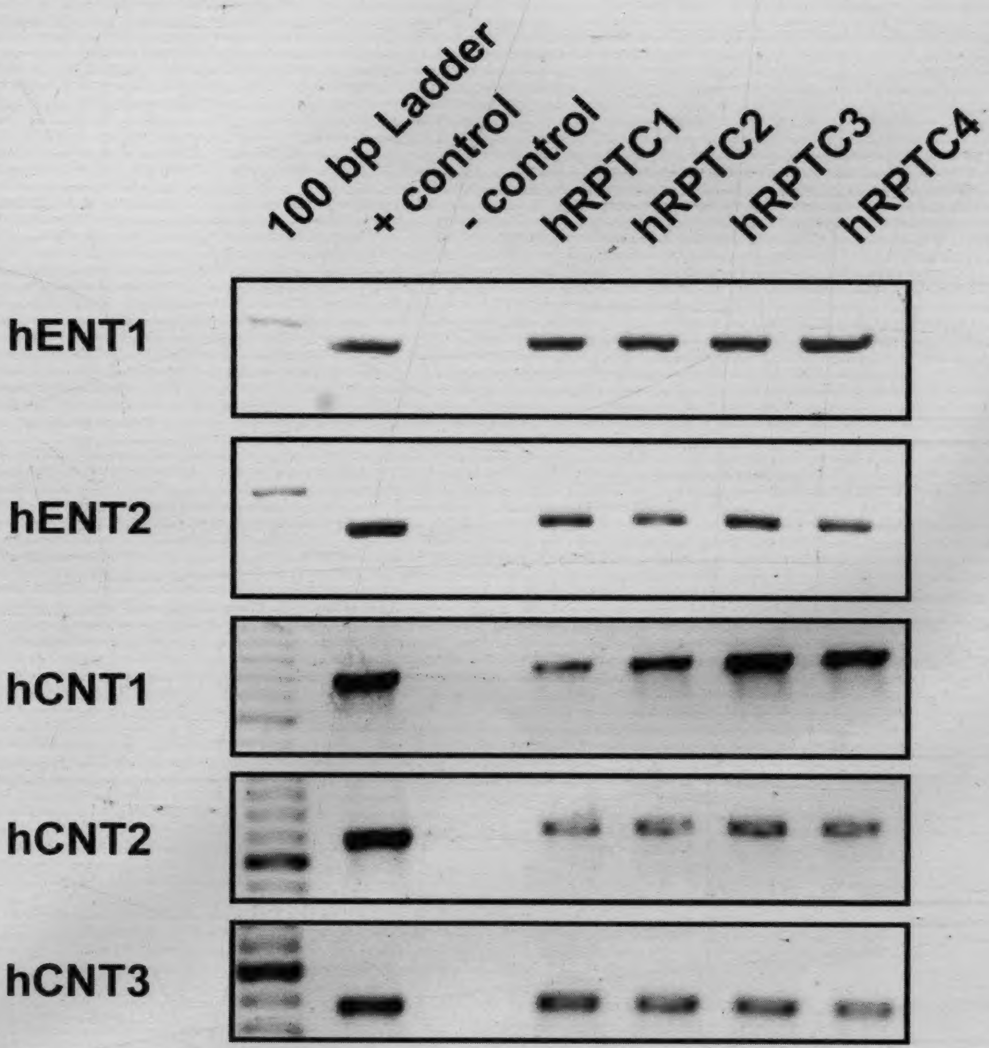
100 bp Ladder
+ control
- control
hRPTC1
hRPTC2
hRPTC3
hRPTC4
hENT1
hENT2
hCNT1
hCNT2
hCNT3

Figure IV-1. Demonstration of hENT1, hENT2, hCNT1, hCNT2, and hCNT3 mRNAs in hRPTCs. Transcripts were assessed by RT-PCR analysis using gene-specific primers in total RNA preparations isolated from different hRPTC cultures as described in Materials and Methods (Section II.8). Positive controls (+) consisted of plasmid DNA with the indicated hNT cDNA insert and negative controls (-) consisted of plasmid without insert.

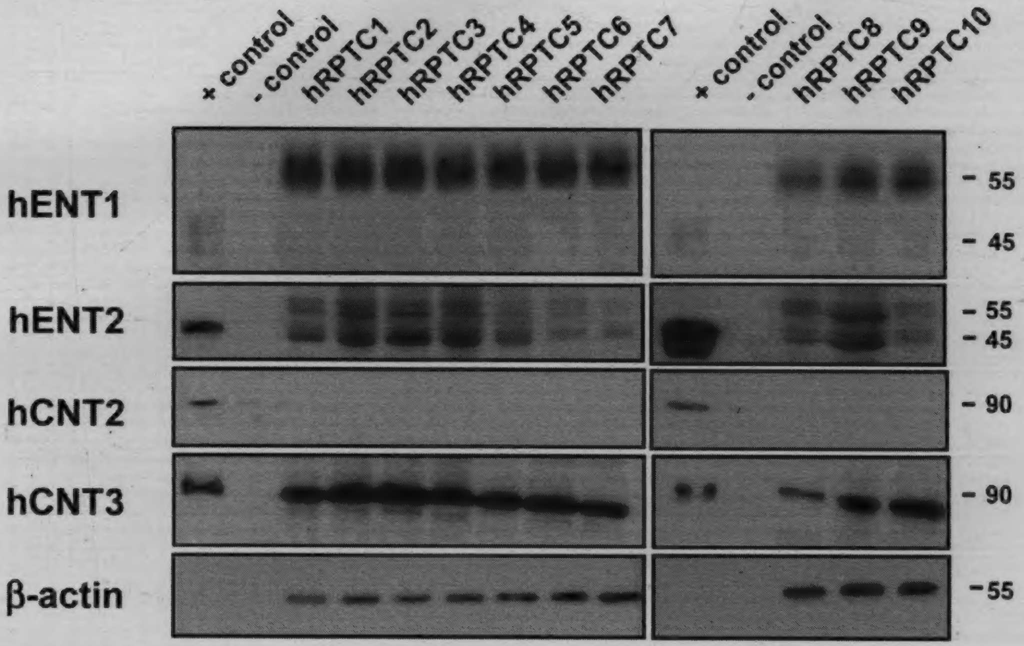
+ control
- control
hRPTC1
hRPTC2
hRPTC3
hRPTC4
hRPTC5
hRPTC6
hRPTC7
+ control
- control
hRPTC8
hRPTC9
hRPTC10
hENT1
hENT2
hCNT2
hCNT3
β-actin
- 55
- 45
- 55
- 45
- 90
- 90
-55

Figure IV-2. Demonstration of hENT1, hENT2, and hCNT3, but not hCNT2, proteins in crude membrane preparations of hRPTCs. hENT1, hENT2, hCNT2, and hCNT3 proteins were assessed by immunoblotting using anti-hNT specific monoclonal antibodies in membrane preparations isolated from each of ten different adherent cultures of hRPTCs (hRPTC1 through hRPTC10, Table II-1) as described in Materials and Methods (Section II.9). Positive controls (+) consisted of crude membrane preparations from yeast transfected with plasmids that contained the indicated hNT cDNA insert and negative controls (-) consisted of crude membrane preparations from yeast transfected with plasmids without inserts. Bands were visualized using horseradish peroxidase conjugated anti-mouse IgG antibodies and enhanced chemiluminescence. Gel mobilities in kDa are denoted by the dashes and numbers beside each immunoblot.

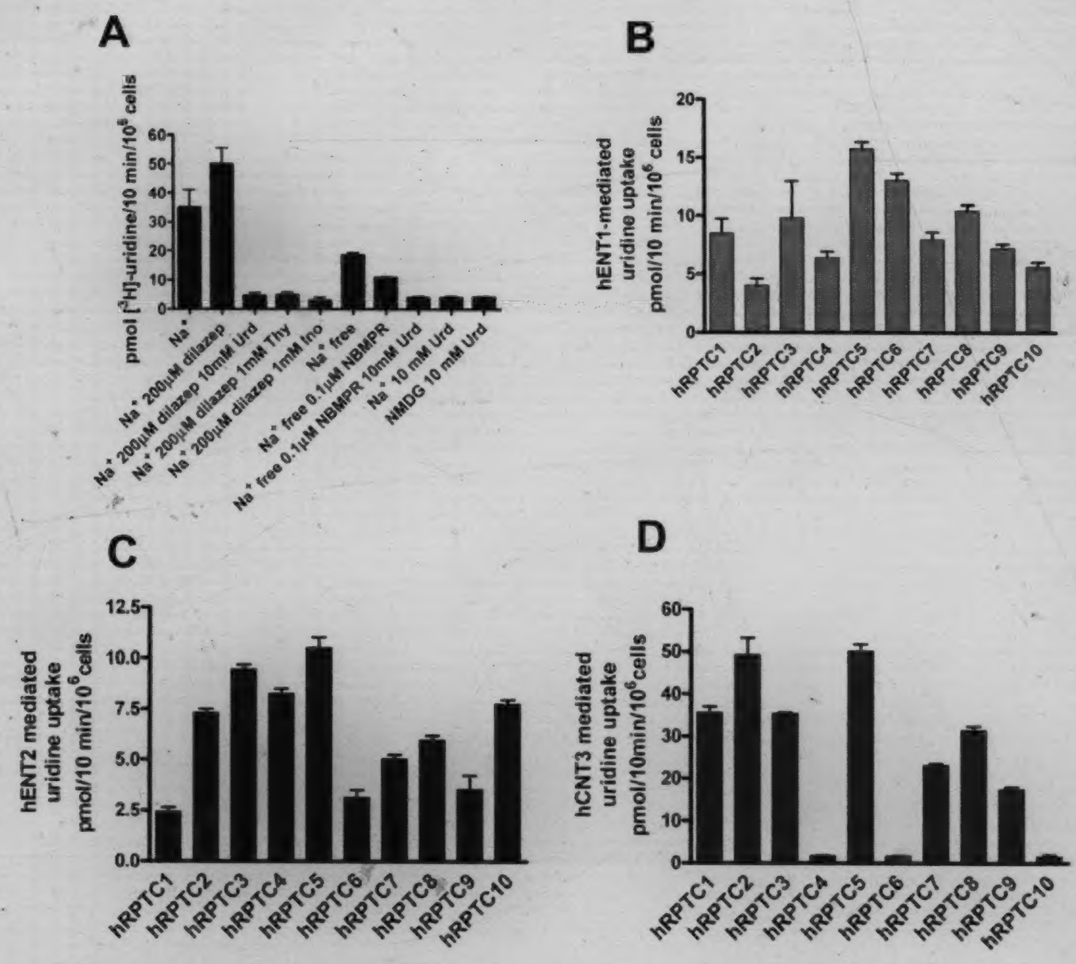

Figure IV-3. hRPTCs exhibit hENT1-, hENT2-, and hCNT3-mediated uptake activities. (A) Values obtained for uptake of 1 μM [^{3}H]-uridine into hRPTC1 cultures in sodium-containing and sodium-free buffers with and without various NT inhibitors (see Figure III-11) were used to calculate NT activities as described in Materials and Methods (Section II.5). A similar approach was used for the other nine hRPTC cultures and results for all ten cultures (hRPTC1 through hRPTC10, Table II-1) are shown for (B) hENT1-, (C) hENT2-, and (D) hCNT3-mediated uridine uptake. Values are means (± standard deviations) of three independent experiments each with triplicate measurements. Samples for which error bars are apparently absent had errors equal or smaller than the border size of the bars.

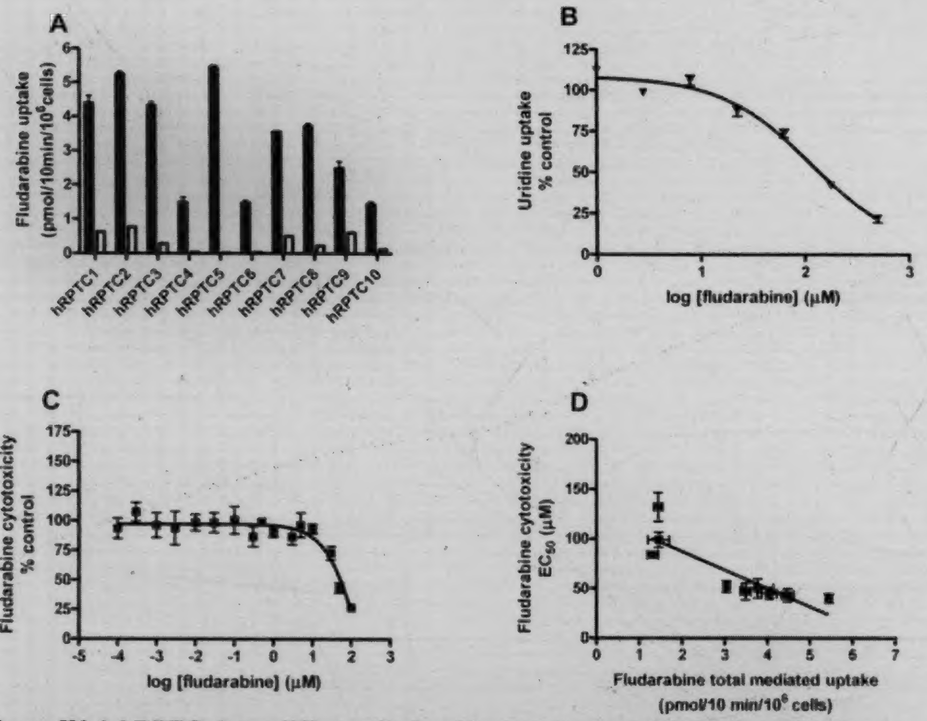

Figure IV-4. hRPTCs have different fludarabine uptake capacities and sensitivities to fludarabine cytotoxicity. (A) Uptake of 1 μM [^{3}H]-fludarabine into hRPTC1 through hRPTC10 cultures (Table II-1) after 10-min exposures in sodium-containing buffer (solid bars) or sodium-containing buffer with 10 mM non-radiolabeled uridine (open bars). (B) Inhibition of 1 μM [^{3}H]-uridine uptake into cultures of hRPTC2 by fludarabine. (C) Cytotoxicities of fludarabine against hRPTC2. (D) Correlation of total mediated fludarabine uptake and sensitivities to fludarabine cytotoxicity in the ten different hRPTC cultures (r^2 0.7356, $p < 0.01$). Uptake of 1 μM [^{3}H]-uridine after 10-min exposures was monitored as described in Materials and Methods (Section II.5) in the presence or absence of fludarabine (1.0, 2.9, 7.9, 22.4, 63.0, 177.5, and 500.0 μM) in sodium-containing buffer with or without 10 mM uridine. Uridine uptake values in the presence of fludarabine for hRPTC2 are expressed as % of values in its absence, correcting all values for non-mediated uptake in the presence of 10 mM uridine. Cultures of hRPTC2 were incubated for 72-hr in the presence or absence of fludarabine (0.0001, 0.0003, 0.001, 0.003, 0.01, 0.03, 0.1, 0.3, 0.5, 1, 3, 5, 10, 30, 50, 100 μM), and cytotoxicities were determined using the MTS assay as described in Materials and Methods (Section II.10). Cytotoxicity values are absorbance at 490 nM of cultures treated with various fludarabine concentrations expressed as a percentage of absorbance of untreated cells. The IC_{50} value in (B) was 122 ± 12 μM for fludarabine inhibition of [^{3}H]-uridine uptake and the EC_{50} value in (C) was 43 ± 10 μM for fludarabine cytotoxicity, both calculated from non-linear regression analysis of sigmoidal dose-response curves. Similar experiments were conducted for the other nine hRPTC cultures and IC_{50} (uptake capacities) and EC_{50} (cytotoxicity sensitivities) values are given in Table IV-1. Values shown in (A), (B), (C), and (D) are means (± standard deviations) of three independent experiments each with triplicate measurements. Samples for which error bars are apparently absent had errors equal to or smaller than the border sizes of the bars or points.

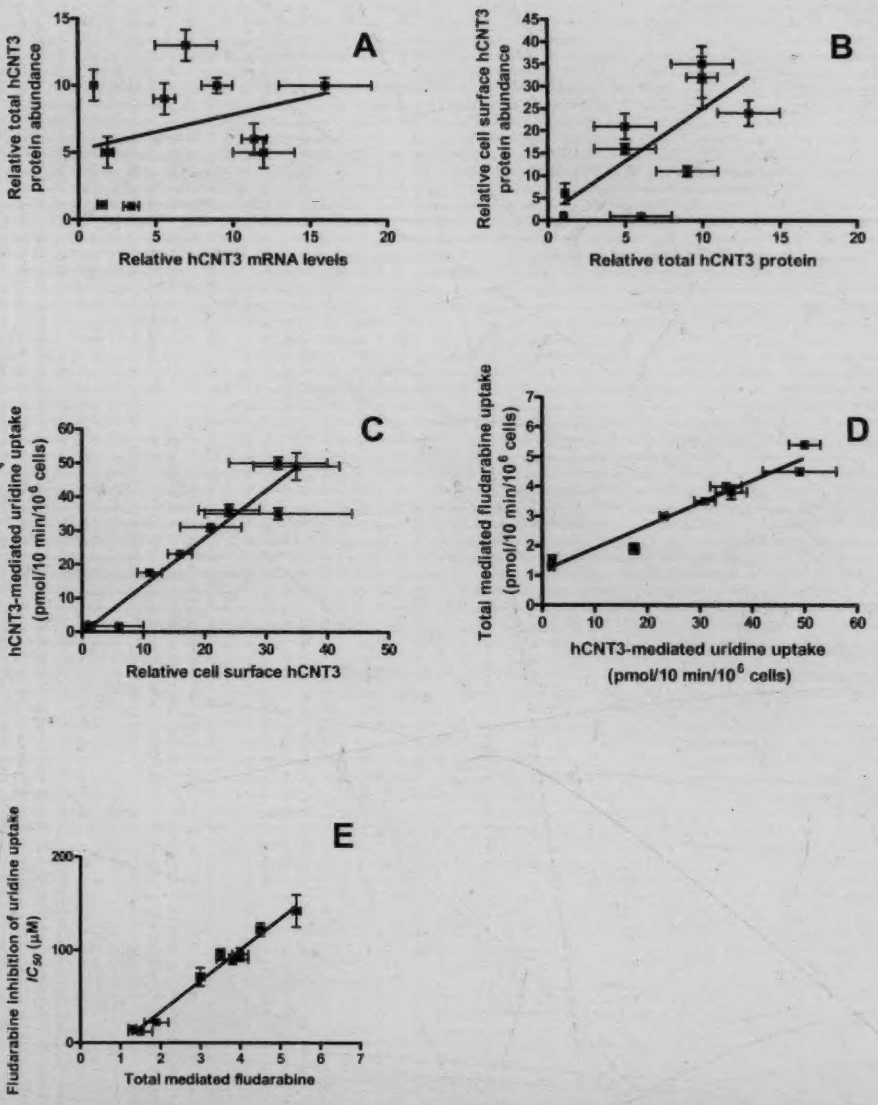

Figure IV-5. Correlation of hCNT3 relative mRNA levels, total protein abundance levels, cell surface protein abundance levels, hCNT3 activity levels, fludarabine uptake levels, fludarabine apparent affinities, and sensitivities to fludarabine cytoxicity in hRPTCs. Experimentally determined values in hRPTCs were obtained as described in Table IV-1. Correlations for experimentally determined values in hRPTCs are plotted: for hCNT3 relative mRNA levels (see Section II.8) versus hCNT3 relative total protein abundance levels (Section II.9) in (A) (r^2 0.0529); for hCNT3 relative total protein abundance levels versus hCNT3 relative cell surface protein abundance (Section II.8) in (B) (r^2 0.5674, $p < 0.05$); for hCNT3 relative cell surface protein abundance versus hCNT3-mediated uridine uptake (Section II.5) in (C) (r^2 0.9439, $p < 0.0001$); for hCNT3-mediated uridine uptake (Section II.5) versus total mediated fludarabine uptake (see Section II.5) in (D) (r^2 0.7356, $p < 0.01$); and for total mediated fludarabine uptake versus IC_{50} value for fludarabine inhibition of uridine uptake (Section II.5) in (E) (r^2 0.9831, $p < 0.0001$). Correlation analysis was done by Pearson's correlation analysis (Section II.11).

Table IV-1. Summary of hCNT3 protein levels, hCNT3 activities, fludarabine uptake capacities (IC_{50} values for fludarabine inhibition of [^{3}H]-uridine uptake), and fludarabine cytotoxicities (EC_{50} values for fludarabine cytotoxicities) in hRPTCs.

Culture	Relative hCNT3 mRNA levels[§]	Relative total hCNT3 protein abundance[*]	Relative cell surface hCNT3 protein abundance[*]	hCNT3-mediated uridine uptake (pmol/10min/10^6 cells)[†]	Total mediated fludarabine uptake (pmol/10min/10^6 cells)[$]	Fludarabine inhibition of uridine uptake IC_{50} (µM)[‡]	Fludarabine cytotoxicity EC_{50} (µM)[‖]
hRPTC1	7 ± 2	13 ± 2	24 ± 5	36 ± 3	3.8 ± 0.4	90 ± 9	50 ± 17
hRPTC2	1.01 ± 0.01	10 ± 2	35 ± 7	49 ± 7	4.5 ± 0.1	122 ± 12	43 ± 11
hRPTC3	16 ± 3	10 ± 1	32 ± 12	35 ± 3	4.0 ± 0.2	95 ± 12	45 ± 10
hRPTC4	3.4 ± 0.5	1.0 ± 0.1	1.0 ± 0.1	1.9 ± 0.1	1.5 ± 0.3	12 ± 5	99 ± 13
hRPTC5	9 ± 1	10 ± 1	32 ± 8	50 ± 3	5.4± 0.1	142 ± 30	40 ± 8
hRPTC6	11.4 ± 0.8	6 ± 2	1.0 ± 0.1	1.8 ± 0.1	1.4 ± 0.1	13 ± 3	132 ± 45
hRPTC7	1.9 ± 0.4	5 ± 2	16 ± 2	23.1 ± 0.7	3.0 ± 0.1	71 ± 17	52 ± 10
hRPTC8	12 ± 2	5 ± 2	21 ± 5	31 ± 2	3.5 ± 0.1	95 ± 10	47 ± 15
hRPTC9	5.6 ± 0.7	9 ± 2	11 ± 2	17.5 ± 0.9	1.9 ± 0.3	22 ± 5	> 200
hRPTC10	1.5 ± 0.3	1.1 ± 0.2	6 ± 4	1.7 ± 0.5	1.3 ± 0.1	15 ± 2	84 ± 4

[§] Determined from quantitative TAQMAN® RT-PCR analysis (Section II.8). Means ± standard errors of measurement.

[*] Determined from semi-quantitative western blot analysis (Section II.9). Means ± standard errors of measurement.

[†] Determined from calculated hCNT3 functional activities; see Figure IV-3. Means ± standard deviations.

[$] Determined from radiolabeled fludarabine uptake assays (Section II.5) see Figure IV-4. Means ± standard deviations.

[‡] Determined from fludarabine inhibition of uridine uptake curves (Section II.5); see Figure IV-4. Means ± standard deviations.

[‖] Determined from fludarabine cytotoxicity curves (Section II.10); see Figure IV-4. Means ± standard deviations.

IV.4 Bibliography

1. Plunkett W, Saunders PP. Metabolism and action of purine nucleoside analogs. Pharmacol Ther. 1991; 49: 239-268.

2. Adkins JC, Peters DH, Markham A. Fludarabine. An update of its pharmacology and use in the treatment of haematological malignancies. Drugs. 1997; 53: 1005–1037.

3. Leporrier M, Chevret S, Cazin B, Boudjerra N, Feugier P, Desablens B, Rapp MJ, Jaubert J, Autrand C, Divine M, Dreyfus B, Maloum K, Travade P, Dighiero G, Binet JL, Chastang C; French Cooperative Group on Chronic Lymphocytic Leukemia. Randomized comparison of fludarabine, CAP, and ChOP in 938 previously untreated stage B and C chronic lymphocytic leukemia patients. Blood. 2001; 98: 2319-2325.

4. Hagenbeek A, Eghbali H, Monfardini S, Vitolo U, Hoskin PJ, de Wolf-Peeters C, MacLennan K, Staab-Renner E, Kalmus J, Schott A, Teodorovic I, Negrouk A, van Glabbeke M, Marcus R. Phase III intergroup study of fludarabine phosphate compared with cyclophosphamide, vincristine, and prednisone chemotherapy in newly diagnosed patients with stage III and IV low-grade malignant Non-Hodgkin's lymphoma. J Clin Oncol, 2006; 24: 1590-1596.

5. Tobinai K, Watanabe T, Ogura M, Morishima Y, Ogawa Y, Ishizawa K, Minami H, Utsunomiya A, Taniwaki M, Terauchi T, Nawano S, Matsusako M, Matsuno Y, Nakamura S, Mori S, Ohashi Y, Hayashi M, Seriu T, Hotta T. Phase II study of oral fludarabine phosphate in relapsed indolent B-Cell non-Hodgkin's lymphoma. J Clin Oncol. 2006; 24: 174-180.

6. Malspeis L, Grever MR, Staubus AE, Young D. Pharmacokinetics of 2-F-ara-A (9-beta-D-arabinofuranosyl-2-fluoroadenine) in cancer patients during the phase I clinical investigation of fludarabine phosphate. Sem Oncol. 1990; 17: 18-32.

7. Hutton JJ, Von Hoff DD, Kuhn J, Phillips J, Hersh M, Clark G. Phase I clinical investigation of 9-beta-D-arabinofuranosyl-2-fluoroadenine 5′-monophosphate (NSC 312887), a new purine antimetabolite. Cancer Res. 1984; 44: 4183-4186.

8. Avramis VI, Champagne J, Sato J, Krailo M, Ettinger LJ, Poplack DG, Finkelstein J, Reaman G, Hammond GD, Holcenberg JS. Pharmacology of fludarabine phosphate after a phase I/II trial by a loading bolus and continuous infusion in pediatric patients. Cancer Res 1990;50: 7226-31.

9. Danhauser L, Plunkett W, Keating M, Cabanillas F. 9-β-D-Arabinofuranosyl-2-fluoroadenine 5′-monophosphate pharmacokinetics in plasma and tumor cells of patients with relapsed leukemia and lymphoma. Cancer Chemother Pharmacol. 1996; 18: 145-152.

10. Carson DA, Wasson DB, Kaye J, Ullman B, Martin DW Jr, Robins RK, Montgomery JA. Deoxycytidine kinase mediated toxicity of deoxyadenosine analogs toward human lymphoblasts in vitro and toward murine L1210 leukemia in vivo. Proc Natl Acad Sci USA. 1980; 77: 6865-6869.

11. Plunkett W, Huang P, Gandhi V. Metabolism and action of fludarabine phosphate. Semin Oncol. 1990; 17: 3-17.

12. Brockman RW, Schabel Jr FM, Montgomery JA. Biological activity of 9-β-D-arabinofuranosyl-2-fluoroadenine, a metabolically stable analog of 9-β-D-arabinofuranosyladenine. Biochem Pharmacol. 1977; 26: 2193-2196.

13. Tseng WC, Derse D, Cheng Y-C, Brockman RW, Bennett LL Jr. In vitro activity of 9-β-D-arabinofuranosyl-2-fluoroadenine and the biochemical actions of its triphosphate on DNA polymerases and ribonucleotidereductase from HeLa cells. Mol Pharmacol. 1982; 21: 474-477.

14. White L, Shaddix SC, Brockman RW, et al. Comparison of the actions of 9-β-D-arabinofuranosyl-2-fluoroadenine and 9-β- D-arabinofuranosyladenine on target enzymes from mouse tumor cells. Cancer Res 1982; 42: 2260-4

15. Parker WB, Bapat AR, Shen J-X, Townsend AJ, Cheng YC. Interaction of 2-halogenated dATP analogs (F, Cl, and Br) with human DNA polymerases. DNA primase and ribonucleotide reductase. Mol Pharmacol. 1988; 34: 485-491.

16. Huang P, Chubb S, Plunkett W. Termination of DNA synthesis by 9-β-D-arabinofuranosyl-2-fluoroadenine: a mechanism for cytotoxicity. J Biol Chem 1990; 265: 16617-25

17. Gandhi V, Huang P, Chapman A, Chen F, Plunkett W. Incorporation of fludarabine and 1-β-D-arabinosylcytosine 5′-triphosphates by DNA polymerase α: affinity, interaction, and consequences. Clin Cancer Res. 1997; 3: 1347-55.

18. Chandra D, Bratton SB, Person MD, Tian Y, Martin AG, Ayres M, Fearnhead HO, Gandhi V, Tang DG. Intracellular nucleotides act as critical prosurvival factors by binding to cytochrome C and inhibiting apoptosome. Cell. 2006; 125:1333-1346.

19. Huang P, Plunkett W. Action of 9-β-D-arabinofuranosyl-2-fluoroadenine on RNA metabolism. Mol Pharmacol. 1991; 39: 449-455.

20. Chen LS, Plunkett W, Gandhi V. Polyadenylation inhibition by the triphosphates of deoxyadenosine analogues. Leuk Res. 2008; 32: 1573-1581.

21. Rao VA, Plunkett W. Activation of a p53-mediated apoptotic pathway in quiescent lymphocytes after the inhibition of DNA repair by fludarabine. Clin Cancer Res. 2003; 9: 3204-3212.

22. Gandhi V, Estey E, Keating MJ, Plunkett W. Fludarabine potentiates metabolism of arabinosylcytosine in patients with acute myelogenous leukemia during therapy. J Clin Oncol 1993; 11: 116-124.

23. Borthakur G, Kantarjian H, Wang X, Plunkett WK Jr, Gandhi VV, Faderl S, Garcia-Manero G, Ravandi F, Pierce S, Estey EH. Treatment of core-binding-factor in acute myelogenous leukemia with fludarabine, cytarabine, and granulocyte colony-stimulating factor results in improved event-free survival. Cancer. 2008; 113: 3181-3185.

24. Gandhi V, Plunkett W. Cellular and clinical pharmacology of fludarabine. Clin Pharmacokinet. 2002; 41: 93-103.

25. Hande KR, Garrow GC. Acute tumor lysis syndrome in patients with high-grade non-Hodgkin's lymphoma. Amer J Med. 1993; 94: 133-139.

26. Cairo MS, Bishop M. Tumour lysis syndrome: new therapeutic strategies and classification. Brit J Haematol. 2004; 127: 3-11.

27. Hussain K, Mazza JJ, Clouse LH. Tumor lysis syndrome (TLS) following fludarabine therapy for chronic lymphocytic leukemia (CLL): case report and review of the literature. Am J Hematol. 2003; 72: 212–215.

28. Young JD, Yao SYM, Sun L, Cass CE, Baldwin SA. Human equilibrative nucleoside transporter (ENT) family of nucleoside and nucleobase transporter proteins. Xenobiotica. 2008; 38: 995-1021.

29. Pastor-Anglada M, Cano-soldado P, Errasti-murugarren E, Casado FJ. SLC28 genes and concentrative nucleoside transporter (CNT) proteins. Xenobiotica. 2008; 38: 972-994.

30. Griffiths M, Beaumont N, Yao SY, Sundaram M, Boumah CE, Davies A, Kwong FY, Coe I, Cass CE, Young JD, Baldwin SA. Cloning of a human nucleoside transporter implicated in the cellular uptake of adenosine and chemotherapeutic drugs. Nat Med. 1997; 3: 89-93.

31. Griffiths M, Yao SY, Abidi F, Phillips SE, Cass CE, Young JD, Baldwin SA. Molecular cloning and characterization of a nitrobenzylthioinosine-insensitive (ei) equilibrative nucleoside transporter from human placenta. Biochem J. 1997; 328: 739-743.

32. Crawford CR, Patel DH, Naeve C, Belt JA. Cloning of the human equilibrative, nitrobenzylmercaptopurine riboside (NBMPR)-insensitive nucleoside transporter ei by functional expression in a transport-deficient cell line. J Biol Chem. 1998; 273: 5288–5293.

33. Baldwin SA, Yao SYM, Hyde RJ, Foppolo S, Barnes K, Ritzel MWL, Cass CE, Young JD. Functional Characterization of novel human mouse equilibrative nucleoside transporters (hENT3 and mENT3) located in intracellular membranes. J Biol Chem. 2007; 280: 15880-15887.

34. Barnes K, Dobrzynski H, Foppolo S, Beal PR, Ismat F, Scullion ER, Sun L, Tellez J, Ritzel MW, Claycomb WC, Cass CE, Young JD, Billeter-Clark R, Boyett MR, Baldwin SA. Distribution and functional characterization of equilibrative nucleoside transporter-4, a novel cardiac adenosine transporter activated at acidic pH. Circ Res. 2006; 99: 510-519.

35. Yao SY, Ng AM, Vickers MF, Sundaram M, Cass CE, Baldwin SA, Young JD. Functional and molecular characterization of nucleobase transport by recombinant human and rat equilibrative nucleoside transporters 1 and 2.

Chimeric constructs reveal a role for the ENT2 helix 5-6 region in nucleobase translocation. J Biol Chem. 2002; 277: 24938-24948.

36. Engel K, Zhou M, Wang J. Identification and characterization of a novel monoamine transporter in the human brain. J Biol Chem. 2004; 279: 50042-50049.

37. Ritzel MW, Yao SY, Huang MY, Elliott JF, Cass CE, Young JD. Molecular cloning and functional expression of cDNAs encoding a human Na+ nucleoside cotransporter (hCNT1). Am J Physiol Cell Physiol. 1997; 272: C707– C714.

38. Wang J, Su SF, Dresser MJ, Schaner ME, Washington CB, Giacomini KM. Na+ dependent purine nucleoside transporter from human kidney: cloning and functional characterization. Am J Physiol Renal Physiol. 1997; 273: F1058–F1065.

39. Ritzel MW, Yao SY, Ng AM, Mackey JR, Cass CE, Young JD. Molecular cloning, functional expression and chromosomal localization of a cDNA encoding a human Na+/nucleoside cotransporter (hCNT2) selective for purine nucleosides and uridine. Mol Membr Biol. 1998; 15: 203– 211.

40. Ritzel MW, Ng AM, Yao SY, Graham K, Loewen SK, Smith KM, Ritzel RG, Mowles DA, Carpenter P, Chen XZ, Karpinski E, Hyde RJ, Baldwin SA, Cass CE, Young JD. Molecular identification and characterization of novel human and mouse concentrative Na+ nucleoside cotransporter proteins (hCNT3 and mCNT3) broadly selective for purine and pyrimidine nucleosides (system cib). J Biol Chem. 2001; 276: 2914– 2927.

41. Slugoski MD, Smith KM, Mulinta R, Ng AM, Yao SY, Morrison EL, Lee QO, Zhang J, Karpinski E, Cass CE, Baldwin SA, Young JD. A conformationally mobile cysteine residue (Cys-561) modulates Na+ and H+ activation of human CNT3. J Biol Chem. 2008; 283: 24922-34.

42. Smith KM, Slugoski MD, Cass CE, Baldwin SA, Karpinski E, Young JD. Cation coupling properties of human concentrative nucleoside transporters hCNT1, hCNT2 and hCNT3. Mol Membr Biol. 2007; 24: 53-64.

43. King KM, Damaraju VL, Vickers MF, Yao SY, Lang T, Tackaberry TE, Mowles DA, Ng AM, Young JD, Cass CE. A comparison of the transportability, and its role in cytotoxicity, of clofarabine, cladribine, and

fludarabine by recombinant human nucleoside transporters produced in three model expression systems. Mol Pharmacol 2006; 69: 346-353.

44. Kuttesch JF Jr, Nelson JA. Renal handling of 2'-deoxyadenosine and adenosine in humans and mice. Cancer Chemother Pharmacol. 1982; 8: 221-229.

45. Kuttesch JF Jr, Robins MJ, Nelson JA. Renal transport of 2'-deoxytubercidin in mice. Biochem Pharmacol. 1982; 31: 3387-3394.

46. Nelson JA, Kuttesch JR Jr, Herbert BH. Renal secretion of purine nucleosides and their analogs in mice. Biochem Pharmacol. 1983; 32: 2323-2332.

47. Nelson JA, Vidale E, Enigbokan M. Renal transepithelial transport of nucleosides. Drug Metab. 1988; 16: 789-792.

48. Aiba T, Sakurai Y, Tsukada S, Koizumi T. Effects of probenecid and cimetidine on the renal excretion of 3'-azido-3'-deoxythymidine in rats. J Pharmacol Exp Ther. 1995; 272: 94–99.

49. Chen R, Nelson JA. Role of organic cation transporters in the renal secretion of nucleosides. Biochem Pharmacol. 2000; 60: 215-219.

50. Green H, Chan T-S. Pyrimidine starvation induced by adenosine in fibroblasts and lymphoid cells: role of adenosine deaminase. Sci. 1973; 182: 836-837.

51. Klenow H. Further studies on the effect of deoxyadenosine on the accumulation of deoxyadenosine triphosphate and inhibition of deoxyribonucleic acid synthesis in Ehrlich ascites tumor cells in vitro. Biochim Biophys Acta. 1962; 61: 885-896.

52. Chen R, Jonker JW, Nelson JA. Renal organic cation and nucleoside transport. Biochem. Pharmacol. 2002; 64: 185-190.

53. Gutierrez MM, Brett CM, Ott RJ, Hui AC, Giacomini KM. Nucleoside transport in brush border membrane vesicles from human kidney. Biochim Biophys Acta. 1992; 1105: 1-9.

54. Mangravite LM, Lipschutz JH, Mostov KE, Giacomini KM. Localization of GFP-tagged concentrative nucleoside transporters in a renal polarized epithelial cell line. Am J Physiol Renal Physiol. 2001; 280: F879-885.

55. Lai Y, Bakken AH, Unadkat JD. Simultaneous expression of hCNT1-CFP and hENT1-YFP in Madin-Darby canine kidney cells. Localization and vectorial transport studies. J Biol Chem. 2002; 277: 37711-37717.

56. Mangravite LM, Xiao G, Giacomini KM. Localization of human equilibrative nucleoside transporters, hENT1 and hENT2, in renal epithelial cells. Am J Physiol Renal Physiol. 2003; 284: F902-910.

57. Mangravite LM, Badagnani I, Giacomini KM. Nucleoside transporters in the disposition and targeting of nucleoside analogs in the kidney. Eur J Pharmacol. 2003; 479: 269-281.

58. Xia L, Engel K, Zhou M, Wang J. Membrane localization and pH-dependent transport of newly cloned organic cation transport (PMAT) in kidney cells. Am. J. Physiol. Renal Physiol. 2007; 292: F682-F690.

59. Govindarajan R, Bakken AH, Hudkins KL, Lai Y, Casado FJ, Pasto-Anglada M, Tse CM, Hayashi J, Unadkat JD. In situ hydribdization and immunolocalization of concentrative and equilibrative nucleoside transporters in the human intestine, liver, kidneys, and placenta. Amer J Physiol Reg Int Comp Physiol. 2007; 293: R1809-R1822.

60. Errasti-Murugarren E, Pastor-Anglada M, Casado FJ. Role of CNT3 in the transepithelial flux of nucleosides and nucleoside-derived drugs. J Physiol. 2007; 582: 1249-60.

61. Lash LH, Putt DA, Cai H. Membrane transport function in primary cultures of human proximal tubular cells. Toxicol. 2006; 228: 200-218.

62. Mackey JR, Jennings LL, Clarke ML, Santos CL, Dabbagh L, Vsianska M, Koski SL, Coupland RW, Baldwin SA, Young JD, Cass CE. Immunohistochemical variation of human equilibrative nucleoside transporter 1 in primary breast cancers. Clin Cancer Res 2002; 8: 110-116.

63. Dabbagh L, Coupland RW, Cass CE, Mackey JR. Immunohistochemical variation of human equilibrative nucleoside transporter 1 protein in primary breast cancers. Clin Cancer Res 2003; 9: 3213-3214.

64. Spratlin J, Sangha R, Glubrecht D, Dabbagh L, Young JD, Dumontet C, Cass C, Lai R, Mackey JR. The absence of human equilibrative nucleoside transporter 1 is associated with reduced survival in patients with gemcitabine-treated pancreas adenocarcinoma. Clin Cancer Res 2004; 10: 6956-6961.

65. Chow L, Lai R, Dabbagh L, Belch A, Young JD, Cass CE, Mackey JR. Analysis of human equilibrative nucleoside transporter 1 (hENT1) protein in non-Hodgkin's lymphoma by immunohistochemistry. Mod Pathol. 2005; 18: 558-564.

66. Mackey JR, Galmarini CM, Graham KA, Joy AA, Delmer A, Dabbagh L, Glubrecht D, Jewell LD, Lai R, Lang T, Hanson J, Young JD, Merle-Béral H, Binet JL, Cass CE, Dumontet C. Quantitative analysis of nucleoside transporter and metabolism gene expression in chronic lymphocytic leukemia (CLL): identification of fludarabine-sensitive and -insensitive populations. Blood 2005; 105: 767-774.

67. Farrell JJ, Elsaleh H, Garcia M, Lai R, Ammar A, Regine WF, Abrams R, Benson AB, Macdonald J, Cass CE, Dicker AF, Mackey JR. Human equilibrative nucleoside ransporter 1 levels predict response to gemcitabine in patients with pancreatic cancer. Gastroenterol. 2008 Oct 7 [Epub ahead of print].

68. Tsang RY, Santos C, Ghosh S, Dabbagh L, King K, Young J, Cass CE, Mackey JR, Lai R Immunohistochemistry for human concentrative nucleoside transporter 3 protein predicts fludarabine sensitivity in chronic lymphocytic leukemia. Mod Pathol. 2008; 21: 1387-1393.

69. Ward JL, Sherali A, Mo ZP, Tse CM. Kinetic and pharmacological properties of cloned human equilibrative nucleoside transporters, ENT1 and ENT2, stably expressed in nucleoside transporter-deficient PK15 cells. Ent2 exhibits a low affinity for guanosine and cytidine but a high affinity for inosine. J Biol Chem. 2000; 275: 8375-8381.

70. Vickers MF, Mani RS, Sundaram M, Hogue DL, Young JD, Baldwin SA, Cass CE. Functional production and reconstitution of the human equilibrative nucleoside transporter (hENT1) in *Saccharomyces cerevisiae*. Interaction of

inhibitors of nucleoside transport with recombinant hENT1 and a glycosylation-defective derivative (hENT1/N48Q). Biochem J. 1999; 339: 21-32.

71. Gray JH, Mangravite LM, Owen RP, Urban TJ, Chan W, Carlson EJ, Huang CC, Kawamoto M, Johns SJ, Stryke D, Ferrin TE, Giacomini KM. Functional and genetic diversity of concentrative nucleoside transporter 1, CNT1, in human populations. Mol Pharmacol 2003; 73: 512-519.

72. Carson DA, Wasson DB, Kaye J, Ueda T. Deoxycytidine kinase mediated toxicity of deoxyadenosine analogs toward human lymphoblasts in vitro and toward murine L1210 leukemia in vivo. Proc Natl Acad Sci USA. 1980; 77: 6865-6869.

Chapter V

V. Transepithelial fluxes of adenosine and 2′-deoxyadenosine across polarized cultures of human renal proximal tubule cells (hRPTCs): the roles of human equilibrative and concentrative nucleoside transporters, hENT1, hENT2, and hCNT3[1]

---

[1] An earlier version of this chapter has been published as a primary authored paper [Elwi AN, Damaraju VL, Kuzma ML, Mowles DA, Baldwin SA, Young JD, Sawyer MB, Cass CE. Transepithelial fluxes of adenosine and 2′-deoxyadenosine across polarized cultures of human kidney proximal tubule cells: the roles of human equilibrative and concentrative nucleoside transporters, hENT1, hENT2, and hCNT3. Am J Physiol Renal Physiol in press; contribution of Elwi AN was 90 %.

V.1 Introduction.

Renal proximal tubular handling of various solutes, such as nucleosides [1-3], in the kidney is accomplished by differential distribution of transporters to apical or basolateral surfaces of epithelial cells. Human nucleoside transporters (hNTs) mediate the passage of physiological nucleosides and nucleoside analog drugs across biological membranes [4,5], which comprise two Solute Carrier (SLC) families, human equilibrative NTs (SLC29/hENTs: hENT1/2/3/4), [4,6-9] and human concentrative NTs (SLC28/hCNTs: hCNT1/2/3) [5,10-13]. Coupling of apical hCNT1/2/3, which are Na^+-nucleoside co-transporters with differing permeant selectivities [10-13], to basolateral hENT1/2, which are facilitative transporters with broad selectivities [6,7], is thought to mediate nucleoside reabsorption [14-17], driven by sodium gradients established by basolateral Na^+K^+-adenosine-5′-triphosphatases (Na^+K^+-ATPases). Endogenous CNT3 activities in murine proximal convoluted tubules and hCNT3 in transfected Madin-Darby Canine Kidney (MDCK) cells were shown to mediate sodium-dependent apical-to-basolateral (*i.e.*, "reabsorptive") transepithelial fluxes of cytidine, adenosine, gemcitabine, fludarabine, and 5′-deoxy-5-fluorouridine, and some anti-viral nucleoside analog drugs [18]. hENT3, which is an intracellular transporter localized to lysosomes and mitochondria [8,19] has minimal mRNA expression in the kidney [8] and hENT4, which is an adenosine transporter localized to apical membranes of transfected MDCK cells [9,20], is present in kidney tissue lysates [20].

The role of hNTs in renal secretion of nucleoside is less clear. While adenosine reabsorption *in vivo* in mice is unaffected by the ENT1 inhibitor nitrobenzylmercaptopurine ribonucleoside (NBMPR), 2′-deoxyadenosine secretion is inhibited by NBMPR, indicating the involvement of ENT1-dependent processes in 2′-deoxyadenosine secretion [1-3]. Previous work with hCNT1 and hENT1 co-transfected renal epithelial cell lines suggested that basolateral-to-apical transepithelial (*i.e.*, "secretive") fluxes of 2′-deoxyadenosine were due to the lower apparent affinity of hCNT1 for 2′-deoxyadenosine than adenosine at physiological concentrations [15]. An activity similar to that of pyrimidine nucleoside-selective hCNT1, but which also transports guanosine, has been previously observed in human kidney brush border membrane vesicles [21] and hCNT1 has been detected in apical membranes of human kidney proximal tubules by immunostaining [22]. While hCNT1 accepts adenosine and 2′-deoxyadenosine as permeants, transport of these purine nucleosides by purine nucleoside-selective hCNT2 and purine/pyrimidine nucleoside-transporting hCNT3 is at much higher capacities [10-13], and both of these transporters have been detected in apical membranes of human kidney proximal tubules by immunostaining [22, Chapter III]. The presence of hCNT2 and hCNT3 in human kidney proximal tubules raises doubt as to the physiological relevance of hCNT1 in selective purine nucleoside proximal tubular handling.

The location of hENT1 in proximal tubules has been controversial, and its role in proximal tubular secretion of nucleosides is currently unclear. In transfected renal proximal tubule epithelial cells producing recombinant hENT1 and grown as differentiated monolayer cultures, hENT1 is found primarily on basolateral membranes, with minor amounts present on apical membranes [15-17]. One immunostaining study identified hENT1 in apical, but not basolateral, membranes of human kidney proximal tubules (Chapter III) while another study found hENT1 in both apical and basolateral membranes [22]. Apical hENT1 may have a role in proximal tubular secretion of nucleosides by equilibration of nucleosides at luminal surfaces, as 2′-deoxyadenosine secretion *in vivo* is known to be ENT1-dependent [1,3]. Members of the human organic cation and anion transporter families (hOCTs and hOATs, respectively), may be involved along with hENT1 in selective secretion of some nucleosides [3,23-25]. hOCT1, which can mediate 7-deaza-2'-deoxyadenosine (2'-deoxytubercidin) transport [23-24] and hOAT2, which can mediate adenosine and 2'-deoxyguanosine transport [25], are both present on basolateral membranes of human kidney proximal tubules [26].

Little is known about renal handling of fludarabine (9-β-D-arabinosyl-2-fluoroadenine), cladribine (2-chloro-2′-deoxyadenosine), and clofarabine (2-chloro-2′-fluoro-deoxy-9-β-D-arabinofuranosyladenine), which are used clinically to treat a variety of hematological malignancies [27-29]. Fludarabine, cladribine and clofarabine can all be transported by hENT1/2 and hCNT2/3, but not by hCNT1 [30]. Following cellular uptake, fludarabine, cladribine, and clofarabine are phosphorylated by intracellular kinases to 5′-monophosphate, -diphosphate, and -triphosphate forms [31]. The active metabolites of all three drugs are nucleoside-5′-triphosphates, which are incorporated into deoxyribonucleic acid

(DNA) resulting in DNA chain termination and which also inhibit ribonucleotide reductase resulting in reduction of 2′-deoxynucleotide intracellular pools [32-34]. All three drugs are renally eliminated with peak plasma concentrations ranging from 1-3 μM [35-38]. Fludarabine displays a terminal half life of 30 hr and plasma concentrations of free drug (<0.1 μM) that persist for 24-72 hr after infusion, with heterogeneity between individuals in levels of fludarabine-5′-triphosphate achieved in leukemia cells [35]. Plasma levels and clearance rates of cladribine show large inter-individual variability, which was not reduced by either dosing according to weight or body surface area [36]. Clofarabine exhibits significant interpatient heterogeneity in peak plasma concentrations of free drug and clofarabine-5′-triphosphate in leukemia cells [37,38].

Renal handling of circulating physiological and pharmacological nucleosides is a major determinant of their plasma levels and tissue availabilities and influences the pharmacokinetics and normal tissue toxicities of nucleoside analog drugs. To investigate the roles of hNTs in renal handling of adenosine, 2′-deoxyadenosine, and their analogs fludarabine, cladribine and clofarabine, the present study used polarized monolayers of hRPTCs because they were previously shown to have endogenous hENT1, hENT2, and hCNT3 activities (Chapter III, Section III.2.3.4; Chapter IV, Section IV.2.4). Transepithelial fluxes of radioactive adenosine and 2′-deoxyadenosine were monitored from apical-to-basolateral sides and *vice versa* under a variety of experimental conditions (*e.g.*, presence or absence of specific transport inhibitors) to assess potential involvement of hNTs, respectively, in reabsorption and secretion processes. The presence of hNTs at either apical or basolateral surfaces was demonstrated functionally by measurements of initial rates of cellular uptake of radioactive adenosine and 2′-deoxyadenosine from apical or basolateral surfaces under conditions that enabled identification of particular transporter types. Adenosine "reabsorptive" fluxes (*i.e.*, apical-to-basolateral) were mediated primarily by apical hCNT3 and basolateral hENT2 while 2′-deoxyadenosine "secretive" fluxes (*i.e.*, basolateral-to-apical) were mediated by apical hENT1 and basolateral hOATs. The extent of reabsorptive fluxes of adenosine across polarized monolayers of various hRPTCs varied between cultures and correlated positively with apical hCNT3 activities. Fludarabine, cladribine, and clofarabine resembled adenosine rather than 2′-deoxyadenosine in that they exhibited reabsorptive rather than secretive fluxes across polarized monolayers of hRPTCs.

V.2 Results

V.2.1 Formation of polarized monolayers

The results of Chapters III and IV showed that adherent cultures of hRPTCs on collagen-coated polystyrene cell culture ware exhibited hENT1, hENT2, and hCNT3 activities. To study roles of hNTs in transepithelial fluxes of nucleosides, polarized monolayer cultures of hRPTCs with experimentally accessible apical and basolateral domains were produced on collagen-coated transwell inserts since earlier studies showed that such cultures exhibit transepithelial transport of folates between apical and basolateral chambers [39,40]. The experiments of Figure 1 were undertaken to demonstrate formation of polarized monolayers of hRPTC cultures prepared on collagen-coated transwell inserts, using cultures prepared from a single individual (*i.e.*, hRPTC11). Formation of tight junctions restricts paracellular movement of ions across polarized monolayers, resulting in potential differences between apical and basolateral chambers that can be reliably quantified by TEER measurements [41,42]. TEER values rose to a plateau of approximately 100 $\Omega \cdot cm^2$ by day ten for hRPTC11 cultures (Figure V-1A), indicating formation of polarized monolayers with leaky tight junctions. This was not unexpected since renal proximal tubules are known to exhibit passive reabsorption of sodium, a significant contributor to sodium reabsorption [41,43]. In comparison, the distal tubular MDCK cell line forms relatively non-leaky polarized monolayers when cultured on transwell inserts, with TEER values reaching a plateau at approximately 400 $\Omega \cdot cm^2$ [42].

To further demonstrate formation of polarized monolayers with distinct apical and basolateral membrane domains, localization of tight junction protein ZO-1 and cell adhesion protein E-CAD was determined in hRPTC11 cultures prepared on collagen-coated transwell inserts by immunofluorescent staining and confocal imaging. Previous localization studies in polarized renal epithelial cell lines have shown ZO-1 in tight junctions between cells at apical domains [44] and E-CAD in basolateral membrane domains [45,46]. Similarly, in polarized hRPTC11 cultures, immunofluorescent staining with anti-ZO-1 antibodies showed ZO-1 in apical tight junctions between cells in xy image sections and orthogonal projections of z-stack images (Figure V-1B-E). Some minimal intracellular background staining of ZO-1 was seen in orthogonal projections of z-stack images (Figure V-1E). On the other hand, immunofluorescent staining with anti-E-CAD antibodies showed E-CAD in basolateral membrane domains between cells in xy image sections and orthogonal projections of z-stack images (Figure 1F-I). No E-CAD staining was observed between cells and inserts, perhaps due to limited resolution at insert boundaries (Figure V-1I). No staining was observed with isotype control antibodies (data not shown). DAPI counterstaining was used to delineate cell positions in the polarized monolayers (Figure 1B-I). Formation of polarized monolayers for four other cultures of hRPTCs (hRPTC12, hRPTC13, hRPTC14, hRPTC15) on transwell inserts was confirmed in parallel experiments that measured rises in TEER values and assessed localizations of ZO-1 and E-CAD (Table V-1). Collectively, these results demonstrated that hRPTC cultures isolated from different individuals consistently formed polarized monolayers with distinct apical and basolateral domains.

V.2.2 Transepithelial fluxes of adenosine and 2′-deoxyadenosine

In vivo studies in a human with an adenosine deaminase deficiency and in mice treated with an adenosine deaminase inhibitor have shown that adenosine is actively reabsorbed and 2′-deoxyadenosine is actively secreted in the kidney. It was previously shown (i) in human kidney by immunohistochemistry that hENT1 and hCNT3 localize to apical membranes of proximal tubules (Chapter III), and (ii) in monolayer cultures of hRPTCs by functional studies that hENT1, hENT2, and hCNT3 mediate uridine uptake (Chapter IV), suggesting that hENT1, hENT2, and hCNT3 are involved in renal handling of adenosine and 2′-deoxyadenosine. Cytidine and adenosine apical-to-basolateral fluxes are mediated by endogenous CNT3 in murine proximal convoluted tubule cells and transfected hCNT3 in MDCK cells [18]. To confirm and extend these observations, transepithelial fluxes of adenosine and 2′-deoxyadenosine across polarized hRPTC11 monolayer cultures were assessed in sodium-containing buffer. Concentrations of [^{3}H]-adenosine and [^{3}H]-2′-deoxyadenosine were 1 μM since circulating physiological and renal concentrations are ≤ 1 μM [47,48]. In the experiments of Figure V-2, substantial apical-to-basolateral fluxes of adenosine were observed across polarized hRPTC11 cultures with significantly higher levels in the presence of 500 μM EHNA, an adenosine deaminase inhibitor ($p < 0.01$) (Figure V-2A) [50], whereas only very small basolateral-to-apical fluxes of adenosine were observed and these were not enhanced by EHNA (Figure V-2C). In contrast, for 2′-

deoxyadenosine, substantial basolateral-to-apical fluxes were observed with small but significant increases in the presence of EHNA ($p < 0.01$) (Figure V-2B), whereas only very small apical-to-basolateral fluxes were observed and these were not enhanced by EHNA (Figure V-2D). Apical-to-basolateral fluxes of adenosine were higher than basolateral-to-apical fluxes of 2′-deoxyadenosine in both the presence and absence of EHNA (p values < 0.01) (Figure V-2A,B).

Results of studies of metabolism of [^{3}H]-adenosine and [^{3}H]-2'-deoxyadenosine during transepithelial flux assays are shown in Table V-2. In the presence of EHNA, the majority of radioactivity recovered when adenosine and 2'-deoxyadenosine moved, respectively, from apical-to-basolateral and basolateral-to-apical compartments was unaltered nucleoside. In contrast, in the absence of EHNA, there was significant degradation of the fluxed adenosine to inosine and hypoxanthine and the fluxed 2'-deoxyadenosine to 2'-deoxyinosine and hypoxanthine (p values < 0.01) (Table V-2). The majority of intracellular recovered radioactivity after apical-to-basolateral transepithelial fluxes of adenosine in the presence of EHNA was adenosine and phosphorylated forms of adenosine and in the absence of EHNA was hypoxanthine and phosphorylated forms of adenosine (Table V-2). Similarly, intracellular recovered radioactivity after basolateral-to-apical transepithelial fluxes of 2'-deoxyadenosine in the presence of EHNA was unaltered 2'-deoxyadenosine and in the absence of EHNA was hypoxanthine (Table V-2). In this work, subsequent experiments with adenosine and 2′-deoxyadenosine were performed in the presence of 500 μM EHNA to inhibit deamination.

Preferential apical-to-basolateral transepithelial fluxes of adenosine and basolateral-to-apical transepithelial fluxes of 2'-deoxyadenosine were confirmed for the five different hRPTC cultures (*i.e.*, isolated from kidneys of five different individuals) and the results are summarized in Tables V-3, V-4, and V-5. The observed lag times in which no transepithelial fluxes were observed (< 30 min) (see Figure V-2 for results with hRPTC11 cultures) may have been due to the accumulation of phosphorylated forms of adenosine and 2'-deoxyadenosine within cells before commencement of subsequent effluxes into the opposite extracellular compartments.

Previous *in vivo* studies in mice have shown that adenosine reabsorption is unaffected by NBMPR whereas 2′-deoxyadenosine secretion is inhibited [1-3]. This behavior was recapitulated in the model proximal tubule system in the experiments of Figure V-3. Apical-to-basolateral fluxes of adenosine and basolateral-to-apical fluxes of 2′-deoxyadenosine across polarized hRPTC11 cultures were almost completely ablated in the absence of sodium and completely inhibited by dilazep at 200 μM ($p < 0.001$), a concentration that inhibits both hENT1 and hENT2, the hENTs known to be present in hRPTC cultures (Figure V-3A,B). On the other hand, NBMPR at 0.1 μM, a concentration that inhibits hENT1 but not hENT2, had no effect on apical-to-basolateral fluxes of adenosine whereas basolateral-to-apical fluxes of 2′-deoxyadenosine were inhibited ($p < 0.001$) (Figure V-3A,B). Theoretically, inhibition of transport at either apical or basolateral membranes could reduce transepithelial fluxes. Therefore, these results indicated that adenosine "reabsorptive" fluxes were dependent on hCNTs and hENT2 but not hENT1 and 2′-deoxyadenosine "secretive" fluxes were dependent on hENT1. Also, apical-to-basolateral fluxes of adenosine were slightly increased in the presence of NBMPR (p values < 0.05) (Figure V-3A), possibly due to inhibition of efflux through hENT1 at apical membranes.

In five different polarized hRPTC cultures, the apical-to-basolateral fluxes of adenosine were significantly higher in the presence of sodium than in its absence (p values < 0.01) (Table V-3) and the basolateral-to-apical fluxes of 2'-deoxyadenosine were significantly lower in the presence of NBMPR than in its absence (p values < 0.01) (Table V-4). These results suggested that apical-to-basolateral fluxes of adenosine were sodium-dependent and mediated by apical hCNTs and that basolateral-to-apical fluxes of 2'-deoxyadenosine were dependent on hENT1. Attempts to localize hENT1, hENT2, and hCNT3 by immunofluorescent staining with anti-hNT-specific monoclonal antibodies in polarized monolayer cultures of hRPTCs were unsuccessful, possibly due to low protein abundance.

While the results presented thus far were consistent with the current understanding of renal nucleoside handling (*i.e.*, that adenosine is reabsorbed by hCNT3 driven by the sodium gradient with significant metabolism to hypoxanthine in the absence of adenosine deaminase inhibition) [18], secretion of 2′-deoxyadenosine cannot be explained by hENT1 involvement alone. Since it has been suggested that hOCTs and hOATs are involved in renal secretion of some nucleosides [23-25], the effects of the nonspecific hOCT inhibitor cimetidine and hOAT inhibitor probenecid on basolateral-to-apical fluxes of 2′-deoxyadenosine across polarized hRPTC11 cultures were examined in the experiments of Figure V-3B. Although 500 μM cimetidine had no effect, 500 μM probenecid reduced 2′-deoxyadenosine basolateral-to-apical fluxes ($p < 0.05$) (Figure V-3B), implicating hOATs in the observed 2′-deoxyadenosine secretive fluxes. The reduction of basolateral-to-apical fluxes of 2′-deoxyadenosine by probenecid was confirmed for the five different hRPTC cultures and the results are summarized in Table V-4 (p values < 0.05).

V.2.3 Cellular uptake of adenosine and 2′-deoxyadenosine from apical and basolateral surfaces

Although immunofluorescent localization of hNTs in polarized hRPTC cultures was unsuccessful, hENT1, hENT2, and hCNT3 were functionally localized by assessing mediated uptake of adenosine and 2′-deoxyadenosine from either apical or basolateral surfaces into polarized hRPTC cultures under experimental conditions designed to functionally identify particular hNTs. In the experiments of Figure V-4, which were conducted with cultures derived from a single individual, apical uptake of 1 μM [^{3}H]-adenosine or [^{3}H]-2′-deoxyadenosine was assessed in sodium-containing or sodium-free buffer for 10 min because: (i) 10 min provided an estimate of initial rates of cellular uptake (*i.e.*, transport) (8), and (ii) transepithelial fluxes were not evident at 10 min (see Figure V-2). Rates of apical uptake of adenosine (Figure V-4A) and 2′-deoxyadenosine (Figure V-4B) in sodium-free buffer were (i) substantially lower than those in sodium-containing buffer ($p < 0.001$), indicating the presence of apical sodium-dependent transport activity, (ii) further reduced by the inclusion of

0.1 μM NBMPR ($p < 0.001$), indicating the presence of apical hENT1 activity, and (iii) still further inhibited by 200 μM dilazep ($p < 0.001$) (*i.e.*, to levels similar to those observed in sodium-free buffer with dilazep and excess non-radiolabeled adenosine or 2′-deoxyadenosine), indicating the presence of apical hENT2 activity. Rates of apical uptake of adenosine were higher than those of 2′-deoxyadenosine in both sodium-containing and sodium-free buffers (p values < 0.001) (Figure V-4A,B). The reduction of rates of uptake of adenosine and 2′-deoxyadenosine by high concentrations of either thymidine or inosine in sodium- and dilazep-containing buffer (p values < 0.001) (Figure V-4A,B) demonstrated that apical sodium-dependent transport of both adenosine and 2′-deoxyadenosine was mediated by apical hCNT3. The slightly increased uptake of adenosine and 2′-deoxyadenosine observed in sodium-containing buffer in the presence of dilazep compared to that in its absence (Figure V-4A,B) (p values < 0.01) was consistent with intracellular trapping due to inhibition of efflux through hENTs.

Basolateral uptake of 1 μM $[^3H]$-adenosine (Figure V-4C) and -2′-deoxyadenosine (Figure 4D) was also assessed at 10 min in sodium-containing or sodium-free buffer. For both nucleosides, uptake rates were unaffected by (i) removal of sodium, indicating the absence of basolateral sodium-dependent transport activity, or (ii) the presence of 0.1 μM NBMPR, indicating the absence of basolateral hENT1 activity. Adenosine and 2′-deoxyadenosine basolateral uptake differed in their sensitivities to inhibition by 200 μM dilazep in that basolateral uptake of adenosine was reduced to non-mediated levels ($p < 0.001$) (*i.e.*, those observed in the presence of excess non-radiolabeled adenosine)

(Figure V-4C) whereas that of 2′-deoxyadenosine was reduced ($p < 0.001$), but not to non-mediated levels (*i.e.*, those observed in the presence of excess non-radiolabeled 2′-deoxyadenosine) (Figure V-4D). These results, which demonstrated basolateral hENT2-mediated transport of both nucleosides, suggested the presence of a basolateral dilazep-insensitive uptake process for 2′-deoxyadenosine. Basolateral 2′-deoxyadenosine uptake was significantly higher than apical 2′-deoxyadenosine uptake or basolateral adenosine uptake in sodium-containing buffer (p values < 0.01) (Figure V-4B,C,D). These results were consistent with the observed vectorial fluxes of 2'-deoxyadenosine from basolateral-to-apical compartments.

It was previously observed that hRPTCs isolated from the kidneys of different individuals exhibited different levels of hCNT3 activity (Chapter IV, Section IV.2.4). To determine if the observed different levels of apical hCNT3 activity were reflected in differences in apical-to-basolateral fluxes of adenosine, the values obtained in experiments with hRPTC cultures from five different individuals for uptake and transepithelial fluxes of adenosine are compared in Table V-3.

Apical uptake of 1 μM [^{3}H]-adenosine by polarized hRPTC cultures was measured in sodium-containing buffer with 200 μM dilazep (to inhibit hENT1 and hENT2) in the absence or presence (to inhibit all mediated uptake) of 1 mM non-radiolabeled adenosine, and the hCNT3-mediated component was calculated by subtracting non-mediated uptake values from the corresponding total uptake values. Table V-3 shows that apical hCNT3-mediated adenosine uptake varied significantly between cultures (p values < 0.05), consistent with the results presented in Chapter IV (Section IV.2.4) in which cultures of hRPTCs from different individuals exhibited different hCNT3 activities. When apical-to-basolateral fluxes of 1 μM [^{3}H]-adenosine across polarized monolayers of the five hRPTC cultures were measured in sodium-containing buffer, the fluxes (i) varied significantly between cultures (p values < 0.05), and (ii) correlated positively with apical hCNT3-mediated adenosine uptake levels (r^2 0.9908 $p < 0.001$) (Table V-3). These results demonstrated that apical hCNT3-mediated uptake activities were determinants of apical-to-basolateral fluxes of adenosine in polarized monolayers of hRPTCs.

Basolateral uptake of 1 μM [^{3}H]-2'-deoxyadenosine by polarized hRPTC cultures was determined in sodium-containing buffer to measure total uptake, and the mediated component was calculated by subtracting non-mediated uptake determined in the presence of 1 mM non-radiolabeled 2'-deoxyadenosine. Basolateral mediated uptake of 2'-deoxyadenosine varied significantly between cultures (p values < 0.05) as did basolateral-to-apical fluxes of 1 μM [^{3}H]-2'-deoxyadenosine across polarized monolayers (p values < 0.05) (Table V-4), and uptake and flux values correlated positively with each other (r^2 0.9566, $p < 0.01$) (Table V-4). These results demonstrated that basolateral transporters were determinants of basolateral-to-apical fluxes of 2'-deoxyadenosine in polarized monolayers of hRPTCs.

Because hOCTs and hOATs have been implicated in renal handling of some nucleosides [23-25] and basolateral-to-apical fluxes of 2′-deoxyadenosine across polarized monolayers of hRPTC11 were sensitive to probenecid (Figure V-3B), rates of apical and basolateral uptake of 2′-deoxyadenosine were assessed in the presence or absence of the non-specific hOCT and hOAT inhibitors cimetidine and probenecid, respectively, in the experiments of Figure V-4B,D. Neither apical (Figure V-4B) nor basolateral (Figure V-4D) uptake of 2′-deoxyadenosine in sodium-containing buffer with 200 μM dilazep (to block hENT1 and hENT2 activities) were inhibited by 500 μM cimetidine. In contrast, although apical uptake of 2′-deoxyadenosine was not affected (Figure V-4B), 500 μM probenecid reduced basolateral uptake to non-mediated levels ($p < 0.001$) (*i.e.*, those observed in sodium-free buffer with 200 μM dilazep and excess non-radiolabeled 2′-deoxyadenosine) (Figure V-4D), suggesting the presence of basolateral hOAT-mediated 2′-deoxyadenosine uptake. Inhibition of basolateral mediated 2'-deoxyadenosine uptake by probenecid was confirmed for the five different hRPTC cultures and the results are summarized in Table V-4 (p values < 0.01).

V.2.4 Expression of human organic anion transporter 2 (hOAT2) mRNA

Previous studies have shown that hOAT mRNAs and proteins are present in non-polarized hRPTC cultures [50]. Since (i) functional studies suggested that hOATs mediated basolateral uptake and basolateral-to-apical transepithelial fluxes of 2'-deoxyadenosine in polarized hRPTC monolayers (Section V.2.3), (ii) 2'-deoxyguanosine and adenosine are permeants of hOAT2 [25], and (iii) hOAT2 is present in basolateral membranes of kidney proximal tubules [26], experiments were undertaken to determine if hOAT2 mRNA was present in polarized hRPTC monolayers. Figure V-5A shows results of RT-PCR analyses with five different cultures. The identities of the amplified bands were confirmed by their predicted PCR product sizes (0.59 kb) and by sequence analysis of amplified PCR products. Genomic DNA contamination was not detected in RT-PCR reactions without reverse transcriptase. hOAT2 mRNA was present in all five cultures, suggesting the involvement of hOAT2 in secretive transepithelial fluxes of 2'-deoxyadenosine.

V.2.5 hCNT3 protein abundance

hRPTC cultures isolated from kidneys of different individuals (hRPTC1 through hRPTC10, Table II-1) and grown as differentiated monolayers exhibited different hCNT3 activity levels that correlated positively with cell surface hCNT3 protein levels but not with hCNT3 mRNA levels (Chapter IV). To determine if the different apical hCNT3 activity levels observed in this study were due to differences in hCNT3 protein levels in apical cell surfaces of polarized hRPTC cultures, the relative abundance of hCNT3 at apical cell surfaces was examined in cultures derived from five different individuals. Immunoreactive bands at 90 kDa were identified in apical cell surface protein preparations with antibodies against hCNT3 (Figure V-5B), and the relative abundance of the immunoreactive material varied over a five-fold range (p values < 0.05) (Figure V-5C). Apical hCNT3-mediated adenosine uptake rates and apical-to-basolateral fluxes of adenosine correlated positively with the relative levels of apical cell surface hCNT3 (r^2 0.8179 and r^2 0.8055, respectively, p values < 0.05) (data from Table V-3, Figure V-5C).

It was shown in Chapter III (Sections III.2.1.2) that, hCNT3 was present in crude membranes of human kidney cortex tissues by immunoblotting. To determine if the polarized hRPTC cultures retained apical cell surface hCNT3 at relative levels similar to those of human kidney cortical proximal tubules, the relative abundance of hCNT3 was examined in crude membranes from the human kidney cortex tissues from which the hRPTC cultures had been isolated. Immunoreactive bands for hCNT3 at 90 kDa were identified in human kidney cortex crude membrane preparations (Figure V-5B), as previously observed (Chapter III, Section III.2.1.2), and their relative abundance correlated positively with apical cell surface hCNT3 protein abundance in the corresponding polarized hRPTC cultures (r^2 0.8107, $p < 0.05$) (Figure V-5C). Collectively, these results showed that polarized hRPTC monolayer cultures retained the same relative hCNT3 protein levels as their tissue cells of origin and suggested that apical hCNT3 protein levels (and activities) are determinants of the extent of adenosine reabsorptive fluxes.

V.2.6 Transportability of adenosine and 2′-deoxyadenosine by recombinant hCNT3

Despite the observed apical sodium-dependent uptake of 2'-deoxyadenosine in polarized hRPTC monolayers, the cultures exhibited preferential basolateral-to-apical transepithelial fluxes of 2'-deoxyadenosine. In the experiments of Figures V-4A,B, apical hCNT3-mediated uptake of 2'-deoxyadenosine was lower than that of adenosine in the same polarized hRPTC monolayers ($p < 0.01$), suggesting that adenosine was a better permeant of hCNT3 than 2'-deoxyadenosine. To investigate the transportability of adenosine and 2'-deoxyadenosine by hCNT3, kinetic studies were undertaken in yeast producing recombinant hCNT3 (Figures V-6A,B). Initial rates of uptake of adenosine and 2'-deoxyadenosine were saturable and conformed to Michaelis-Menten kinetics with apparent K_m values of 1.3 ± 0.2 and 3.6 ± 0.5 μM, respectively, and V_{max} values of 110.3 ± 5.4 and 80.4 ± 4.8 pmol/mg protein/min, respectively (Figure V-6A,B). The efficiencies of transport of adenosine and 2'-deoxyadenosine by hCNT3 (V_{max}:K_m ratio) were 83.1 and 22.4 pmol/mg protein/min/μM, respectively, indicating greater hCNT3 transportability of adenosine than 2'-deoxyadenosine. These results were consistent with the higher observed apical hCNT3-mediated uptake of adenosine than 2'-deoxyadenosine in polarized hRPTC monolayers.

V.2.7 Fludarabine, cladribine, and clofarabine transepithelial fluxes and cellular uptake

Little is known about renal handling of the purine nucleoside analogs fludarabine, cladribine, and clofarabine, which are used clinically to treat hematological malignancies. In previous studies, CNT3 was found to be a determinant of cytidine and fludarabine reabsorptive fluxes in murine proximal convoluted tubule cells and apical-to-basolateral fluxes in polarized transfected renal epithelial cell lines, respectively [18]. In the experiments of Figure V-7, transepithelial fluxes and polarized uptake of fludarabine, cladribine and clofarabine were investigated in polarized hRPTC cultures. Transepithelial fluxes of 10 μM [^{3}H]-fludarabine, -cladribine, or -clofarabine across polarized hRPTC11 cultures were measured in sodium-containing buffer. Apical-to-basolateral fluxes

(Figure V-7A) of all three analogs were observed whereas basolateral-to-apical fluxes were not (Figure V-7B). Thus, the directionality of transepithelial fluxes of fludarabine, cladribine, and clofarabine resembled that of adenosine, which is reabsorbed in human kidney proximal tubules. Apical and basolateral cellular uptake of 10 μM [^{3}H]-fludarabine, -cladribine, and -clofarabine was measured in sodium-containing buffer in the absence (total uptake) or presence (non-mediated uptake) of 1 mM non-radiolabeled adenosine (Figures V-7C,D). For all three analogs apical uptake was higher than basolateral uptake (p values < 0.01) (Figures V-7C,D), similar to the results obtained with adenosine (Figure V-4A,C).

Because of the observed positive correlations for adenosine between relative apical-to-basolateral fluxes and rates of apical hCNT3-mediated uptake in polarized hRPTC monolayers from different individuals (Section V.2.3), similar studies were undertaken for fludarabine, cladribine, and clofarabine. Apical-to-basolateral fluxes and apical mediated cellular uptake of all three analogs were assayed in polarized hRPTC monolayer cultures isolated from five different individuals (Table V-6). Positive correlations were found between apical-to-basolateral fluxes and mediated apical uptake for fludarabine and clofarabine (r^2 values 0.9218 and 0.9372, respectively, p values < 0.01) but not for cladribine (r^2 0.7448) (Table V-6) and between apical hCNT3 activities (Table V-3) and apical-to-basolateral fluxes for fludarabine and clofarabine (r^2 values 0.7944 and 0.8183, respectively, p values < 0.05), but not for cladribine (r^2 0.4204) (Table V-6).

V.3 Discussion.

Evidence presented in this Chapter supports a model for proximal tubular reabsorption of adenosine, fludarabine, cladribine, and clofarabine mediated by hCNT3 and hENT2 asymmetrically distributed, respectively, to apical and basolateral membranes. Furthermore, a model for proximal tubular secretion of 2'-deoxyadenosine is proposed from evidence presented in this Chapter that demonstrated asymmetric distribution of hOATs and hENT1, respectively, to basolateral and apical membranes. Both of these models fit well with current evidence in the literature. This study also confirmed findings [18] that suggested that hCNT3 is a determinant of proximal tubular reabsorption of nucleosides, including adenosine, fludarabine and clofarabine.

Apical-to-basolateral (*i.e.*, reabsorptive) fluxes of adenosine were mediated by coupling of sodium-driven apical hCNT3 to basolateral hENT2 (Figures V-2,3,4, Table V-3). These findings agreed with a recent report that attributed transepithelial fluxes of cytidine and adenosine across murine proximal convoluted tubule cells to endogenous CNT3 and across hCNT3-transfected renal epithelial cell lines grown as polarized monolayers to introduced hCNT3 [18]. Theoretically, inhibition of transport at either apical or basolateral sides could inhibit transepithelial fluxes; however, hENT1, found on apical membranes, did not contribute to apical-to-basolateral fluxes of adenosine across polarized hRPTC monolayers in the current study (Figure V-3). The lack of involvement of hENT1 in adenosine apical-to-basolateral fluxes may reflect its lower apparent affinity for adenosine than hCNT3 and the presence of abundant hCNT3 at the apical side [6,13].

hENT3, which appears to be an intracellular pH-dependent transporter that localizes to lysosomes and mitochondria [8,50], has minimal expression in human kidney [8]. hENT4, which was originally identified as plasma monoamine transporter (PMAT) [52] and appears to be a cell surface adenosine pH-dependent transporter [9], is present in human kidney tissue lysates and apical membranes of transfected MDCK cells [20].

This results described in this Chapter extended the role of hCNT3 in mediating transepithelial fluxes of nucleosides to include cladribine and clofarabine in human kidney proximal tubule cells with endogenous hCNT3 activities (Figure V-7, Table V-6). Interestingly, cladribine, which, like 2′-deoxyadenosine, contains a 2′-deoxyribosyl moiety, also exhibited apical-to-basolateral (*i.e.*, reabsorptive) transepithelial fluxes across polarized hRPTC cultures (Figures V-7A, Table V-6). These results may explain, in part, the delayed and variable elimination of some nucleoside analog drugs from the body [35-37] and highlight the high selectivity of transport machinery involved in renal handling of physiological nucleosides and therapeutic nucleoside analogs. hCNT3 was also shown to be involved in transepithelial fluxes of various nucleoside analogs in transfected renal epithelial cell lines [18], and to be a determinant of fludarabine mediated uptake and cytotoxicity in hRPTC cultures (Chapter IV, Section IV.2.4, IV.2.5, IV.2.6). Relative levels of apical mediated uptake of fludarabine and clofarabine were shown to be determinants of their apical-to-basolateral transepithelial fluxes (Figure V-7, Table V-6). These results suggested that differences in kidney proximal tubule hCNT3 levels may result in differences in renal handling of physiological nucleosides and nucleoside analogs that affect their pharmacokinetics and, for nucleoside analogs, their normal tissue toxicities.

Axial heterogeneity of hNTs in different proximal tubular cell types in hRPTC cultures from kidneys of different individuals may have contributed to the observed variability in transepithelial fluxes and cellular uptake of nucleosides. However, the results of Chapter III (Sections III.2.1.3) showed that hCNT3 and hENT1 staining was present in apical membranes uniformly throughout cortical and corticomedullary proximal tubules of human kidney tissues. Other studies have also demonstrated hENT1 staining in apical and basolateral membranes of proximal tubules adjacent to corticomedullary junctions [22]. In the current study, polarized hRPTC cultures exhibited similar relative hCNT3 protein levels on apical cell surfaces as were observed in the corresponding human kidney cortex crude membranes (Figure V-5B,C), of which the majority were from cortical convoluted proximal tubule cells [53]. This correspondence suggested that hRPTCs retained the characteristics of nucleoside transport processes present in their cortical proximal tubular cells of origin.

A model of renal secretion of 2′-deoxyadenosine through apical hCNT1 and basolateral hENT1 was previously proposed based on results of studies with hCNT1- and hENT1-overexpressing animal kidney cell lines in which it was suggested that the selectivity of adenosine reabsorption and 2′-deoxyadenosine secretion was the result of the higher affinity of hCNT1 for adenosine than for 2′-

deoxyadenosine [15]. However, apical membranes of kidney tubule epithelial cells also possess hCNT2 [22] and hCNT3 (Chapter III, Section III.2.1.3), both of which have higher transport capacities for adenosine and 2′-deoxyadenosine than hCNT1 [10-13], making the contributions of hCNT1 to selective purine proximal tubular handling doubtful. hCNT3-mediated apical uptake of 2′-deoxyadenosine was significantly lower than that of adenosine under similar conditions (Figures V-4A,B), consistent with the higher hCNT3 transportability of adenosine than of 2′-deoxyadenosine observed in the recombinant yeast expression system (Figures V-6A,B). The results shown in this Chapter support a new model of renal secretion of 2′-deoxyadenosine that involves apical hENT1 and basolateral hOATs (Figures V-3B,4B,D, Table V-4). This model is supported by results of *in vivo* studies in mice treated with 2′-deoxycoformycin in which adenosine reabsorption was not inhibited by the classical hENT inhibitors, NBMPR or dipyridamole, whereas 2′-deoxyadenosine secretion was inhibited by both [2,3].

hOATs have been reported to share some permeants with hNTs – *e.g.*, 2′-deoxyguanosine and adenosine are permeants of hOAT2 [25]. hOAT2 is known be present in basolateral membranes of kidney proximal tubules [26] and, since hOAT2 mRNA transcripts were found in polarized hRPTC monolayer cultures (Figure V-5A), may account, in part, for the observed inhibitions of secretive fluxes and basolateral uptake of 2′-deoxyadenosine by probenecid (Figure V-2B,3D, Table V-4). While hOCT1 is known to transport 2′-deoxytubercidin, a nucleoside analog almost identical in structure to 2′-deoxyadenosine, the nonspecific hOCT inhibitor cimetidine had no inhibitory effects on secretive transepithelial fluxes of 2′-deoxytubercidin in mice [2] or on apical and basolateral uptake of 2′-deoxyadenosine in the present study (Figure V-2B,3B,3D), suggesting that it was not involved.

Both hOAT2 and hOCT1, along with other hOCTs and hOATs, are known to be asymmetrically distributed in apical and basolateral membrane domains in human kidney proximal tubules [26]. hOAT1, hOAT2 and hOAT3 appear to be basolateral transporters while hOAT4 appears to be an apical transporter in kidney epithelia [26]. While hOAT1, hOAT2, and hOAT4 are facilitative transporters like hENTs, hOAT3 is a dicarboxylate-exchanger that is driven by the sodium gradient [26]. While apical sodium-driven hCNT3-mediated 2'-deoxyadenosine uptake was observed in polarized hRPTC cultures (Figures V-4B), basolateral sodium-independent 2'-deoxyadenosine uptake was higher, resulting in preferential basolateral-to-apical fluxes of 2'-deoxyadenosine (Figure V-4D, Table V-4). This may have been due to more efficient transport of 2'-deoxyadenosine by basolateral hOATs than by apical hCNT3, which was shown to have a lower transport efficiency for 2'-deoxyadenosine than for adenosine (Figure V-6). Furthermore, the basolateral mediated uptake values for 2'-deoxyadenosine were positively correlated with basolateral-to-apical fluxes. The driving forces for 2′-deoxyadenosine secretive transepithelial fluxes across polarized hRPTC cultures are unknown. Development of more transporter-specific inhibitors will allow further delineation of the roles of specific hOATs in renal secretion of 2′-deoxyadenosine [54].

Inter-individual differences in hOAT and hOCT abundances have been demonstrated previously in cultures of hRPTCs from different individuals [50]. In Chapter IV it was shown that differences in hCNT3 abundance and activities in adherent cultures of hRPTC from different individuals correlated positively with mediated uptake rates and cytotoxicities of fludarabine. Therefore, inter-individual variation in renal reabsorption or secretion of physiological nucleosides and nucleoside drugs may be due to differences in kidney transporter types and/or levels as suggested by the variations in apical hCNT3 activities shown in Table V-3. Because proximal tubular luminal pH is highly variable and regulated, ranging from pH 5.5 to 7.4 [55], hCNT3, which co-transports nucleosides with either sodium and/or protons [56], is ideally suited to play a role in nucleoside reabsorption in human kidney proximal tubules. hCNT3 can function under varying conditions and thus enable continuous reabsorption of energetically expensive physiological nucleosides for tissues that lack *de novo* nucleotide biosynthesis pathways.

As observed for hCNT3-mediated transepithelial fluxes of adenosine across polarized monolayers of transfected renal tubular epithelial cells [18], the majority of fluxed molecules across polarized hRPTC cultures in the absence of inhibition of adenosine deaminase by EHNA (Table V-2,5) were, respectively, for adenosine and 2'-deoxyadenosine: (i) adenosine, inosine, and hypoxanthine, and (ii) 2'-deoxyadenosine and hypoxanthine. In the absence of adenosine deaminase inhibition, intracellular metabolites for both adenosine and 2'-deoxyadenosine were phosphorylated nucleotides and hypoxanthine (Table V-2). While the contribution of various transporters to transepithelial fluxes of a given nucleoside depends on their relative abundances, turnover numbers, and apparent affinities, the extent and nature of transepithelial fluxes of particular nucleosides also depends on their intracellular metabolism.

In summary, the results presented in this Chapter provided evidence for a descriptive model of purine nucleoside renal handling in which adenosine reabsorptive fluxes are mediated by hCNT3 at apical domains and hENT2 at basolateral domains and 2′-deoxyadenosine secretive fluxes are mediated by hENT1 at apical domains and hOATs at basolateral domains. A better understanding of renal handling of nucleosides by hNTs, the main route of elimination of nucleosides from the body, could lead to strategies aimed at improving drug dosing for therapeutic nucleoside analogs that maximize their efficacies and minimize their toxicities.

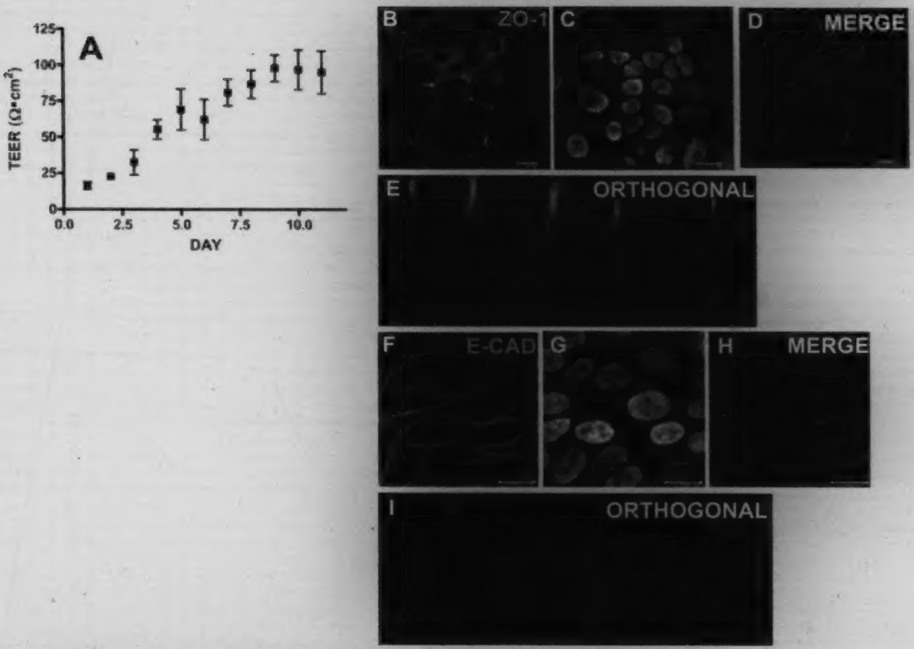

Figure V-1. Demonstration that cultures of hRPTC11 on transwell inserts form polarized monolayers. (A) TEER was measured for hRPTC11 cultures on transwell inserts at daily intervals for 10 days as described in Materials and Methods (Section II.3). Values are means (± standard deviation) for three experiments each with triplicate measurements. Error bars are absent where the data symbols were larger than the standard deviation values. (B-I) Immunofluorescent staining with anti-ZO-1 (green) and anti-E-CAD (green) antibodies and DAPI (blue) was performed in triplicate on polarized cultures of hRPTC11 on transwell inserts as described in Materials and Methods. (B) xy section of ZO-1 stained z-stack. (C) xy section of DAPI counterstained z-stack. (D) Merged image of xy sections of ZO-1 and DAPI stained z-stacks. (E) Orthogonal projection of ZO-1 and DAPI stained z-stacks. (F) xy section of E-CAD stained z-stack. (G) xy section of DAPI counterstained z-stack. (H) Merged image of xy sections of E-CAD and DAPI stained z-stacks. (I) orthogonal projection of E-CAD and DAPI stained z-stacks.

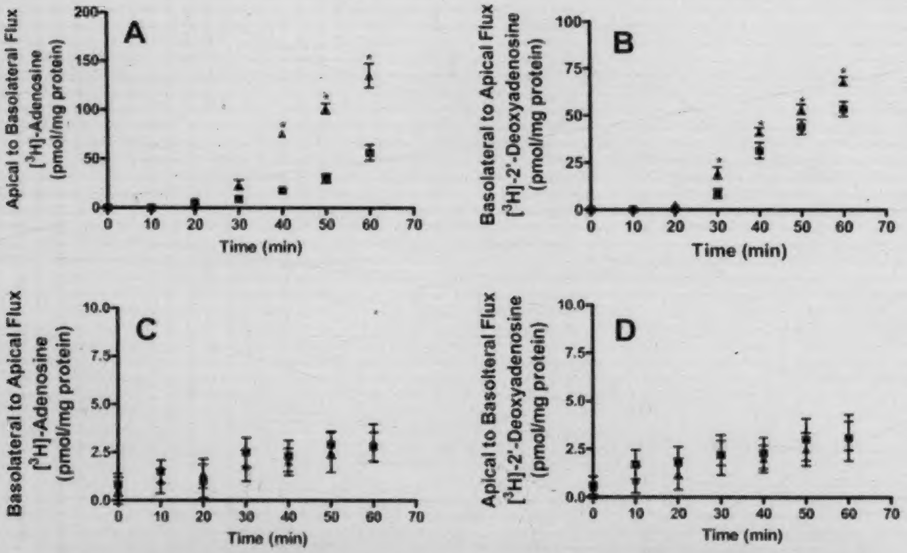

Figure V-2. Demonstration of apical-to-basolateral fluxes of adenosine and basolateral-to-apical fluxes of 2′-deoxyadenosine across polarized hRPTC11 cultures. Apical-to-basolateral fluxes of 1 μM (A) [^{3}H]-adenosine or (D) [^{3}H]-2′-deoxyadenosine and basolateral-to-apical fluxes of 1 μM (C) [^{3}H]-adenosine or (B) [^{3}H]-2′-deoxyadenosine were measured over time across polarized monolayers of hRPTC11 cultures in sodium-containing buffer with (▲) or without (■) 500 μM EHNA as described in Materials and Methods (Section II.5). (*) denotes significantly different values in the presence versus the absence of EHNA (p values < 0.01). Values are means (± standard deviation) for three independent experiments each with triplicate measurements. Error bars are absent where the data symbols were larger than the standard deviation values.

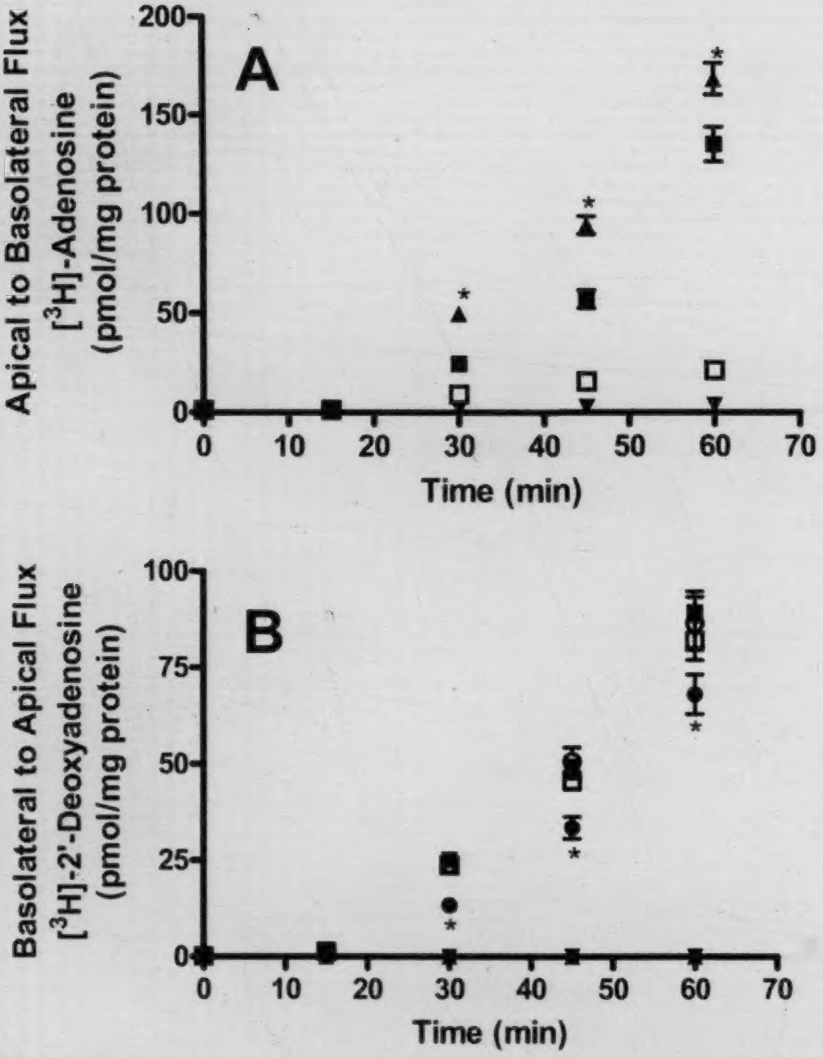

Figure V-3. Sodium dependence and inhibitor sensitivities of apical-to-basolateral fluxes of adenosine and basolateral-to-apical fluxes of 2′-deoxyadenosine across polarized hRPTC11 cultures. (A) Apical-to-basolateral fluxes of 1 μM $[^3H]$-adenosine were measured over time across polarized monolayers of hRPTC11 cultures, as described in Materials and Methods (Section II.5), in sodium-containing buffer that contained 500 μM EHNA alone (■) or with 0.1 μM NBMPR (▲) or 200 μM dilazep (▼), or in sodium-free buffer that contained 500 μM EHNA (□). (B) Basolateral–to-apical fluxes of 1 μM $[^3H]$-2′-deoxyadenosine were measured over time across polarized monolayers of hRPTC11 cultures, as described in Materials and Methods, in sodium-containing buffer that contained 500 μM EHNA alone (■) or with 0.1 μM NBMPR (▲) or 200 μM dilazep (▼), or with 500 μM cimetidine (○), or with 500 μM probenecid (●), or in sodium-free buffer that contained 500 μM EHNA (□). (*) denotes significantly different values in sodium-containing buffer in the presence or absence of NBMPR or probenecid (p values < 0.05). Values are means (± standard deviation) for three independent experiments each with triplicate measurements. Error bars are absent where the data symbols were larger than the standard deviation values.

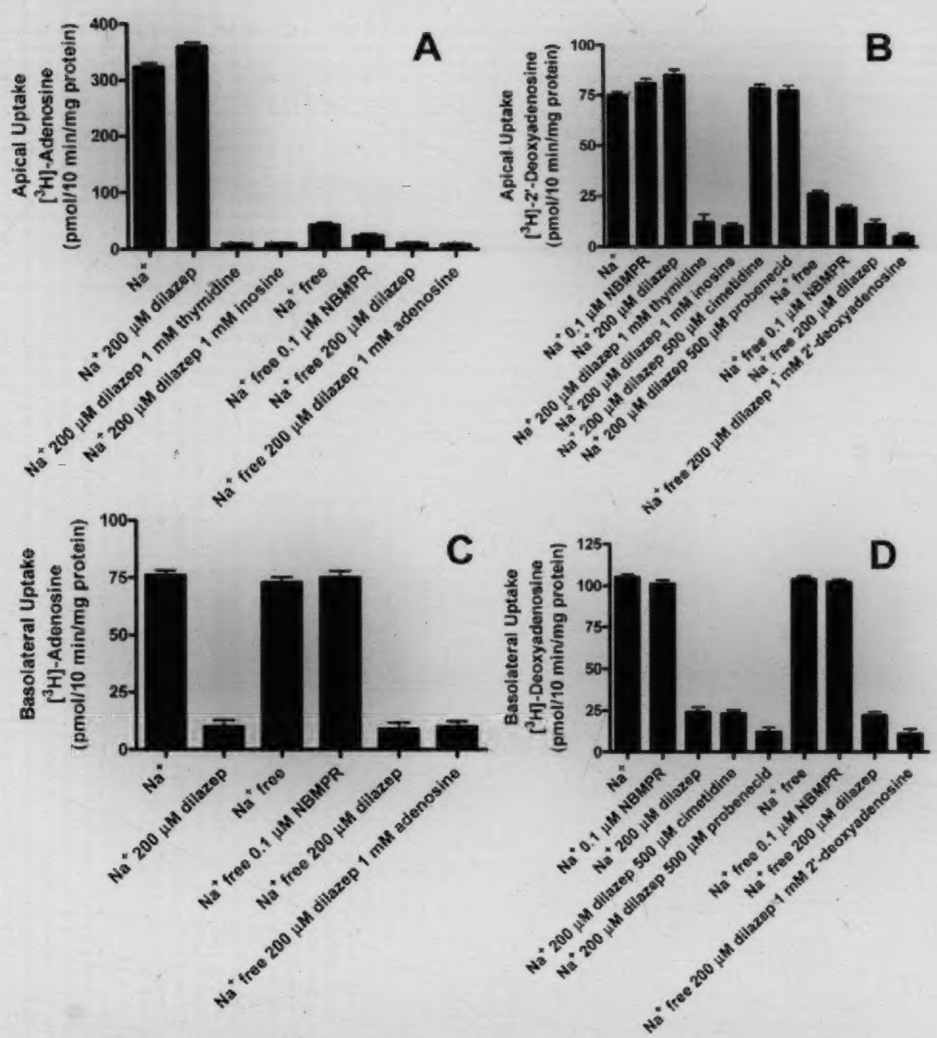

Figure V-4. Sodium dependence and inhibitor sensitivities of apical and basolateral uptake of adenosine and 2′-deoxyadenosine into polarized hRPTC11 cultures. Apical uptake of 1 µM (A) [^{3}H]-adenosine or (B) [^{3}H]-2′-deoxyadenosine and basolateral uptake of 1 µM (C) [^{3}H]-adenosine or (D) [^{3}H]-2′-deoxyadenosine was measured at 10 min into polarized monolayers of hRPTC1 in various buffers containing 500 µM EHNA with or without the indicated inhibitors as described in Materials and Methods (Section II.5). Values are means (± standard deviation) for three independent experiments each with triplicate measurements. Error bars are absent where the data symbols were larger than the standard deviation values.

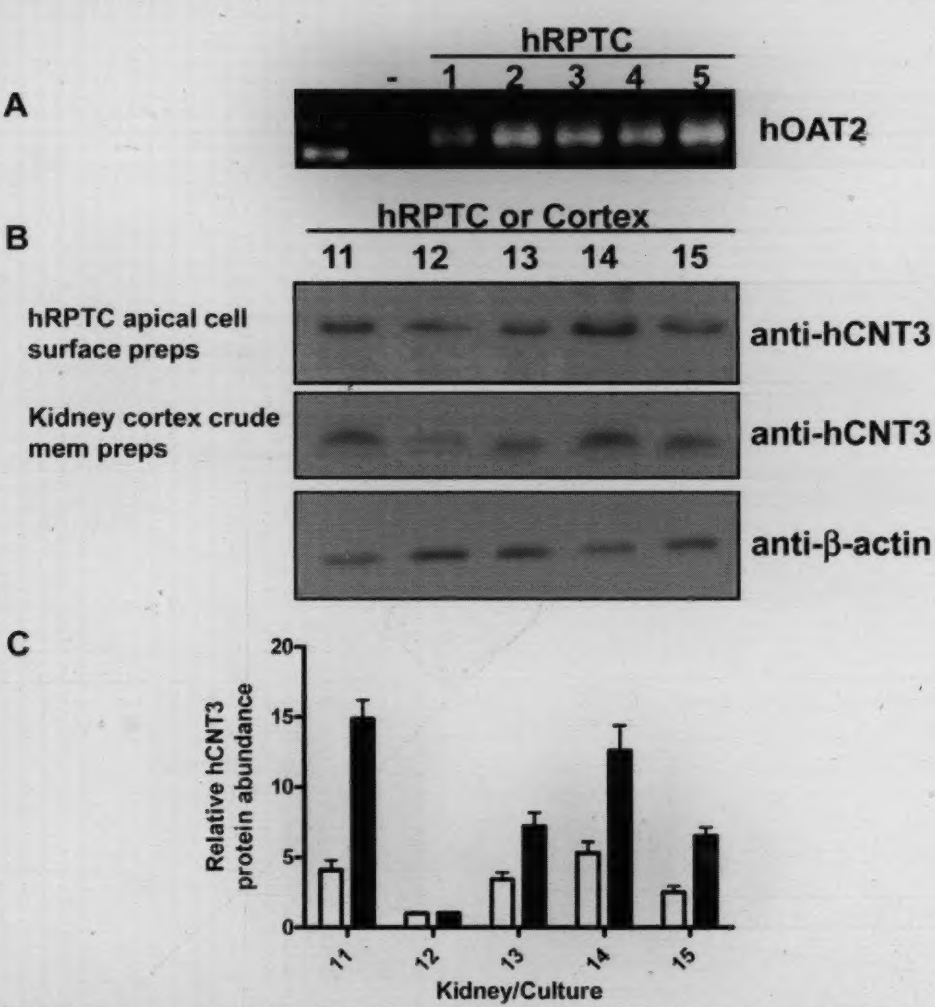

Figure V-5. Expression of hOAT2 mRNA and abundance of hCNT3 protein on apical cell surfaces in polarized hRPTC cultures. (A) Transcripts were assessed by RT-PCR analysis using hOAT2-specific primers in total RNA preparations from each of five different polarized hRPTC monolayer cultures as described in Materials and Methods (Section II.8). Negative controls (-) consisted of reactions in the absence of reverse transcriptase to control for genomic DNA contamination. (B) The presence of hCNT3 in apical cell surface protein preparations of polarized hRPTC cultures and crude membranes from corresponding human kidney cortex tissues (*i.e.*, from which the hRPTCs were isolated) were assessed by immunoblotting using anti-hCNT3 monoclonal antibodies as described in Materials and Methods (Section II.9). Bands corresponding to hCNT3 or β-actin (loading control) were visualized using horseradish peroxidase conjugated anti-IgG antibodies and Enhanced Chemiluminescence. (C) The relative quantities of apical cell surface hCNT3 were assessed by quantitative immunoblotting using anti-hCNT3 monoclonal antibodies as described in Materials and Methods (Section II.9) in (i) apical cell surface protein preparations from each of five different hRPTC cultures (open bars), and (ii) crude membranes from corresponding human kidney cortex tissues (*i.e.*, from which the hRPTCs were isolated) (solid bars). Bands corresponding to hCNT3 were quantified using AlexaFluor488 conjugated anti-IgG antibodies and a Typhoon multimode scanner. Bar graph values are means (± standard errors of measurement) from triplicate experiments. Samples for which error bars are absent had errors equal to or smaller than the border size of the bars.

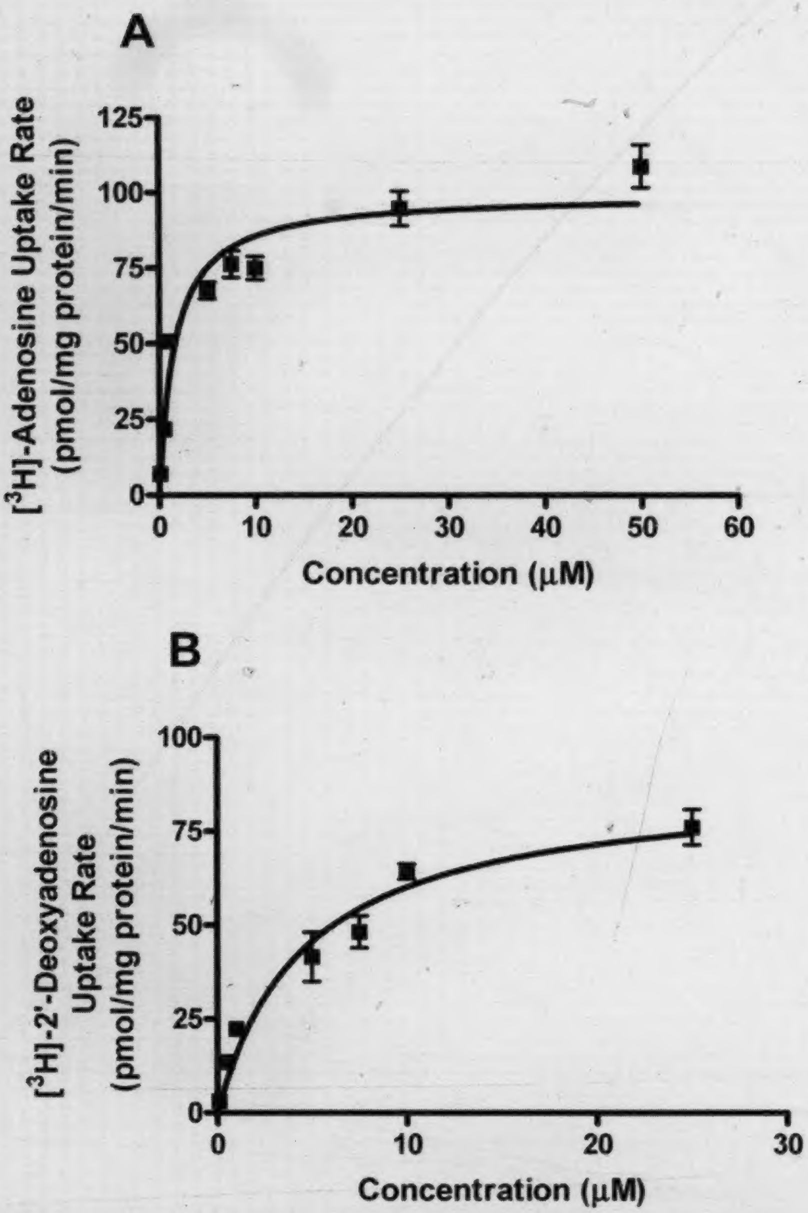

Figure V-6. Transportability of adenosine and 2'-deoxyadenosine by recombinant hCNT3 in yeast. The concentration dependence of initial rates of uptake of (A) [^{3}H]-adenosine and (B) [^{3}H]-2'-deoxyadenosine into yeast producing recombinant hCNT3 was determined in sodium-containing buffer as described in Materials and Methods (Section II.5). Values are means (± standard deviation) from triplicate independent experiments.

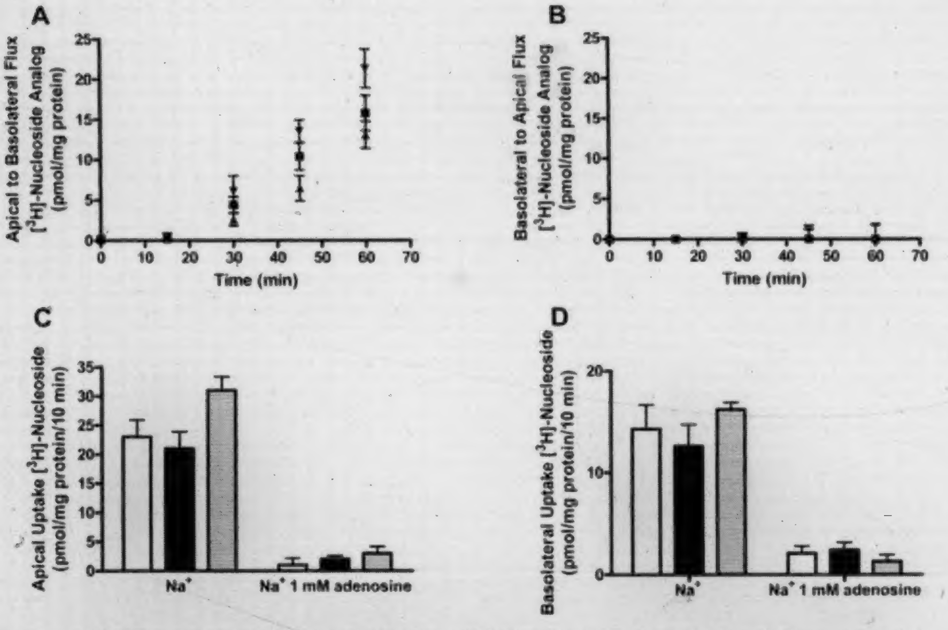

Figure V-7. Demonstration of preferential apical-to-basolateral fluxes and apical mediated uptake of fludarabine, cladribine, and clofarabine across polarized hRPTC11 cultures. Apical–to-basolateral (A) and basolateral-to-apical (B) fluxes of 10 μM [^{3}H]-fludarabine (■),[^{3}H]-cladribine (▲), or [^{3}H]-clofarabine (▼) across polarized hRPTC11 cultures in sodium-containing buffer were measured as described in Materials and Methods (Section II.5). Apical (C) and basolateral (D) uptake of 10 μM [^{3}H]-fludarabine (open bars), [^{3}H]-cladribine (solid bars), or [^{3}H]-clofarabine (hatched bars) into polarized hRPTC11 cultures was measured in sodium-containing buffer in the presence (non-mediated uptake) or absence (total uptake) of 1 mM non-radiolabeled adenosine as described in Materials and Methods. Values are means (± standard deviation) for three independent experiments each with triplicate measurements. Error bars are absent where the data symbols were larger than the standard deviation values.

Table V-1. Summary of TEER measurements[a] and immunoflourescent staining[b] for tight junction protein ZO-1 and cell adhesion protein E-CAD in polarized hRPTC monolayer cultures.

Culture	TEER values after 10 days in culture[a]	Immunofluorescent staining	
	Ω·cm^2	ZO-1	E-CAD
hRPTC11	97 ± 5	apical between cells	basolateral between cells
hRPTC12	102 ± 8	apical between cells	basolateral between cells
hRPTC13	94 ± 6	apical between cells	basolateral between cells
hRPTC14	112 ± 11	apical between cells	basolateral between cells
hRPTC15	107 ± 9	apical between cells	basolateral between cells

a - TEER measurements were performed on polarized monolayer cultures of hRPTCs isolated from five different individuals (hRPTC11 through hRPTC15, Table II-1) as described in Materials and Methods (Section II.3). Values represent means ± standard deviations from three independent experiments, each with triplicate measurements.

b - Immunofluorescence with anti-ZO-1 or -E-CAD antibodies was performed on polarized monolayer cultures of hRPTCs isolated from five different individuals (hRPTC11 through hRPTC15, Table II-1) as described in Materials and Methods (Section II.4).

Table V-2. Analysis of adenosine and 2'-deoxyadenosine metabolites after apical-to-basolateral transepithelial fluxes of 1 µM [^{3}H]-adenosine and after basolateral-to-apical transepithelial fluxes of 1 µM [^{3}H]-2'-deoxyadenosine across polarized hRPTC11 monolayers after 60 min.[a]

Metabolite	Adenosine metabolites recovered in basolateral (% radioactivity loaded)		Adenosine metabolites recovered intracellularly (% radioactivity loaded)	
	Na^{+}[c]	Na^{+} 500 µM EHNA[c]	Na^{+}[c]	Na^{+} 500 µM EHNA[c]
Phosphorylated	10.7 ± 1.8	15.6 ± 2.1	29.1 ± 2.3	37.6 ± 5.1
Adenosine	31.5 ± 3.3	72.3 ± 5.8	6.5 ± 0.9	45.7 ± 4.3
Inosine	21.2 ± 2.6	3.2 ± 2.6	3.3 ± 0.7	5.1 ± 1.3
Hypoxanthine	20.9 ± 4.1	4.3 ± 1.9	53.2 ± 4.5	6.8 ± 1.2
Other[b]	15.7 ± 2.5	4.6 ± 2.6	7.9 ± 2.3	4.8 ± 2.6
Metabolite	2'-Deoxyadenosine metabolites recovered in (% radioactivity loaded)		2'-Deoxyadenosine metabolites recovered (% radioactivity loaded)	
	Na^{+}[c]	Na^{+} 500 µM EHNA[c]	Na^{+}[c]	Na^{+} 500 µM EHNA[c]
Phosphorylated	15.2 ± 1.7	20.7 ± 2.5	9.8 ± 1.1	11.2 ± 2.4
2'-Deoxyadenosine	35.6 ± 4.5	68.3 ± 3.9	7.2 ± 1.5	73.5 ± 5.3
2'-Deoxyinosine	10.1 ± 3.2	5.2 ± 1.8	6.6 ± 1.6	5.4 ± 1.0
Hypoxanthine	30.4 ± 2.7	4.5 ± 1.3	75.9 ± 6.3	4.7 ± 1.6
Other[b]	9.2 ± 2.5	1.3 ± 2.3	0.5 ± 2.6	5.2 ± 2.5

a - Thin layer chromatography analyses of metabolites were performed as described in Materials and Methods (Section II.6). Values represent means ± standard deviations from three independent experiments.

b - "Other" constitutes unidentified spots on thin layer chromatography plates that were pooled.

c - Na^{+} denotes sodium-containing buffer.

Table V-3. Summary of 1 µM [^{3}H]-adenosine transepithelial fluxes[a] and uptake[b] in polarized hRPTC monolayers.

Culture	Adenosine			
	Apical-to-basolateral transepithelial fluxes[a]			Apical hCNT3-mediated uptake[b,d]
	Sodium-containing buffer (Control)[c]	Sodium-free buffer[c]		
	(pmol/mg protein/60 min)	(pmol/mg protein/60 min)	(% reduction of control values)	(pmol/mg protein/10 min)
hRPTC11	133 ± 17	20 ± 2	85.3 ± 9.8	352 ± 14
hRPTC12	42 ± 8	4.7 ± 0.4	88.8 ± 7.8	97 ± 7
hRPTC13	79 ± 8	5.5 ± 0.6	93.7 ± 10.7	221 ± 13
hRPTC14	118 ± 13	11 ± 1	90.6 ± 11.1	307 ± 15
hRPTC15	71 ± 6	8 ± 1	80.8 ± 7.5	192 ± 11

a - Measurements of transepithelial fluxes of radiolabeled adenosine were performed as described in Materials and Methods (Section II.5). Values represent means ± standard deviations from three independent experiments.

b - Measurements of uptake of radiolabeled adenosine were performed as described in Materials and Methods (Section II.5). Values represent means ± standard deviations from three independent experiments.

c - Apical-to-basolateral fluxes of 1 µM [^{3}H]-adenosine across polarized hRPTC monolayers in sodium-containing buffer (Control) or in sodium-free buffer were measured as described in Materials and Methods (Section II.5).

d - Apical hCNT3-mediated uptake were measured as described in Materials and Methods (Section II.5) and calculated as described in Results (Section V.2.3).

Table V-4. Summary of 1 μM $[^3H]$-2'-deoxyadenosine transepithelial fluxes[a] and uptake[b] in polarized hRPTC monolayers

Culture	Basolateral-to-apical transepithelial fluxes[a]				
	Control[c]	0.1 μM NBMPR[c]		500 μM probenecid[c]	
	(pmol/mg protein/60 min)	(pmol/mg protein/60 min)	(% reduction of control values)	(pmol/mg protein/60 min)	(% reduction of control values)
hRPTC11	68 ± 7	0.065 ± 0.006	99.9 ± 9.1	56 ± 2	17.6 ± 4.2
hRPTC12	88 ± 9	0.18 ± 0.01	99.8 ± 7.9	68 ± 3	23.2 ± 4.1
hRPTC13	95 ± 10	2.8 ± 0.3	97.1 ± 9.8	81 ± 3	15.2 ± 4.2
hRPTC14	92 ± 7	0.83 ± 0.07	99.1 ± 8.9	73 ± 4	20.2 ± 5.9
hRPTC15	49 ±6	0.54 ± 0.05	98.9 ± 9.7	43 ± 2	12.6 ± 4.3

Culture	Basolateral mediated uptake[b,d]				
	Control[e]	200 μM dilazep[e]		200 μM dilazep, 500 μM probenecid[e]	
	(pmol/mg protein/10 min)	(pmol/mg protein/60 min)	(% reduction of control values)	(pmol/mg protein/60 min)	(% reduction of control values)
hRPTC11	94 ± 6	22 ± 1	77.1 ± 4.8	15.0 ± 0.7	84.0 ± 4.6
hRPTC12	119 ± 11	22 ± 2	81.3 ± 7.2	15.2 ± 0.8	87.2 ± 5.4
hRPTC13	124 ± 9	27 ± 1	78.3 ± 5.2	17.8 ± 0.9	85.7 ± 4.9
hRPTC14	133 ± 12	35 ± 2	73.9 ± 6.7	21 ± 1	83.9 ± 6.3
hRPTC15	76 ± 8	15.6 ± 0.9	79.5 ± 5.9	11.3 ± 0.4	85.2 ± 3.9

a - Measurements of transepithelial fluxes of radiolabeled 2'-deoxyadenosine were performed as described in Materials and Methods (Section II.5). Values represent means ± standard deviations from three independent experiments.
b - Measurements of uptake of radiolabeled 2'-deoxyadenosine were performed as described in Materials and Methods (Section II.5). Values represent means ± standard deviations from three independent experiments.

c - Basolateral-to-apical fluxes of 1 μM $[^3H]$-2'-deoxyadenosine across polarized hRPTC monolayers in sodium-containing buffer in the presence or absence (Control) of 0.1 μM NBMPR or 500 μM probenecid were measured as described in Materials and Methods (Section II.5).

d - Basolateral mediated uptake of 2'-deoxyadenosine were measured as described in Materials and Methods (Section II.5) and calculated as described in Results (Section V.2.3).

e - Basolateral mediated uptake of 1 μM $[^3H]$-2'-deoxyadenosine across polarized hRPTC monolayers in sodium-containing buffer in the presence or absence (Control) of 200 μM dilazep or 200 μM dilazep and 500 μM probenecid were measured as described in Materials and Methods (Section II.5).

Table V-5. Recovery of adenosine in basolateral compartments and 2'-deoxyadenosine in apical compartments after apical-to-basolateral transepithelial fluxes of 1 µM [^{3}H]-adenosine and after basolateral-to-apical transepithelial fluxes of 1 µM [^{3}H]-2'-deoxyadenosine across polarized hRPTC monolayers after 60 min.[a]

Culture	Adenosine recovered in basolateral compartments (% radioactivity loaded)		2'-Deoxyadenosine recovered in apical compartments (% radioactivity loaded)	
	Na^{+}[b]	Na^{+} 500 µM EHNA[b]	Na^{+}[b]	Na^{+} 500 µM EHNA[b]
hRPTC11	31.5 ± 3.3	72.3 ± 5.8	35.6 ± 4.5	68.3 ± 3.9
hRPTC12	24.3 ± 4.5	60.7 ± 4.2	39.4 ± 3.2	63.8 ± 5.7
hRTPC13	36.6 ± 3.1	79.8 ± 4.7	34.6 ± 4.8	75.3 ± 5.5
hRPTC14	30.1 ± 3.6	75.9 ± 6.2	36.3 ± 4.6	71.9 ± 5.8
hRPTC15	28.6 ± 3.8	72.3 ± 5.7	35.1 ± 5.5	77.8 ± 6.5

a - Thin layer chromatography analyses of metabolites were performed as described in Materials and Methods (Section II.6). Values represent means ± standard deviations from three independent experiments.

b - Na^{+} denotes sodium-containing buffer.

Table V-6. Summary of apical-to-basolateral transepithelial fluxes and apical mediated uptake of 1 µM [^{3}H]-fludarabine, -cladribine, and -clofarabine in polarized hRPTC monolayers.[a]

Culture	Apical-mediated uptake[b] (pmol/mg protein/10 min)			Apical-to-basolateral fluxes (pmol/mg protein/60 min)		
	fludarabine	cladribine	clofarabine	fludarabine	cladribine	clofarabine
hRPTC11	22 ± 5	19 ± 5	28 ± 4	16 ± 4	13 ± 3	21 ± 4
hRPTC12	8 ± 2	7 ± 1	13 ± 4	9 ± 1	10 ± 2	8 ± 2
hRPTC13	19 ± 4	28 ± 5	30 ± 5	14 ± 3	15 ± 3	19 ± 4
hRPTC14	24 ± 3	18 ± 5	32 ± 6	19 ± 5	15 ± 6	24 ± 3
hRPTC15	15 ± 3	19 ± 4	23 ± 3	11 ± 2	13 ± 4	17 ± 5

a - Uptake and transepithelial flux assays performed as described in Materials and Methods (Section II.5). Values represent means ± standard deviations from three independent experiments.
b - Apical mediated uptake was calculated as described in Results (Section V.2.7).

V.4 Bibliography

1. Kuttesch JF Jr Nelson JA. Renal handling of 2′-deoxyadenosine and adenosine in humans and mice. Cancer Chemother Pharmacol. 1982; 8: 221-229.

2. Nelson JA, Kuttesch JR Jr, Herbert BH. Renal secretion of purine nucleosides and their analogs in mice. Biochem Pharmacol. 1983; 32: 2323-2327.

3. Nelson JA, Vidale E, Enigbokan M. Renal transepithelial transport of nucleosides. Drug Metab. 1988; 16: 789-792.

4. Young JD, Yao SYM, Sun L, Cass CE, Baldwin SA. Human equilibrative nucleoside transporter (ENT) family of nucleoside and nucleobase transporter proteins. Xenobiotica. 2008; 38: 995-1021.

5. Pastor-Anglada M, Cano-soldado P, Errasti-murugarren E, Casado FJ. SLC28 genes and concentrative nucleoside transporter (CNT) proteins. Xenobiotica. 2008; 38: 972-994.

6. Griffiths M, Beaumont N, Yao SYM, Sundaram M, Boumah CE, Davies A, Kwong FYP, Coe I., Cass CE, Young JD, Baldwin SA. Cloning of a human nucleoside transporter implicated in the cellular uptake of adenosine and chemotherapeutic drugs. Nat Med. 1997; 3: 89–93.

7. Griffiths M, Yao SYM, Abidi F, Phillips SEV, Cass CE, Young JD, Baldwin SA. Molecular cloning and characterization of a nitrobenzylthioinosine-insensitive (ei) equilibrative nucleoside transporter from human placenta. Biochem J. 1997; 328: 739–743.

8. Baldwin SA, Yao SYM, Hyde RJ, Foppolo S, Barnes K, Ritzel MWL, Cass CE, Young, JD. Functional characterization of novel human mouse equilibrative nucleoside transporters (hENT3 and mENT3) located in intracellular membranes. J Biol Chem. 2005; 280: 15880-15887.

9. Barnes K, Dobrzynski H, Foppolo S, Beal PR, Ismat F, Scullion ER, Sun L, Tellez J, Ritzel MW, Claycomb WC, Cass CE, Young JD, Billeter-Clark R, Boyett MR, Baldwin SA. Distribution and functional characterization of equilibrative nucleoside transporter-4, a novel cardiac adenosine transporter activated at acidic pH. Circ Res. 2006; 99: 510-9.

10. Ritzel MW, Yao SY, Huang MY, Elliott JF, Cass CE, Young JD. Molecular cloning and functional expression of cDNAs encoding a human Na+ nucleoside cotransporter (hCNT1). Am J Physiol Cell Physiol 1997; 272: C707– C714.

11. Wang J, Su SF, Dresser MJ, Schaner ME, Washington CB, Giacomini KM. Na+ dependent purine nucleoside transporter from human kidney: cloning and functional characterization. Am J Physiol Renal Physiol 1997; 273: F1058–F1065.

12. Ritzel MW, Yao SY, Ng AM, Mackey JR, Cass CE, Young JD. Molecular cloning, functional expression and chromosomal localization of a cDNA encoding a human Na+/nucleoside cotransporter (hCNT2) selective for purine nucleosides and uridine. Mol Membr Biol 1998; 15: 203– 211.

13. Ritzel MW, Ng AM, Yao SY, Graham K, Loewen SK, Smith KM, Ritzel RG, Mowles DA, Carpenter P, Chen XZ, Karpinski E, Hyde RJ, Baldwin SA, Cass CE, Young JD. Molecular identification and characterization of novel human and mouse concentrative Na+ nucleoside cotransporter proteins (hCNT3 and mCNT3) broadly selective for purine and pyrimidine nucleosides (system cib). J Biol Chem 2001; 276: 2914–2927.

14. Mangravite LM, Lipschutz JH, Mostov KE, Giacomini KM. Localization of GFP-tagged concentrative nucleoside transporters in a renal polarized epithelial cell line. Am J Physiol Renal Physiol. 2001; 280: F879-F885.

15. Lai Y, Bakken AH, Unadkat JD. Simultaneous expression of hCNT1-CFP and hENT1-YFP in Madin-Darby canine kidney cells. Localization and vectorial transport studies. J Biol Chem. 2002; 277: 37711-7.

16. Mangravite LM, Badagnani I, Giacomini KM. Nucleoside transporters in the disposition and targeting of nucleoside analogs in the kidney. Eur J Pharmacol. 2003; 479: 269-281.

17. Mangravite LM, Xiao G, Giacomini KM. Localization of human equilibrative nucleoside transporters, hENT1 and hENT2, in renal epithelial cells. Am J Physiol Renal Physiol. 2003; 284: F902-F910.

18. Errasti-Murugarren E, Pastor-Anglada M, and Casado FJ. Role of CNT3 in the transepithelial flux of nucleosides and nucleoside-derived drugs. J Physiol. 2007; 582: 1249-60.

19. Govindarajan R, Leung GP, Zhou M, Tse CM, Wang J, Unadkat JD. Facilitated Mitochondrial Import of Anti-viral and Anti-cancer Nucleoside Drugs by Human Equilibrative Nucleoside Transporter-3 (hENT3). Am J Physiol Gastrointest Liver Physiol 2009 Jan 22. [Epub ahead of print]

20. Xia L, Engel K, Zhou M, Wang J. Membrane localization and pH-dependent transport of a newly cloned organic cation transporter (PMAT) in kidney cells. Am J Physiol Renal Physiol. 2007; 292: F682-90.

21. Gutierrez MM, Brett CM, Ott RJ, Hui AC, Giacomini KM. Nucleoside transport in brush border membrane vesicles from human kidney. Biochim Biophys Acta. 1992; 1105: 1-9.

22. Govindarajan R, Bakken AH, Hudkins KL, Lai Y, Casado FJ, Pasto-Anglada M, Tse CM, Hayashi J, Unadkat JD. In situ hydribdization and immunolocalization of concentrative and equilibrative nucleoside transporters in the human intestine, liver, kidneys, and placenta. Amer J Physiol Reg Int Comp Physiol. 2007; 293: R1809-R1822.

23. Chen R, Nelson JA. Role of organic cation transporters in the renal secretion of nucleosides. Biochem Pharmacol. 2000; 60: 215-219.

24. Chen R, Jonker JW, Nelson JA. Renal organic cation and nucleoside transport. Biochem Pharmacol. 2002; 64: 185-190.

25. Cropp CD, Komori T, Shima JE, Urban TJ, Yee SW, More SS, Giacomini KM. Organic anion transporter 2 (SLC22A7) is a facilitative transporter of cGMP. Mol Pharmacol. 2008; 73: 1151-1158.

26. Pastor-Anglada M, Cano-Soldado P, Molina-Arcas M, Lostao MP, Larráyoz I, Martínez-Picado J, Casado FJ. Cell entry and export of nucleoside analogues. Virus Res. 2005; 107: 151-164.

27. Johnson S, Smith AG, Löffler H, Osby E, Juliusson G, Emmerich B, Wyld PJ, Hiddemann W. Multicentre prospective randomised trial of fludarabine versus cyclophosphamide, doxorubicin, and prednisone (CAP) for treatment of advanced-stage chronic lymphocytic leukaemia. The French Cooperative Group on CLL. Lancet. 1996; 347: 1432-1438.

28. Robak T, Wierzbowska A, Robak E. Recent clinical trials of cladribine in hematological malignancies and autoimmune disorders. Rev Recent Clin Trials. 2006; 1: 15-34.

29. Jeha S, Gaynon PS, Razzouk BI, Franklin J, Kadota R, Shen V, Luchtman-Jones L, Rytting M, Bomgaars LR, Rheingold S, Ritchey K, Albano E, Arceci RJ, Goldman S, Griffin T, Altman A, Gordon B, Steinherz L, Weitman S, Steinherz P. Phase II study of clofarabine in pediatric patients with refractory or relapsed acute lymphoblastic leukemia. J Clin Oncol. 2006; 24: 1917-1923.

30. King KM, Damaraju VL, Vickers MF, Yao SY, Lang T, Tackaberry TE, Mowles DA, Ng AM, Young JD, Cass CE. A comparison of the transportability, and its role in cytotoxicity, of clofarabine, cladribine, and fludarabine by recombinant human nucleoside transporters produced in three model expression systems. Mol Pharmacol 2006; 69: 346-353.

31. Parker WB, Shaddix SC, Rose LM, et al. Comparison of the mechanism of cytotoxicity of 2-chloro-9-(2-deoxy-2-fluoro-ß-D-arabinofuranosyl)adenine, of 2-chloro-9-(2-deoxy-2-fluoro-ß-D-ribofuranosyl)adenine, and of 2-chloro-9-(2-deoxy-2,2-difluoro-ß-D-arabinofuranosyl)adenine in CEM cells. Mol Pharmacol 1999;55:515–20

32. Gandhi V, Huang P, Chapman A, et al. Incorporation of fludarabine and arabinosylcytosine 5′-triphosphates by DNA polymerase α: affinity, interaction, and consequences. Clin Cancer Res. 1997; 3: 1347-1355

33. Parker WB, Shaddix SC, Chang CH, et al. Effects of 2-chloro-9-(2-deoxy-2-fluoro-ß-D-arabinofuranosyl) adenine on K562 cellular metabolism and the inhibition of human ribonucleotide reductase and DNA polymerases by its 5'-trisphosphate. Cancer Res. 1991; 51: 2386–2394.

34. Parker WB, Bapat AR, Shen JX, Townsend AJ, Cheng YC. Interaction of 2-halogenated dATP analogs (F, Cl, and Br) with human DNA polymerases, DNA primase, and ribonucleotide reductase. Mol Pharmacol. 1988; 34: 485–491.

35. Gandhi V, Plunkett W. Cellular and clinical pharmacology of fludarabine. Clin Pharmacokinet. 2002; 41: 93−103.

36. Lindemalm S, Savic RM, Karlsson MO, Juliusson G, Liliemark J, Albertioni F. Application of population pharmacokinetics to cladribine. BMC Pharmacol. 2005; 5: 4.

37. Gandhi V, Plunkett W, Bonate PL, Du M, Nowak B, Lerner S, Keating MJ. Clinical and pharmacokinetic study of clofarabine in chronic lymphocytic leukemia: strategy for treatment. Clin Cancer Res. 2006; 12: 4011-4017.

38. Kantarjian HM, Gandhi V, Kozuch P, Faderl S, Giles F, Cortes J, O'Brien S, Ibrahim N, Khuri F, Du M, Rios MB, Jeha S, McLaughlin P, Plunkett W, Keating MPhase I clinical and pharmacology study of clofarabine in patients with solid and hematologic cancers. J Clin Oncol. 2003; 21: 1167-1173.

39. Morshed KM, McMartin KE. Reabsorptive and secretory 5-methyltetrahydrofolate transport pathways in cultured human proximal tubule cells. Am J Physiol Renal Physiol. 1997; 272: F380-388.

40. Morshed KM, Ross DM, McMartin KE. Folate transport proteins mediate the bidirectional transport of 5-methyltetrahydrofolate in cultured human proximal tubule cells. J Nutr. 1997; 127: 1137-1147.

41. Morshed KM, McMartin KE. Transient alterations in cellular permeability in cultured human proximal tubule cells: implications for transport studies. In Vitro Cell Dev Biol Anim. 1995; 31: 107-114.

42. Whitin JC, Bhamre S, Tham DM, Cohen HJ. Extracellular glutathione peroxidase is secreted basolaterally by human renal proximal tubule cells. Am J Physiol Renal Physiol 2002; 283: F20-28.

43. Dantzler WH. Regulation of renal proximal and distal tubule transport: sodium, chloride and organic anions. Comp Biochem Physiol A Mol Integr Physiol. 2003; 136: 453-478.

44. Siliciano JD, Goodenough DA. Localization of the tight junction protein, ZO-1, is modulated by extracellular calcium and cell-cell contact in Madin-Darby canine kidney epithelial cells. J Cell Biol. 1988; 107: 2389-2399.

45. Miranda KC, Khromykh T, Christy P, Le TL, Gottardi CJ, Yap AS, Stow JL, Teasdale RD. A dileucine motif targets E-cadherin to the basolateral cell

surface in Madin-Darby canine kidney and LLC-PK1 epithelial cells. J Biol Chem. 2001; 276: 22565-22572.

46. Wu JC, Gregory CW, DePhilip RM. P-cadherin and E-cadherin are co-expressed in MDCK cells. Biochem Biophys Res Commun. 1993; 195: 1329-1335.

47. Saito H, Nishimura M, Shinano H, Makita H, Tsujino I, Shibuya E, Sato F, Miyamoto K, Kawakami Y. Plasma concentrations of adenosine during normoxia and moderate hypoxia in humans. Am J Respir Crit Care Med. 1999; 159: 1014–1018.

48. Zou AP, Nithipatikom K, Li PL, Cowley AW Jr. Role of renal medullary adenosine in the control of blood flow and sodium excretion. Am J Physiol Reg Int Comp Physiol. 1999; 45: R790–798.

49. Wiginton DA, Coleman MS, Hutton JJ. Purification, characterization and radioimmunoassay of adenosine deaminase from human leukaemic granulocytes. Biochem J. 1981; 195: 389-397.

50. Lash LH, Putt DA, Cai H. Membrane transport function in primary cultures of human proximal tubular cells. Toxicol. 2006; 228: 200-218.

51. Govindarajan R, Leung GP, Zhou M, Tse CM, Wang J, Unadkat JD. Facilitated Mitochondrial Import of Anti-viral and Anti-cancer Nucleoside Drugs by Human Equilibrative Nucleoside Transporter-3 (hENT3). Am J Physiol Gastrointest Liver Physiol 2009 Jan 22. [Epub ahead of print]

52. Engel K, Zhou M, Wang J. Identification and characterization of a novel monoamine transporter in the human brain. J Biol Chem. 2004; 279: 50042-50049.

53. Blackburn JG, Hazen-Martin DJ, Detrisac CJ, Sens DA. Electrophysiology and ultrastructure of cultured human proximal tubule cells. Kidney Int. 1988; 33: 508-516.

54. Hayer-Zillgen M, Brüss M, Bönisch H. Expression and pharmacological profile of the human organic cation transporters hOCT1, hOCT2 and hOCT3. Br J Pharmacol. 2002; 136: 829-836.

55. Dantzler WH. Regulation of renal proximal and distal tubule transport: sodium, chloride and organic anions. Comp Biochem Physiol A Mol Integr Physiol 2003; 136: 453-478.

56. Slugoski MD, Ng AM, Yao SY, Smith KM, Lin CC, Zhang J, Karpinski E, Cass CE, Baldwin SA, Young JD. A proton-mediated conformational shift identifies a mobile pore-lining cysteine residue (C561) in human concentrative nucleoside transporter 3 (hCNT3). J Biol Chem. 2008; 283:8496-8507.

Chapter VI.

VI. Conclusion

The significant achievement of this thesis was the development of a descriptive model for renal proximal tubular handling of physiological nucleosides and nucleoside analog drugs (Figure VI-1). In the studies of Chapter III, the purine and pyrimidine nucleoside-transporting human equilibrative nucleoside transporter 1 (hENT1) and human concentrative nucleoside transporter 3 (hCNT3) were demonstrated to be present on apical membranes of human kidney proximal tubules by immunostaining methods. The nucleoside- and nucleobase-transporting hENT2 was demonstrated to be present in human kidney cortex tissue of which the majority of cells are proximal tubular epithelial cells. The production (from normal kidney specimens obtained from different individuals) of human renal proximal tubule cell (hRPTC) cultures that retained proximal tubular characteristics and endogenous hENT1, hENT2, and hCNT3 activities provided an *in vitro* model system that was used to investigate the roles of hENT1, hENT2, and hCNT3 in proximal tubular reabsorption or secretion of nucleosides. The studies described in Chapter V provided evidence for a framework in which the direction and extent of proximal tubular transepithelial fluxes of nucleosides could be understood. Coupling of apical hCNT3 to basolateral hENT2 mediated proximal tubular apical-to-basolateral (*i.e.*, ”reabsorptive”) transepithelial fluxes of adenosine, fludarabine (9-β-D-arabinosyl-2-fluoroadenine), cladribine (2-chloro-2′-deoxyadenosine), and clofarabine (2-chloro-2′-fluoro-deoxy-9-β-D-arabinofuranosyladenine) in polarized hRPTC monolayer cultures (Figure V1-1). On the other hand, coupling of basolateral human organic anion transporters (hOATs) to apical hENT1 mediated proximal tubular basolateral-to-apical (*i.e.*, "secretive") transepithelial fluxes of 2′-deoxyadenosine in polarized hRPTC monolayer cultures (Figure VI-1). Evidence was presented that demonstrates that hCNT3 was a determinant of cellular uptake and cytotoxicity of fludarabine (see also Chapter IV) and of adenosine, fludarabine, and clofarabine reabsorptive fluxes in different polarized hRPTC monolayer cultures.

VI.1 Model for renal proximal tubular handling of nucleosides by hENTs and hCNTs

Previous proposed models for renal handling of nucleosides by hNTs have attributed renal reabsorption of nucleosides to coupling of apical hCNT1/2/3 with basolateral hENT1/2 [1] and renal secretion of 2′-deoxyadenosine to lower apparent affinities of hCNT1 for 2′-deoxyadenosine than for adenosine [2]. Those models relied on evidence from localization studies of recombinant hNT-Green Fluorescent Protein (GFP) fusion proteins in transfected renal epithelial cell lines of non-human origin [1,2]. An important aspect of generating a detailed model for renal handling by hNTs of nucleosides in humans, was to first acquire knowledge of the segmental distribution, anatomic locations, and functional activities of endogenous hENTs and hCNTs in human nephrons. This was accomplished for both human kidney tissues and hRPTCs by a combination of reverse transcriptase polymerase chain reaction (RT-PCR), immunoblotting, immunostaining, whole cell radiolabeled nucleoside uptake, and transepithelial radiolabeled nucleoside flux assays.

Analysis of the expression profiles of hNT messenger ribonucleic acid (mRNA) and the relative abundances of hNT proteins in human kidney cortex tissues and hRPTCs (Chapter III, Section III.2.1.2; Chapter IV, Section IV.2.1, IV.2.2) and characterization of hNT activities in hRPTCs (Chapter III, Section III.2.3; Chapter IV, Section IV.2.4) revealed hENT1, hENT2, and hCNT3 as the endogenous hNTs present in human kidney proximal tubule cells (Chapter III, IV), the main site of reabsorption of solutes [3]. Although mRNA transcripts for hCNT1 and hCNT2 were present in both human kidney cortex tissues (Chapter III, Section III.2.1.1) and hRPTCs (Chapter IV, Section IV.2.1), hCNT1 and hCNT2 were either not present, or below the limits of detection of immunological and/or functional assays, in human kidney cortex tissues (Chapter III, Section III.2.1.2) and hRPTCs (Chapter III, Section III.2.3.4; Chapter IV, Section IV.2.4; Chapter V, Section V.2.3). The evidence that hENT1, hENT2, and hCNT3 are endogenous hNTs in human kidney proximal tubule cells fits well with previous observations of the presence of mRNA transcripts for all seven known hNTs in human kidney tissue RNA [4-13], of which many cell types other than proximal tubules are present. hCNT1-like activities have been observed in human kidney brush border membrane vesicles [14], derived primarily from apical membranes of human kidney proximal tubules. The hCNT1-like activities observed were also able to transport guanosine, perhaps reflecting the effects of a known naturally occurring variant of hCNT1 which enhances sensitivity to inhibition of transport by guanosine [15]. The evidence for lack of hCNT1 involvement as an endogenous hNT of human kidney proximal tubules is evidenced by functional assays in hRPTCs (Chapter IV, Section IV.2.4; Chapter V, Section V.2.3). The discrepancy between the present work and the previous demonstration of the presence of hCNT1-like activities in apical membranes [14] of human kidney proximal tubules may be a result of: (i) the limits of detection of functional assays, or (ii) the unclear molecular identity of hCNT1-like activities observed [14,15]. Later studies showed that the hCNT1-like activities in human kidney brush border membrane vesicles were not sensitive to inhibition by zidovudine or cytarabine [16], both known permeants of hCNT1 (Table I.3).

Analysis of the immunostaining patterns of anti-hENT1 and -hCNT3 antibodies in human kidney tissues and the characterization of hNT activities at apical and basolateral membranes of polarized hRPTC monolayer cultures revealed that hENT1 and hCNT3 were present on apical membranes and hENT2 was present on basolateral membranes of human kidney proximal tubules (Chapter III, Section III.2.1.3; Chapter V, Section V.2.3). hCNT2 was not detected in crude membranes of human kidney cortex tissues or hRPTCs, of which the majority is composed of proximal tubule cells, by immunoblotting assays (Chapter III, Section III.2.1.2, Chapter IV, Section IV.2.2). Additionally, hCNT1 and hCNT2 activities were not detected in hRPTCs by whole cell nucleoside uptake assays (Chapter IV, Section IV.2.4; Chapter V, Section V.2.3). Subsequent to the present work, *in situ* hybridization and immunostaining studies in human kidney tissues identified hCNT1/2 in apical domains of proximal tubules and hENT1 in apical and basolateral domains of proximal tubules adjacent to corticomedullary junctions [17]. The latter studies relied on histological identification of nephron segments while the present work relied on antigenic identification, which is more stringent. The discrepancy between the present work and other immunostaining studies [17] over the identification of hCNTs in human kidney proximal tubules may be a result of: (i) the limits of detection of immunological and/or functional assays in the present study and other studies [17], or (ii) the less stringent histological identification of nephron segments of other studies [17]. The novel finding of the present study that hENT1 is strictly an apical protein in human kidney proximal tubules and an apical and basolateral protein in other nephron segments clarifies the previous experimental discrepancies in the location of hENT1-Green Fluorescent Protein (GFP) fusion proteins in transfected renal epithelial cell lines, which has been a contentious issue [2,18]. The apical localization of hENT1 in the present study is also supported by: (i) evidence from previous studies with human kidney brush border membrane vesicles which identified sodium-independent uridine uptake processes [14], likely mediated by hENT1, and (ii) evidence from other immunostaining studies demonstrating hENT1 in apical membranes of human kidney proximal tubule cells adjacent to corticomedullary junctions [17]. Other immunostaining studies also identified hENT1 in basolateral membranes of human kidney proximal tubule cells adjacent to corticomedullary junctions [17], while the present work identified hENT1 only in apical membranes of human kidney cortical proximal tubules. The discrepancy between those studies [17] and the present work over the distribution and location of hENT1 in human kidney proximal tubules may be a result of: (i) differences in limits of detection of antibodies employed in respective studies, or (ii) less stringent histological identification of nephron segments of other studies [17].

Analysis of transepithelial fluxes of adenosine and 2′-deoxyadenosine across polarized hRPTC monolayer cultures (Chapter V, Section V.2.2), combined with the findings discussed above, led to the model for renal proximal tubular handling of nucleosides by hNTs presented in Figure VI-1. This model accounts for both the simultaneous renal reabsorption of adenosine and secretion of 2′-deoxyadenosine previously observed in mice and humans [19] and the apical location of hENT1 in proximal tubules (Chapter III, Section 2.1.3; Chapter V, Section V.2.3). Proximal tubular reabsorption of nucleosides from the lumen is accomplished by coupling of sodium- and proton-driven apical hCNT3 to basolateral equilibrating hENT2 (Figure VI-1). Proximal tubular secretion of nucleosides into the lumen is accomplished by coupling of basolateral electrogenically driven hOATs to apical equilibrating hENT1 (Figure VI-1). A previous model suggested that apical hCNT1 mediates selective reabsorption of adenosine and secretion of 2′-deoxyadenosine [2] on the basis of hCNT1 having a lower apparent affinity for 2′-deoxyadenosine than for adenosine [10-13]; however, the presence of hCNT2 [16] and/or hCNT3 (Chapter III, Section III.2.1.3; Chapter V, Section V.2.3), which both have higher transport capacities for adenosine and 2′-deoxyadenosine than hCNT1 [11-13], in apical membranes of proximal tubules raises doubt as to the physiological significance of hCNT1 involvement in renal proximal tubular handling of purine nucleosides. No evidence of hCNT2 in human kidney cortex tissues or hRPTCs by immunological and/or functional studies was found in the present work (Chapter III, Section III.2.1.1, III.2.3.4; Chapter IV, Section IV.2.2, IV.2.4; Chapter V, Section V.2.3). Additionally, there was no evidence of hCNT1 activity in the functional studies conducted with hRPTC cultures (Chapter III, Section III.2.3.4). Results of studies, performed during the course of the present work, in cultures of murine proximal convoluted tubule cells and hCNT3-GFP fusion protein transfected Madin-Darby Canine Kidney (MDCK) cell lines also suggested that coupling of apical CNT3 drives reabsorptive fluxes of various nucleosides [20].

Analysis of the uptake and transepithelial fluxes of fludarabine, cladribine, and clofarabine in polarized hRPTC monolayer cultures provided a basis for understanding the applicability of the proposed model for renal proximal tubular handling of nucleoside by hNTs to nucleoside analogs. Proximal tubular reabsorption of all three nucleosides appeared to be driven primarily by apical hCNT3 (Chapter IV, Section IV.2.5; Chapter V, Section V.2.7). These findings are consistent with recently reported results by others that suggested that CNT3 drives reabsorptive fluxes of fludarabine and various other nucleosides [20].

Analysis of uptake and cytotoxicity of fludarabine in different hRPTC monolayer cultures revealed strong relationships between hCNT3 cell surface protein abundance (Chapter IV, Section IV.2.3) and activities (Chapter IV, Section IV.2.4), extents of cellular fludarabine uptake (Chapter IV, Section IV.2.5), and fludarabine cytotoxicities (Chapter IV, Section IV.2.6). The degree of sensitivity of different hRPTC cultures to fludarabine was reflected in the differing protein and activity levels of hCNT3. Whether or not differences in hCNT3 protein or activity levels in proximal tubules exist in patient populations remains to be determined; however, such variations, primarily for hENT1, have been documented in tumors of several patient populations [21-27]. One prospective study has determined that hENT1 immunostaining levels in pancreatic tumor biopsies predict response to gemcitabine [26].

The proposed model shown in Figure VI-1 predicts that the direction and extent of a nucleoside's proximal tubular transepithelial fluxes depend on the relative abundances, turnover numbers, and apparent affinities of its various transporters, as well as their anatomic locations. This was confirmed by several findings in this thesis. First, the magnitude of cellular uptake of fludarabine into different hRPTCs was positively correlated with hCNT3 cell surface protein abundance and activity (Chapter IV, Section IV.2.5). Second, reabsorptive transepithelial fluxes of adenosine, fludarabine, and clofarabine across different polarized hRPTC monolayer cultures were positively correlated with levels of apical hCNT3 cell surface protein abundance and activities (Chapter V, Section V.2.2, V.2.3, V.2.5, V.2.7). Third, secretive transepithelial fluxes of 2′-deoxyadenosine across different polarized hRPTC monolayer cultures were related to (i) the levels of basolateral mediated uptake (Chapter V, Section V.2.2, V.2.3), (ii) the presence of basolateral hOAT activities and apical hENT1 activities (Section V.2.3, V.2.3, V.2.4), and (iii) the lower transportability of 2′-deoxyadenosine by hCNT3 as compared to that of adenosine (Chapter V, Section V.2.6). Precedents for inter-individual differences in hNT levels come from several immunohistochemical studies in various cancer tissues [21-27]. Previous experiments that demonstrated significant variations of hOAT and human organic cation transporter (hOCT) protein abundances in cultures of hRPTCs from different individuals [28] lend credence to the findings of variations in hCNT3 protein abundances and activities between different hRPTC cultures in the present work.

The extent and nature of nucleoside proximal tubular transepithelial fluxes are predicted by the model presented in Figure VI-1 to also depend on intracellular metabolism. Analysis of metabolism of adenosine during transepithelial fluxes across hRPTCs by thin layer chromatography confirmed this prediction. In the absence of inhibition of adenosine deaminase, intracellular and fluxed metabolites included the nucleobase hypoxanthine (Chapter V, Section V.2.2). Others in studies performed in murine proximal convoluted tubule cells with endogenous CNT3 and hCNT3-GFP fusion protein transfected MDCK cells observed similar phenomena with adenosine [20]. The presence of hENT2, which transports nucleosides and nucleobases [29], on basolateral membranes of proximal tubules in the proposed model (Figure VI-1) allows for equilibration of adenosine, 2′-deoxyadenosine and their nucleobase metabolite, hypoxanthine. Thus, basolateral hENT2 provides the potential of almost complete proximal tubular reabsorption of adenosine and its metabolic equivalents.

Future research to confirm the model proposed in this thesis should be aimed at identifying the hOATs present in polarized hRPTC monolayer cultures and delineating their involvement in 2′-deoxyadenosine secretive transepithelial fluxes. Work done in this study identified mRNA transcripts for hOAT2 (Chapter V, Section V.2.4), a transporter now implicated in 2′-deoxyguanosine and adenosine transport [30]. Furthermore, hENT4 has been identified in human kidney tissue lysates by immunoblotting [31], therefore, its anatomic locations in human kidney tissues should be defined once suitable antibodies for immunostaining experiments become available. The roles of hENT1, hENT2, and hCNT3 in transepithelial fluxes of other nucleosides across polarized hRPTC monolayer cultures should be defined including the purine physiological nucleosides guanosine and 2′-deoxyguanosine and the pyrimidine physiological and pharmacological nucleosides cytidine, 2′-deoxycytidine, gemcitabine, uridine, 5′-deoxy-5-fluorouridine, thymidine, and zidovudine (3′-azido-2′,3′-dideoxythymidine). Preliminary work has suggested that guanosine, cytidine, gemcitabine, uridine, thymidine, and 5′-deoxy-5-fluorouridine undergo reabsorptive transepithelial fluxes across polarized hRPTC monolayer cultures (Elwi AN & Cass CE, unpublished observations).

Lastly, an important question that should be addressed to obtain insights into regulation of hNTs in proximal tubules is why hCNT3 cell surface protein abundances and activities varied significantly between different hRPTC cultures. The present work examined hCNT3 levels with respect to its RNA expression by quantitative TaqMan RT-PCR (Chapter IV, Section IV.2.3), its total cellular and cell surface protein abundance by quantitative immunoblotting (Chapter IV, Section IV.2.3; Chapter V, Section V.2.5), and its uptake activities by whole cell radiolabeled nucleoside uptake assays (Chapter IV, Section IV.2.4; Chapter V, Section V.2.3). Variations in apical cell surface hCNT3 protein abundance between polarized hRPTC monolayer cultures were reflected in similar variations in total hCNT3 protein abundance in their matching proximal tubular tissues of origin (Chapter V, Section V.2.5) – *i.e.*, the variations were likely not a result of different growth states of hRPTC cultures or differences in proximal tubular cell type composition. No relationships between RNA and either protein or activity levels were observed in different hRPTC cultures; however, variations in total cellular hCNT3 protein abundance explained, in part, the variations in hCNT3 cell surface protein abundance and activities (Chapter IV, Section IV.2.4). This suggests that translational and post-translational, but not transcriptional, differences with respect to hCNT3 between cultures may have accounted for variations in hCNT3 protein and activity levels. Further studies should be undertaken to determine if hCNT3 in hRPTCs is regulated by post-translational modifications. Although hCNT3 possesses consensus sites for phosphorylation by protein kinase C, whether or not it is regulated by phosphorylation has not been determined. A connection between protein kinase C δ and/or ε and phorbol ester-mediated activation of cell surface hENT1 has been reported, but whether or not hENT1 is phosphorylated in the process is unknown [32]

V1.2 Other physiological roles of renal hNTs

The evidence presented in this thesis not only provided information useful to the proposal of a model for renal proximal tubular handling of nucleosides (Figure VI-1), but also contributed to a body of knowledge with respect to the anatomic locations of hENT1 and hCNT3 in other nephron segments. In the thick ascending limb of loop of Henle, hCNT3 is present in apical membranes while hENT1 is present in apical and basolateral membranes (Chapter III, Section III.2.1.3). In collecting ducts, hENT1 is present in apical and basolateral membranes while hCNT3 is absent (Chapter III, Section III.2.1.3). In the thick ascending limb of loop of Henle, where sodium gradient varies [3], hCNT3 may complete the reabsorption process of purine and pyrimidine nucleosides that was started in the proximal tubules. The unique ability of hCNT3, among hCNTs, to transport nucleosides with 2:1 sodium-to-nucleoside coupling ratio and co-transport nucleosides with protons [13,21], makes hCNT3 amenable to driving continuous nucleoside reabsorption throughout the human kidney nephron with varying sodium and proton gradients, including the proximal tubule and loop of Henle.

It is now being recognized that hNTs play more than just a salvage role in various tissues in which they are present. Knowledge of the relationship between hNTs and adenosine signalling has been expanding in recent years in brain cells, vascular endothelial cells, and cardiomyocytes [33,34]. Modulation of nephron tubule luminal adenosine concentrations available for interaction with adenosine receptors by hNTs is an unexplored area. Adenosine receptor signalling has important functions along the human nephron [35]. In proximal tubules, adenosine A_1 receptor activation stimulates sodium, bicarbonate, and phosphate reabsorption [35]. On the other hand, adenosine A_1 receptor activation in thick ascending limb of loop of Henle inhibits fluid reabsorption [35]. In collecting ducts, adenosine A_1 receptor activation decreases water permeability [35]. The work in this thesis provides a basis from which these relationships could be investigated. The presence of apical hENT1, along with apical hCNT3, in proximal tubules and thick ascending limb of loops of Henle (Chapter III, Section

III.2.1.3) suggests that hCNT3 may be involved in clearing adenosine from tubular lumens thereby limiting its availability to interact with adenosine receptors while hENT1 may release adenosine thereby prolonging its presence in tubular lumens. These physiological functions would be in addition to the involvement of apical hENT1 in nucleoside secretion and apical hCNT3 in nucleoside reabsorption. In collecting ducts, adenosine A_1 receptor stimulation inhibits the ability of the hormone vasopressin to stimulate formation of cAMP necessary for protein kinase A activation of water channel aquaporin 2 [35]. The resulting enhanced water permeability in collecting ducts is required for fluid reabsorption and formation of urine [35]. Collecting duct hENT1 may be involved in regulating extracellular concentrations of adenosine available for adenosine receptor activation and subsequent inhibition of vasopressin stimulation of water reabsorption. Similar roles for hENTs in physiology and pathophysiology has previously been defined in the heart, vasculature, and the brain [33]. Likewise, hENT1, along with hCNT3, in the thick ascending limb of the loop of Henle may be involved in tubuloglomerular feedback [34]. Investigations into the regulation of renal fluid reabsorption and glomerular filtration by hNTs may be fruitful in animal models in which genes encoding various hNTs are deleted.

Future research into relationships between renal hNTs and adenosine signalling could be aimed at investigating the distribution of hENT1 and adenosine receptors in human kidney tissue and the effects of renal hNTs on adenosine receptor functions in hRPTC cultures.

V1.3 Clinical consequences of renal hNTs

The concept that renal hNTs determine, in large part, the pharmacokinetics of nucleoside analogs was a guide to the experimental investigations undertaken in this thesis. In different polarized hRPTC monolayer cultures, the extent of reabsorptive fluxes of fludarabine and clofarabine reflected hCNT3 apical cell surface protein abundance and activities (Chapter V, Section V.2.7). It may be possible to rationally design individual chemotherapeutic schedules that take advantage of such differences, if they exist in patient populations, to minimize normal tissue toxicities and maximize therapeutic effects. Knowledge of the elimination kinetics of naturally occurring nucleosides, such as adenosine, may be useful in prediction of the pharmacokinetics of nucleoside analogs, such as fludarabine, in individual patients. Alternatively, if the hNT expression profile of a given tumor was shown to exhibit other hNTs than, or in addition to, hCNT3, the development and application of a hCNT3-specific inhibitor could be useful in modulating pharmacokinetics of nucleoside analogs given the prominent role of hCNT3 in renal proximal tubular reabsorption of nucleosides discovered in this work. Future research could be aimed at simultaneous investigations of pharmacokinetics of naturally occurring nucleosides and their structurally similar nucleoside analogs in patient populations.

Fludarabine nephrotoxicity is rare; nevertheless, it is potentially fatal [36-39]. Renal failure with fludarabine treatment is thought to occur by tumor lysis syndrome, whereby rapid killing of tumor cells releases uric acid which crystallizes in distal tubules [40]. Alternative mechanisms for tumor lysis syndrome include direct drug toxicity to constituent kidney epithelial cells resulting in renal flow defects, uric acid crystallization, and subsequent renal dysfunction. The present work demonstrated that fludarabine is directly cytotoxic to hRPTC cultures (Chapter IV, Section IV.2.6), highlighting a connection between renal proximal tubular handling by hNTs and renal proximal tubule cell toxicities. The degree of cytotoxicity of fludarabine to different hRPTC cultures was reflected in cellular fludarabine uptake and hCNT3 cell surface protein abundance and activities (Chapter IV, Section IV.2.4, IV.2.5, IV.2.6). Fludarabine is known to be cytotoxic to non-dividing cells [41-43], but the mechanisms behind this toxicity are not well defined. It has been suggested that inhibition of deoxyribonucleic acid (DNA) repair processes or RNA processing or transcription in non-dividing cells may account for this toxicity [41-43]. Alternatively, mounting evidence has implicated direct mitochondrial toxicity as a mechanism of nucleoside analog cytotoxicity in normal peripheral tissues composed of non-dividing cells [44]. Fludarabine-mediated mitochondrial toxicity in human leukemia cells treated in combination with a histone deacetylase inhibitor has been reported [45] as has cladribine- and clofarabine-mediated mitochondrial toxicity in chronic lymphocytic leukemia cells [46]. Fludarabine, cladribine, and clofarabine can be phosphorylated in mitochondria by deoxyguanosine kinase and their triphosphates incorporated into mitochondrial DNA by DNA polymerase γ [36]. Inhibition of mitochondrial DNA synthesis, decreases in 2′-deoxynucleotide pools available for cytochrome c binding and inhibition of apoptosome formation, or direct binding of nucleoside analog triphosphates to proteins on inner mitochondrial membrane are all conceivable avenues that could lead to mitochondria damage and/or mitochondria-mediated programmed cell death [45-47]. Potential cytotoxicity of cladribine and clofarabine to hRPTCs should also be investigated, as should differences in intracellular metabolism of fludarabine, cladribine, and clofarabine between different hRPTC cultures. Future research could also be aimed at investigating mechanisms of cytotoxicity of these purine nucleoside analogs in hRPTC cultures.

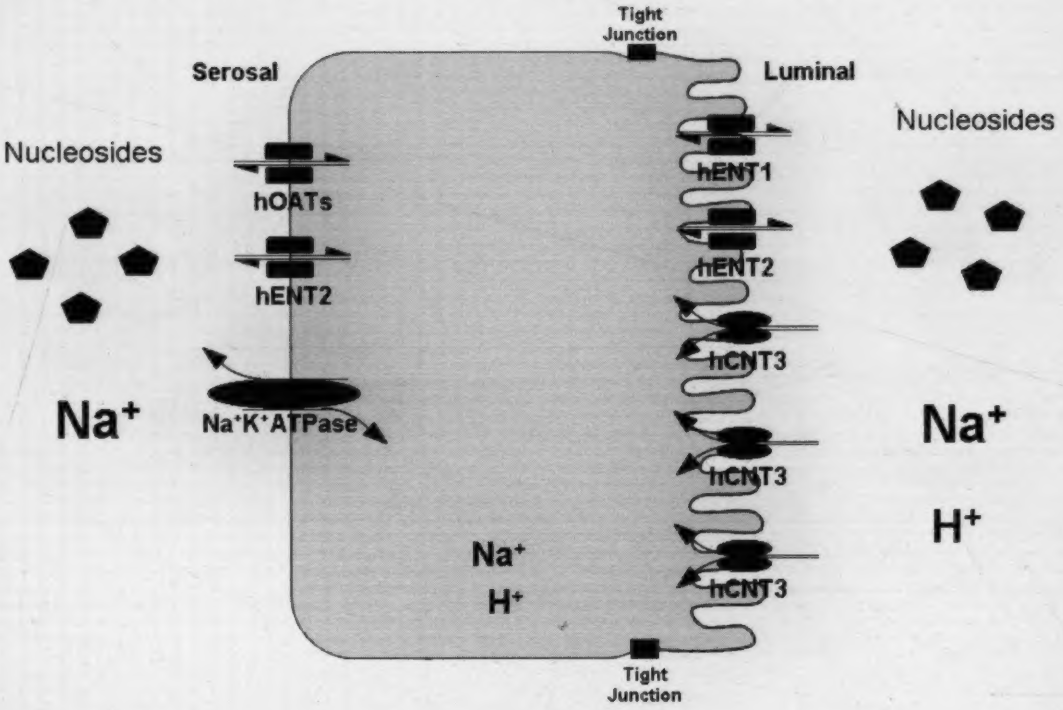
Tight Junction
Serosal
Luminal
Nucleosides
hOATs
hENT2
Nucleosides
hENT1
hENT2
hCNT3
Na+
Na+K+ATPase
Na+
hCNT3
H+
Na+
H+
hCNT3
Tight Junction

Figure VI-1. Model of renal proximal tubule handling of nucleoside by hNTs.

V1.4 Bibliography

1. Mangravite LM, Badagnani I, Giacomini KM. Nucleoside transporters in the disposition and targeting of nucleoside analogs in the kidney. Eur J Pharmacol. 2003; 479: 269-281.

2. Lai Y, Bakken AH, Unadkat JD. Simultaneous expression of hCNT1-CFP and hENT1-YFP in Madin-Darby canine kidney cells. Localization and vectorial transport studies. J Biol Chem. 2002; 277: 37711-37717.

3. Wheater PR, Burkitt HG, Daniels VG. Urinary system. In Wheaters Functional Histology: A Text and colour atlas. Edited by Wheater PR, Burkitt HG, Daniels VG. Churchill Livingstone: New York, 1987, pp. 236-257.

4. Griffiths M, Beaumont N, Yao SY, Sundaram M, Boumah CE, Davies A, Kwong FY, Coe I, Cass CE, Young JD, Baldwin SA. Cloning of a human nucleoside transporter implicated in the cellular uptake of adenosine and chemotherapeutic drugs. Nat Med. 1997; 3: 89-93.

5. Griffiths M, Yao SY, Abidi F, Phillips SE, Cass CE, Young JD, Baldwin SA. Molecular cloning and characterization of a nitrobenzylthioinosine-insensitive (ei) equilibrative nucleoside transporter from human placenta. Biochem J. 1997; 328: 739-743.

6. Crawford CR, Patel DH, Naeve C, Belt JA. Cloning of the human equilibrative, nitrobenzylmercaptopurine riboside (NBMPR)-insensitive nucleoside transporter ei by functional expression in a transport-deficient cell line. J Biol Chem. 1998; 273: 5288–5293.

7. Yao SY, Ng AM, Vickers MF, Sundaram M, Cass CE, Baldwin SA, Young JD. Functional and molecular characterization of nucleobase transport by recombinant human and rat equilibrative nucleoside transporters 1 and 2. Chimeric constructs reveal a role for the ENT2 helix 5-6 region in nucleobase translocation. J Biol Chem. 2002; 277: 24938-24948.

8. Baldwin SA, Yao SYM, Hyde RJ, Foppolo S, Barnes K, Ritzel MWL, Cass CE, Young JD. Functional Characterization of novel human mouse equilibrative nucleoside transporters (hENT3 and mENT3) located in intracellular membranes. J Biol Chem. 2007; 280: 15880-15887.

9. Barnes K, Dobrzynski H, Foppolo S, Beal PR, Ismat F, Scullion ER, Sun L, Tellez J, Ritzel MW, Claycomb WC, Cass CE, Young JD, Billeter-Clark R, Boyett MR, Baldwin SA. Distribution and functional characterization of equilibrative nucleoside transporter-4, a novel cardiac adenosine transporter activated at acidic pH. Circ Res. 2006; 99: 510-519.

10. Ritzel MW, Yao SY, Huang MY, Elliott JF, Cass CE, Young JD. Molecular cloning and functional expression of cDNAs encoding a human Na+ nucleoside cotransporter (hCNT1). Am J Physiol Cell Physiol. 1997; 272: C707– C714.

11. Wang J, Su SF, Dresser MJ, Schaner ME, Washington CB, Giacomini KM. Na+ dependent purine nucleoside transporter from human kidney: cloning and functional characterization. Am J Physiol Renal Physiol. 1997; 273: F1058– F1065.

12. Ritzel MW, Yao SY, Ng AM, Mackey JR, Cass CE, Young JD. Molecular cloning, functional expression and chromosomal localization of a cDNA encoding a human Na+/nucleoside cotransporter (hCNT2) selective for purine nucleosides and uridine. Mol Membr Biol. 1998; 15: 203– 211.

13. Ritzel MW, Ng AM, Yao SY, Graham K, Loewen SK, Smith KM, Ritzel RG, Mowles DA, Carpenter P, Chen XZ, Karpinski E, Hyde RJ, Baldwin SA, Cass CE, Young JD. Molecular identification and characterization of novel human and mouse concentrative Na+ nucleoside cotransporter proteins (hCNT3 and mCNT3) broadly selective for purine and pyrimidine nucleosides (system cib). J Biol Chem. 2001; 276: 2914– 2927.

14. Gutierrez MM, Brett CM, Ott RJ, Hui AC, Giacomini KM. Nucleoside transport in brush border membrane vesicles from human kidney. Biochimica et Biophysica Acta. 1992; 1105: 1-9.

15. Lai Y, Lee EW, Ton CC, Vijay S, Zhang H, Unadkat JD. Conserved residues F316 and G476 in the concentrative nucleoside transporter 1 (hCNT1) affect guanosine sensitivity and membrane expression, respectively. Am J Physiol Cell Physiol. 2005; 288: C39-45.

16. Brett CM, Washington CB, Ott RJ, Gutierrez MM, Giacomini KM. Interaction of nucleoside analogues with the sodium-nucleoside transport system in brush border membrane vesicles from human kidney. Pharm Res. 1993; 10: 423-426

17. Govindarajan R, Bakken AH, Hudkins KL, Lai Y, Casado FJ, Pasto-Anglada M, Tse CM, Hayashi J, Unadkat JD. In situ hydribdization and immunolocalization of concentrative and equilibrative nucleoside transporters in the human intestine, liver, kidneys, and placenta. Amer J Physiol Reg Int Comp Physiol. 2007; 293: R1809-R1822.

18. Mangravite LM, Xiao G, Giacomini KM. Localization of human equilibrative nucleoside transporters, hENT1 and hENT2, in renal epithelial cells. Am J Physiol Renal Physiol. 2003; 284: F902-F910.

19. Kuttesch JF Jr, Nelson JA. Renal handling of 2'-deoxyadenosine and adenosine in humans and mice. Cancer Chemother Pharmacol. 1982; 8: 221-229.

20. Errasti-Murugarren E, Pastor-Anglada M, Casado FJ. Role of CNT3 in the transepithelial flux of nucleosides and nucleoside-derived drugs. J Physiol. 2007; 582: 1249-60.

21. Mackey JR, Jennings LL, Clarke ML, Santos CL, Dabbagh L, Vsianska M, Koski SL, Coupland RW, Baldwin SA, Young JD, Cass CE. Immunohistochemical variation of human equilibrative nucleoside transporter 1 in primary breast cancers. Clin Cancer Res 2002; 8: 110-116.

22. Dabbagh L, Coupland RW, Cass CE, Mackey JR. Immunohistochemical variation of human equilibrative nucleoside transporter 1 protein in primary breast cancers. Clin Cancer Res 2003; 9: 3213-3214.

23. Spratlin J, Sangha R, Glubrecht D, Dabbagh L, Young JD, Dumontet C, Cass C, Lai R, Mackey JR. The absence of human equilibrative nucleoside transporter 1 is associated with reduced survival in patients with gemcitabine-treated pancreas adenocarcinoma. Clin Cancer Res 2004; 10: 6956-6961.

24. Chow L, Lai R, Dabbagh L, Belch A, Young JD, Cass CE, Mackey JR. Analysis of human equilibrative nucleoside transporter 1 (hENT1) protein in non-Hodgkin's lymphoma by immunohistochemistry. Mod Pathol. 2005; 18: 558-564.

25. Mackey JR, Galmarini CM, Graham KA, Joy AA, Delmer A, Dabbagh L, Glubrecht D, Jewell LD, Lai R, Lang T, Hanson J, Young JD, Merle-Béral H, Binet JL, Cass CE, Dumontet C. Quantitative analysis of nucleoside

transporter and metabolism gene expression in chronic lymphocytic leukemia (CLL): identification of fludarabine-sensitive and -insensitive populations. Blood 2005; 105: 767-774.

26. Farrell JJ, Elsaleh H, Garcia M, Lai R, Ammar A, Regine WF, Abrams R, Benson AB, Macdonald J, Cass CE, Dicker AF, Mackey JR. Human equilibrative nucleoside ransporter 1 levels predict response to gemcitabine in patients with pancreatic cancer. Gastroenterol. 2008 Oct 7 [Epub ahead of print].

27. Tsang RY, Santos C, Ghosh S, Dabbagh L, King K, Young J, Cass CE, Mackey JR, Lai R Immunohistochemistry for human concentrative nucleoside transporter 3 protein predicts fludarabine sensitivity in chronic lymphocytic leukemia. Mod Pathol. 2008; 21: 1387-1393.

28. Lash LH, Putt DA, Cai H. Membrane transport function in primary cultures of human proximal tubular cells. Toxicol. 2006; 228: 200-218.

29. Yao SY, Ng AM, Vickers MF, Sundaram M, Cass CE, Baldwin SA, Young JD. Functional and molecular characterization of nucleobase transport by recombinant human and rat equilibrative nucleoside transporters 1 and 2. Chimeric constructs reveal a role for the ENT2 helix 5-6 region in nucleobase translocation. J Biol Chem. 2002; 277: 24938-24948.

30. Cropp CD, Komori T, Shima JE, Urban TJ, Yee SW, More SS, Giacomini KM. Organic anion transporter 2 (SLC22A7) is a facilitative transporter of cGMP. Mol Pharmacol. 2008; 73: 1151-1158.

31. Xia L, Engel K, Zhou M, Wang J. Membrane localization and pH-dependent transport of a newly cloned organic cation transporter (PMAT) in kidney cells. Am J Physiol Renal Physiol. 2007; 292: F682-90.

32. Coe I, Zhang Y, McKenzie T, Naydenova Z. PKC regulation of the human equilibrative nucleoside transporter, hENT1. FEBS Lett. 2002; 517: 201-205.

33. Young JD, Yao SYM, Sun L, Cass CE, Baldwin SA. Human equilibrative nucleoside transporter (ENT) family of nucleoside and nucleobase transporter proteins. Xenobiotica. 2008; 38: 995-1021.

34. Pastor-Anglada M, Cano-soldado P, Errasti-murugarren E, Casado FJ. SLC28 genes and concentrative nucleoside transporter (CNT) proteins. Xenobiotica. 2008; 38: 972-994.

35. Vallon V, Muhlbauer B, and Osswald H. Adenosine and kidney function. Physiol Rev. 2006; 86: 901-940.

36. Gandhi, V., and Plunkett, W. 2002. Cellular and clinical pharmacology of fludarabine. Clin. Pharmacokinet. 41: 93–103.

37. List, A.F., Kummet, T.D., Adams, J.D., and Chun, H.G. 1990. Tumor lysis syndrome complicating treatment of chronic lymphocytic leukemia with fludarabine phosphate. Am. J. Med. 89: 388-390.

38. Piro L.D., Carrera, C.J., Beutler, E., and Carson, D.A. 1988. 2-Chlorodeoxyadenosine: an effective new agent for the treatment of chronic lymphocytic leukemia. Blood 72: 1069-1073.

39. McCroskey R.D., Mosher, D.F., Spencer, C.D., Prendergast, E., and Longo, W.L. 1990. Acute tumor lysis syndrome and treatment response in patients treated for refractory chronic lymphocytic leukemia with short-course, high-dose cytosine arabinoside, cisplatin, and etoposide. Cancer 66: 246-250.

40. Cairo, M.S., and Bishop, M. 2004. Tumor lysis syndrome: new therapeutic strategies and classification. Br. J. Haematol. 127: 3-11.

41. Huang P, Plunkett W. Action of 9-β-D-arabinofuranosyl-2-fluoroadenine on RNA metabolism. Mol Pharmacol. 1991; 39: 449-455.

42. Chen LS, Plunkett W, Gandhi V. Polyadenylation inhibition by the triphosphates of deoxyadenosine analogues. Leuk Res. 2008; 32: 1573-1581.

43. Rao VA, Plunkett W. Activation of a p53-mediated apoptotic pathway in quiescent lymphocytes after the inhibition of DNA repair by fludarabine. Clin Cancer Res. 2003; 9: 3204-3212.

44. Lai Y, Tse CM, Unadkat JD. Mitochondrial expression of the human equilibrative nucleoside transporter 1 (hENT1) results in enhanced

mitochondrial toxicity of antiviral drugs. J Biol Chem. 2004; 279: 4490–4497.

45. Maggio SC, Rosato RR, Kramer LB, Dai Y, Rahmani M, Paik DS, Czarnik AC, Payne SG, Spiegel S, Grant S. The histone deacetylase inhibitor MS-275 interacts synergistically with fludarabine to induce apoptosis in human leukemia cells. Cancer Res. 2004; 64: 2590-2600.

46. Genini D, Adachi S, Chao Q, Rose DW, Carrera CJ, Cottam HB, Carson DA, Leoni LM. Deoxyadenosine analogs induce programmed cell death in chronic lymphocytic leukemia cells by damaging the DNA and by directly affecting the mitochondria. Blood. 2000; 96: 3537-3543.

47. Chandra D, Bratton SB, Person MD, Tian Y, Martin AG, Ayres M, Fearnhead HO, Gandhi V, Tang DG. Intracellular nucleotides act as critical prosurvival factors by binding to cytochrome C and inhibiting apoptosome. Cell. 2006; 125: 1333-1346.